

This electronic thesis or dissertation has been downloaded from the King's Research Portal at <https://kclpure.kcl.ac.uk/portal/>



The role of fluoride in erosion, attrition and abrasion of human enamel and dentine in vitro

Austin, Rupert

Awarding institution:
King's College London

The copyright of this thesis rests with the author and no quotation from it or information derived from it may be published without proper acknowledgement.

END USER LICENCE AGREEMENT



Unless another licence is stated on the immediately following page this work is licensed

under a Creative Commons Attribution-NonCommercial-NoDerivatives 4.0 International

licence. <https://creativecommons.org/licenses/by-nc-nd/4.0/>

You are free to copy, distribute and transmit the work

Under the following conditions:

- Attribution: You must attribute the work in the manner specified by the author (but not in any way that suggests that they endorse you or your use of the work).
- Non Commercial: You may not use this work for commercial purposes.
- No Derivative Works - You may not alter, transform, or build upon this work.

Any of these conditions can be waived if you receive permission from the author. Your fair dealings and other rights are in no way affected by the above.

Take down policy

If you believe that this document breaches copyright please contact librarypure@kcl.ac.uk providing details, and we will remove access to the work immediately and investigate your claim.

Title:The role of fluoride in erosion, attrition and abrasion of human enamel and dentine in vitro

Author:Rupert Austin

KING'S COLLEGE LONDON DENTAL INSTITUTE AT
GUY'S, ST. THOMAS' AND KING'S COLLEGE HOSPITALS

*The role of fluoride on
erosion, attrition and
abrasion of human
enamel and dentine in
vitro*

Thesis submitted for the degree of
Doctor of Philosophy

Rupert Austin

BDS (Hons) MJDF RCS Eng AHEA

Department of Biomaterials Science
King's College London Dental Institute
London SE1 9RT
United Kingdom

April 2011

Abstract

The effect of trace elements such as fluoride on multi-factorial tooth wear is poorly understood. This study examined the role of varying fluoride compounds and products in multi-factorial tooth wear models. Dedicated software for surface profile measurement of dental hard tissues using white light confocal profilometry was developed and a measurement uncertainty evaluation completed. Microhardness techniques were validated and the remineralisation protocol developed. Human teeth were donated in line with research ethics and enamel and dentine samples were prepared. A series of three distinct experiments involving varying fluoride preparations and concentrations were completed. Firstly, the effect of an aqueous sodium fluoride solution of increasing concentration on citric acid erosion and attrition of enamel and dentine was investigated. 5000 ppm and 19000 ppm sodium fluoride solutions significantly reduced enamel loss versus control after 15 cycles of erosion-attrition, however no other groups showed significant differences. Secondly, the effect of a single application of highly concentrated sodium fluoride, stannous fluoride and titanium fluoride solutions and a sodium fluoride/calcium fluoride varnish on hydrochloric acid erosion and tooth brush abrasion of enamel was investigated. The titanium fluoride solution and the sodium/calcium fluoride varnish reduced enamel loss significantly after erosion, however, in the erosion-abrasion protocol only the sodium fluoride solution and the sodium/calcium fluoride varnish showed a statistically significant reduction in enamel loss after 15 cycles. Chemical and ultra-structural analyses supported these findings. Finally, the effect of a single application of two highly concentrated sodium fluoride varnishes and a fluoride-free self-etch adhesive on citric acid erosion and attrition of enamel was investigated. Both fluoride varnishes resulted in statistically significant reductions of enamel loss versus the self-etch adhesive and the negative control, at all stages of the study. Overall, these studies showed potential for highly concentrated fluoride preparations to provide protection against erosion-abrasion and erosion-attrition *in vitro*.

Acknowledgements

Professor David Bartlett, my first supervisor and research mentor, to whom I owe so much. Your energy and enthusiasm have been truly inspirational throughout every stage of this process. I have greatly enjoyed taking my first research steps under your tutelage and am ever grateful for all you have done.

Dr Rebecca Moazzez, my second supervisor, who first provided the opportunity to join her research team and who has been a beacon of guidance and good sense throughout. Your kind words and deeds are hugely appreciated.

Professor Stephen Dunne, my third supervisor, who nurtured and mentored me from the outset. You made this work possible and I am very grateful for your unwavering support.

Dr Ron Wilson; whose discerning mind and sage advice has been immensely beneficial. Your rigorous analysis and sound judgement during our many debates and discussions on study design and research planning (and much else in between!) is much appreciated.

Dr Jose Rodriguez, my friend and colleague, whose admirable ability of blending duty and fun in equal measures has made this journey all the more enjoyable!

Dr. Ryan Olley, my fellow PhD student and friend, who has shared the hopes, aspirations (and occasional frustrations) whilst researching together.

Messrs Peter Pilecki and Richard Mallett, whose sound guidance around the finery and foibles of their research laboratories has resulted in practical solutions where, at first, none seemed possible. Thank you for your patience!

Dr Fred Festy, who has provided insights and a robustness of scientific discipline that broadened my vision of the possibilities and potentials of this project.

Mr Tom Bull, Dr. Kevin Cross and Professor John McBride from TaiCaan® Technologies Ltd., whose profound understanding of metrology equipment and science is truly admirable.

Mr Claudiu Giuscu and Professor Richard Leach and from the Dimensional Engineering Measurement division of the National Physical Laboratory, and Dr Michael McCarthy and Dr Andy Robinson from the Freeform Measurement & Analysis division. Your willingness to transfer your expertise in the science of measurement has provided a deeper level of insight and analysis and has proved invaluable to this project.

Dr Kjersti R. Stenhagen, Dr. Lene Hove and Professor Anne Bjørg Tveit at the Faculty of Dentistry University of Oslo, Norway and Dr. Børge Holme from The Foundation for Scientific and Industrial Research, Oslo, Norway. Your collaborative work and efforts have been outstanding and I have greatly enjoyed working with you on this project.

My parents Michael and Shelia, my sisters Ismay and Rowena and my brother Geoffrey, whose love and support has defined my path in life.

And finally to Deborah, whose love, intelligence and humanity are incomparable.

Declaration of collaborative work

Professor David Bartlett, Professor Stephen Dunne and Dr Rebecca Moazzez contributed to the design, analysis and discussion of all Chapters contained within this thesis.

Professor Richard Leach and Mr Claudiu Giuscu contributed to the design and analysis of Section 2.1 of Chapter 2 of this thesis.

Dr Kjersti Stenhagen, Dr. Lene Hove and Professor Anne Bjorg Tveit contributed to the design and analysis of Chapter 4 of this thesis. Dr Kjersti Stenhagen and Dr. Lene Hove contributed to the sample preparation (Section 4.2.2), the application of the fluoride treatments (Section 4.2.3) and the cyclic tooth wear modelling (Section 4.2.4) of Chapter 4 of this thesis.

All other work presented in this thesis is my own. All references are cited accordingly.

Rupert Sloan Austin

April 2011, London.

Table of Contents

Abstract.....	2
Acknowledgements	3
Declaration of collaborative work.....	5
List of Tables.....	13
List of Figures.....	17
List of Equations	23
Chapter 1 Review of the literature	24
1.1. Tooth wear.....	24
1.1.1 Aetiology	25
Erosion	25
Attrition.....	27
Abrasion	28
Abfraction	28
1.1.2 Clinical features.....	28
1.1.3 Management.....	30
1.2. Fluoride and tooth wear	30
1.2.1. Fluoride and the oral environment.....	31
Effects on enamel	31
Effects on dentine	33
Fluoride concentration in teeth	33
Fluoride metabolism and toxicity	34
1.2.2. Physicochemical interactions between topical fluoride and enamel/dentine during tooth wear	35

1.2.3.	Fluoride products	39
	Self-applied products	40
	Fluoride toothpastes	40
	Fluoride gels	42
	Fluoride rinses	42
	Professionally-applied products	43
	Fluoride gels	43
	Fluoride varnishes	43
1.3.	Tooth wear measurement	44
1.3.1.	Direct visual measurement, dental casts and indices	45
1.3.2.	Surface topography and texture measurement	46
	Contacting stylus profilometry	50
	Optical profilometry	52
	Projected surface topography measurement	53
	Photogrammetry	53
	Confocal laser scanning microscopy	53
	Laser triangulation profilometry	54
	Confocal profilometry	56
	Interferometry	57
	Optical coherence tomography	57
	Atomic force microscopy	58
	Software for surface profile and surface texture measurement	59
1.3.3.	Surface hardness	61
	Microhardness	61
	Nanoindentation	64
1.3.4.	Chemical analysis	65
	Iodide permeability test	65
	Chemical analysis of dissolved minerals	65
	Energy Dispersive X-Ray Spectroscopy	65
1.3.5.	Scanning electron microscopy	66
	Quantitative light-induced fluorescence	68

Microradiography	68
1.4. Tooth wear modelling.....	69
1.4.1. <i>In vivo</i>	71
Clinical trials of investigational medicinal products	72
1.4.2. <i>In situ</i>	73
1.4.3. <i>In vitro</i>	74
Studies modelling erosion only.....	75
Simple erosion models.....	76
Cyclic erosion models.....	78
Studies modelling erosion with a physical impact.....	79
Abrasion components	79
Attrition components.....	79
Overall aims of Chapter 2, 3, 4 and 5.....	80
 Chapter 2 Development and validation of techniques used to model and measure tooth wear <i>in vitro</i>	 81
Introduction.....	81
2.1 Section 2.1: Uncertainty of tooth wear measurement <i>in vitro</i>	84
2.1.1 Aim, objectives and hypothesis	84
2.1.2 Materials and methods.....	84
2.1.2.1 Quantification of flatness and noise errors	90
2.1.2.2 Quantification of enamel and dentine shrinkage errors	92
2.1.2.3 Quantification of lateral (x, y) scale linearity errors	97
2.1.2.4 Quantification of vertical (z) scale linearity errors.....	101
2.1.2.5 Quantification of software errors	104
2.1.2.6 Combine the Standard Uncertainties	111
2.1.2.7 Determine the Overall Combined Uncertainty	111
2.1.3 Results.....	114
2.1.3.1 Flatness and noise errors	114

2.1.3.2	Enamel and dentine shrinkage errors.....	115
2.1.3.3	Lateral (x, y) scale linearity errors.....	118
2.1.3.4	Vertical (z) scale linearity errors	119
2.1.3.5	Software errors	120
2.1.3.6	Standard Combined Uncertainty	122
2.1.3.7	Overall Combined Uncertainty	123
2.2	Section 2.2: Validity of microhardness measurement	125
2.2.1	Introduction	125
2.2.2	Aim, objectives and null hypothesis	126
2.2.3	Materials and methods.....	126
2.2.4	Statistical analysis	129
2.2.5	Results.....	129
2.3	Section 2.3: Validity of remineralisation protocol	130
2.3.1	Introduction	130
2.3.2	Aim, objectives and null hypothesis	131
2.3.3	Materials and methods.....	131
2.3.3.1	Study design.....	131
2.3.3.2	Sample preparation	131
2.3.3.3	Baseline microhardness measurements.....	131
2.3.3.4	Erosion cycling model	132
2.3.3.5	Artificial saliva	132
2.3.3.6	Human saliva.....	133
2.3.3.7	Microhardness	133
2.3.4	Statistical analysis	133
2.3.5	Results.....	134
	Discussion.....	135
	Section 2.1.....	135

Section 2.2.....	141
Section 2.3.....	142
Chapter 3 The effect of increasing sodium fluoride concentrations on erosion and attrition of enamel and dentine <i>in vitro</i>.....	144
Introduction.....	144
3.1 Aim, objectives and null hypotheses	145
3.2 Materials and methods.....	146
3.2.1 Study design	146
3.2.2 Sample preparation	147
3.2.3 Cyclic tooth wear model	147
3.2.4 Profilometry	150
3.3 Statistical analysis	150
3.4 Results	151
Discussion.....	158
Chapter 4 The effect of a single application of topical fluoride treatments on enamel surfaces subjected to erosion or erosion-abrasion <i>in vitro</i>.....	162
Introduction.....	162
4.1 Aim, objectives and null hypotheses	163
4.2 Materials and methods.....	164
4.2.1 Study design	164
4.2.2 Sample preparation	165
4.2.3 Application of fluoride treatments	165
4.2.4 Cyclic tooth wear model	165

4.2.5	Profilometry	167
4.2.6	Scanning electron microscopy (SEM) and energy-dispersive X-ray spectroscopy (EDS)	167
4.2.7	Microhardness	168
4.3	Statistical analysis	169
4.4	Results	169
4.4.1	Profilometry	169
4.4.2	SEM analysis.....	174
4.4.3	EDS analysis.....	177
4.4.4	Microhardness	180
	Discussion.....	182
 Chapter 5 The effect of sodium fluoride varnishes and a resin-based adhesive on enamel erosion-attrition <i>in vitro</i>		
	Introduction.....	189
5.1	Aim, objectives and null hypothesis	189
5.2	Materials and methods.....	190
5.2.1	Study design	190
5.2.2	Sample preparation	190
5.2.3	Application of surface treatments	191
5.2.4	Cyclic tooth wear model	192
5.2.5	Profilometry	193
5.2.6	Scanning electron microscopy (SEM) and energy-dispersive X-ray spectroscopy (EDS)	194

5.3	Statistical analysis	194
5.4	Results	195
5.4.1	Profilometry	195
5.4.2	SEM analysis.....	200
5.4.3	EDS analysis.....	203
	Discussion.....	207
Chapter 6 General discussion and conclusions; clinical implications and suggestions for future work.....		212
	General discussion	212
	Conclusions.....	215
	Clinical implications.....	217
	Future developments	219
Appendices.....		220
	Appendix 1 Effect of varying measurement control settings on the time and accuracy of <i>in vitro</i> tooth wear measurement using the white light confocal profilometer	220
	Appendix 3 Informed Consent Form (ICF) for donation of extracted tooth	226
	Appendix 4 Uncertainty budget used to evaluate the Standard Combined Uncertainty of the step height and volume measurement with the white light confocal profilometer	227
	Appendix 5 Uncertainty budget used to evaluate the Overall Combined Uncertainty of the step height and volume measurement with the white light confocal profilometer	230
Bibliography		233

List of Tables

Table 1 Percentage by weight (wt %) and the equivalent parts per million (ppm) fluoride of sodium fluoride and sodium monofluorophosphate in toothpastes (Adapted from Ellwood et al 2008)	40
Table 2 Nominal stage specifications of the XYRIS™ 4000 white light confocal profilometer	86
Table 3 Nominal sensor specifications of the XYRIS™ 4000 white light confocal profilometer	89
Table 4 Principle inclusion and exclusion criteria for recruitment of participants to donate extracted teeth for the research study ' <i>Protection of erosive wear</i> '	94
Table 5 Mean (SD) and maximum Sz flatness error (μm) and Sq noise error (μm) of a 5 mm x 3 mm scanned area of the optical flat measured at different locations of the x/y stage	114
Table 6 Mean (SD) linearity error (μm) on the vertical scale over step heights of 0.3 μm , 2.97 μm , 17 μm and 30 μm	119
Table 7 BODDIES® software error (μm) associated with the step height measurement of 0.3 μm , 3 μm , 17 μm and 30 μm soft gauges, in comparison to Mountains® software	120
Table 8 ImageJ step height (SH) macro software error (μm) associated with the step height measurement of 0.3 μm , 3 μm , 17 μm and 30 μm soft gauges, in comparison to Mountains® software	121
Table 9 ImageJ volume (Vol) macro software error ($\text{M } \mu\text{m}^3/\text{mm}$) associated with the volume measurement of 0.3 μm , 3 μm , 17 μm and 30 μm soft gauges, in comparison to Mountains® software	121
Table 10 Standard combined uncertainties associated with the step height (μm) and volume ($\text{M } \mu\text{m}^3/\text{mm}$) measurements of 0.3 μm , 2.97 μm , 17 μm and 30 μm step height reference standards	122
Table 11 Overall Combined Uncertainty associated with step height (μm) and volume ($\text{M } \mu\text{m}^3/\text{mm}$) measurement of 0.3 μm , 3 μm , 17 μm and 30 μm soft gauge reference standards	124

Table 12 Varying conditions of measurement used in order to determine the repeatability and reproducibility of a measurement instrument, as described in the International Vocabulary of Metrology (BIPM et al., 2008).....	126
Table 13 Measurement settings used to determine the “true” microhardness of the transfer-standard block as stated in the calibration certificate	127
Table 14 Knoop microhardness values (KHN) of the transfer-standard block using the Leitz-Wetzlar microhardness tester and the calibration microhardness tester.....	130
Table 15 Median (IQR) step height (μm) enamel wear after five, ten and 15 cycles of attrition, by control and test fluoride solutions ($n=10/\text{gp}$).....	153
Table 16 Median (IQR) step height (μm) enamel wear after five, ten and 15 cycles of erosion-attrition, by control and test fluoride solutions (μm) ($n=10/\text{gp}$).....	153
Table 17 Mean (SD) step height (μm) dentine wear after five, ten and 15 cycles of attrition, by control and test fluoride solutions (μm) ($n=10/\text{gp}$).....	154
Table 18 Mean (SD) step height (μm) dentine wear after five, ten and 15 cycles of erosion-attrition, by control and test fluoride solutions ($n=10/\text{gp}$).....	154
Table 19 Mean (SD) volume ($\text{M } \mu\text{m}^3/\text{mm}$) surface change by fluoride group after three, six and nine cycles of erosion ($n=6/\text{gp}$).....	170
Table 20 Mean (SD) volume ($\text{M } \mu\text{m}^3/\text{mm}$) of surface change by fluoride group after three, six and nine cycles of erosion-abrasion ($n=6/\text{gp}$).....	170
Table 21 Fluoride concentration (ppm), starting pH and composition of the self-etch adhesive and the two fluoride varnishes applied to the enamel samples prior to erosion-attrition.....	192
Table 22 Median (IQR) step height (μm) surface change of treated enamel surface after application of product/deionized water (deionized water) and after five, ten and 15 cycles of erosion-attrition, by product group ($n=10/\text{gp}$).....	195
Table 23 Median (IQR) volume ($\text{M } \mu\text{m}^3/\text{mm}$) surface change after application of product/deionized water and after five, ten and 15 cycles of erosion-attrition, by product group ($n=10/\text{gp}$).....	196

Table 24 Median (IQR) step height (μm) enamel loss after application of product/deionized water and after five, ten and 15 cycles of erosion-attrition, by product group ($n = 10/\text{gp}$)	199
Table 25 Median (IQR) volume ($\text{M } \mu\text{m}^3/\text{mm}$) enamel loss after application of product/deionized water and after five, ten and 15 cycles of erosion-attrition, by product group ($n = 10/\text{gp}$)	200
Table 26 Individual uncertainty budget contributions from each source of error to the Standard Combined Uncertainty (μm and %) of the step height measurement of a $0.3 \mu\text{m}$ step height reference standard	227
Table 27 Individual uncertainty budget contributions from each source of error to the Standard Combined Uncertainty (μm and %) of the step height measurement of a $2.97 \mu\text{m}$ step height reference standard	227
Table 28 Individual uncertainty budget contributions from each source of error to the Standard Combined Uncertainty (μm and %) of the step height measurement of a $17 \mu\text{m}$ step height reference standard	227
Table 29 Individual uncertainty budget contributions from each source of error to the Standard Combined Uncertainty (μm and %) of the step height measurement of a $30 \mu\text{m}$ step height reference standard	228
Table 30 Individual uncertainty budget contributions from each source of error to the Standard Combined Uncertainty ($\text{M } \mu\text{m}^3/\text{mm}$ and %) of the volume measurement of a $0.3 \mu\text{m}$ step height reference standard	228
Table 31 Individual uncertainty budget contributions from each source of error to the Standard Combined Uncertainty ($\text{M } \mu\text{m}^3/\text{mm}$ and %) of the volume measurement of a $2.97 \mu\text{m}$ step height reference standard	228
Table 32 Individual uncertainty budget contributions from each source of error to the Standard Combined Uncertainty ($\text{M } \mu\text{m}^3/\text{mm}$ and %) of the volume measurement of a $17 \mu\text{m}$ step height reference standard	229

Table 33 Individual uncertainty budget contributions from each source of error to the Standard Combined Uncertainty ($\text{M } \mu\text{m}^3/\text{mm}$ and %) of the volume measurement of a $30 \mu\text{m}$ step height reference standard	229
Table 34 Individual uncertainty budget contributions from each source of error to the Overall Combined Uncertainty (μm and %) of the step height measurement of a $0.3 \mu\text{m}$ soft gauge reference standard	230
Table 35 Individual uncertainty budget contributions from each source of error to the Overall Combined Uncertainty (μm and %) of the step height measurement of a $3 \mu\text{m}$ soft gauge reference standard	230
Table 36 Individual uncertainty budget contributions from each source of error to the Overall Combined Uncertainty (μm and %) of the step height measurement of a $17 \mu\text{m}$ soft gauge reference standard	230
Table 37 Individual uncertainty budget contributions from each source of error to the Overall Combined Uncertainty (μm and %) of the step height measurement of a $30 \mu\text{m}$ soft gauge reference standard	231
Table 38 Individual uncertainty budget contributions from each source of error to the Overall Combined Uncertainty ($\text{M } \mu\text{m}^3/\text{mm}$ and %) of the volume measurement of a $0.3 \mu\text{m}$ soft gauge reference standard	231
Table 39 Individual uncertainty budget contributions from each source of error to the Overall Combined Uncertainty ($\text{M } \mu\text{m}^3/\text{mm}$ and %) of the volume measurement of a $3 \mu\text{m}$ soft gauge reference standard	231
Table 40 Individual uncertainty budget contributions from each source of error to the Overall Combined Uncertainty ($\text{M } \mu\text{m}^3/\text{mm}$ and %) of the volume measurement of a $17 \mu\text{m}$ soft gauge reference standard	232
Table 41 Individual uncertainty budget contributions from each source of error to the Overall Combined Uncertainty ($\text{M } \mu\text{m}^3/\text{mm}$ and %) of the volume measurement of a $30 \mu\text{m}$ soft gauge reference standard	232

List of Figures

Figure 1 Intra-oral clinical photographs of a 36 year old male patient with severe tooth wear	29
Figure 2 Classification of surface topography measurement techniques. [Adapted from (Blunt, 2008)]	47
Figure 3 Example of a single profile measurement taken from a 5 mm x 3 mm ‘areal’ measurement of an optical flat	49
Figure 4 Schematic illustrating the relationship between (a) the overall surface geometry and (b) the profile, (c) the waviness and (d) the roughness of a surface.	50
Figure 5 Potential sources of measurement uncertainty associated with the use of contacting profilometry techniques for 3D surface topography measurement [adapted from (Leach, 2008)]	52
Figure 6 Schematic of optical principles of surface topography measurement using laser triangulation profilometry	55
Figure 7 Schematic of resistance to motion of dislocations created by a diamond indenter [From (Sirdeshmukh et al., 2006)]	61
Figure 8 Photograph of the component parts of the white light confocal profilometer	85
Figure 9 Close-up photograph of the component parts of the white light confocal profilometer	86
Figure 10 Schematic of the optical principles of the white light confocal sensor	88
Figure 11 Schematic showing the relationship between the overall surface geometry (a), profile (b) waviness (c) and roughness (d) of a measured surface.	91
Figure 12 Photograph of the National Physical Laboratory optical flat.....	91
Figure 13 Photograph of the hard-anodized aluminium and brass sample former used to embed enamel and dentine sections in bis-acryl composite	95
Figure 14 Overview photograph of the National Physical Laboratory optical dimensional standard and close up photograph of the lateral scale SC6	98
Figure 15 Schematic of the image analysis workflow for the length measurement the NPL optical dimensional standard lateral scale SC6 using Mountains® surface analysis software	100

Figure 16 Overview and close up photographs of the 0.3 μm , 2.97 μm and 17 μm step height reference standards	101
Figure 17 Analysis of the 3D step height of the 0.3 μm step height reference standard using Mountains® surface analysis software	103
Figure 18 Framework for the validation of surface analysis software (after Blunt et al 2008)	104
Figure 19 Profiles showing the typical geometry of erosion; erosion-abrasion and erosion-attrition lesions created by the <i>in vitro</i> tooth wear models used in this thesis	105
Figure 20 3D images of the 0.3 μm , 3 μm , 17 μm and 30 μm common 3D data sets ('soft gauges')	106
Figure 21 ISO profile method for measurement of step height (as defined by ISO 3274, 1996)	107
Figure 22 Schematic of the step height measurement technique of the 0.3 μm , 3 μm , 17 μm and 30 μm soft gauges using Mountains® reference software	107
Figure 23 Schematic of the volume measurement technique of the 0.3 μm , 3 μm , 17 μm and 30 μm soft gauges using Mountains® reference software	108
Figure 24 Schematic of the image analysis workflow for calculation of the volume of the 0.3 μm , 3 μm , 17 μm and 30 μm soft gauges using ImageJ volume macro	110
Figure 25 3D images of (a) the 3D data set created by scanning the optical flat and (b-e) the 0.3 μm , 3 μm , 17 μm and 30 μm soft gauge reference standards	113
Figure 26 Representative images of the 3D scans of the optical flat analysed with Mountains® surface analysis software to assess (a) the flatness errors and (b) the noise errors.....	115
Figure 27 Mean percent change (%) of the relative humidity and measured step height of pre-worn enamel (n =2) and dentine (n =2) samples over time	117
Figure 28 Mean percent change (%) of the relative humidity and measured volume of pre-worn enamel (n =2) and dentine (n =2) samples over time.....	118
Figure 29 Mean (SD) linearity error (μm) on the x axis over 5 mm linear distance	118
Figure 30 Mean (SD) linearity error (μm) on the y axis over 5 mm linear distance	119

Figure 31 Mean Standard Combined Uncertainty (%) of the step height and volume measurement using the white light confocal profilometer by the depth (z axis height) of the wear (μm) being measured.....	123
Figure 32 Mean Overall Combined Uncertainty (%) of the step height and volume measurement using the white light confocal profilometer by the depth (z axis height) of the wear (μm) being measured.....	125
Figure 33 Photograph of the transfer-standard block used to assess the accuracy and precision of the microhardness tester	127
Figure 34 Median (IQR) Knoop microhardness of enamel samples before and after an acid challenge and after immersion in either a diluted solution of stimulated human parotid saliva or an artificial saliva solution over time ($n = 5/\text{gp}$)	134
Figure 35 Mean (SD) percent surface microhardness recovery (%SMR) of enamel samples after an acid challenge and after immersion in either a diluted solution of stimulated human parotid saliva or an artificial saliva solution over time ($n = 5/\text{gp}$)	135
Figure 36 Flowchart of protocols for the attrition and erosion-attrition	148
Figure 37 Photograph of the set up of the attrition wear machine with taped sample immersed in artificial saliva.....	150
Figure 38 Median (IQR) enamel step height wear (μm) and mean (SD) dentine step height wear (μm) after five, ten and 15 cycles of attrition and erosion-attrition of the enamel samples allocated to the control group ($n = 10/\text{gp}$)	152
Figure 39 Effect of increasing the concentration of the sodium fluoride solution on the mean step height (μm) of enamel loss by the number of cycles of attrition ($n = 10/\text{gp}$)	155
Figure 40 Effect of increasing the concentration of the sodium fluoride solution on the mean step height (μm) of enamel loss by the number of cycles of erosion-attrition ($n = 10/\text{gp}$)	155
Figure 41 Effect of increasing the concentration of the sodium fluoride solution on the mean step height (μm) of dentine loss by the number of cycles of attrition ($n = 10/\text{gp}$)	156

Figure 42 Effect of increasing the concentration of the sodium fluoride solution on the mean step height (μm) of dentine loss by the number of cycles of erosion-attrition (n =10/gp).....	156
Figure 43 Effect of varying concentration of a sodium fluoride solution on the median (IQR) rate ($\mu\text{m}/\text{cycle}$) of enamel wear by experimental wear method (n =10/gp).....	157
Figure 44 Effect of varying concentration of a sodium fluoride solution on the mean (SD) rate ($\mu\text{m}/\text{cycle}$) of dentine wear by experimental wear method (n =10/gp).....	157
Figure 45 Flowchart of protocols for the erosion and erosion-abrasion.....	166
Figure 46 Mean (SD) volume of enamel and product loss (M $\mu\text{m}^3/\text{mm}$) after nine cycles of erosion and erosion-abrasion by fluoride/control group (n = 6/gp)	171
Figure 47 Comparison of volume change (M $\mu\text{m}^3/\text{mm}$) of enamel samples subjected to (a) three cycles (b) six cycles and (c) nine cycles of erosion and erosion-abrasion by fluoride/control group (n = 6/gp)	173
Figure 48 Representative SEM images from the control group, immediately after deionized water treatment; after nine cycles of erosion and after nine cycles of erosion-abrasion	174
Figure 49 Representative SEM images from the NaF treated group, immediately after treatment; after nine cycles of erosion and after nine cycles of erosion-abrasion.....	175
Figure 50 Representative SEM images from the TiF_4 treated group, immediately after treatment; after nine cycles of erosion and after nine cycles of erosion-abrasion.....	175
Figure 51 Representative SEM images from the SnF_2 treated group, immediately after treatment; after nine cycles of erosion and after nine cycles of erosion-abrasion.....	176
Figure 52 Representative SEM images from the Bifluorid10® treated group, immediately after treatment; after nine cycles of erosion and after nine cycles of erosion-abrasion.....	177
Figure 53 Elemental surface composition (wt %) of a sample from the deionized water treated (control) group after application; after nine cycles of erosion and after nine cycles of erosion-abrasion	178
Figure 54 Elemental surface composition (wt %) of a sample from the NaF treated group after treatment; after nine cycles of erosion and after nine cycles of erosion-abrasion.....	178

Figure 55 Elemental surface composition (wt %) of a sample from the SnF ₂ treated group after treatment; after nine cycles of erosion and after nine cycles of erosion-abrasion.....	179
Figure 56 Elemental surface composition (wt %) of a sample from the TiF ₄ treated group after treatment; after nine cycles of erosion and after nine cycles of erosion-abrasion.....	179
Figure 57 Elemental surface composition (wt %) of a sample from the Bifluorid10® treated group after treatment; after nine cycles of erosion and after nine cycles of erosion-abrasion	180
Figure 58 Mean Knoop microhardness (KHN) of fluoride groups and control after 3, 6 and 9 cycles of erosion (n =6/gp).....	181
Figure 59 Mean percent Knoop microhardness change (%KHC) of fluoride groups vs. control after 3, 6 and 9 cycles of erosion (n =6/gp)	182
Figure 60 Flowchart of the protocols for the erosion-attrition	193
Figure 61 Representative image of Bifluorid10® treated enamel sample after ten cycles of erosion attrition	197
Figure 62 Images from a representative enamel sample (a) after application of Duraphat® varnish (b) after ten cycles of erosion-attrition and (c) after virtual removal of the coating using BODDIES® software.....	198
Figure 63 SEM images from a sample from the control group: after application of de-ionized water (deionized water); after five, ten and 15 cycles of erosion-attrition (x 1.5 k magnification)...	201
Figure 64 SEM images from a sample from the Adper™ Prompt™ self-etch adhesive group: after application of Adper™ Prompt™ self-etch adhesive; after five, ten and 15 cycles of erosion-attrition (x 1.5 k magnification).....	202
Figure 65 SEM images from a sample from the Bifluorid10® varnish group: after application of Bifluorid10® varnish; after five, ten and 15 cycles of erosion-attrition (x 1.5 k magnification)	202
Figure 66 SEM images from a sample from the Duraphat® varnish group: after application of Duraphat® varnish; after five cycles of erosion-attrition, after ten cycles of erosion-attrition and after 15 cycles of erosion-attrition (x 1.5 k magnification).....	203

Figure 67 Mean elemental surface composition (wt %) of the enamel surface of a sample from the control group after application of deionized water (deionized water) and after five, ten and 15 cycles of erosion-attrition	204
Figure 68 Mean elemental surface composition (wt %) of the enamel surface of a sample from the Adper™ Prompt™ treated group after application of Adper™ Prompt™ self-etch adhesive and after five, ten and 15 cycles of erosion-attrition	205
Figure 69 Mean elemental surface composition (wt %) of the enamel surface of a sample from the Bifluorid10® varnish treated group after application of Bifluorid10® varnish and after five, ten and 15 cycles of erosion-attrition.....	206
Figure 70 Mean elemental surface composition (wt %) of the enamel surface of a sample from the Duraphat® treated group after application of Duraphat® varnish and after five, ten and 15 cycles of erosion-attrition	207
Figure 71 Geometry of a developing erosion-attrition lesion <i>in vitro</i>	213
Figure 72 Scatter plot showing the relationship between step height enamel loss and volume enamel loss ($M \mu m^3/mm$) after multiple cycles of erosion ($n = 55$)	214
Figure 73 Scatter plot showing the relationship between step height enamel loss and volume enamel loss ($M \mu m^3/mm$) after multiple cycles of erosion-abrasion ($n = 36$).....	214
Figure 74 Scatter plot showing the relationship between step height enamel loss and volume enamel loss ($M \mu m^3/mm$) after multiple cycles of erosion-abrasion ($n = 30$).....	215
Figure 75 Time taken (minutes) for the white light confocal profilometer to scan a 15 mm ² measurement area at 5 x 5 μm , 10 x 10 μm and 15 x 15 μm x/y measurement spacing and at 'fast', 'medium' and 'slow' measurement speeds	220
Figure 76 Mean accuracy (μm) of the white light confocal profilometer at measuring a Taylor-Hobson 0.39 μm and a 2.64 μm step height reference standard measured at 5 x 5 μm , 10 x 10 μm and 15 x 15 μm x/y measurement spacing and at 'fast', 'medium' and 'slow' measurement speeds	221

List of Equations

Equation 1 Formation of fluorhydroxyapatite from hydroxyapatite in the presence of ionic fluoride.....	32
Equation 2 Formation of calcium fluoride from hydroxyapatite in the presence of ionic fluoride.....	32
Equation 3 Formula for calculation of step height using Mountains® surface analysis software	107
Equation 4 The American Society for the Testing of Materials (ASTM) formula for calculation of the Knoop Hardness Number (KHN)	128
Equation 5 Indenter constant defined by the angulation of the opposite edges of the vertex of the Knoop diamond indenter.....	128
Equation 6 Calculation of percent surface microhardness recovery (%SMR) of eroded enamel samples immersed in either human or artificial saliva over time (Gelhard et al., 1979)	133

Chapter 1 Review of the literature

1.1. Tooth wear

Tooth wear is defined as the irreversible, non-traumatic loss of dental hard tissues due to processes classified as erosion, attrition and abrasion (Bartlett and Smith, 2000; Ganss, 2006) and abfraction (Lee and Eakle, 1984). Erosion is chemical wear as a result of extrinsic or intrinsic acids acting on tooth surfaces. Attrition is physical wear as a result of the action of antagonistic teeth. Abrasion is physical wear as a result of mechanical processes involving foreign bodies. Abfraction is thought to be a type of fatigue wear which occurs as a result of tensile or shear stress in the cemento-enamel junction which initiate micro fractures in enamel and dentine (Lee and Eakle, 1984).

The terms 'tooth wear' and 'tooth surface loss' are interchangeable however the former term is preferred by the author.

Considered from a historical or anthropological perspective, some degree of tooth wear is considered a natural part of aging. (Whittaker, 2000) and Berry and Poole (1974) first advocated the theory that the human dentition was designed to wear (even extensively) and that a certain degree of tooth wear optimized the functional capabilities of the human dentition. Within the dental community however, Smith and Knight (1984a) were the first to distinguish between 'physiological' tooth wear and 'pathological' tooth wear. This classification depends on the age of the patient and the rate of progression of the tooth wear, with pathological tooth wear being that which threatens the survival of the tooth, or causes aesthetic concerns, sensitivity, loss of vitality and failure of restorations or results in occlusal problems. This remains a subjective assessment however it is generally agreed that excessive levels of tooth wear may be a cause for major concern to patients and clinicians alike and the World Health Organisation (1992) has included attrition, abrasion and erosion in the International Classification of Diseases.

1.1.1 Aetiology

When a patient is diagnosed with tooth wear, elements of abrasion, attrition and erosion are commonly co-diagnosed as contributing to the overall clinical picture (Addy and Shellis, 2006; Smith and Knight, 1984b). This multifactorial process is further modified by risk factors such as stress, parafunction, salivary buffering capacity and dietary habits and other biological factors. The main aetiological factors should be identified prior to any treatment because if left unchecked, the success of any restorative work may be compromised (O'Sullivan and Milosevic, 2007).

Erosion

Of the three main tooth wear processes, erosion is considered to be the most common and important aetiological factor (Bartlett, 1997; Nunn, 2000). Erosion is chemical dissolution (complete mineral loss) of apatite crystals in enamel and dentine, due to the chemical action of acids, which are not produced by the oral flora (Ten Cate et al., 2008). This chemical dissolution is preceded by demineralisation, which is partial loss of mineral resulting in softening of the enamel and dentin, without bulk loss of tissue. The source of the acids may either be from extrinsic (dietary and environmental acids) or intrinsic (regurgitated stomach acid) sources.

The most common proposed source of extrinsic acid is from dietary sources, such as acidic drinks and foodstuffs. The extent of an erosive attack from a dietary erosive source is effected by the pH value, titratable acidity, calcium, phosphate and fluoride content of the acidic drink or foodstuff (Lussi and Jaeggi, 2006). However, this relationship between the intake of dietary acids (which have erosive potential) and dental erosion (as observed clinically) is not as clear as often suggested. In a pair of studies, Millward et al (1994; 1997) investigated firstly, the relationship between erosion and dietary constituents in a group of children and secondly, the salivary flow rate and pH at the tooth surface of individuals consuming an acidic beverage (1 % w/v citric acid solution). The results from the former study could not establish a direct causal

link between an increased consumption of acidic beverages and an increased severity of erosive wear. The latter study revealed that after the acid intake, the pH on the tooth surface was below pH 5.5 for a shorter time period than expected. These studies highlight that the erosive effect of dietary acids is modified by intra-oral biological factors, such the role of the salivary pellicle and the effect of salivary neutralisation and oral clearance. Carbonated beverages, fruit juices, smoothies and some alcoholic drinks have an erosive potential, whether or not that translates into erosion is difficult to predict with any degree of certainty (Hara et al., 2006b). There is therefore, no clear-cut critical pH for erosion (in contrast to caries). Even a low pH acid attack may not cause erosion, if the chemical and biological factors mentioned above are strong enough to prevent an erosive lesion developing *in vivo* (Lussi and Jaeggi, 2006).

Intrinsic erosion results from the regurgitation of gastric contents, of which hydrochloric acid is a major component. Pure gastric juice has been shown to have a mean pH of 2.92 and mean titratable acidity 0.68 ml and therefore gastric contents have erosive potential (Bartlett and Coward, 2001). Gastro-oesophageal reflux disease (GORD) has been shown to be associated with dental erosion in case reports and observational studies (Bartlett et al., 1996a; Bartlett et al., 1996b; Meurman et al., 1994). GORD is a common condition affecting up to 65 % of adults in the western world (Jones and Lydeard, 1989), however as it is often asymptomatic patients may be unaware that they are affected (O'Sullivan and Milosevic, 2007). Repeated vomiting in conditions such as anorexia nervosa, bulimia nervosa and cyclic vomiting syndrome has also been associated with dental erosion (Milosevic and Slade, 1989). The practice of regurgitating the stomach contents into the mouth to be later re-swallowed (rumination) has been reported and this is also associated with dental erosion (Gilmour and Beckett, 1993).

Increased alcohol consumption increases the exposure of teeth to extrinsic acids and also promotes gastric reflux (Bartlett, 1995). Therefore increased alcohol intake can result in erosion from both an intrinsic and an extrinsic source (Robb and Smith, 1990). Food stuffs

which have erosive potential include citrus fruits, pickled foods and foods prepared with or containing vinegar (Milosevic et al., 2004). Many medications are formulated using acidic preparations which therefore have erosive potential, and case reports have proposed vitamin C preparations as a potential contributing cause of erosion (Giunta, 1983). Lifestyle factors such as the use of recreational drugs, occupational factors such as acid fumes in battery factories and other lifestyle factors such as frequent swimming in low pH gas-chlorinated pools have also been cited as potential sources of extrinsic erosion (Centerwall et al., 1986; Milosevic et al., 1997b; Milosevic et al., 1999; Petersen and Gormsen, 1991).

The relevance of modifying factors such as impaired salivary characteristics (flow rate, buffering capacity etc), acquired pellicle composition, dental anatomy and occlusion, physiological soft tissue movements and soft tissue position and finally the nature of the hard tissue substrate have all been shown to influence dental erosion (Hara et al., 2006b).

Attrition

Attrition is the physical wear of dental hard tissues through tooth to tooth contact. In normal function teeth will only be in contact for a small amount of time and therefore tooth-to-tooth contact that occurs when not eating or swallowing is termed parafunction or bruxism. The cause of bruxism is not entirely understood, however, it may be a form of stress relief overnight (Bartlett and Smith, 2000). This can result in tooth contact at much higher loads causing particles of enamel to detach and converting the two body wear into a three body wear process as the particles create an abrasive slurry (Xhonga, 1977).

The role of attrition in tooth wear has been relatively under-investigated, with most tooth wear research preferentially focusing on the role of erosion in tooth wear. This has perhaps contributed to the recent contention that *"The scientific evidence of the use of occlusal concepts and the knowledge regarding the role of occlusal factors in the management of tooth wear is fragmented and ambiguous, as is the relationship between management of tooth wear and dysfunction"* (Van't Spijker et al., 2007).

Abrasion

The most commonly cited cause for abrasion in Western populations is tooth brushing (Addy and Hunter, 2003). The main factors regarding the development of abrasion are the frequency, duration and force of brushing and the relative dentine abrasivity of the toothpaste. It has however, been shown that when using a standard toothpaste with normal tooth brushing duration and force the amount of wear is negligible (Addy and Hunter, 2003). Once an acid induced softening occurs then erosion and abrasion have been shown to act synergistically (Attin et al., 2004; Jaeggi and Lussi, 1999).

Abfraction

The theory of abfraction was proposed to explain wedge shaped cervical cavities; however the evidence to support this as an important contributing factor in tooth wear remains unclear (Bartlett and Shah, 2006; Litonjua et al., 2003).

1.1.2 Clinical features

Early signs of erosive tooth wear include cupped out lesions on the occlusal surfaces of molars and translucency of the incisal edges of upper incisors as the enamel or dentine wears thin. Later, erosion of enamel and dentine may result in restorations appearing proud of the tooth surface and symptoms of sensitivity may result (Smith, 1991). Attritional wear presents itself as flattening of inter-digitating cusp tips with wear facets seen in both arches as the occlusal aspects of the teeth contact in static and dynamic occlusions (Smith, 1991). Abrasion manifests itself on the buccal-cervical areas as rounded, wide lesions usually on the incisors, canines and premolars (Smith, 1991).

Figure 1 below shows Intra-oral clinical photographs of a 36 year old male patient with severe tooth wear the aetiology of which included intrinsic erosion (from gastro-oesophageal reflux and vomiting) and attrition.

Figure 1 Intra-oral clinical photographs of a 36 year old male patient with severe tooth wear



1.1.3 Management

Sensitive investigation to identify the sources of acid, either from intrinsic or extrinsic sources should be followed by provision of tailored, specific advice for each individual patient. Preventative measures should involve patient education; dietary analysis and advice, modifying behavioural and oral hygiene factors and reducing oral exposure to intrinsic and extrinsic sources of acid. Patients should be made aware of habits which exacerbate the effects of erosion such as brushing after acid intake or after vomiting; acid intakes last thing at night and retaining acid drinks in mouth before swallowing; and patients should be encouraged and supported to stop these habits. Suspected vomiting or signs or symptoms of GORD should be managed by liaising with the patient's general medical practitioner or a gastroenterologist.

Although fluoride products are often recommended for patients with tooth wear, the evidence to support their use is currently lacking (DoH/BASCD, 2009). Resin-based adhesives have also been recommended, however use of such adhesives may only result in short term protection against erosive wear (Sundaram et al., 2004). Interventional restorative dental treatment is only indicated if the patient has functional or aesthetic concerns and should be as minimally destructive as possible using adhesive techniques such as direct composite restorations (O'Sullivan and Milosevic, 2007) or resin-bonded metal alloys (Chana et al., 2000). Finally conventional indirect restorative procedures, such as full coverage metal, metal-ceramic or all ceramic crowns should be considered as the treatment of last resort.

1.2. Fluoride and tooth wear

Fluoride is a chemical compound containing the element fluorine in combination with another element. Fluorine is the most reactive non-metallic chemical element and is represented by the symbol F in the periodic table, with atomic number 9 and atomic weight: $18.9984 \text{ g}\cdot\text{mol}^{-1}$. In its elemental state fluorine is a pale yellow-green, corrosive, toxic gas; however due to its

reactivity, fluorine in the environment is most commonly found combined with other elements as a mineral, especially as fluorite, cryolite and phosphate rock (Curzon and Cutress, 1983).

The dental profession has had an intimate relationship with the element fluorine since the early inception of dental research as a scientific discipline. This began in 1908, when the mine chemist F. S. McKay suggested, at a meeting of the El Paso Texas Dental Society, that the caries-resistance of mottled teeth may be related to an element in the drinking water. Subsequently, fluorine was observed to become incorporated as a trace element into the apatite of enamel and dentine, thus influencing its chemical, crystallographic and biologic characteristics (Curzon and Cutress, 1983) and over the intervening century. Fluoride has become ubiquitously utilised in dentistry for its caries-properties, both as systemically ingested and as topically applied delivery systems.

Current scientific evidence regarding the optimal pharmacokinetics for effective anti-caries mechanism of fluorides considers the low concentrations of fluoride present in solution in the immediate oral environment as being more important than the incorporation of high levels (100 – 1000 ppm F) into the apatite of enamel and dentine during tooth formation (ten Cate and Duijsters, 1983a; b). Accordingly, based upon this knowledge and the observation from section 1.1 above, that tooth wear is effectively a surface phenomena, this thesis will only explore the role of topical fluorides in the prevention and management of tooth wear. Therefore, no further consideration in this thesis will be given to the role of systemically applied fluorides.

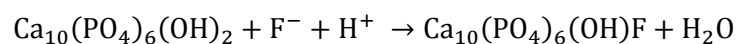
1.2.1. Fluoride and the oral environment

Effects on enamel

When topical fluoride is present in the oral environment surrounding teeth (i.e. in saliva, plaque, crevicular fluid, oral soft tissues and directly on the enamel/dentine surface itself), there are two distinct post-eruptive effects on enamel. Low concentrations of ionic fluoride interact with enamel during the process of demineralisation to either modify the chemical and

biologic characteristics of enamel apatite by forming fluorhydroxyapatite or calcium fluoride. The former is more likely to occur when the fluoride concentration is less than around 50 ppm and the environment is acidic. Formation of fluorhydroxyapatite occurs only in the outermost layers of enamel and forms an integral part of the tissue that will be lost if the tissue is worn away.

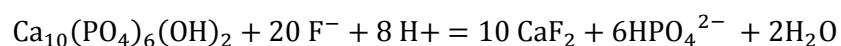
Equation 1 Formation of fluorhydroxyapatite from hydroxyapatite in the presence of ionic fluoride



Under neutral conditions this is a slow process, however in a low pH solution the solubility of enamel increases considerably and fluorhydroxyapatite formation increases under such conditions. Ionic fluoride promotes conversion of brushite and octacalcium phosphate to apatite and promoting formation of fluorhydroxyapatite, in preference to brushite or β -tricalcium phosphate in acidic conditions (Ten Cate et al., 2008).

At higher fluoride concentrations (>100 ppm) calcium fluoride is formed thus:

Equation 2 Formation of calcium fluoride from hydroxyapatite in the presence of ionic fluoride



Therefore the higher the concentration of fluoride and the more acidic the solution the more calcium fluoride is formed on the tooth surface. In the oral environment, calcium fluoride is also precipitated in plaque, in pellicle, in porosities and other plaque retention factors. Calcium fluoride is formed in the shape of spherical globules scattered across the tooth surface which can be seen using scanning electron microscopy as a round globule with a nodular surface around 0.6 μm in diameter (Petzold, 2000). Formation of calcium fluoride globules is the only surface event that is detectable using chemical means after application of high fluoride

concentrations. Subsequently, after the calcium fluoride is worn away and all chemical traces have disappeared, a reduced caries incidence in the following months is noted (ten Cate and Featherstone, 1996).

Effects on dentine

On a physicochemical level, the fluoride interactions for dentine are the same as for enamel, however the fluoride levels that are required to inhibit demineralisation in dentine are 10 times those required in enamel (ten Cate and Duijsters, 1983a; b; Ten Cate, 1997). Possible reasons for this have been explored by researchers investigating root caries remineralisation, who proposed that the high organic content of dentine (in comparison to enamel) complicates the role of fluoride in remineralising dentine after demineralisation, perhaps due to the presence of non-collagenous proteins such as phosphoproteins, which have been shown to block the remineralisation of dentine (Fejerskov and Clarkson, 1996).

Fluoride concentration in teeth

Mineralised tissues are able to retain fluoride because apatite can bind fluoride into its crystal lattice. According to the level of fluoride intake, the duration of fluoride exposure and other biological factors, the concentrations of fluoride in mineralized tissues varies, with studies showing that the fluoride concentration is greatest in surface regions i.e. the outer 100 µm of surface enamel and the dentine-pulp interface (those closest to the fluids that will be delivering the fluoride) (Robinson et al., 1996). Within the inner area of the enamel and dentine the fluoride concentration plateaus to reach a consistently relatively lower concentration of fluoride compared to these surface regions (Nakagaki et al., 1987). The fluoride concentration of dentine is slightly higher than non-surface enamel and the above described pattern of fluoride concentration is similar for the teeth of those living in non-fluoridated areas, albeit at a slightly lower level. This slight reduction in concentration of fluoride has been investigated in relation to caries incidence (Poulsen and Larsen, 1975) and tooth wear *in vitro* (Bartlett et al., 1994). Both studies found no relationship between fluoride

concentrations in enamel and either caries incidence or tooth wear severity, which further reinforces the topical mode of action of fluorides.

Fluoride metabolism and toxicity

As use of topical fluorides results in varying amounts of ingestion of fluoride and as both an acute intake of a large dose and a chronic intake of a lower dose results in a variety of side effects which include death, therefore a brief review of the metabolism and toxicity of fluoride is indicated here (Fomon and Ekstrand, 1996).

Ingested fluoride is absorbed by the gastrointestinal tract and in adults 50 % is excreted at the kidney. The other 50 % is distributed via the blood plasma almost entirely into mineralised tissues where a physiological balance is achieved determined by the rate of bone remodelling, amongst others (Ekstrand, 1996). The probably toxic dose (PTD: the amount that if ingested, should result in the individual receiving emergency treatment and hospitalisation) is 5 mg/ kg body weight (Whitford, 1996). Chronic ingestion of lower amounts of excess fluoride during tooth formation results in dose-related enamel hypomineralisation and increased enamel porosity due to mechanisms which are not fully understood (Aoba and Fejerskov, 2002). This appears clinically as an increase in enamel opacity resulting in a variety of changes ranging from fine white lines appearing along the striae of Retzius to widespread severely weakened chalky enamel which breaks down and is lost soon after eruption. Together these effects are known as dental fluorosis (Fejerskov et al., 2009).

The development of dental fluorosis following ingestion of fluoride products is only a risk during development of the dentition, which for the permanent maxillary central incisors occurs between the age of 15 and 30 months of age (Evans and Stamm, 1991). Calculations of fluoride ingestion and development of fluorosis have estimated that a 12 kg 2-year-old ingesting 1.2 mg fluoride/day would be at high risk of developing aesthetically compromising fluorosis i.e. 0.1 mg F per kg of body weight per day (Richards et al., 1986). This equates to a daily ingestion of 0.8 mg of 1500 ppm fluoride toothpaste; 1.2 mg of 1000 ppm toothpaste and 2.4 mg of 500

ppm toothpaste. However, these calculations are heavily dependent on factors such as: the amount of product used per day; age and weight of child; concentration of fluoride in the product and in other sources including the drinking water; per cent ingestion of used product and bioavailability of ingested fluoride according to varying stomach contents at the time of ingestion (Ellwood et al., 2008). In general, manufacturers of fluoride products therefore formulate lower concentrations of fluoride toothpastes for children and advise discouraging younger children from eating toothpastes, especially if using higher concentrations of fluoride toothpastes in areas of water fluoridation. In the United Kingdom, however, government guidelines recommend use of 1350-1500 ppm fluoride toothpaste for all ages; although smaller volumes are recommended (a 'smear' of toothpaste rather than a 'pea-sized' amount) for young children up to 3 years of age (DoH Delivering better oral health).

1.2.2. Physicochemical interactions between topical fluoride and enamel/dentine during tooth wear

Caries research has shown that following topical application of fluoride to the enamel/dentine surface, the only measureable chemical event in the subsequent months (apart from initial formation of calcium fluoride) is a reduction in caries incidence (ten Cate and Featherstone, 1996). This effect was first demonstrated by Dean et al (1950) in a series of seminal studies which found a 50 % reduction in caries incidence after water fluoridation, a finding which was later replicated and validated by other workers around the world (Murray et al., 1991). Over the intervening years, the cariostatic action of fluoride has become so widely accepted that it would now be considered unethical to conduct a caries related clinical trial with a non-fluoride control toothpaste.

However, the role of fluoride in erosion, attrition and abrasion of enamel and dentine remains controversial. Although some authors advocate that on a physicochemical level, fluoride may have the potential to modify the erosive process (Featherstone and Lussi, 2006), others see no

theoretical or practical possibility for fluorides to provide protection before, during or after the formation of an erosive *in vivo* lesion (Larsen and Richards, 2002; Ten Cate et al., 2008).

The view that there is no role for fluoride therapy in erosive tooth wear is twofold. Firstly the presence of calcium fluoride on smooth surfaces *in vivo* is too short-lived to be considered potentially effective against all but the mildest of erosive challenges. This is based on the high solubility of CaF_2 in acidic drinks, as demonstrated by an *in vitro* study in which 1 litre of Coca Cola® (pH 2.5) had the potential to remove all CaF_2 from up to 5000 teeth (Larsen, 2001). The second reason is due to the differing histology of the initial erosive lesion in contrast to the initial carious lesion. In short, caries begins as a 20-50 μm thick relatively-well mineralised surface layer with a more demineralised (30-50 % mineral loss) subsurface area extending deep into the tissue (Ten Cate et al., 2008). In contrast, it has traditionally been thought that erosion lesions demonstrate surface features of complete demineralisation which results in layer by layer dissolution of the dental hard tissues. Following removal of the demineralised surface layer by mechanical attritive or abrasive forces, it was then thought that the underlying newly exposed tissue showed no signs of demineralisation meaning that the mineral content is essentially unaltered. This would therefore mean therefore there is no role for fluoride interactions to modify or inhibit this process. Evidence for this histological description was backed by clinical observations: carious lesions appear chalky white and softened whereas erosion leaves the enamel looking hard and shiny. This view has been challenged by developments in qualitative and quantitative surface analysis techniques which have furthered knowledge of the complex surface effects that occur during early enamel and dentine erosion (Cheng et al., 2009). However, the relative clinical importance of the role of acid demineralisation on surface softening and bulk wear and, more importantly, the role of fluorides and other compounds to modify this process and promote subsequent remineralisation and repair of enamel and dentine during tooth wear remains to a large extent unclear.

Despite (or perhaps because of) these observations, there is a large body of research on-going into the role of fluoride compounds to modify the erosive process. Correspondingly, there is growing industry interest in the development of fluoride containing oral health care products, targeted at those suffering from erosive tooth wear. There is also substantial commercial interest in products with modified calcium and phosphate levels (Grenby, 1996; Jensdottir et al., 2007), albeit to a lesser extent than fluoride containing products. This has led to development of such a range of products, the formulation of which will be reviewed in more detail in Section 1.2.3 below. Varying fluoride compounds have been successfully incorporated, licensed and marketed into a variety of oral care products, some of which are specifically designed and marketed to have varying methods of action on enamel and dentine during tooth wear. Other fluoride compounds remain solely experimental, having never been incorporated into any products, for reasons of expense, toxicity or licensing issues.

The fluoride compounds with relevance to this thesis are inorganic salts such as sodium fluoride (NaF); calcium fluoride (CaF_2); stannous fluoride (SnF_2) and titanium tetrafluoride (TiF_4). These are water soluble compounds which thus have the potential to readily provide free fluoride on exposure to the oral environment. Whilst other fluoride compounds, such as monofluorophosphates (e.g. sodium monofluorophosphate [Na_2FPO_3] in which the fluoride is covalently bound as FPO_3^{2-} and requires hydrolysis to release the F^- (ten Cate and Featherstone, 1996)); and organic fluorides (e.g. amine fluoride: AmF) are of relevance to the wider context of fluorides and dental caries, they are not of direct relevance to this thesis and therefore will not be considered hereafter.

Considering these differing classifications, NaF can be delivered either as a pH neutral toothpaste at low concentrations, in order to be self-applied and thus, on contact with the oral environment, immediately provide free fluoride; or NaF can be delivered as an acidulated varnish at high concentrations, in order to be professionally-applied to susceptible sites and thus promote the surface precipitation of a CaF_2 rich store, which will subsequently release

available fluoride over an extended period of time. Both methods will result in the presence of free fluoride to effectively modify the demineralisation and remineralisation seen during caries, however the relative advantages and disadvantages of each mode of action in erosive tooth wear remains to be comprehensively elucidated.

Any potential role for use of SnF_2 in the prevention and management of tooth wear, is much less clearly understood. SnF_2 has been formulated as a topical fluoride agent, mainly for use as a self-applied product in toothpastes and mouthrinses. At low concentrations SnF_2 provides fluoride ions (which have the same mechanism of action as described above) and stannous ions (which have an antibacterial and therefore an anti-caries and anti-gingivitis effect). The antibacterial effect of the SnF_2 is thought to be due to the rapid uptake of Sn by *S. mutans* (Attramadal and Svaton, 1980) and by Sn^{2+} mediated inhibition of *S. mutans* growth and metabolism (Camosci and Tinanoff, 1984). At higher concentrations, tin containing stannous phosphate fluoride precipitates are formed, resulting in tin-rich layers on and in the enamel surface, which are also thought to contain CaF_2 (Wei and Forbes, 1974), which has the same mechanism of action as described above.

TiF_4 is unique in comparison with conventional fluoride compounds in that an acid resistant coating (ARC) is formed on the enamel/dentine surface after topical application (Shrestha, 1983). This coating has been described as a soft but stable hydrophobic structure and has been shown to be more effective at reducing enamel dissolution from erosion than conventional topical fluoride compounds (Buyukyilmaz et al., 1997; Hove et al., 2006; Hove et al., 2007b; Hove et al., 2008; Mundorff et al., 1972; Tveit et al., 1983; Tveit et al., 1988; Vieira et al., 2005; Wei et al., 1976). Various possible mechanisms by which the TiF_4 solution may reduce demineralisation during erosion have been proposed. These include the formation of TiO_2 by complex binding to phosphate bound oxygen in the outer enamel layer and another possibility is that HF (hydrofluoric acid), formed in the acidic TiF_4 solution, may promote a deeper penetration of the F^- than native pH solutions and thus enhance the formation of CaF_2

on the surface (Wiegand et al., 2009). Therefore, both Ti and F appear to act synergistically to produce acid-resistant enamel, with the roles of Ti thought to be secondary to the role of the F (Shrestha, 1983). However, despite the ability of this ARC to reduce enamel erosion, the potential role for use of TiF_4 in the prevention and management of multifactorial tooth wear, is much less uncertain.

1.2.3. Fluoride products

Fluorides products for topical application in tooth wear may be formulated as pH neutral or acidulated products. Fluoride-containing calcium-phosphates have been shown to precipitate from oral fluids at a neutral pH (ten Cate and Featherstone, 1996) and on first principles, neutral or alkaline products may seem preferable in an acid mediated condition such as erosive tooth wear. However, as shown in Equation 1 and Equation 2 above, formation of calcium fluoride and fluorhydroxyapatite in the presence of ionic fluoride, is greatly enhanced by an acidic environment. Therefore acidulated fluoride toothpastes, rinses, gels and varnishes at concentrations ranging from 225 ppm to 19500 ppm may have a potential role in tooth wear (Horowitz and Ismail, 1996).

Another way of classifying topical fluorides for use in tooth wear is by their intended mode of application. Therefore the role of self-applied products such as fluoride toothpastes, fluoride gels and fluoride rinses in the prevention and management of tooth wear will be reviewed below and the role of professionally-applied products such as gels and varnishes will be reviewed below.

In solutions used for *in vitro* tooth wear studies, ionic fluoride levels are measured by a fluoride ion specific electrode, developed by Frant and Ross (1966). The fluoride electrode responds to free fluoride ions and requires for the test solution to be maintained between pH 5 and pH 6 and for the ionic strength and composition to be the same in both sample and standard solutions. Therefore the measurement of fluoride requires the addition of a total strength ionic buffer (TISAB) prior to measurement (Venkateswarlu and Vogel, 1996). The

amount of fluoride in products can be difficult to ascertain because the percentage by weight (wt %) of the active ingredient, as opposed to the parts per million (ppm), is often provided by the manufacturer. This is potentially confusing because the weight of varying fluoride species is clearly different for different fluoride species, as shown in Table 1 below. Consequently, many manufacturers currently provide labelling in ppm fluoride in order to provide more meaningful information on the clinical effectiveness of the product.

Table 1 Percentage by weight (wt %) and the equivalent parts per million (ppm) fluoride of sodium fluoride and sodium monofluorophosphate in toothpastes (Adapted from Ellwood et al 2008)

Fluoride (ppm)	Sodium fluoride (wt %)	Sodium monofluorophosphate (wt %)
1500	0.32	1.14
1000	0.22	0.76
500	0.11	0.38

Self-applied products

In general, the self-applied products supply relatively low concentrations of fluoride (from approximately 250 ppm for a low concentration rinse up to 5000 ppm for a high concentration toothpaste) on a regular basis. This has the effect of elevating the fluoride concentration in the oral fluids, soft tissues and plaque for periods of minutes to hours. Therefore these products deliver fluoride to the immediate enamel/dentine environment of the substrate at the time of demineralisation and remineralisation.

Fluoride toothpastes

Toothpastes are used as an integral part of the daily hygiene regime by many people worldwide, mainly for cosmetic motivations related to cleanliness, removal of stains, whiteness and avoidance of oral malodour (Nyvad, 2008). As such, toothpastes formulated with fluoride are by far the most widely used method of applying fluoride. It is, however, interesting to note that toothpaste containing fluoride up to 1500 ppm is classified as a cosmetic rather than a pharmaceutical product by many government regulatory agencies worldwide, for example in most European countries by the European Cosmetics Directive.

Manufacturers have three main aims when formulating toothpastes (Scheie and Peterson, 2008):

1. To remove stains from teeth
2. To provide a feeling of freshness and cleanliness of the oral cavity
3. To serve as a vehicle for delivery of active components such as fluorides or antimicrobial agents.

Apart from active components toothpastes contain the following ingredients (Scheie and Peterson, 2008):

1. An abrasive for stain removal
2. A component to carry the abrasive and active agents
3. A surfactant for foam and detergent action
4. A binder for desirable rheology
5. Flavour to make tooth brushing taste pleasant.

However, formulation of active and non-active components can result in interactions which inactivate or reduce the bioavailability of incorporated fluorides, thereby negating any potential for anti-caries or anti-erosion effects. For this reason the use of chalk-based abrasives, which inactivate free fluoride by forming insoluble calcium fluoride have been replaced in modern toothpaste formulation with silica-based abrasives.

Despite the first toothpaste approved for marketing in the USA in 1955 containing 0.4 % stannous fluoride, currently sodium fluoride and sodium monofluorophosphate are the two most popular fluoride species incorporated into toothpastes. These two species are believed to have comparable anti-caries efficacy (Bowen, 1995). Stannous fluoride and amine fluoride toothpastes are also available in some parts of the world (Mühlemann et al., 1957) however since the 1960's few clinical trials have been conducted into the anti-caries efficacy of stannous fluorides toothpastes in comparison to sodium fluoride and sodium

monofluorophosphate (Clarkson et al., 1993). There has been growing interest into the potential anti-erosion effects of stannous fluoride in recent years with a recent *in situ* study finding a reduction of enamel loss from a stannous based sodium fluoride toothpaste, in comparison to a sodium fluoride toothpaste (West et al., 2011).

Toothpastes specifically marketed for dental erosion contain similar levels of fluoride than other toothpastes however the formulation has been modified to increase the availability of free fluoride, to reduce the abrasivity and to also supply a desensitising agent to reduce hypersensitivity (Layer, 2009).

Toothpastes containing more than 1500 ppm fluoride are available as prescription only medications for high caries risk individuals who are of an age where fluorosis is no longer a possibility. In the UK 2800 ppm sodium fluoride toothpaste is available for those aged 10 and over and 5000 ppm sodium fluoride for those aged 16 and over. These high fluoride toothpastes have been shown to have greater anti-caries efficacy clinical trials however the ability of an increased concentration to provide confer greater protection against erosion has only began to be demonstrated *in vitro* studies (Joziak et al., 2011).

Fluoride gels

A gel is a thickened aqueous solution which does not contain abrasive or foaming agents. Gels have the advantage of being compatible with a wide range of active ingredients such as antimicrobial agents and fluorides, including as acidulated formulations (Scheie and Peterson, 2008). Gels also allow formulations of range of appearances and colours that appeal to the consumer. Fluoride gels are thought to be as effective as solution counterparts and many fluoride gels are now being specifically marketed as anti-erosion products (Ivoclar-Vivadent, 2010).

Fluoride rinses

Mouthrinses are usually a mixture of the active component in water and alcohol with the addition of a surfactant and a flavour. Fluoride rinses are most often formulated with 0.05 %

sodium fluoride (227 ppm) for daily rinsing and 0.2 % sodium fluoride (909 ppm) for weekly rinsing (Ellwood et al., 2008). Use of both daily and weekly rinses has been shown to achieve an average caries reduction of around 30 % (Ripa, 1991).

Manufacturers of fluoride rinses have recently formulated sodium fluoride rinses specifically for use against dental erosion, with fluoride concentrations increased to 450 ppm and these rinses have been evaluated *in vitro* (Venasakulchai et al., 2009) and *in situ* (Maggio et al., 2010). However, apart from these initial investigations the only clinical study to find an anti-erosion effect is an observational study which found a reduced prevalence of erosion amongst children using a fluoride rinse (Pieterse et al., 2006).

Professionally-applied products

In general, these products can deliver relatively high fluoride concentrations in comparison to self-applied products. Professionally-applied products are targeted to deliver fluoride susceptible sites (and individuals), usually at a minimum of three monthly periods, and thus promote the surface precipitation of a CaF₂ rich store of fluoride, which will subsequently release available fluoride over an extended period of time.

Fluoride gels

Fluoride gels, foams and solutions for professional application in the dental surgery are formulated with fluoride concentrations of 5000 – 12 3000 ppm fluoride (Øgaard et al., 1994). Either stock or custom trays hold the gel and allow close contact of the gel to the tooth for a prolonged period of time under supervision of a dental professional. These techniques have been shown to reduce caries incidence (Ripa, 1991), however as of yet there has been little research into the effect of professionally applied gels on tooth wear.

Fluoride varnishes

Fluoride varnishes have been used by dental professionals for over 30 years in order to deliver high levels of fluoride to specific sites within the mouth that are at risk of caries. Varnishes are formulated to adhere to the tooth surface and harden to aid retention and slow release of

fluoride over time. Studies into fluoride release overtime have shown that varnishes released fluoride for five to six months (Castillo et al., 2001). One of the most widely researched varnishes contains 2.26 % sodium fluoride (22 600 ppm) in an alcoholic solution of natural resins which sets on contact with water. Meta-analysis of clinical trials of with this varnish have shown a 38 % reduction in caries incidence (Helfenstein and Steiner, 1994). Although this product was initially marketed and formulated against caries, more recently the following sentence has been added under Section of pharmacodynamic properties of the product on the UK based Colgate website: *'In the management of dental erosion associated with the frequent consumption of acidic beverages or gastric reflux, high concentration topical fluoride agents are considered to be of value. Duraphat® is at least as effective as 2 % sodium fluoride solution in inhibiting erosion in vitro.'* however the product is not specifically licensed to be marketed for this use and treatment of dental erosion is not stated as an indication of use, which perhaps reflects the lack of evidence of clinical effectiveness of fluoride varnishes against tooth wear.

1.3. Tooth wear measurement

A wide range of tooth wear measurement techniques have been used *in vivo* and *in vitro*. These include visual examination of macroscopic changes of teeth (either intra-orally or using dental casts) with and without the adjunctive use of clinical indices; surface topography measurement (profilometry, interferometry, projected surface topography measurement); scanning electron microscopy, polarized light microscopy, microradiography, digital image analysis, quantitative light fluorescence, chemical techniques (iodide permeability, calcium and phosphorous dissolution, energy dispersive x-ray spectroscopy) and surface hardness (microhardness and nanoindentation) (West and Jandt, 2000). However, the main techniques with relevance to this thesis are surface topography measurement, surface microhardness and scanning electron microscopy and therefore the use of these and relevant related techniques will be reviewed below.

1.3.1. Direct visual measurement, dental casts and indices

Direct visual measurement is the most commonly used method for clinically measuring tooth wear. Although being quick, easy and without expense, it is thought to be highly subjective, with potential for large inter- and intra- operator variability (Rodriguez et al., 2011). A clinician who relies upon visual assessment alone when monitoring the progression of tooth wear in an individual with a worn dentition will be relying on visual recall of the condition of the dentition from the last recall period, which may be six months ago.

Sequential construction of gypsum dental casts may be used to supplement visual comparison to assessment progression of tooth wear. Comparison between sequential models is recommended at a minimum of 6 monthly intervals and the assessment may be made either with or without the use of indices (O'Sullivan and Milosevic, 2007). Azzopardi et al (2000b) highlighted the potential for poor sensitivity of this method due to the relatively subtle surface changes that occur in all but the most aggressive forms of tooth wear. Therefore, solely basing the clinical judgement that an individual's tooth wear is active/inactive on visual assessment remains highly subjective, as slight levels of tooth wear progression are difficult to detect with the naked eye. If progression can be detected, this suggests that the tooth wear is rapidly progressing, at a rate which would compromise the longevity of teeth (Azzopardi et al., 2000b) and therefore it is difficult to monitor progression reliably without more discriminating tools.

An index is a rating scale i.e. a set of numbers derived from a series of observations of specified variables (Last, 2000). Tooth wear indices record an aspect of tooth wear at a given moment in time. A multitude of indices have been devised and their evolution and development has been reviewed (Bardsley, 2008). Each index differs in its intended use (e.g. epidemiological prevalence studies, clinical staging and monitoring, other research purposes) making comparison between studies difficult without a universally accepted, validated, 'gold standard' index (Berg-Beckhoff et al., 2008). Review of the literature from 2000 - current

shows that in adults the Smith and Knight tooth wear index (Smith and Knight, 1984a) is that most commonly used, followed by the Eccles index (Eccles, 1979) and Lussi index (Lussi, 2002).

The Smith and Knight Tooth Wear Index (Smith and Knight, 1984a) does not differentiate between different aetiologies of tooth wear. The index scores four surfaces per tooth (cervical/buccal/incisal/occlusal and lingual) and uses five possible grades based upon observation of severity of tooth wear with a threshold set for dentine exposure. Uniquely the index defined acceptable and non-acceptable levels of tooth wear based upon age defined limits and consideration of expected tooth survival based upon predicted wear rates which inevitably involved an element of judgement. Validation and improvements of indices continue following recommended quality criteria for index development (Berg-Beckhoff et al., 2008).

In summary therefore, tooth wear indices have practical advantages over alternative measurement techniques, such as profilometry, which is time-consuming and costly. In order to achieve good inter- and intra-examiner reliability, good calibration of examiners is required and direct scoring of indices from subjects is advised as measurement of wear from dental casts is limited by loss of detail in tooth colour and texture.

1.3.2. Surface topography and texture measurement

A surface is 'the outermost part of a material body, considered with respect to its form, texture, or extent' (Oxford English Dictionary, November 2010). ISO 4287 (1997) differentiates between a real surface as the "surface limiting the body and separating it from the surrounding medium" and the measured surface as the "profile that results from the intersection of the real surface by a specified plane". This definition differentiates between the real surface as perceived with the human senses of touch and sight and the results from a surface topography and texture measuring instrument. The earliest method for assessment of surface profile and finish was by simply running a fingernail across the surface of the object, a technique which remains useful today in industrial manufacturing for tactile comparison of the surface texture of machined and finished products. Following this early tactile comparison, in

the 1930's, the aerospace industry required accurate comparison of the surfaces of finely finished bearing surfaces of aircraft engine parts which led to the development of stylus profilometers (Leach, 2010a). Subsequently, a wide variety of instrumentation for 2D and 3D surface topography measurement has been developed. A Classification of surface topography measurement techniques is illustrated in Figure 2 below. This figure shows the complete spectrum of techniques available and the main surface topography measurement technique that will be used in this thesis operates using the confocal method of focus detection. As shown highlighted in yellow in Figure 2 below, the confocal method of focus detection is classified as a non-contacting optical surface measurement technique.

Figure 2 Classification of surface topography measurement techniques. [Adapted from (Blunt, 2008)].



STM: Scanning Tunnelling Microscopy; AFM: Atomic Force Microscopy; LFM: Lateral Force Microscopy; MFM, Magnetic Force Microscopy; NSOM, Near-field Scanning Optical Microscopy

Since its inception, the use of profilometry has been widely adopted into for tooth wear research, including for *in vivo* tooth wear measurements (Bartlett et al., 1997a; Pintado et al.,

1997; Sundaram et al., 2007a). Stylus profilometry was the first surface measurement technique to be applied to tooth wear research and the technique is still widely used in tooth wear research to date. However, the relevance of stylus profilometry to *in vivo* tooth wear research will only be described briefly on page 50 below, as the technique has not been used in this thesis. Scanning Probe Microscopes operate on near-field optical principles by using a physical probe that scans the sample, following which an image of the surface is obtained recording the probe-surface interaction as a function of position. The use of atomic force microscopy for tooth wear surface measurement research will be briefly reviewed on page 58 below and also in relation to nano-indentation on page 64 below.

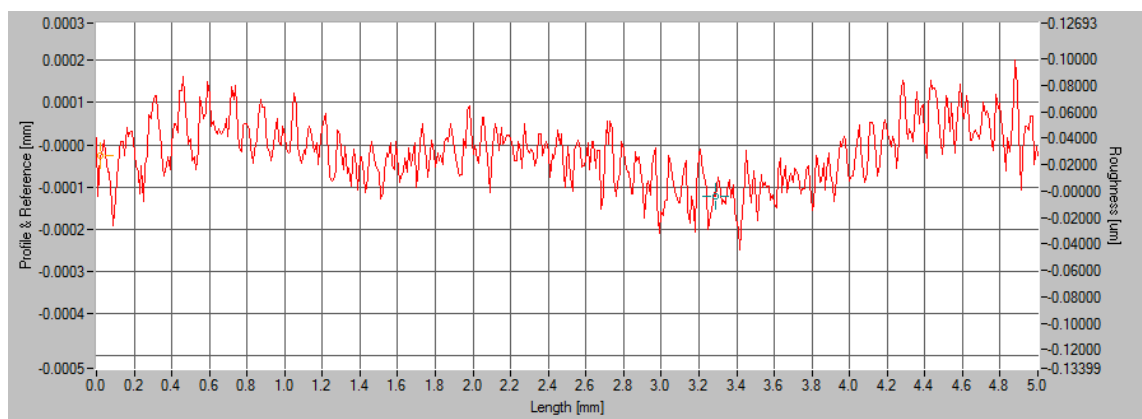
Non-contacting 'optical' instruments dominate in tooth wear research where 3D 'areal' measurements are required. The confocal method of focus detection has been widely used throughout this thesis and therefore the application of optical instruments to tooth wear research will be described in more detail below with the confocal measurement system specific to this thesis being described in Section 2.1.2 below.

Surface topography measurement and characterisation is an indispensable element of all precision engineering industries, for the simple reason that 90 % of all engineering component failures are surface initiated through mechanisms which are described within the discipline of tribology (wear, lubrication and friction) (Blunt, 2008). In engineering industries, surface measurement is used firstly in quality control, diagnosis and monitoring during the manufacturing process and secondly in analysis and prediction of function of the manufactured workpiece. In dental research, this knowledge is transferred and adapted for various purposes including examining the biofunctionality of dental hard tissues (Stout and Blunt, 1995); to allow comparisons of surface texture (Field et al., 2010) and bulk tissue loss of enamel and dentine from tooth wear (Bartlett et al., 1997a).

Surface topography measurement is differentiated into surface form and surface texture. Surface form relates to the overall surface geometry of an object and surface texture is what is

left when the overall form has been removed, leaving three elements profile; waviness and roughness (ISO 4287, 1997). Surface profile measurement is defined as the measurement of a line over the surface of an object, that can be represented mathematically in two dimensions as a height function (z axis) with lateral displacement (x or y axes) (Leach, 2010a). Figure 3 shows an example of the result of a profile measurement with the z axis height (mm) appearing on the left vertical axis and the x axis length (mm) appearing on the horizontal axis.

Figure 3 Example of a single profile measurement taken from a 5 mm x 3 mm ‘areal’ measurement of an optical flat

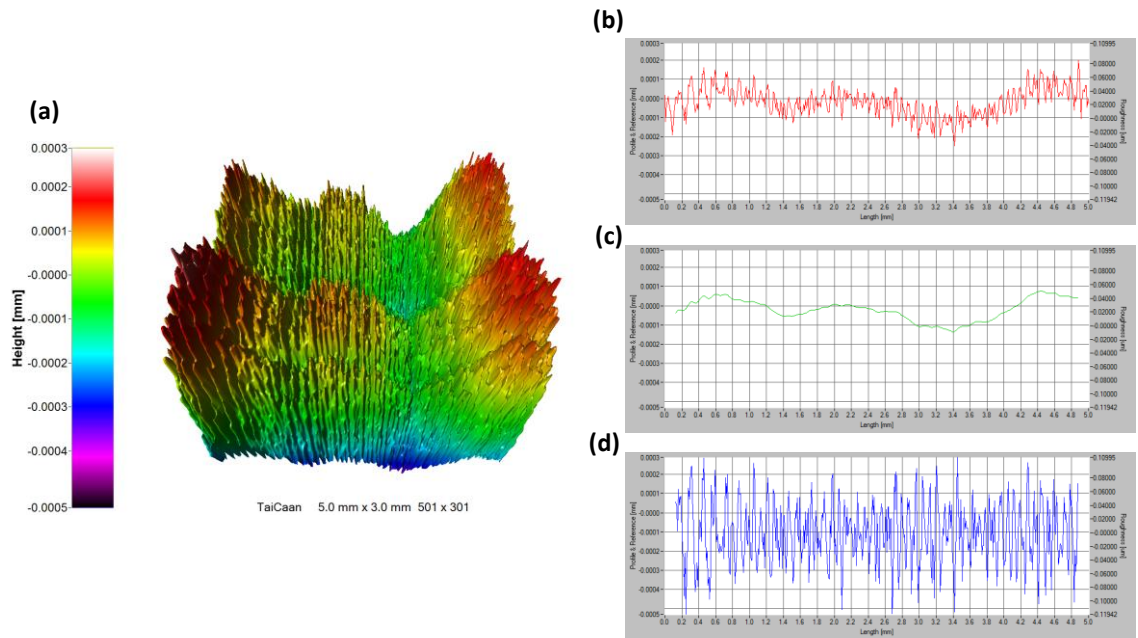


This single 2D surface profile provides some limited information about the surface being investigated. In order to obtain a more complete representation of the whole surface of an object, a three-dimensional or ‘areal’ measurement is required. For this, a profilometer is used to scan the stylus or light beam across the surface of the object line by line in a raster pattern. This creates a set of multiple parallel profile measurements which are then juxtaposed using the software to produce a 3D topographic image of the overall object surface in z, x and y axes (Suga, 2007).

The overall form of a surface is removed by filtering, which is a means for selecting for analysis a range of structure in the total profile which is judged to be of significance to that particular situation (Leach, 13th August 2008). A low-pass filter is applied to remove form or set up errors and thereby create the surface profile; a band-pass filter is applied to create the surface waviness and finally a high pass filter is applied to reduce noise thereby creating the surface

roughness. Figure 4 shows a schematic illustrating the relationship between (a) the overall surface geometry and (b) the profile, (c) the waviness and (d) the roughness of a surface.

Figure 4 Schematic illustrating the relationship between (a) the overall surface geometry and (b) the profile, (c) the waviness and (d) the roughness of a surface.



Contacting stylus profilometry

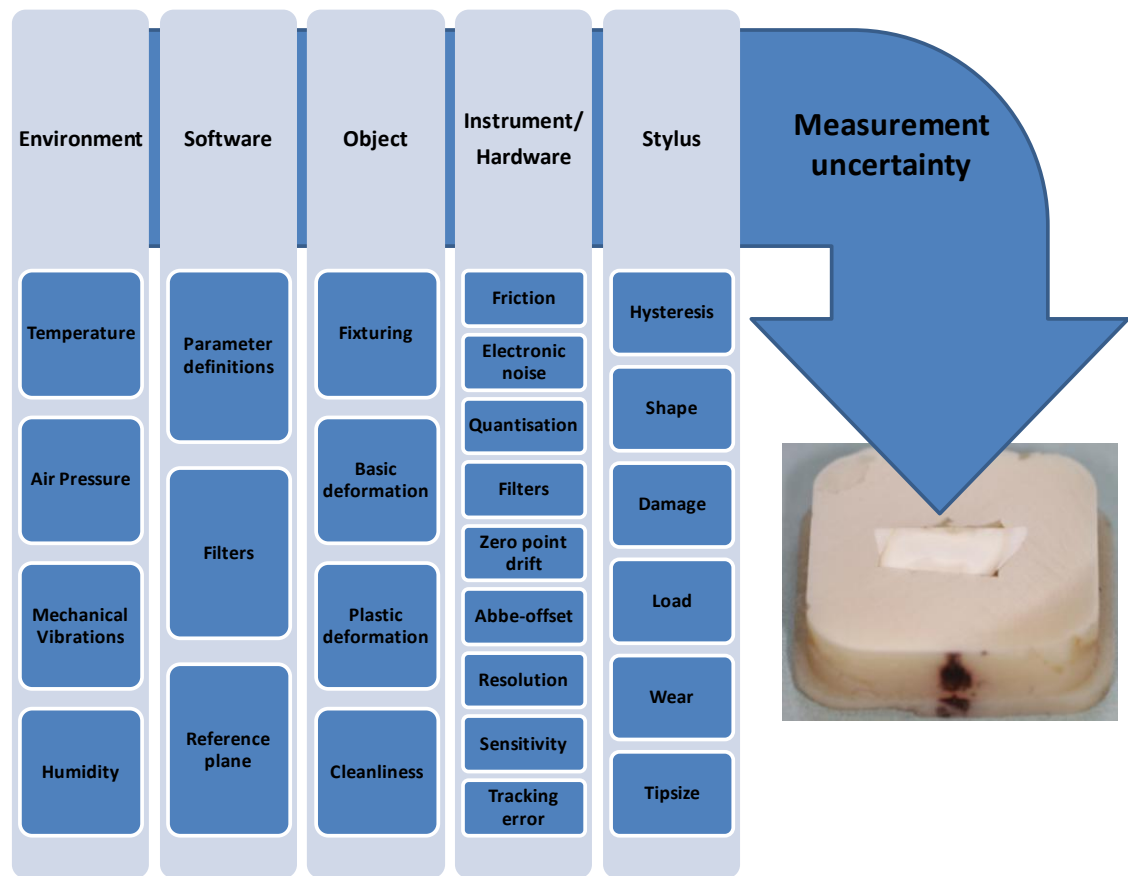
Stylus profilometers typically consist of a stylus that physically contacts the surface being measured and a transducer to convert its vertical movement into an electrical signal. For a complete reference regarding the specifications of contact (stylus) instruments the reader is referred to the ISO publication “*Geometrical product specifications (GPS) Surface texture: Profile method–Nominal characteristics of contact (stylus) instruments*” (ISO 3274 1996), however the characteristics of stylus instrument which have relevance to tooth wear measurements will be considered briefly in this Section.

A potential disadvantage of stylus profilometry is that the demineralised surface layer of eroded enamel is very fragile to mechanical forces and therefore the effect of the stylus force could have significant influence on the measurement results, with too high a measurement force resulting in damage to the demineralised enamel surface (Attin, 2006). ISO 3274 (1996)

states that the stylus force should be 0.75 mN however this force is rarely checked and can vary from the value given by the instrument manufacturer (Leach, 2010a).

There are many potential sources of measurement error from contacting surface topography measurement techniques (surface profilers) (Figure 5). These are derived from environmental factors such as temperature, air pressure, mechanical vibrations and humidity; software factors such as parameter definitions, filters and reference plane; object factors such as fixturing, relocation, basic deformation, plastic deformation, cleanliness; instrument/hardware factors such as friction, electronic noise, quantisation, filters, zero-point drift, Abbe-offset, resolution, sensitivity, and tracking error and finally stylus errors such as hysteresis, shape, damage, load, wear and tipsize (Leach, 2008). The dimensions and geometry of the stylus will affect lateral resolution because a tip with a given radius will be unable to record information of a concave surface feature with a smaller radius than the stylus tip (DeVries and Li, 1985; McCool, 1984; O'Donnell, 1993). Generally the radii of the diamond tip in commercial profilometers ranges from 2 μm to 10 μm , however the styli diameter can vary (Stachowiak et al., 2004) and styli tips of varying geometry have been developed for specialist applications such as for determination of tribological characteristics such as friction, rheology and wear.

Figure 5 Potential sources of measurement uncertainty associated with the use of contacting profilometry techniques for 3D surface topography measurement [adapted from (Leach, 2008)]



In order to compensate for some of these potential errors the speed of the stylus traversing the surface of the sample is often reduced; however this in turn increases the scan time depending on the area that is needed to be scanned.

Optical profilometry

Optical profilometers use a beam of electromagnetic radiation to measure the actual surface topography, most commonly using the focus detection concept which broadly implies that the surface profile is measured by maintaining the focus of the optical system making use of the principle of optical focus detection (Blunt, 2008). Two of the most commonly used optical techniques for tooth wear research are triangulation laser instruments and confocal instruments and these will therefore be reviewed below.

Projected surface topography measurement

Xhonga et al (1995) described a technique using projected profilometry (a shadow graph of dental casts) and gravimetric approach to dental erosion measurement, however when this was applied to a clinical study they found the measurement lacked the ability to quantitatively measure tooth wear (Xhonga and Sognnaes, 1973) and therefore use of this projected profilometry was discontinued.

Photogrammetry

Photogrammetry is the process of taking measurements from 2D images to obtain 3D coordinates of points on an object. Common points (groups of pixels) are identified and measured in two or more images and are processed with a mathematical model that relates the camera sensor/s, referred to as image space, to the object space. The generation of a large number of 3D coordinates leads to a point cloud of surface data or digital surface model (DSM). The quality of the DSM is dependent on the accuracy of the measurements taken from the 2D images and the fidelity of the mathematical model, which generally contains terms to account for focal length, lens distortions, and the location and orientation of the cameras in 3D object space. Grenness et al (2009) have described the application of this technique for measurement of tooth wear progression on the bucco-cervical area of an upper canine from digital images of sequential dental casts taken over a two year period. An accuracy of 6 μm and a repeatability of 18.5 μm were quoted and the authors concluded that this methodology may provide valuable information of the pattern of tooth wear *in vivo*. However, unlike surface profilers, the process fails to provide any qualitative data, for example regarding surface texture.

Confocal laser scanning microscopy

Confocal laser scanning microscopy (CLSM) is a tool for obtaining high-resolution images, 3-D reconstructions and optical sections through 3-D samples. CLSM has been used to provide a qualitative 3D insight into erosively altered substrate (Duschner et al., 2000; Lussi and Hellwig,

2001), However, as with all microscopy techniques CLSM is limited in its application to dental erosion research by the lack of information about the textural nature of the eroded surface and by limited information on the exact nature of the degree of demineralisation, therefore CLSM is commonly combined with other quantitative analytical techniques such as microhardness or analysis of mineral loss (Attin, 2006).

For dental erosion research, in addition to its non-destructive nature, CSLM has advantages over other microscopic techniques; namely the ability to image wet surfaces and to concurrently image surface and subsurface effects. As a result of these advantages, CSLM lends itself well to studies considering the effect of dental pellicle on tooth wear, especially with regard to dentine. CSLM has been used to study the structure, thickness and properties of the dental pellicle at different oral sites (Amaechi et al., 1999; Hannig and Joiner, 2006) and, in combination with microhardness, to analyse the ability of an intact dental pellicle, formed over varying time periods, to protect dentine against an erosive challenge *in vitro* (Duschner et al., 2000).

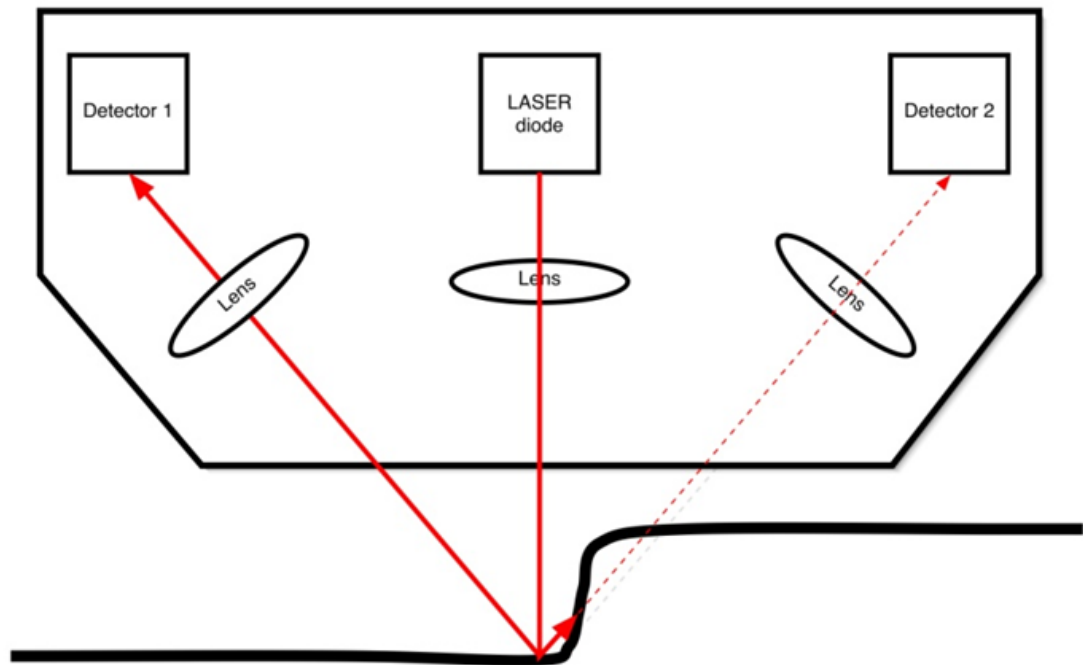
CLSM has increased understanding of the role of the dental pellicle in dental erosion, especially by illustrating the nature of subsurface phenomena occurring during the formation of erosive lesions. These subsurface phenomena have clinical relevance, in that calcium and phosphate from saliva before loss of substance has the potential to remineralisation these subsurface erosive lesions and fluoride containing products may expedite this process clinically.

Laser triangulation profilometry

Laser triangulation is classified as a light scattering optical profiling technique. Figure 6 below shows the optical principles of surface topography measurement using laser triangulation profilometry. Light from a laser source is projected onto a surface and is scattered on the surface, focussed through a lens on one (or both) of elements which focuses the light on to a

spot on a detector. As the surface of the object changes, the position of the spot is displaced on the detector and thus the distance of the sample surface from the laser source is recorded.

Figure 6 Schematic of optical principles of surface topography measurement using laser triangulation profilometry



This results in a typical 1 μm vertical resolution and up to 30 mm vertical range and is ideal for measurement of diffuse surfaces which scatter and reflect incident rays at many angles rather than at just one angle. Examples include surfaces built from a non-absorbing powder such as plaster, or from fibres such as paper, or from a polycrystalline material such as white marble. Laser triangulation also has the advantage of high speed surface profiling, which can measure slopes up to 90° and is of relatively low cost (Blunt, 2008). This makes laser triangulation useful in tooth wear measurement for measuring macro geometry of entire teeth that have been reproduced in dental stone or in an impression material which has a uniform colour (Rodriguez et al., 2009). Figure 6 shows a schematic of the optical principles of a laser triangulation laser which illustrates how the presence of two detectors reduces shadowing caused by areas of steep angulations in the surface profile which could potentially block the return path of the reflected light.

However, laser triangulation is limited by factors such as spot size variation over the vertical measuring range; shadow effects due to uneven detection of the reflected laser and problems with smooth, highly reflective specular surfaces. This is due to specular, mirror-like reflection of light from a surface, in which light from a single incoming direction (a ray) is reflected into a single outgoing direction. This lack of scattering means that triangulation lasers are not able to directly measure enamel and dentine; unlike other optical surface measurement instruments such as white light confocal sensors and white light interferometers. Instead, a replica technique is required which introduces further potential sources of measurement error and loss of surface information which therefore invalidates this technique for *in vitro* tooth wear measurement.

Triangulation laser profilometry has been used to measure tooth wear *in vivo* (Rodriguez et al., 2011; TBC) and *in vitro* (Rodriguez and Bartlett, 2010). For *in vitro* measurement the inherent accuracy and repeatability of the laser profilometer was 1.3 μm and 1.6 μm respectively (Rodriguez et al., TBC) however careful consideration of the choice and handling of replica materials was required for these techniques.

Confocal profilometry

The confocal profilometer used in this thesis will be described further in Section 2.1.2 below, however the advantages of confocal profilometry in comparison to other techniques will be reviewed here. These include the rapid scanning time, high vertical resolution (around 1 nm) and the small spot size which is maintained at a constant size throughout the depth of focus. The principle of confocal imaging yields an excellent spatial resolution regardless of ambient illumination, which therefore may reduce the impact of environmental light noise. The chromatic coding ensures that measurement is insensitive to reflectivity variations in the sample and therefore enables measurement of varying types of materials, transparent and opaque, specular or scattering, polished or not. This eliminates the need to replicate or treat the sample surface prior to measurement. The use of a white light source and not of a

coherent source (laser) eliminates completely all the difficulties associated with speckle and artefacts such as the 'batwing' effect seen with confocal laser and coherence scanning interferometry (Boltryk et al., 2009; Leach et al., 2008). However the system is limited by not being able to measure features with an angulation of greater than 30° and by having a depth of field limited to around 350 µm (Boltryk et al., 2008); combined with the expense of this instrument. Therefore the white light confocal sensor is more suitable for measurement of flat or curved surfaces with micro features where high accuracy and precision measurements are required (Boltryk et al., 2009).

Interferometry

Interferometry is based on the idea that amplitudes of two waves (e.g. light, sound, water) with the same frequency will add to each other, i.e. when the two waves are in phase, the result will summate to twice the amplitude and when the two waves are out of phase by 180° the result will summate to zero amplitude. This adding and cancelling wave property is known as superposition and results in a set of dark and light bands known as interference fringes when viewed on a screen or through a microscope (Leach et al., 2008). The advantages of white light interference for measuring tooth wear are direct areal surface measurements at high speeds with no contact and therefore no surface damage from a traversing stylus tip, with a lateral resolution typically < 1 µm and a vertical resolution typically < 1 nm. However disadvantages are the potential for a large amount of 'drop out' of image information when examining a highly diffuse surface such as etched enamel prisms and a limited vertical range requiring careful fixturing and relocation of objects onto the examining stage (Blunt, 2008).

Optical coherence tomography

Optical coherence tomography (OCT) is an interferometric technique, typically employing near-infrared light, which is similar to the confocal microscopy in that it uses light to penetrate a sample. The use of relatively long wavelength light allows it to penetrate into the scattering

medium and captures micrometer-resolution, three-dimensional images from within optical scattering media (e.g., biological tissue).

OCT has been used to assess enamel thickness, reflectivity and absorbance of bovine enamel *in vivo* (Amaechi et al., 2001) and for *in vitro* caries research (Jones et al., 2006). *In vivo*, OCT for tooth wear research is limited by difficulties with accurate and reliable re-positioning of the probe on the same position of the tooth surface, however in the first study of its kind Wilder-Smith et al (2009) reported the use of OCT to measure enamel loss in a randomised controlled trial comparing the effectiveness of esomeprazole at reducing enamel loss in patients with GORD when compared with placebo. This study standardized the imaging location and angle by inserting the OCT probe into fitted holes drilled into a 5 – 7 mm thick dental impression previously made of each patient's upper and lower teeth using a heavy bodied silicone impression material (Wilder-Smith et al., 2009). The study reported significant differences in decreases in enamel thickness and demineralisation as quantified by increased reflectivity, results which show much promise for future *in vivo* applications of this technique.

Atomic force microscopy

The atomic force microscope (AFM) is the most widely used member of the family of scanning probe microscopes because of its versatility in imaging a different materials with atomic resolution in varying operating modes which provide information about surface topography, lateral surface composition and differences in elasticity (Leach, 2010c). AFM probes the sample surface using a sharp tip which is either moved back and forward across the surface (contact mode), in essentially the same fashion as a profilometer, or is held in close proximity to the surface (tapping mode) whilst being oscillated at close to its resonant frequency (Barbour and Rees, 2004). Contacting mode is used to provide information about the frictional properties of a surface and mapping mode is more desirable when imaging delicate surface features (Field et al., 2010).

The advantage of AFM over profilometry is the far greater resolution of AFM and the advantage over SEM and scanning tunnelling microscopy is that no sample preparation is required and that samples can be imaged wet (Barbour and Rees, 2004), however the images can be subject to artefacts (Field et al., 2010). AFM has been used to evaluate erosion in human enamel and the authors report that the technique is suitable for measuring the early stages of enamel demineralisation (Finke et al., 2000; Marshall et al., 2001).

Software for surface profile and surface texture measurement

Surface texture helps to determine the overall physical and mechanical characteristics of a surface, of which roughness is the most important part because it describes the finest measureable detail of the surface geometry. Roughness is characterised by small, short-wavelength random variations in surface height which are superimposed on larger longer-wavelength regular patterns of waviness that, in turn, are superimposed on the overall profile of the surface (Suga, 2007).

Roughness average (Ra) is the most common parameter used to express roughness and is defined as the average of the absolute values of the profile height deviations recorded within the evaluation length measured from the mean line in micrometers (Suga, 2007). Roughness is relevant to clinical tooth wear research as the roughness of a surface is often closely related to its friction and wear properties i.e. a surface with a large Ra value, will usually have high friction and wear quickly. When assessing an area of tooth surface for roughness, it is considered good practice to make assessments of Ra over a number of consecutive sampling lengths (usually a total of 5) as the effect of a single non-typical peak will only have a small effect on the overall value and therefore an average of multiple measurements provides a more representative value (Leach, 2010b).

However, solely quoting Ra values in tooth wear research has limitations in that the value contains no information about the textural characteristics of a profile, the likelihood of future wear or wear-resistance, the rate of future wear or the potential of a surface to retain

fluids/lubricant. In light of these limitations, Field (2010) has postulated that use of bearing parameters to qualify the effects of a multi-factorial wear process (i.e. erosion and abrasion or attrition) may provide more information about the surface texture resulting from these processes which may allow prediction of, for example, surfaces with pooling/lubricative potential vs. surfaces which are likely to suffer more early wear.

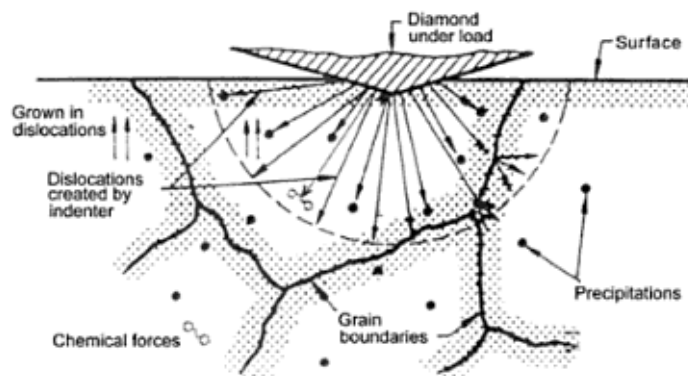
Surface topography measurement tooth wear has traditionally required an assessment of the interface between an unchanged 'reference' area and an area that was subjected to wear (Schlueter et al., 2005). The practicalities of achieving this *in vivo* meant that the technique relied on either acid resistant metal restorations (Chadwick et al., 1997) or metal circular or star shaped disks/stars circular star shaped discs (Bartlett et al., 1997a; Schlueter et al., 2005) cemented to the tooth. However, this technique was limited by debonding of the metal disks. Therefore the use of surface matching software which superimposes sequential scans of teeth was proposed (Chadwick et al., 2005). Surface matching software allows superimposition of scans through the use of surface matching and difference detection algorithms. These profile comparison techniques can be used on scans of experimental surfaces at different time intervals which can be expressed graphically from which 2D/3D step-height and volumetric measurements can be made. The underlying theory of profile comparison is based on the 'least squares technique' where the sum of the squares in the vertical direction is minimized in order to allow for surface matching and difference detection (Chadwick et al., 1997; Mitchell and Chadwick, 1998). This has been used *in vivo* (Pintado et al., 1997; Rodriguez et al., 2011; TBC) and *in vitro* (Chadwick et al., 1997) and to date the longest longitudinal study measuring the progression of tooth wear on a cohort of adults has run for over two years and found that at the subject and tooth level over 70 % of subjects had wear less than 15 μm over a six month period (Rodriguez et al., 2011)

1.3.3. Surface hardness

Microhardness

'Hardness' of a material is defined as 'resistance to permanent indentation' and is measured by the size of penetration of a diamond indenter forced into a sample under load, with 'microhardness' being measurements taken at low loads (<200 g). The size and depth of an indentation is affected by the physical characteristics of the material, not only in the immediate vicinity of the indentation but also up to a distance of ten times the dimensions of the indentation itself. Figure 7 is a schematic showing the physical characteristics that determine hardness of a material by providing resistance to motion of dislocations created by an indenter (Sirdeshmukh et al., 2006).

Figure 7 Schematic of resistance to motion of dislocations created by a diamond indenter [From (Sirdeshmukh et al., 2006)]



Knoop microhardness is the measure used most commonly by dental researchers to assess erosive potential *in vitro* (Attin et al., 1997; Lussi et al., 1993; Lussi et al., 1995; Lussi and Hellwig, 2001; Van Meerbeek et al., 1993; West et al., 1998). Typical Knoop hardness values for dental hard tissues range from 272 to 440 KHN for enamel and from 50 to 70 KHN for dentine (Meredith et al., 1996), therefore enamel is around five times harder than dentine. Although Craig and Peyton (1958) found no trends between hardness values from human teeth from different sites in the arch or between different sites within enamel and dentine, Meredith et al (1996) found in human molar teeth a decrease in enamel hardness with increased depth from

the surface and this corresponded with increasing hardness of dentine with distance from the amelodentinal junction.

Knoop microhardness testing has the advantage of being simple and non-time consuming and it can be used on brittle materials. Furthermore, it is considered more suitable for testing enamel and dentine than Vickers indentation, partly as the elongated nature of the Knoop indenter reduces measurement inaccuracies due to rebound from plastic deformation and also the relatively blunt Knoop indenter gives a shallower indentation and therefore less subsurface cracking and crazing (Sirdeshmukh et al., 2006; Waters, 1980). Microhardness provides useful information which allows prediction of other physical properties of the material and therefore the technique has been used widely for assessment of surface softening in dental erosion models, especially for enamel hardness testing, using either the Knoop or Vickers indenters (Attin, 2006). The technique has proven to provide useful information for discrimination of the erosive potential of various substances on dental hard tissues (Lussi et al., 1997; Lussi et al., 2000). The role of microhardness indentations to assess wear has been described for ruling out the possibility of any bulk loss of enamel or dentine in studies which consider the earliest stages of erosive demineralisation which is characterized by surface softening without loss of bulk tissue. It is considered essential that studies of this phase of erosion should always include checks that the effects of erosion have indeed been confined to softening. i.e. that no tissue loss has occurred. This method requires indentations using a microhardness tester under various loads to create varying indentation depths (calculated from the indentation length). After the exposure to the erosive challenge, one or more of these indentations will have disappeared if tissue loss has taken place.

Microhardness has also been described for measuring the extent of bulk loss of enamel or dentine. This is made possible by calculating the depth of the indentations before and after the tooth wear challenge, because the body of the indentation has not changed and only the surrounding tissue on the surface is removed so that the pyramidal geometry the contour of

the indentation (and thereby its length) is reduced, this difference represents the loss of substance. This technique has been used by various authors for abrasion studies (Jaeggi and Lussi, 1999; Joiner et al., 2004a; Joiner et al., 2004b; Lussi et al., 2004), however its role for studies into erosion and abrasion has been criticised due to the acid removing substance from the body of the indentation and not only from its surrounding area (Attin, 2006). Therefore more recent reviews of techniques for simulation and measurement of *in vitro* tooth wear studies have concluded that microhardness cannot be used to assess wear studies resulting in bulk tissue loss.

A further application for microhardness testing is for assessing the potential for remineralisation of eroded enamel by exposure to various products or solutions which promote remineralisation. This potential can be measured either by the surface microhardness recovery test or the relative erosion resistance test (Hara et al., 2009). These will be briefly reviewed below.

The percentage surface microhardness recovery (%SMR) test of enamel is carried out by calculating the mean length of five indentations made at three time points: initially at baseline prior to exposure to an erosive challenge (Lb); immediately after an erosive challenge (Ld) and thirdly after exposure to a remineralising agent (Lr). The further indentations are made 100µm to one side of the previous indentations. The %SMR is then calculated as: $\%SMR = 100 [(Ld1 - Lr) / (Ld1 - Lb)]$. Higher values indicate higher microhardness recovery and therefore greater remineralising potential for the agent or product under consideration (Hara et al., 2009).

Advantages of microhardness testing over nano-indentation include its relatively low costs, relative simplicity and a long history of use. However, for accurate results flat and highly polished surfaces samples are needed. Polishing removes the outer layer of fluoride rich/magnesium and carbonate poor enamel, exposing the inner layer of enamel. The inner layer has a higher solubility in acidic solutions than the outer layer, which may cause *in vitro* erosive lesions to progress more quickly than would occur in an intact enamel surface

(Meurman and Frank, 1991) To combat this, Fosse (1986) devised an instrument for taking *in vivo* hardness measurements and Caldwell et al (1957) reported microhardness data from natural tooth surfaces. Despite these developments, this technique has not been widely adopted *in vivo*, with only two studies reporting having used this instrument *in vivo* (Albrecht et al., 1991; Takats et al., 1991).

Nanoindentation

Nanoindentation describes a series of indentation hardness tests that are applied to very small volumes. First documented in the late 1980's (Bhushan et al., 1988) it has since been applied to biological testing of mineralised tissues, including research into dental erosion (Rios et al., 2006; Sales-Peres et al., 2007; Zheng et al., 2009). Measurement of hardness and elastic modulus using nanoindentation is considered a valuable technique for quantifying the earliest stages of softening. Moreover, due to the small volumes occupied by each indentation and the high sensitivity of the technique, micro-structural features of enamel can be assessed and the ability of variations of factors such as calcium and phosphate concentration, degree of saturation and pH of acid solutions at exposure times which are comparable to the clearance time of acids in the mouth can be investigated (Barbour et al., 2003a; b; Barbour et al., 2003c; Barbour and Shellis, 2007). Using these techniques, Habelitz et al (2002) reported changes in the mechanical properties of enamel after storage in the commonly used mediums of deionized water and saline. Following this some authors have advised caution in the choice of storage medium for tooth samples during *in vitro* research into tooth wear (Barbour and Rees, 2004) such as the saturated mineral solution (1.5 mmol/l CaCl_2 , 1.0 mmol/l KH_2PO_4 , 50 mmol/l NaCl, pH = 7.0) described by Zero (1990) for storage of enamel samples when not being used for experiments

1.3.4. Chemical analysis

Iodide permeability test

Iodide permeability testing (IPT) was introduced by Bakhos et al (1977). This technique involves allowing enamel samples to soak in potassium iodide for a few minutes, after which the remaining iodide is recovered from the enamel using paper discs (Attin, 2006). The amount of iodide recovered in the discs is determined and provides information about the pore volume of enamel and provides sensitive information about the early stages of de- and remineralisation (Brudevold et al., 1982) and has been shown to correlate well with measurement of calcium loss during demineralisation (Bakhos and Brudevold, 1982). Therefore this can be considered a low cost, rapid screening technique for assessment of the early stages of demineralisation and remineralisation (Attin, 2006).

Chemical analysis of dissolved minerals

Using the knowledge that dental enamel consists of 34-39 % m/m (g per 100 g) calcium (dry weight) and 16-18 % m/m phosphorous (Ten Cate et al., 2008) the amount of dental enamel dissolution can be determined by measuring the amount of calcium and phosphate dissolved from the apatite crystals of dental hard tissue. Various calcium or phosphorous specific assessments have been used (de Josselin de Jong et al., 1987; Grenby et al., 1989; Hannig et al., 2003; van Rijkom et al., 2003) and are now well established methods for assessing early erosion *in vitro*, albeit as a technique that lacks information on structural changes that are occurring.

Energy Dispersive X-Ray Spectroscopy

Energy Dispersive X-Ray Spectroscopy (EDS) is a form of microanalysis that can be incorporated into the instrumentation of SEM or ESEM. EDS provides information about the elemental composition of the surface of the sample being investigated. Essentially, the physical principle of the technique is that each element in the sample will emit a unique and characteristic pattern of x-rays when excited by electrons of sufficient energy. Furthermore, when examined

under the same conditions, the number of x-rays emitted by each element bears a direct relationship to the concentration of the element in the sample. In order to convert the x-ray emission into analysable data, the emitted x-ray is processed into a unique digital signal which contributes a single count to the appropriate channel of a multichannel analyser. After time, an x-ray spectrum is formed and processed for quantitative analysis. This processing involves accounting for and removal of outlying peaks; identification of the elements giving rise to the spectrum; removal of the background noise; resolution of the spectral peaks and finally computation of the element concentrations (Woldseth, 1973). The advantage of EDS is that it can reliably detect ion concentrations with a concentration of as little as 1 wt. % within a highly mineralised tissue such as enamel. This ability to detect minor ion concentrations has led the technique to be used in studies investigating the effects of amine fluoride on eroded enamel (Rosin-Grget et al., 2000) and more recently the remineralising potential of fluoride toothpastes on enamel erosion have been assessed using EDS (Arnold et al., 2006; Arnold et al., 2007).

1.3.5. Scanning electron microscopy

The scanning electron microscope (SEM) was one of the first techniques described for assessing the structural changes of dental hard tissues (Boyde and Lester, 1967) and is a technique that is still widely used today in research into dental erosion (Schmidlin et al., 2003; Sorvari et al., 1996).

The SEM uses a very fine beam of electrons, which is scanned across the surface of the sample as a raster of parallel contiguous lines. Upon hitting the sample surface the electrons are either reflected as backscattered electrons or secondary electrons are generated by the interaction of the primary electrons with the sample surface. The number of secondary electrons depends on the surface topography or nature of the sample. These secondary electrons are collected, amplified and analysed before modulating the beam of a cathode ray, scanned in sympathy with the scanning beam. The resulting image resembles that seen through an optical lens but

at a much higher resolution and a greater depth of field. The ultimate resolving power of a SEM is dependent on the dimensions of the probe beam which in turn is controlled by diffraction at the final aperture, chromatic aberration and the size of the electron source. A resolution of up to 1 nm is achievable with a field emission system and an in-lens detector. A typical SEM can achieve magnifications of x400000. The magnification is dependent on the excitation of the scan coils, as modified by any residual magnetic or stray fields. The magnification also depends sensitively upon the working distance between the lens and the sample (Egerton, 2008; Goodhew et al., 2000).

For conventional SEM, the sample surface must be coated with a material that is electrically conductive, in order to prevent a reduction in image quality due to accumulation of negative electrostatic charge. These so called charging effects result in artefacts which appear on microscope images as irregular, featureless bright patches, or streaks, and are generally accompanied by loss in resolution (Shaffner and Van Veld, 1971). The coating material is usually gold and therefore a disadvantage of this technique is that the samples will be irreversibly altered during the desiccation and sputtering process. Alternatively casts can be made from the samples if their loss/destruction is unacceptable, however the replication technique results in a degree of dimensional inaccuracies and loss of information (Faria Ac Fau - Rodrigues et al.; Field et al., 2010). This has led to the development of environmental SEM (ESEM) which allows imaging in a low vacuum and wet conditions and is thus designed for imaging biological samples in an uncoated manner (Barbour and Rees, 2004). However, to date few studies have used ESEM to investigate *in vitro* or *in situ* tooth wear.

As with all forms of microscopy image degradation can result from factors such as poor sample preparation, flare, astigmatism, chromatic aberrations, type and intensity of illumination and the numerical apertures of the condenser and lens. It has been reported that the indicated magnification shown on the instrument should not be relied upon for accuracy better than $\pm 10\%$ (Cuenat, 2010).

Quantitative light-induced fluorescence

Quantitative light-induced fluorescence (QLF) is an optical technique developed for detection of early demineralisation found in enamel caries. The fundamental physical principles of this technique are reviewed fully elsewhere (Angmar-Mansson and Ten Bosch, 2001; Tranæus et al., 2001; van der Veen and de Josselin de Jong, 2000), however essentially QLF is based on the principle that autofluorescence of the enamel alters as the mineral content of the dental hard tissue changes (Karlsson, 2010), for example during the process of de- and remineralisation of dental enamel. QLF is now a well-established optical technique for the detection of early enamel caries *in vivo* and *in vitro* (Karlsson, 2010) and its application for quantification of erosive lesions *in vitro* has been investigated (Ablal et al., 2009; Elton et al., 2009; Pretty et al., 2003). In an *in vitro* validation study comparing the use of QLF with contacting profilometry and transverse microradiography (TMR) to measure the depth of erosive lesions Elton et al (2009) found that QLF correlated poorly with TMR for measuring the depth of wear. However, QLF proved highly useful for measuring the subsurface demineralisation. Elton concluded that QLF is reliable for shallow erosive lesions but becomes less consistent as the depth of the erosive lesion increases.

QLF is therefore, an emerging technique for non-destructive measurement of the subsurface effects of dental erosion and has potential for *in vivo* quantification of erosive areas without significant wear (Pretty et al., 2004).

Microradiography

Microradiography is a technique that quantifies mineral loss according to the attenuation of x-radiation passing through enamel and/or dentine (Attin, 2006). The number of x-ray photons that transmit a dental hard tissue sample can be recorded either by photo counting-ray detectors which can allow the mineral mass to be calculated by knowing the appropriate mass attenuation coefficient or alternatively x-ray sensitive photographic plates or films can record the grey values from which the mineral mass can be calculated by determining photographic

density measurements calibrated using an aluminium step wedge (Anderson and Elliott, 2000; de Josselin de Jong et al., 1987; De Josselin de Jong et al., 1988). Microradiography was initially developed for analysing transversely cut thin sections (50-200 μm) of enamel to assess lesion depth and mineral loss of carious lesions, a technique that is known as transverse microradiography (TMR). This technique has been widely used in caries research for determining mineral changes in de- and remineralisation during caries and has more recently been adapted for dental erosion research. Hall et al (1997) found that TMR had a strong correlation with profilometry for measuring mineral loss even for detection of early erosive lesions with short immersion times in a demineralising solution. However, TMR was further modified for detecting erosive mineral loss using thicker sections of enamel or dentine that do not need to be transversely cut. This technique is known as longitudinal microradiography (LMR) and the technique can be used in cyclical models of erosion that require measurement at more than one time point. Although LMR is not able to determine the mineral profile of a sample from surface to depth it can record the mineral loss both in an erosive crater and in the surface softened zone, albeit less sensitively than TMR, with recommendations made that LMR should not be used to assess enamel losses less than 20 μm due to wide standard deviations when using this technique to assess minimal wear. Despite this, LMR can be used to assess erosion progression in both enamel and dentine (Ganss et al., 2001; Ganss et al., 2004a; Ganss et al., 2004b) and LMR correlates well with profilometry and with analysis of dissolved calcium/phosphorous (Ganss et al., 2005). In summary therefore, the main advantage of this technique for assessing *in vitro* tooth wear is that it can simultaneously determine wear and demineralisation.

1.4. Tooth wear modelling

A model can be defined as 'a simplified or idealized description or conception of a particular system, situation, or process...that is put forward as a basis for theoretical or empirical understanding, or for calculations, predictions, etc...' (Oxford English Dictionary). In biology,

'modelling' commonly refers to the use of complex simulational models *in silico* which are mathematically constructed in order to represent and analyse the role of all relevant biological processes (Peck, 2004; Winsberg, 2001). With regard to tooth wear modelling, the philosophical aim is to create a system that mimics the complex tribochemical processes occurring during *in vivo* tooth wear. Unlike nature though, the model can be manipulated in ways that would be impossible, too costly or unethical to do clinically. Within this thesis therefore, modelling of tooth wear describes an experimental system which can be used to explore theories about how the clinical phenomenon of tooth wear really works, through use of an artificial environment that researchers can control, in order to: identify areas where more data are needed; to propose and test hypotheses regarding the aetiology and management of tooth wear and, finally; to evaluate possible management options for tooth wear.

The role of topical fluoride for management of tooth wear lacks scientific evidence supported by randomised controlled double-blind trials because these studies are difficult and expensive and also because of ethical constraints due to the irreversible cumulative nature of tooth wear (Larsen, 2008). Therefore the majority of tooth wear research has involved modelling and simulating the tooth wear process in one form or another.

Validation is defined as the process of establishing that a method is sound (Last, 2000). The word validation is derived from the Latin *validus* meaning 'strong' and the concept of validity in biomedical research has several meanings according to its accompanying word or phrase.

For all studies aiming to model erosion with or without a physical component the question needs to be posed as to whether the model includes all elements of the current understanding of the disease (content validity). On this basis, *in vitro* erosion only models are incomplete, but *in situ* and *in vivo* models more closely approximate the intra-oral tooth wear process, especially if an element of physical wear is involved. Much work on the concepts of construct validity and prediction validity has been carried out with regard to assessing dental caries

(Nyvad et al., 2003) using well accepted and validated measurement techniques with known sensitivities and specificities. However, unlike caries, tooth wear is often seen to develop in patients without a single (or multiple) clear identifiable aetiology (Ganss, 2008), resulting in clinical signs and symptoms which (even using current best *in vivo* measurement techniques) are almost impossible to quantify (Holbrook and Ganss, 2008) with any degree of sensitivity and specificity. Perhaps as a result of this, tooth wear is a condition which lacks a consensus on which clinical risk factors are most reliable in predicting tooth wear progression.

This may explain some of the uncertainty regarding which therapeutic measures would be most beneficial for any given individual with tooth wear. This lack of definite theoretical predictions for use in tooth wear research explains the current state of variation of current research techniques being employed (Berg-Beckhoff et al., 2008; Last, 2000; Young et al., 2008) especially when the content validity of the methodology is negated by disregarding the importance of the contribution of attrition or abrasion to the tooth wear process (Bartlett, 2005).

1.4.1. *In vivo*

There few studies which have simulated *in vivo* tooth wear in human subjects, or aetiological tooth wear factors. This may be because *in vivo* simulation of tooth wear is limited by ethical considerations as tooth wear, by its very nature, is an irreversible damaging process to the dental hard tissues. However the initial surface softening is reversible and future studies may be able to simulate the initial erosion lesion which is then assessed and repaired *in vivo* however the assessment techniques are currently not discriminating enough for this type of research.

Young et al (2006) investigated the effect of stannous fluoride and sodium fluoride toothpastes on enamel erosion in a study which simulated acid erosion, by passing diluted citric acid over healthy anterior teeth of human subjects, using a peristaltic pump. The calcium content in the citric acid applied before and after the treatment with toothpaste was measured and the

authors concluded that the stannous fluoride toothpaste markedly reduced the enamel dissolution of teeth *in vivo*, whereas the NaF toothpaste provided no protection (Young et al., 2006).

Bartlett et al (1997b) compared the effects of a bland meal versus a high fat content meal taken with alcohol on GOR measured by oesophageal and oral pH and found that pathological levels of GOR were provoked by the high fat meal in 6 of the 12 subjects whereas the bland meal provoked pathological levels of reflux in only two out of the twelve subjects. Moreover, there was a significantly lower pH in the anterior palatal region of the oral cavity after consumption of the high fat content meal (Bartlett et al., 1997b).

If an erosive challenge were to be simulated *in vivo*, use of an acidic gel may reduce unnecessary exposure of enamel/dentine to damage by reducing the flow rate of an erosive challenge over tooth surfaces, which are not of interest to the measurement technique, to nil (Shellis et al., 2005). Localisation of the erosive challenge would also have the secondary advantage of allowing a split-mouth or even split-tooth design to be employed.

One area which is potentially under-researched in the field of dental erosion is the role of biological factors such as saliva and the acquired dental salivary pellicle in modifying the erosive wear process *in vivo* (Hara et al., 2006b). Therefore, immediate saliva analysis could be included for *in vivo* models which would reduce the changes in the salivary pH that occur during storage of the saliva (Jensdottir et al., 2005).

Clinical trials of investigational medicinal products

In vivo clinical trials that measure the effectiveness of an intervention on tooth wear are, to date, limited and therefore the current best evidence about strategies to manage erosive tooth wear is based upon observational, *in situ* and *in vitro* studies (DoH/BASCD, 2009).

On an epidemiological level, there have been no interventional studies with an outcome of tooth wear progression or incidence. This may be partially because of the large sample size

required to determine a statistically significant outcome and also because of the current gold standard for measuring tooth wear which would make a clinical trial in such a large group unfeasibly long (Mason, 2009). Therefore, research into the validity of clinical indices to measure and monitor the clinical outcomes of tooth wear continues.

On an individual level, the only interventional clinical trial into treatment of tooth wear investigated the effectiveness of a proton pump inhibitor (PPI) compared with placebo at reducing enamel loss as measured using OCT in a population of individuals with GORD (Wilder-Smith et al., 2009). The study found significant reduction in decreases in enamel thickness and also significant reduction in demineralisation in the PPI group when compared with the placebo group, results which provide some support for the use of PPI's at reducing erosion in individuals with GORD.

1.4.2. *In situ*

In situ tooth wear studies use a methodology which was originally developed for caries research and has since been adopted for use in dental erosion studies. *In situ* studies involve human subjects wearing intraoral appliances which carry mounted enamel and dentine slabs which have previously been sterilised or disinfected.

The advantages of the *in situ* methodology over *in vitro* studies are that the influence of biological factors that influence the tooth wear process can be taken into account, such as saliva flow rate and buffering capacity; acquired salivary pellicle (diffusion limiting properties, composition, maturation and thickness); positioning in the oral cavity; physiological soft tissue movements (Hara et al., 2006b). The finding that *in situ* enamel erosion was drastically reduced by an order of 10 times compared to *in vitro* enamel erosion (West et al., 1998), provides an indication of the cumulative impact of these biological effects. According to the study design and hypothesis of interest, experimental tooth wear regimes may be carried out, either intra-orally or extra-orally. In order to replicate intra-oral physiology as close as possible to the erosive challenge it should ideally be carried out *in situ*; however the use of intra-oral

erosive challenges is limited by ethical considerations, especially if the outcome of the study is substance loss. Therefore *in situ/ex vivo* models typically employ a cyclic study design where extra-oral acid challenges are followed by periods of intra-oral exposure to remineralising conditions (Hara et al., 2009). On removal from the appliance the enamel or dentine slabs are subjected to measurements of the outcome of interest.

1.4.3. *In vitro*

In vitro tooth wear models are carried out in the laboratory with no patient contact or involvement. They can involve techniques that solely mimic the earliest stages of erosive demineralisation (in which surface changes including softening occur without loss of bulk tissue) and techniques which involve bulk tissue loss (in which acids initiate surface softening followed by a mechanical process which removes the vulnerably softened tissue). The later model aims to mimic the clinical situation where the outcome is loss of enamel and dentine usually due to a multifactorial tooth wear process. In order to further simulate a process of alternate demineralisation and remineralisation a cyclic design may be employed to simulate tooth wear causing tissue loss.

Most work in the field of tooth wear research has taken place *in vitro* and the advantages of this approach to modelling of tooth wear include the following:

- achievability of a high degree of standardisation;
- ability to control numerous variables (including acidic challenge and concentration, substrate type and nature);
- inclusion of large sample sizes and use of control groups;
- results can be obtained relatively rapidly with minimal expenditure in comparison with *in vivo* and *in situ* tooth wear research.

Extrapolating the results of *in vitro* studies to the clinical tooth wear is problematical, in part due to the inability to replicate the complexity of the oral environment in the laboratory but

also due to by the heterogeneity of the applied methodologies used in the laboratory. Therefore only potential trends may be suggested by early erosion models and tissue loss models (Lambrechts et al., 2006).

Review of the literature of all *in vitro* tooth wear research reveals some of the wide variation in methods employed for the following parameters:

- type of tooth wear simulated (erosion; attrition; abrasion)
- substrate (human enamel/dentine; bovine enamel/dentine; hydroxyapatite)
- sample preparation (polished, virgin tooth surface)
- study design (single/cyclic/alternating order of challenge and remineralisation periods, timing and number of cycles)
- Erosive agent (chemistry/pH/immersion time/flow rate/temperature/volume-substrate ratio)
- Tooth brush abrasion wear simulation, (tooth brush machine, brush design, brushing behaviour, toothpaste)
- Attritional wear (two or three body wear behaviour, wear machine, , type of antagonist, antagonist geometry, frequency of change of antagonist, total number of strokes, number of strokes per cycle, load applied, temperature, lubricant)
- Remineralising agent (artificial saliva, human saliva, pooled, frozen, stimulated/unstimulated, presence/absence of pellicle formation)
- Fluoride details (chemistry, concentration, formulation, application method, time)
- Outcome measure
- Measurement technique (validation, accuracy and repeatability)
- Statement of clinically significant effect size, sample size calculation, power calculation, loss to follow up.

Studies modelling erosion only

The erosive challenge can be applied as a single challenge or as part of a cyclic study design.

Simple erosion models

Common themes which appear from reviewing the methodology of studies of this kind include:

- a. Choice of substrate: Most commonly either bovine or human enamel or dentine was investigated in the studies, however previous workers have also used hydroxyapatite blocks (Barbour et al., 2003c). Although most studies seem to prefer to use human tissues, the use of human tissues for research requires donation and use in line with the UK law of the Human Tissue Act 2004 (Good Clinical Practice and Current Regulations, 2010). Studies which have compared bovine substrates with human substrates have found that the bovine substrate reacts in a similar fashion to human substrates (Rios et al., 2008). Therefore due to it being easier to acquire and suitable for most purposes, results from studies using bovine substrate can be considered equally valid to those using human substrates.
- b. Choice of erosive agent: The choice of erosive agent varies according to the aim of the study. For modelling erosion from extrinsic sources of acid, the options are either a commercially available product, such as carbonated soft drinks and fruit juices, or a laboratory made acid solution, most commonly citric or phosphoric acids (Eisenburger et al., 2001a) although malic, lactic, tartaric, oxalic and acetic acids have also been used (Hannig et al., 2005). Previous authors have also modelled erosion with wine (Willershausen et al., 2009) and other alcoholic beverages (Lissera et al., 1998), acidic medicines, lozenges (Lussi et al., 1997) and snack foods (Dodds et al., 1997). The advantages of a commercially available product are that there is a degree of verisimilitude to the clinical situation, however due to variations in geographical and market availability of products this introduces the possibility that repeating a previously published experiment may be complicated by a manufacturer changing the formulation of a product or even due to simple variations in batches of a product. Laboratory made acid solutions are easily reproducible, inexpensive and can be precisely formulated to produce

repeatable results. For studies modelling erosion due to intrinsic sources of acid, a solution of HCL is most commonly used (Holme et al., 2005) however gastric juice has also been used (Bartlett and Coward, 2001).

- c. Control of the flow rate of solution across the substrate surface: In order to ensure that the samples across the groups are exposed to the erosive medium in a consistent fashion it has been recommended that studies employ a methods to control the flow rate (Eisenburger and Addy, 2003) such as use of a calibrated stirrer (Hemingway et al., 2008) or and the use of a chamber through which the erosive solution is pumped at a known rate (Attin et al., 2003).
- d. Temperature control: Previous studies have shown that erosion depth and surface softening increased significantly with acid temperature (Eisenburger and Addy, 2003) and therefore the temperature of the erosive medium should be controlled, either by ensuring the ambient temperature remains constant and is stated or by use of a water bath. The temperature chosen in the reviewed studies varies from body temperature (37°C), average intra-oral temperature (36°C) or 'room temperature', which is often stated as a mean temperature with maximal and minimal fluctuations in order to compensate for geographically, seasonally and diurnal variations.
- e. The pH of the acid: The pH of the erosive challenge reported in the studies varied considerably (between pH 1.18 (West et al., 2001) – pH 6.3 (McNally et al., 2006) depending on the aim of the study.
- f. The duration of erosive challenge and volume used: The choice of duration fluctuated according to parameters described above.
- g. Sample preparation: Most models use a polishing procedure with a standardised polishing procedure using sequentially finer grit size grinding/polishing discs thereby removing a uniform depth of material during the grinding/polishing process in order to produce a flattened surface.

In order to allow for extrapolation of findings of studies of this type, researchers have attempted to choose, as far as possible, parameters which are considered clinically relevant. However this poses study design complications as for example, acid exposure time cannot often be specified prior to a pilot study in order to determine that the chosen methodology will produce softening or wear of the desired magnitude and moreover the acid exposure time will depend on other parameters; notably pH, acid type and concentration, temperature and stirring and the ability of the measurement technique to detect the resulting degree of softening or wear.

Cyclic erosion models

Cyclic erosion models aim to investigate the effect of periods of demineralisation and remineralisation that occur during tooth wear. These models can also involve physical impacts, if the aim of the study is to model bulk wear of enamel and dentine. Studies have employed one cycle or several cycles by either manual transfer between media or by automated systems with storage in an appropriate storage media between cycles.

In order to promote remineralisation, a choice exists between artificial saliva and natural human saliva. Whilst artificial saliva has been shown to induce remineralisation of eroded enamel and dentine in the laboratory (Eisenburger et al., 2001a), erosion in absence of natural saliva has greater impact on enamel and dentine than the use of artificial saliva as a remineralising agent (West et al., 1998). This is due to artificial saliva not forming a salivary pellicle (Hara et al., 2006a) and also due to the absence of salivary mucins having a lubricating action, which reduces cyclic erosion-abrasion (Hara et al., 2008). Salivary pellicle is known to be a protective agent against erosive demineralisation and saliva mucins are lubricants which have been shown, in laboratory conditions, to reduce erosion and abrasive wear (Hara et al., 2006a; Hara et al., 2008). Therefore artificial saliva without mucins has the potential to influence the clinical relevance of the tooth wear models. Although the use of natural saliva may be considered ideal, its use introduces a number of challenges, including collection,

storage and disposal in line with the Human Tissue Act and is prone to degradation if stored incorrectly (Hara et al., 2006b). Therefore, there is a need for further research into developing a remineralising medium with properties closer to that of natural saliva with a standardised electrolyte composition which would obviate the need for donation of saliva by human subjects.

Studies modelling erosion with a physical impact

Abrasion components

Clinically, tooth wear is rarely seen as a result of erosion in isolation. Therefore studies modelling erosion may also include a physical impact, which most commonly involves tooth brush abrasion. This component of the challenge will involve a rubbing action often, but not exclusively, involving brushing with a toothbrush. Whilst tooth brushing may not always be clinically relevant to the site and location of the erosive wear it is a convenient representation of the intra-oral process. The force, the number of strokes, the type of brush (including electric/manual), and the length of time of brushing should be controlled. The application of the agent must reflect the clinical situation.

Attrition components

The synergistic role of erosion and attrition in tooth wear is thought to be due to acids creating surface/subsurface softening of tooth tissue which is then mechanically removed by the attritional or abrasive elements; however few studies have modelled erosion with a physical impact due to attrition. Vieira et al (2006b) used a cyclic erosion-attrition model and Shabanian and Richards (2002) investigated attritional wear of enamel at varying antagonistic loads and pH of erosive agent. The methodological parameters chosen for these studies varied considerably and further work is needed to develop a valid and reliable cyclic erosion and attrition model.

Overall aims of Chapter 2, 3, 4 and 5

The aim of Chapter 2 was to validate the techniques used to measure tooth wear modelled *in vitro*; in particular the use of white light confocal profilometry in combination with a range of generic and bespoke software for volume and step height measurement of enamel and dentine wear.

The aim of Chapter 3 was to use an *in vitro* wear model simulating attrition and dietary erosion to investigate the effect of an aqueous sodium fluoride solution of varying concentrations on erosive and attritional wear of human enamel and dentine, in comparison to a negative control.

The aim of Chapter 4 was to use an *in vitro* wear model simulating abrasion and gastric erosion to investigate the effect of increasing three varying aqueous fluoride solutions and a fluoride varnish on erosive and abrasive wear of human enamel, in comparison to a negative control.

The aim of Chapter 5 was to use an *in vitro* wear model simulating attrition and dietary erosion to investigate the effect of two fluoride varnishes and a resin-based adhesive on erosive and attritional wear of human enamel, in comparison to a negative control.

Overall, the null hypothesis of the thesis was that fluoride has no effect on erosion, erosion and abrasion or erosion and attrition *in vitro*.

Chapter 2 Development and validation of techniques used to model and measure tooth wear *in vitro*

Introduction

Many different techniques have been proposed for modelling and measuring tooth wear *in vitro*. Measurement is the “process of experimentally obtaining information about the magnitude of a quantity” (BIPM et al., 2008). Implicit in this definition are both procedures based on a theoretical model and, in practice, a measuring system. Many of the procedures and systems which have been described in the literature for measurement of tooth wear operate using fundamentally different physical or chemical properties, as described in Chapter 1. This means that each procedure and system has advantages and disadvantages (which partially depend on the aspect of tooth wear which is trying to be measured) and also makes comparison and synthesis of the outcomes of tooth wear research very difficult. There is, however, one similarity between all measurement systems which is that each will provide results which will have a margin of doubt about them i.e. no system will provide perfect measurements. The corollary of which is that there will always be error attributable to the outcome of tooth wear research, the extent of which is usually unknown. Central to this principle is the concept of the ‘true value’ which is defined as the “quantity value consistent with the definition of a quantity” (BIPM et al., 2008) i.e. the true value of a measurement is the hypothetical result that would be returned by an ideal measuring instrument if there were no errors in the measurement procedure and system (Leach, 2010d).

In practice, this can never be achieved and the scientific discipline dedicated to understanding and managing measurement uncertainty and improving the quality of measurement is called metrology: “the field of knowledge concerned with measurement” (BIPM et al., 2008). Metrology includes all theoretical and practical aspects of measurement, whichever the field of application and the concept of “uncertainty” in measurement, is based upon the Guide to the Expression of Uncertainty in Measurement (GUM), the first edition of which was published

in 1993 (British Standard Institution, 1995) This seminal reference is read in conjunction with the International vocabulary of basic and general terms in metrology (VIM) (BIPM et al., 2008) which is promoted, revised and updated on a regular basis by the Joint Committee for Guides on Metrology (JCGM). Uncertainty in measurement is not a concept that has been widely adopted by researchers within the field of tooth wear research. However, it has been recently stated that with regard to carrying out surface topography measurement of tooth wear '*The accuracy and reproducibility of any system under the experimental conditions.*' Must be reported. This statement introduces the terms 'accuracy' and 'reproducibility' which, although commonly used to refer to the performance of a measurement instrument, are frequently interpreted incorrectly or are used indistinguishably (Flack and Hannaford, 2005). These terms are explored in more detail in relation to the validation of the hardness tester in Section 2 of this chapter on on page 125 below.

An understanding of these terms is important when attempting to determine the performance of a tooth wear measurement system and thus interpret the clinical significance of the results of a study. However, in the field of research into dental erosion there remains a lack of consensus on how to determine the accuracy and precision for a system used to quantify or qualify the changes occurring to enamel or dentine during simulated tooth wear *in vitro*.

Possible sources of error from the confocal measurement system can come from (Bell, 2010):

- The measuring instrument instruments can suffer from errors including bias, changes due to ageing, wear, or other kinds of drift, poor readability, noise (for electrical instruments) and many other problems.
- The item being measured: dimensional instability of enamel and dentine samples relates to changes due to the fragility of the remaining organic matrix of demineralised dental hard tissues. A concern regarding the measurement of wear using profilometry is that extensive drying prior to measurement of enamel and dentin samples may have

a detrimental effect on measuring step height and volume loss of enamel and dentine (Attin et al., 2009).

- Errors introduced from mounting samples onto the stage to avoid movement measurement process: the measurement itself may be difficult due to practical.
- 'Imported' uncertainties: calibration of reference standards and calibration of other measurement instruments, and calibration of the measurement system has an uncertainty which is then built into the uncertainty of the measurements. However the alternative option of not calibrating the system and therefore having unquantified uncertainties would be much worse.
- Operator skill: some measurements depend on the skill and judgement of the operator. One person may be better than another at the delicate work of setting up a measurement, or at reading fine detail by eye. The use of an instrument such as a stopwatch depends on the reaction time of the operator.
- Sampling issues: the measurements must be properly representative of the process that is being assessed. Therefore the uncertainty evaluation must be carried out under the experimental conditions that will be used in the study.
- The environment - temperature, air pressure, humidity and many other conditions can affect the measuring instrument or the item being measured. Variations in the temperature of the enamel and dentine samples may vary the dimensions. The beam of light passing through air will be affected by air currents in the room and vibrations in the room will affect the measurement.

Despite Ganss (2005; 2007b) finding that non-contacting profilometry measures relatively less tooth wear than other techniques and that careful training and understanding is required to ensure reliability (especially with sophisticated surface matching software); 3D profilometry has been described as 'validated' (Rodriguez, 2009; Schlueter et al., 2005); being 'highly accurate and precise' (Suga, 2007) and has been promoted as the 'gold standard' for

measurement of bulk wear of tooth tissue (Schlueter et al., 2005). However to date no research group within the field of tooth wear research has fully applied the metrological principles behind the Guide to the Uncertainty of Measurement to tooth wear systems. Currently, most research groups using profilometry fail to report basic contributions to the measurement uncertainty such as the accuracy and repeatability of the measurement system being used and how the system was validated for the purpose for which it is being used. An understanding of the limitations of the measurement tools used and an evaluation of how 'fit for purpose' the system is, remains an important and under investigated area of tooth wear research, which requires further development and investigation.

2.1 Section 2.1: Uncertainty of tooth wear measurement *in vitro*

2.1.1 Aim, objectives and hypothesis

The aims of Section 2.1 were to:

- Quantify all possible sources of measurement error associated with the measurement of wear using the measurement system.
- Propagate all assessed measurement errors in an uncertainty budget and carry out an analysis of uncertainty.

The hypothesis was that:

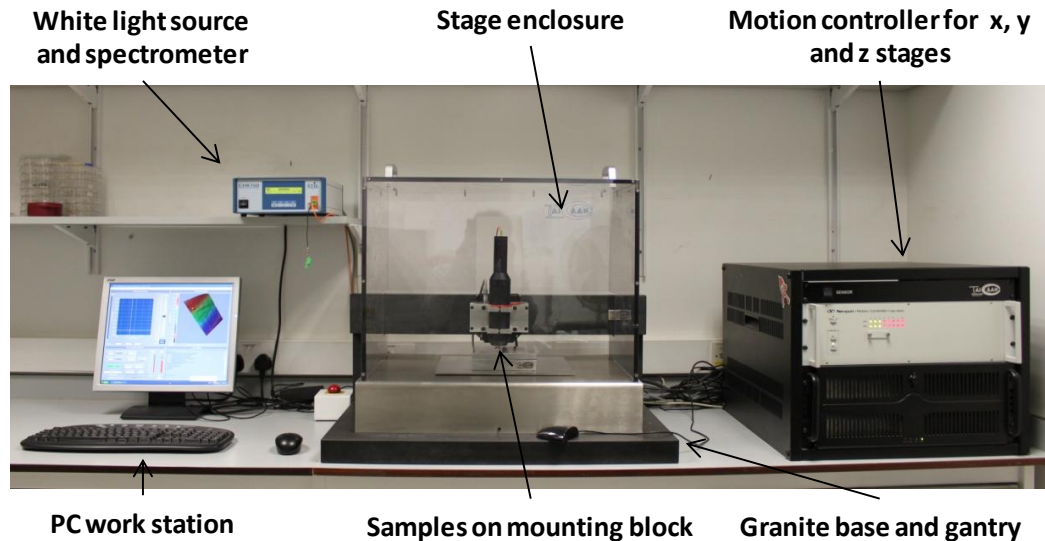
- The uncertainty of step height and volume measurement using the white light confocal profilometer did not exceed the maximum permissible level of uncertainty, which for the purposes of this thesis was set at 10 %.

2.1.2 Materials and methods

The surface topography measurement system used in this study consisted of a white light confocal profilometer (XYRIS 4000 WL, TaiCaan Technologies Ltd., Southampton, UK), in

combination with a range of generic and bespoke measurement software. Figure 8 below shows a photograph of the component parts of the white light confocal profilometer

Figure 8 Photograph of the component parts of the white light confocal profilometer



The granite support structure consisted of a flat base, onto which the x/y axes motion system (stage) was attached and a horizontal gantry, onto which the z stage was attached, in order to position the z stage directly over the x/y stage. Granite was chosen for high inertial mass, stiffness and excellent dimensional stability, in order to form a rigid ‘measurement loop’ between the horizontal and vertical measurement components. These characteristics not only determined the relative position of the x, y and z stages but also dampened the effect of instability in the surrounding environment and thus reduced background ‘noise’ in the measurement system. The transparent polycarbonate stage enclosure was designed to minimise air movement and dust contamination in the immediate area during measurement, whilst allowing sample visualisation during sample positioning and measurement set-up.

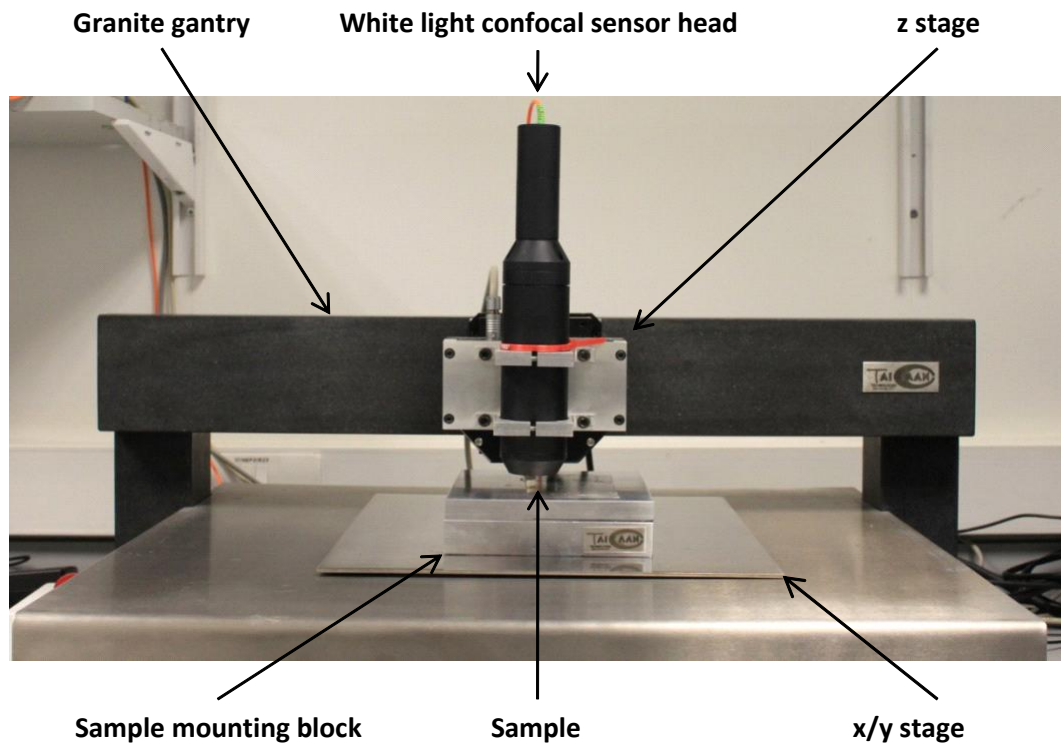
The motion controller regulated the movement of the ball bearing mounted x, y and z stages which, as shown in Table 2 below, had a maximum travel of 10 mm in the x/y axes and 25 mm in the z axis. The motion control system had a nominal resolution of 0.1 μm (x, y and z axes) and a nominal unidirectional repeatability of 0.4 μm (x/y axes) (XYRIS Series Precision 3D Surface Profilers Brochure, 2009).

Table 2 Nominal stage specifications of the XYRIS™ 4000 white light confocal profilometer

Stages	Resolution	Travel	On axis repeatability	Maximum Speed	Drives and Bearings
x and y	0.1 μm	10 mm x 10 mm	0.4 μm	25 mm/s	DC servo Ball bearing
z	0.1 μm	25 mm	Not specified	n/a	DC servo Ball bearing

Figure 9 below shows a close-up photograph of the component parts of the white light confocal profilometer, which remained covered by the stage enclosure during measurement.

Figure 9 Close-up photograph of the component parts of the white light confocal profilometer



The z stage mounting assembly supported the white light confocal sensor head, underneath which, objects to be measured were fixed to aluminium sample mounting blocks using double adhesive tape (Adhesive Paper, Struers A/S, Copenhagen, Denmark). The aluminium blocks were polished and lapped flat so that when they were placed onto the flat aluminium plate of the x/y stage using a sliding action, an adhesive bond of considerable strength was formed

(due to the 'wringing' phenomenon) which thus prevented unwanted slipping of the mounting blocks during x/y stage movement (Siddall and Willey, 1970).

The white light confocal sensor operates following the confocal chromatic length aberration principle (ISO 25178-602 2010 ; Sciences et Techniques Industrielles de la Lumière (STIL), 2007). Figure 10 below shows a schematic of the optical principles of the white light confocal sensor. Polychromatic (i.e. white) light was emitted from a halogen light source (a) and was transmitted through a fibre optic cable (the orange cable seen entering the top of the sensor head in Figure 9 above) to a spectral aberration lens (b) in the sensor head. The spectral aberration lens split the polychromatic light into its constituent wavelengths and the resulting dispersed light was projected onto the sample surface (c), where the light of different wavelengths was focussed at different distances from the lens. As shown in Figure 10 below, areas on the sample surface that are closer to the sensor (i.e. at a higher z axis position) were exposed to the blue end of the spectrum of chromatic focus points and areas on the sample surface that were further from the sensor (i.e. at a lower z axis position) were exposed to the red end of the spectrum. The resulting reflected light from the focal area was therefore mostly monochromatic with all other wavelengths out of focus. The reflected light was transmitted back through the fibre optic cable via a beam splitter (d) in the sensor head to a spectrometer (e) consisting of an optical pin hole, a spectrometer grating and a charge coupled device (CCD) sensor. The spectrometer analysed the spectral distribution of the reflected light by determining the position of maximum intensity on the CCD signal which correlates to the maximum wavelength peak of the received signal (f). Therefore the wavelength of peak intensity directly correlates with the average z axis position of the sample surface, within the area of the light spot projected onto the sample surface (Leach, 2010a; Sciences et Techniques Industrielles de la Lumière (STIL), 2007).

Figure 10 Schematic of the optical principles of the white light confocal sensor

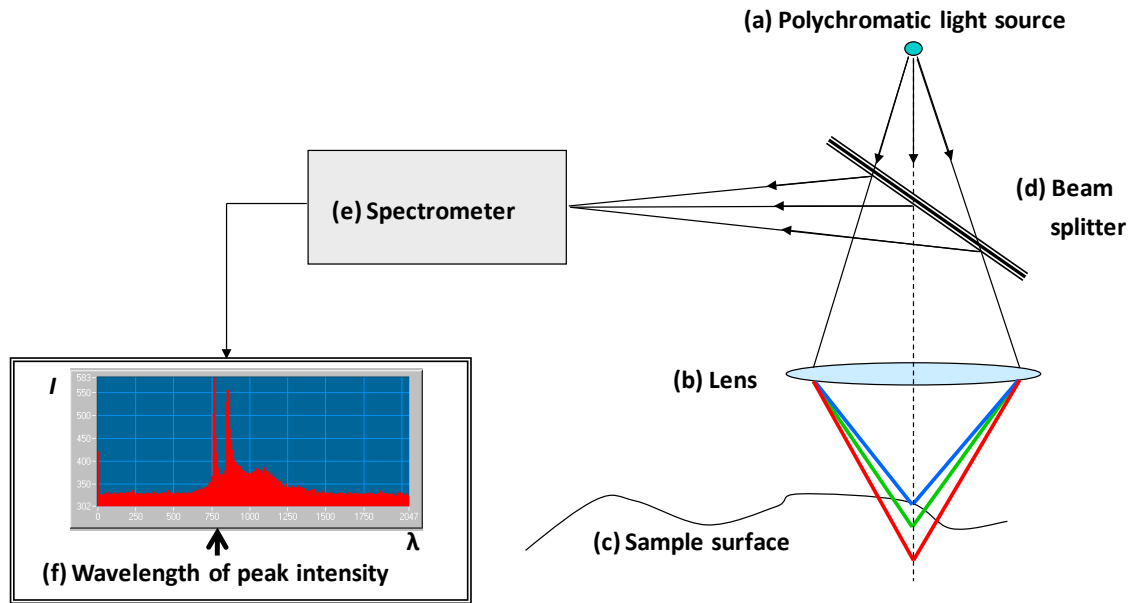


Table 3 below shows the nominal sensor specifications of the XYRIS™ 4000 white light confocal profilometer. The light spot on the measured surface had a diameter (spot size) of 7 μm , throughout the 350 μm z axis distance over which the sensor could operate (gauge range). The stand-off distance (z axis distance between the surface of the lens and the object surface, when the surface is brought to the centre of the sensor gauge range) was 12.7 mm and the minimum z axis distance increment that could be detected by the sensor was 10 nm (sensor resolution). As a result of the confocal chromatic length aberration principle, all sample surfaces can be measured with the exception of surfaces with an a surface angle greater than 30° and matte surfaces which exhibit entirely diffuse reflection such that the intensity of the reflected beam is less than 1 % of the incident light. Both of these surfaces result in no signal being detected by the CCD sensor and thus no z axis measurement was possible (XYRIS Series Precision 3D Surface Profilers Brochure, 2009), however in practice most surfaces exhibit both diffuse and specular reflection such that measurement ‘drop-out’ is rarely reported for white light confocal sensors (Boltryk et al., 2008; Boltryk et al., 2009).

Table 3 Nominal sensor specifications of the XYRIS™ 4000 white light confocal profilometer

Light Source	Spot size	Vertical resolution	Angular tolerance	Gauge Range	Stand-off distance	Sampling rate
Halogen	7 µm	10 nm	Approx. 30°	350 µm	12.7 mm	1/4/30 kHz

The white light confocal sensor and the motion control system were connected to a personal computer running Microsoft® Windows® XP SP2 with an Intel Pentium® 3GHz processor. The personal computer controlled the CWLP using the proprietary measurement control software (STAGES™, TaiCaan Technologies Ltd., Southampton, England).

STAGES™ software was used to control the measurement process. The object surface was brought into the gauge range and an areal measurement was carried out by moving the x/y stage over a specified measurement area, at a medium speed. The sample was moved line by line in a raster pattern from a specified negative x axis position to a specified positive x axis position (i.e. from left to right) whilst individual data points are allocated a z co-ordinate (according to the sensor output) and x/y co-ordinates (according to the motion controller output) at every 10 µm in the x axis. Thus a single line profile of data points is recorded, following which the sensor stopped data capture whilst the x/y stage moved the sample rapidly back to the x axis start position. From here, a new y axis start position was chosen, 10 µm from the initial start point and the sensor renewed data capture whilst the next line profile is swept out from left-to-right. This is repeated for a specified length in the y axis a resulting in a 'point cloud' of individual data points each 10 µm apart from each other. The 3D data is then saved in ASCII format as a .tai filename for later data analysis by the chosen software.

Prior to a detailed investigation of validity of the CWLP for *in vitro* tooth wear measurement, a pilot investigation was conducted in order to determine the ideal measurement speed and x/y spacing settings, following which a 'medium' scanning speed and a 10 x 10 µm x/y measurement spacing was chosen. These settings were chosen as optimal, because this speed and spacing represented an ideal balance between optimum scanning time and instrument

accuracy. As seen in Figure 75 on page 220 of Appendix 1 below, the time taken for the white light confocal profilometer to scan a 15 mm^2 measurement area at $10 \times 10 \text{ }\mu\text{m}$ x/y measurement spacing at 'medium' measurement speed was 8 minutes, whilst Figure 76 on page 221 of Appendix 1 below shows that the mean accuracy of the white light confocal profilometer at measuring a Taylor-Hobson $0.39 \text{ }\mu\text{m}$ and a $2.64 \text{ }\mu\text{m}$ step height reference standard $10 \times 10 \text{ }\mu\text{m}$ at x/y measurement spacing at 'medium' measurement speed was $0.04 \text{ }\mu\text{m}$. Therefore, these settings represented an optimal balance between scanning time and instrument accuracy, whilst also ensuring that the measurement spacing approximated the area of the light spot (a circular area with a minimum diameter of $7 \text{ }\mu\text{m}$). Therefore maximal information about the surface topography could be collected whilst maintaining optimal instrument performance, whilst all sources of instrument error were investigated in detail.

2.1.2.1 Quantification of flatness and noise errors

The flatness error of an instrument is the planarity deviation when measuring a perfect plane. The effect of the flatness error of the white light confocal profilometer on surface topography measurement can be assessed by examining the waviness of the measured surface of a perfect plane, as seen in Section (c) of Figure 11 below. Noise error is unwanted data affecting the resolution of the measurement system. Noise error can result from external environmental sources (e.g. lack of cleanliness; draughts; temperature gradients and vibrations) or from internal equipment sources (e.g. machine defects, electronic noise or quantisation) (BIPM et al., 2008). The effect of the noise error of the white light confocal profilometer noise can be assessed by examining the roughness of the measured surface of a perfect plane, as seen in Section (d) of Figure 11 below.

Figure 1 consists of four panels. Panel (a) is a 3D surface plot of the TaiCaan specimen, showing its complex, porous structure. The height is color-coded, with a vertical color bar on the left ranging from -0.0005 mm (dark blue) to 0.0003 mm (dark red). The specimen is labeled 'TaiCaan 5.0 mm x 3.0 mm 501 x 301'. Panels (b), (c), and (d) are line plots showing the height profile of the specimen along its length (0.0 to 5.0 mm). Panel (b) shows a red line plot with high-frequency oscillations. Panel (c) shows a green line plot with lower-frequency oscillations. Panel (d) shows a blue line plot with high-frequency oscillations. All three line plots have a y-axis labeled 'Height (mm)' ranging from -0.0005 to 0.0003 and an x-axis labeled 'Length (mm)' ranging from 0.0 to 5.0.

Figure 12 Photograph of the National Physical Laboratory optical flat



91

flatness errors, the scanned surface of the optical flat would have a maximum limit of variation between two parallel planes enclosing all measurement points (i.e. the Sz parameter), should be around 0.025 μm . If the measurement instrument had zero noise errors the scanned surface of the optical flat would have a root mean square length of the scale limited surface of around 0.00306 μm .

Therefore, to assess the flatness and noise of the measurement system over the entire measurement area (10 cm x 10 cm), the optical flat was placed onto the aluminium mounting block and scanned in four positions across the stage (top right, bottom right, bottom left, top left).

Three scans were carried out of the optical flat, in each of the four positions and the resulting 3D (areal) surface profile was analysed with Mountains[®] surface analysis software (Version 5.1.1.5374; SARL Digital Surf, 16 rue Lavoisier, 25000 Besançon, France). The software was used to first level the 3D profile using a best-fit plane, following which the flatness contribution to the measurement uncertainty was evaluated by quantifying the surface texture parameter Sz (the maximum 3D height (ISO 25178-2, 2010)) of the waviness of the surface, after a 500 μm Gaussian filter had been applied. After levelling the 3D profile using a best-fit plane, noise was evaluated by the surface texture parameter Sq (root mean square of the 3D height (ISO 25178-2, 2010)) of the roughness of the surface after a 500 μm Gaussian filter had been applied. Finally, a mean (SD) and maximum Sq and Sz of the overall surface was calculated.

2.1.2.2 Quantification of enamel and dentine shrinkage errors

In order to assess the effect of partial dehydration on the dimension stability of worn enamel and dentine, enamel and dentine samples were firstly prepared as described below.

In line with UK legislation (Human Tissue Act, 2004) and guidelines (Good practice in research and consent to research, 2010; HTA Codes of Practice, 2009) regulating activities concerning the removal, storage, use and disposal of human tissue in the UK, teeth were sourced for use

in the studies that form Chapters 3, 4 and 5 of this thesis. In order to achieve this, ethical approval for the research was sought from a local research ethics committee (King's College Hospital NHS Foundation Trust Research Ethics Committee Approval reference 09/H0808/109). Once granted, Research and Development approval was sought from both King's College Hospital NHS Foundation Trust (where the teeth were donated) and from Guy's and St. Thomas' NHS Foundation Trust (where the laboratory work was carried out). Once this was granted a Material Transfer Agreement between the two NHS partner sites (King's College Hospital NHS Foundation Trust, Denmark Hill, London, SE5 9RS and Guy's and St. Thomas' NHS Foundation Trust, Great Maze Pond, London, SE1 9RT) was sought in order to safely transfer the human tissue approximately 3.2 miles across South-East London.

In order to source suitable teeth for the research, potential subjects for tooth donation were sought from patients attending for an assessment appointment at the Oral Surgery Department at King's College Hospital NHS Foundation Trust, prior to undergoing routine extractions of their third molars (required for the enamel and dentine samples in these studies) or premolars (required for the enamel attrition antagonists in these studies). Those patients who needed one or more of their teeth extracted were invited to participate in the study by the clinician from the oral surgery department who was taking first stage clinical consent at this assessment appointment. All clinicians who were identifying potential subjects had been provided with information and training by the research team in order to ensure that the clinicians could identify suitable subjects (according to the principle inclusion and exclusion criteria for recruitment of participants to donate extracted teeth for the research study '*Protection of erosive wear*' as shown in Table 4 below) and to ensure that the clinicians were familiar with the proposed research work so that they would be able to answer any questions that subjects may have at that stage.

Table 4 Principle inclusion and exclusion criteria for recruitment of participants to donate extracted teeth for the research study ‘Protection of erosive wear’

Principle inclusion criteria
Adults aged 18-65
Patients who need teeth extracted for clinical reasons
The teeth free from dental caries
Able to provide written informed consent
Principle exclusion criteria
Patients aged > 18 years or < 65

At this assessment appointment a copy of the participant information sheet (Appendix 2 Patient Information Sheet (PIS) for donation of extracted teeth) was administered to the potential participant. At the subsequent appointment (for the extractions of the teeth), any further questions were answered and subjects were asked to confirm consent to allow their extracted teeth to be used for this research, by completing an informed consent form (Appendix 3 Informed Consent Form (ICF) for donation of extracted tooth) by a member of the research team. Patients who changed their mind about participating in the research were able to do so without the decision affecting their clinical care.

Once consent had been obtained the teeth were then extracted following normal procedures. The extracted teeth were then collected by the research team and anonymised (i.e. there was to be no link to the patient because samples were anonymised after collection and no personal data was to be collected or stored). From this point onwards, no further participation from the donor was required and their participation in the study was completed. Following their collection, the teeth were placed for 1 hour in a 5 % sodium hypochlorite solution (20000 ppm available chlorine) before being placed in a de-ionized water container for transfer to the Department of Biomaterials located on Floor 17 of Guy's Tower, King's College London Dental Institute, Guy's and St. Thomas' NHS Foundation Trust, London Bridge, SE1 9RT.

After transfer to the laboratory, 5mm x 3mm x 2mm sections of enamel and dentine were subsequently prepared from the mid-coronal portion of the buccal and lingual surfaces of the

teeth, using a diamond wafering blade (XL 12205, Benetec Ltd., London, UK). Samples were embedded in a self curing bis-acryl composite (Protemp™4, 3M ESPE, Seefeld, Germany) using a hard-anodized aluminium and brass sample former (Syndicad Ingenieurbüro, München, Germany) as shown in Figure 13 below.

Figure 13 Photograph of the hard-anodized aluminium and brass sample former used to embed enamel and dentine sections in bis-acryl composite



Following sample forming, an outer layer of 400 µm of enamel (for the enamel samples) or approximately 1 mm of enamel and dentine (for the dentine samples) was removed by grinding and polishing the samples in a water-cooled rotating polishing machine (Meta-Serv 3000 Grinder-Polisher, Buehler, Lake Bluff, Illinois, USA) following a standardised grinding-polishing protocol developed specifically for these studies. Custom made polishing jigs were constructed from bis acryl composite (Protemp™4, 3M ESPE, Seefeld, Germany). These jigs allowed the samples to be held face down in a sample holder attached to a semi-automated polishing head (Vector LC Power Head, Buehler, Lake Bluff, Illinois, USA) during polishing. The polishing head applied 10 N of constant force to each sample whilst ensuring that the samples were consistently held perpendicular to the polishing disc, which itself was rotating in a contra-direction to the polishing head. Copious water irrigation was used whilst the samples were sequentially polished with 500, 1200, 2400 and 5000 grit silica carbide discs (Versocit, Struers A/S, Copenhagen, Denmark).

Finally, in order to create protected reference areas, adhesive polyvinyl chloride tape was placed over the sides of the enamel and dentine samples, thus creating an exposed window of 3 mm x 3 mm of the polished sample surface which became the area subjected to the experimental wear.

Two enamel and two dentine samples were then pre-worn using the attrition and erosion-attrition model as described in Section 3.2.3 below. This resulted in attrition and erosion-attrition lesions with dimensions covering the range likely to be seen in the tooth wear studies of this thesis (i.e. an approximate depth of 1 μm to 15 μm for enamel and 5 μm to 50 μm for dentine). Following a 24 hour storage period, during which the samples were kept completely immersed in deionized water, the samples were removed and placed in a weigh boat next to a temperature and humidity data logger (EL-USB-2, Lascar Electronics, Module House, Whiteparish, Salisbury, Wiltshire, UK. SP5 2SJ). This arrangement allowed the temperature and humidity data logger to record the change in the humidity of the air in the immediate proximity of the enamel and dental samples whilst they were repeatedly scanned, during which time the samples dehydrated through moisture loss. The data logger measured and stored relative humidity (RH) readings over a measurement range of 0 to 100% RH. The specifications stated that for humidity measurements the typical accuracy was $\pm 3.0\%$ RH and the maximum Overall Uncertainty was $\pm 6.0\%$ RH.

The samples were scanned three times every five minutes with each sample scanned 20-four times, therefore the total dehydration and measurement time was two hours. A relative humidity logging rate of one measurement per minute was recorded whilst the measurements were taking place. After the two hours dehydration time the samples were then rehydrated for a further 20 four hours and rescanned. This cyclical process was then repeated a third and final time.

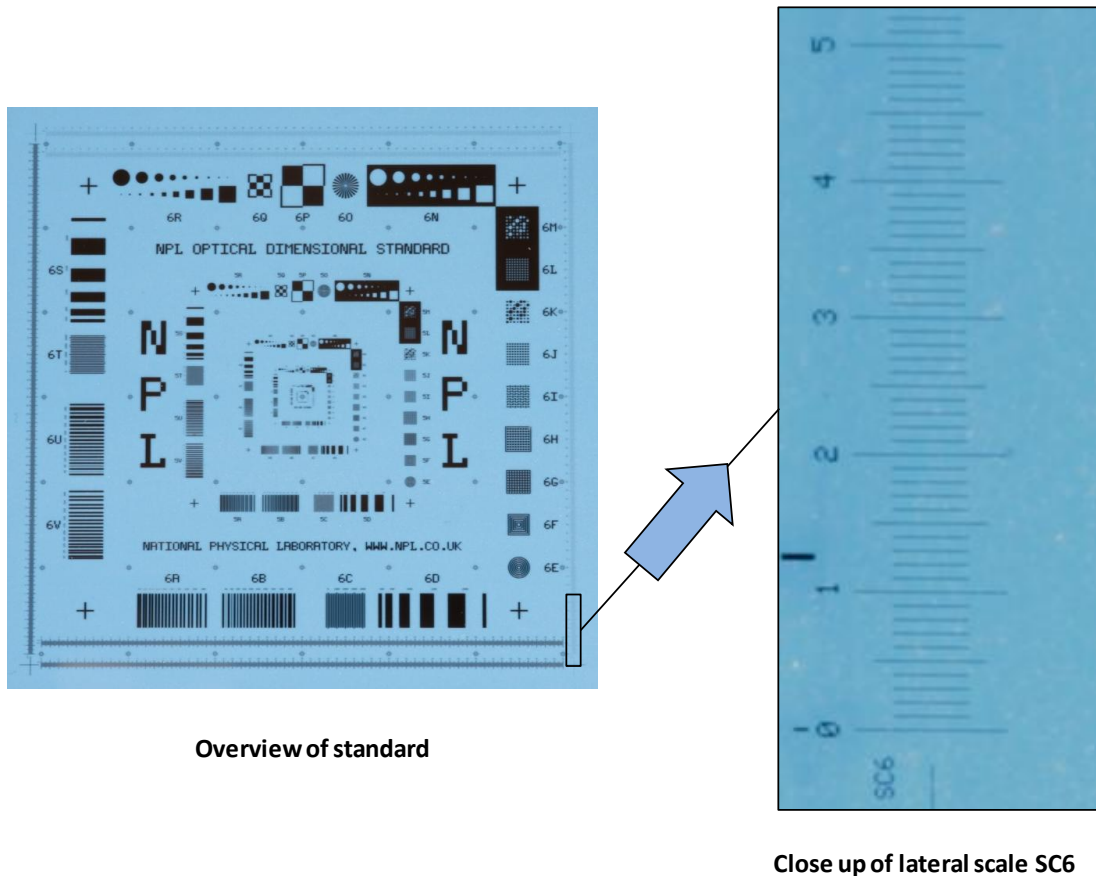
Once the measurements were complete, the stored relative humidity data was downloaded from the data logger using the supplied software under Windows XP. Relative humidity was

then graphed, printed and exported to Excel software for comparison with change in step height and volume measurements of each sample as the sample dehydrated over time. Step height and volume were calculated as described in Section 2.1.2.5 above and a mean (SD) of the three scans was outputted over time.

2.1.2.3 Quantification of lateral (x, y) scale linearity errors

An example of a linearity error on the lateral scale would be a measurement result that was not directly proportional to the qualities of an item of known length, for example a ruler or line scale. Linearity errors on the lateral scale can be assessed by carrying out a length measurement of a calibrated line scale, orientated parallel to the x and y axes. Figure 14 below shows an overview photograph of the National Physical Laboratory optical dimensional standard and a close up photograph of the lateral scale SC6 that was used to assess the contribution from linearity errors on the lateral scale, to the uncertainty of tooth wear measurement using the white light confocal profilometer.

Figure 14 Overview photograph of the National Physical Laboratory optical dimensional standard and close up photograph of the lateral scale SC6



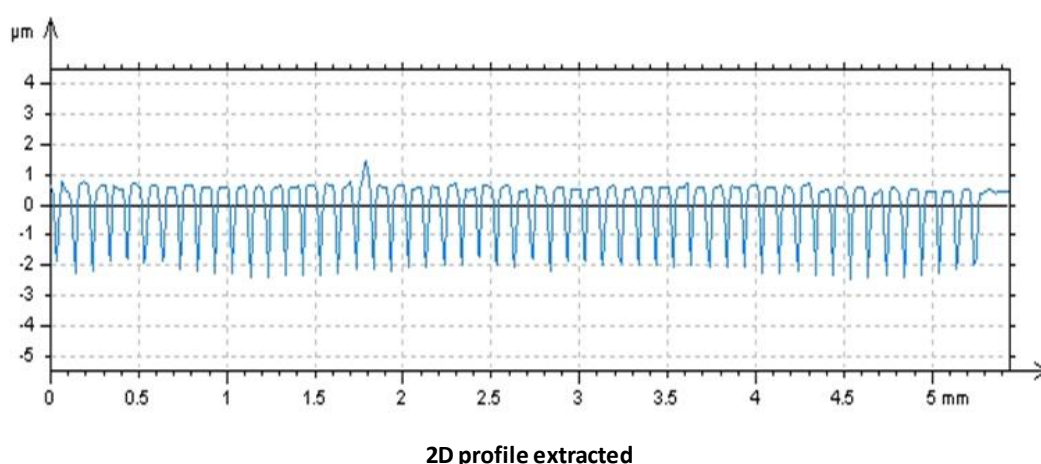
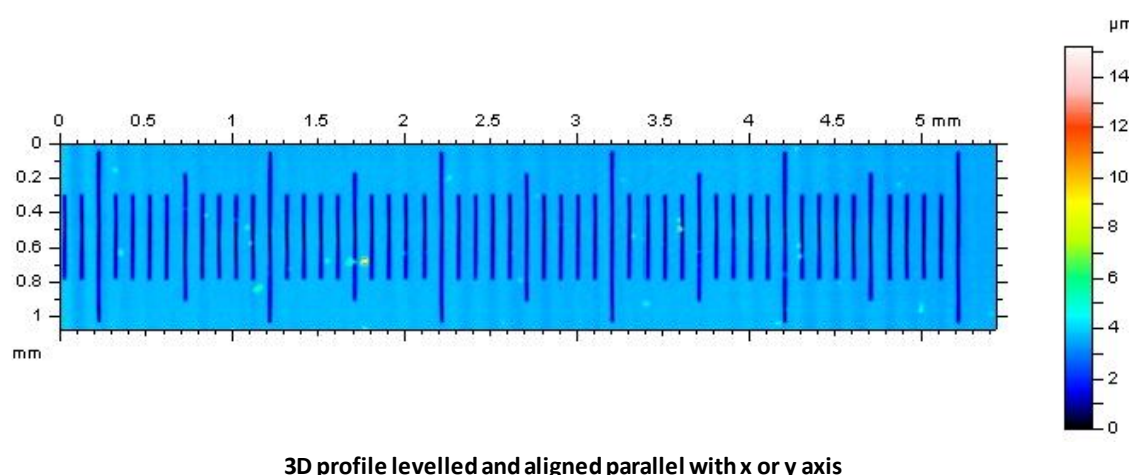
The National Physical Laboratory (NPL) optical dimensional standard is a correct reading, bright chrome on a 100 mm square quartz photomask. The dark areas seen in Figure 14 above indicate the opaque chrome layer on the quartz (which was placed against a blue background for the purposes of the photographs seen in Figure 14 above). 22 distinct patterns can be observed on the standard, which are scaled and repeated six times to enable the use of the standard at different magnifications, with an additional six linear scales and an x/y stage position calibration grid. The pattern that was used to quantify the non-linearity on the lateral scale was the vertical linear optical scale SC6 found on the bottom left of the standard, as seen in the close up photograph in Figure 14 above. All the quoted dimensions were in micrometres unless otherwise stated and all the scales were 60 mm in length, and the SC6 scale had a nominal line width of 10 μm . Every tenth line was 1 mm long and was numbered from 1-60. The nominal pitch was 100 μm and the fifth line between each numbered line was 0.75 mm

long (NPL Optical Dimensional Standard For Vision Machines & Microscopy Range 1 μm - 60 mm).

The NPL optical dimensional standard was placed onto the aluminium mounting block. Three repeated scans of the first 50 lines (i.e. a total length of 5 mm) of the SC6 lateral scale were carried out in four positions across the x/y stage (top right, bottom right, bottom left, top left), in order to quantify the contribution of non-linearity on the lateral scale over the entire x/y measurement range (10 cm x 10 cm). At each of these four positions the scale was scanned both in a vertically orientation (i.e. parallel with the y axis) and then the scale was repositioned in a horizontal orientation (i.e. parallel with the x axis), in order to evaluate non-linearity in both axes. At both orientations the scale was scanned three times.

The resulting 3D profiles were analysed with Mountains® surface analysis software (Version 5.1.1.5374; SARL Digital Surf, 16 rue Lavoisier, 25000 Besançon, France) and spreadsheet software (Microsoft® Office Excel® 2007, Microsoft® Corporation, USA). Figure 15 below shows a schematic of the image analysis workflow for the length measurement the NPL optical dimensional standard lateral scale SC6 using Mountains® surface analysis software. After levelling and fine alignment of the long axis of the scale with the x (or y axis), the 2D profile was extracted from the overall 3D profiles, thus creating a 2D profile as seen in the lower panel of Figure 15 below.

Figure 15 Schematic of the image analysis workflow for the length measurement the NPL optical dimensional standard lateral scale SC6 using Mountains® surface analysis software



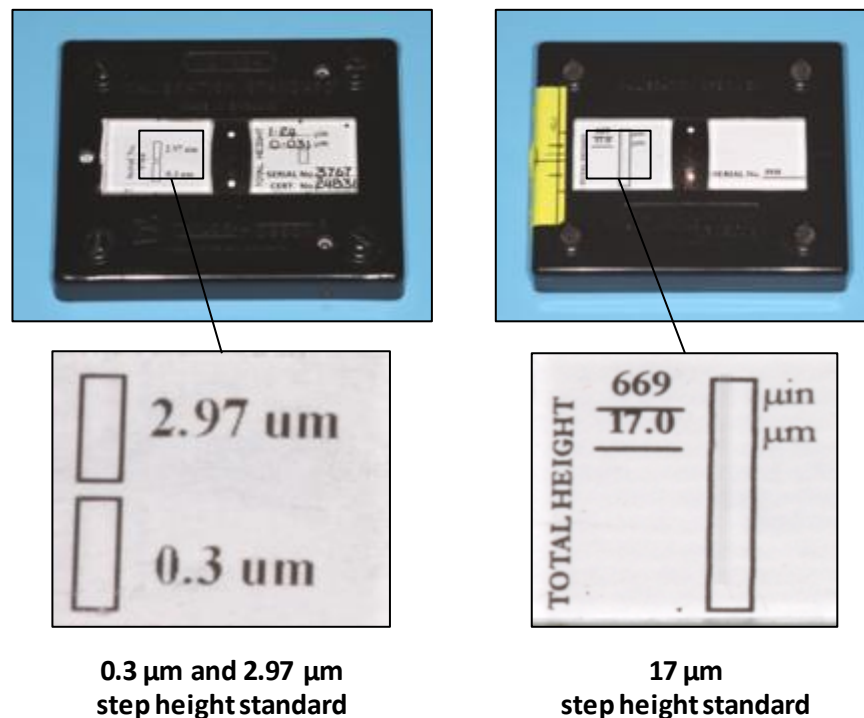
The raw 2D data was then pasted directly into spreadsheet software, in order to identify the central point of each of the 50 scanned lines on the lateral scale. This was carried out by means of a 'centre of gravity' analysis, whereby the x/y variables for each data point were analysed and the central point which represented the middle of each of the 50 lines was identified. Because each line on the line scale had a nominal width of 10 μm and each line was nominally 100 μm apart (from centre to centre), this central data point represented the measured result of each 100 μm length on the lateral scale. Finally, in order to determine the non-linearity of the lateral scale for each axis, a mean of the difference between the nominal position of the centre of each line on the lateral scale and the measured position of the centre of each line on the lateral scale was calculated.

2.1.2.4 Quantification of vertical (z) scale linearity errors

An example of non-linearity on the vertical scale would be in a measurement result of a known distance in the z axis (i.e. a vertical step) which was not directly proportional to the stated qualities of the step being measured. In order to quantify the non-linearity on the z scale, four calibrated type A1 step height reference standards were chosen (Taylor Hobson Ltd, Leicester, United Kingdom). These four step height reference standards were chosen with vertical steps of 0.3 μm , 2.97 μm , 17 μm and 30 μm , to match the range likely to be created by the tooth wear models described in the studies that form Chapters 3, 4 and 5 of this thesis.

Figure 16 below shows an overview and a close up photograph of the 0.3 μm , 2.97 μm and 17 μm step height reference standards that were used to assess the contribution from the linearity error on the vertical scale, to the uncertainty of tooth wear measurement using the white light confocal profilometer.

Figure 16 Overview and close up photographs of the 0.3 μm , 2.97 μm and 17 μm step height reference standards

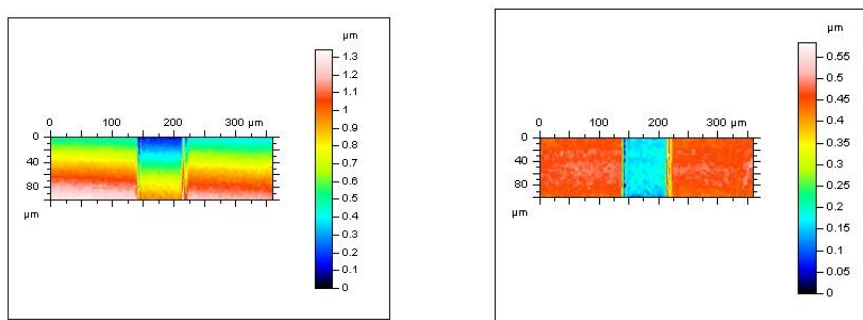


Each step height reference standard was placed onto the aluminium mounting block and three repeated scans of the central part of each step height were carried out, at three positions

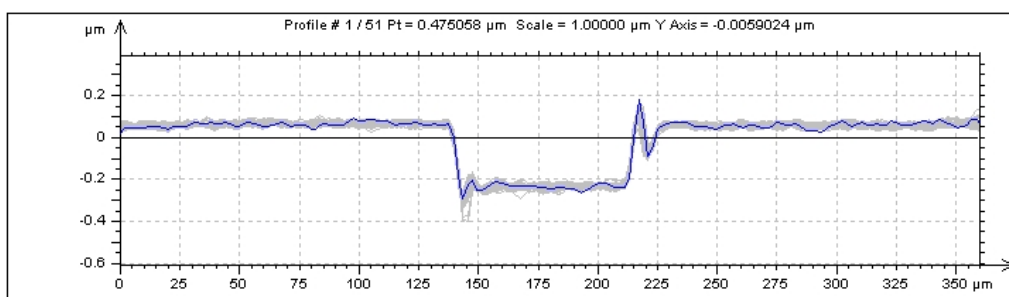
across the z stage (high, middle, low), in order to quantify the contribution of non-linearity on the vertical scale over the entire z axis measurement range (25 cm). At each of these three positions the step height reference standard was scanned three times.

The resulting 3D profiles were analysed with Mountains® surface analysis software (Version 5.1.1.5374; SARL Digital Surf, 16 rue Lavoisier, 25000 Besançon, France). Figure 17 below shows the workflow for the analysis of the 3D step height of the 0.3 µm step height reference standard using Mountains® surface analysis software. After levelling of 3D profile, the mean 3D profile was extracted and the mean 3D step height calculated, by comparing the mean height of the central third of the bottom of the step with the mean height of the central third of the reference plane. The surface analysis software specifically ignores the areas immediately adjacent to the step transitions, because of the high probability of artefacts/spikes in the step transition area.

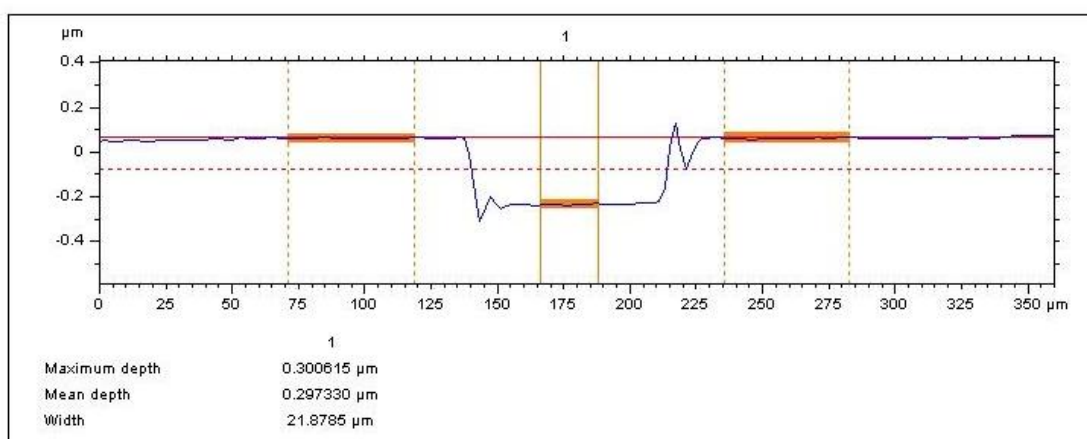
Figure 17 Analysis of the 3D step height of the 0.3 μm step height reference standard using Mountains® surface analysis software



3D profile opened and levelled



Mean 3D profile extracted



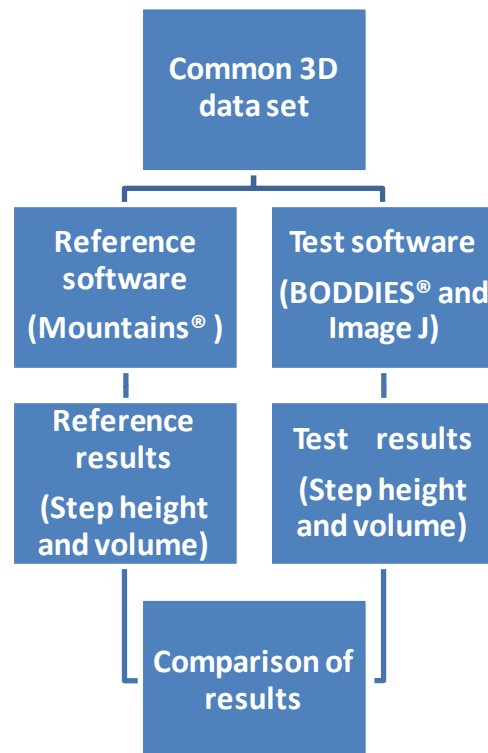
Mean 3D step height calculated

Thus three mean step height measurements were obtained for each reference standard at each of the three z axis positions (high, middle, low). Finally, in order to determine the non-linearity on the vertical scale, a mean of the differences between the nominal step height and the measured result was calculated.

2.1.2.5 Quantification of software errors

As shown in Figure 5 above, the choice of surface analysis software can influence the overall measurement uncertainty through factors such as parameter definitions and algorithms, filters and use of reference planes. A framework by which surface analysis software can be tested has been described by Blunt et al (2008) and the overall protocol for this is shown in Figure 18 below. This protocol involves the use of a common data set, which has the relevant surface features of interest (i.e. step height and volume loss) with known dimensions. The common data set is then input into both the test software and the specified reference software and the results of each are then compared. The difference is then expressed as the software error.

Figure 18 Framework for the validation of surface analysis software (after Blunt et al 2008)

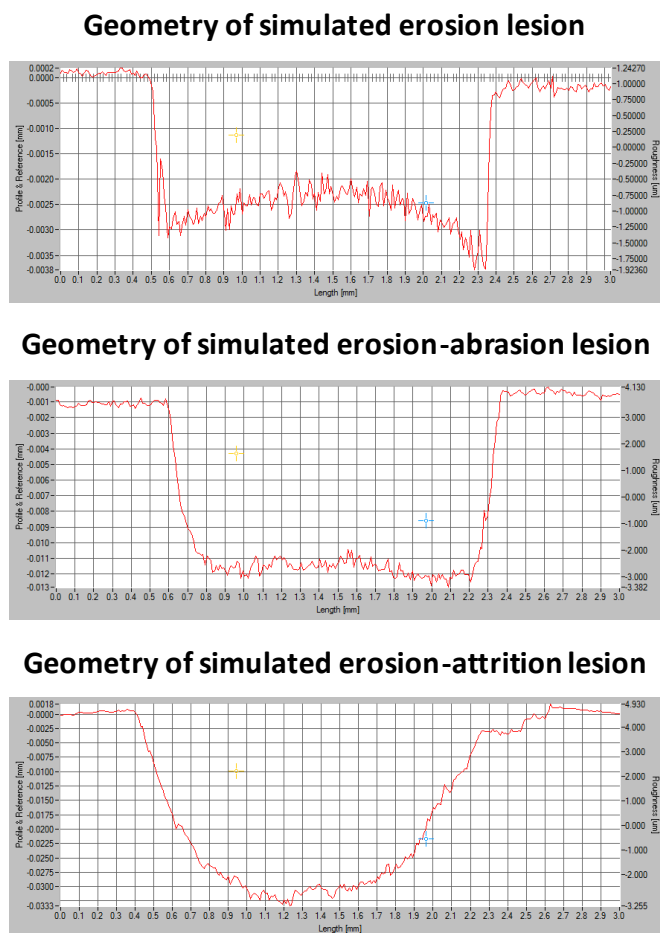


ISO 5436-2 (2001) describes the development and use of software measurement standards ('soft gauges') which are the common 3D data sets that can be used for validation of the software aspects of a measurement instrument. These soft gauges are essentially digital representations of a profile which contains the relevant surface feature of interest, which for this thesis was bulk wear of enamel and dentine, which can be quantified as either step height

(μm) or volume (μm^3) loss. Therefore the soft gauges would contain surface profiles (with known dimensions of step height and volume) with similar geometry to the lesions created in the enamel and dentine samples subjected to the *in vitro* tooth wear models described in Chapters 3, 4 and 5 below.

As shown in Figure 19 below, the overall geometry of these erosion, erosion-attrition and erosion-abrasion lesions can be described as steep-sided grooves or valleys with a flat (or slightly concave or convex) bottom, with varying depths of up to around $30\ \mu\text{m}$. Therefore the digital profiles used to create the common data sets would require surface features of similar geometry with known step height and volume dimensions.

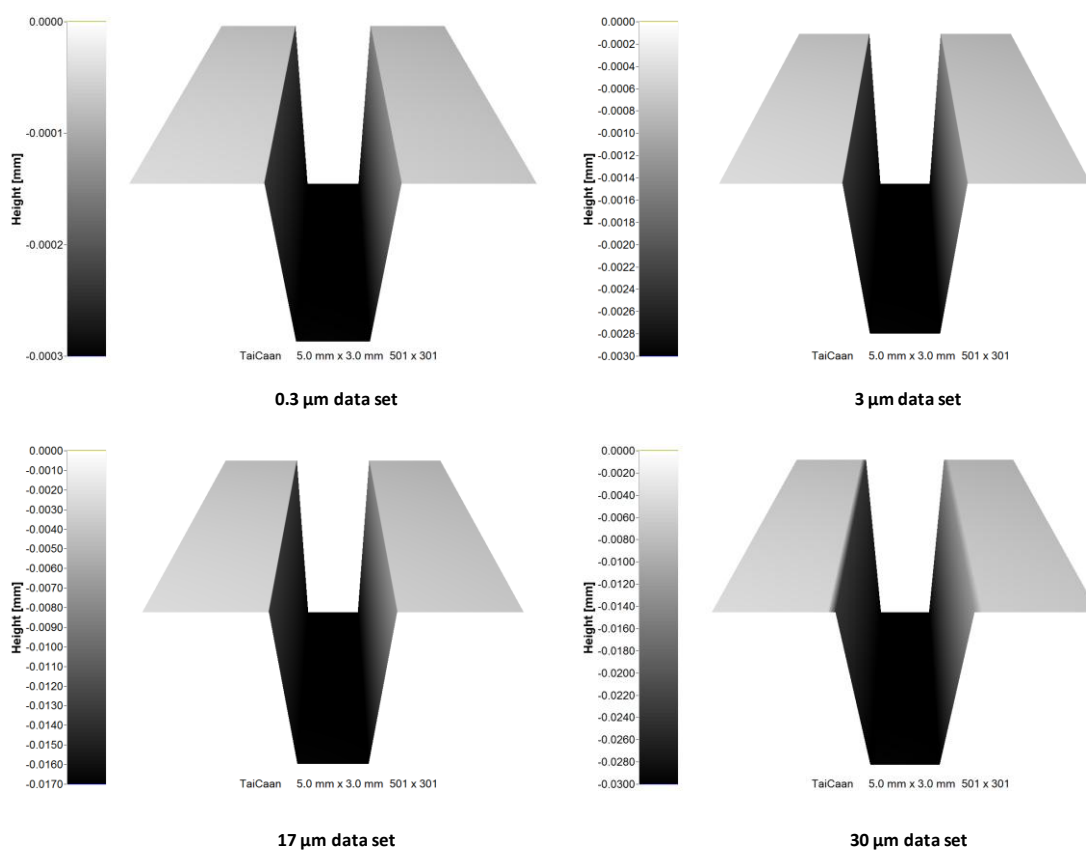
Figure 19 Profiles showing the typical geometry of erosion; erosion-abrasion and erosion-attrition lesions created by the *in vitro* tooth wear models used in this thesis



Therefore, 3D data sets were written using spread sheet software (Microsoft® Office Excel® 2007, Microsoft® Corporation, USA) and converted into ASCII format (which can be read and

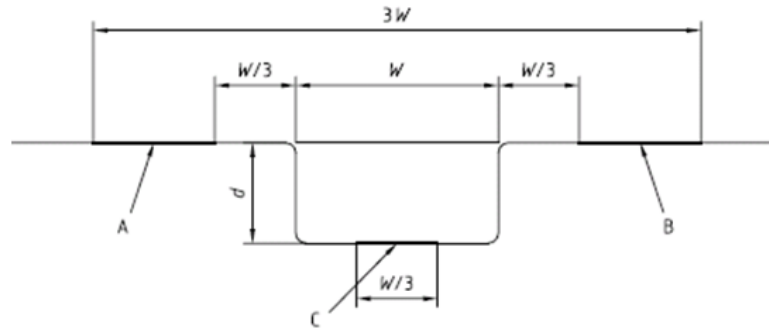
analysed by the reference and test surface analysis software). All enamel and dentine samples used in this thesis had an overall surface area of 5 mm (x axis) by 3 mm (y axis) and the reference areas created by the placement of the tape was standardised to ensure that only the central third of the enamel or dentine was exposed to tooth wear, thus resulting in an lesion of 1.67 mm (x axis) by 3 mm (y axis) with a depth (z axis) of 0 μm up to around 30 μm . Therefore, as seen in Figure 20 below, four data sets were digitally created following this geometry, with lesions of depth varying from 0.3 μm to 30 μm and with flat peripheral reference areas and central lesions of tissue loss, shaped as a steep sided groove with a flat bottom.

Figure 20 3D images of the 0.3 μm , 3 μm , 17 μm and 30 μm common 3D data sets ('soft gauges')



Mountains® surface analysis software (Mountains® Version 5.1.1.5374; SARL Digital Surf, 16 rue Lavoisier, 25000 Besançon, France) was chosen as the reference software for measurement of step height and volume loss. The ISO profile method for measurement of step height (ISO 3274 1996), as shown in Figure 21 below, was used to calculate the step height within Mountains® surface analysis software.

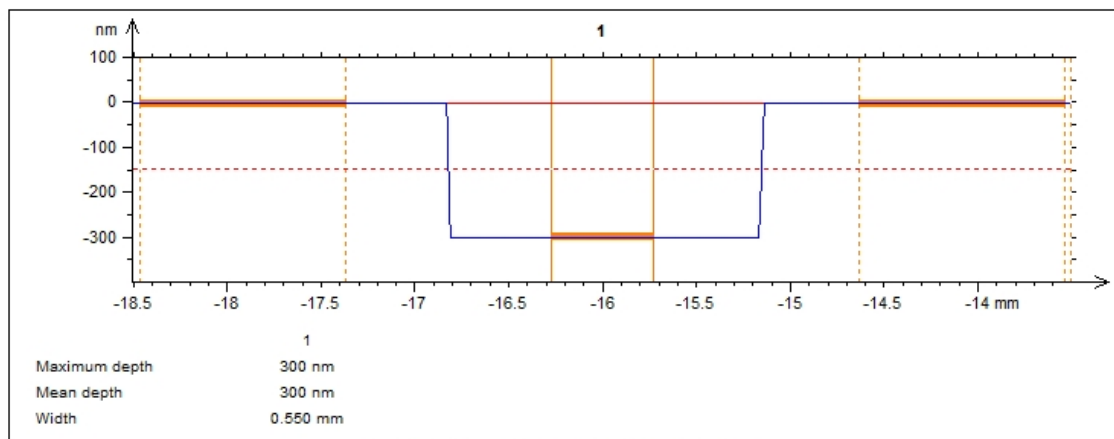
Figure 21 ISO profile method for measurement of step height (as defined by ISO 3274, 1996)



δ = Step height of groove
 W = Width of groove
 A = Section of reference area $W/3$ away from left edge of groove
 B = Section of reference area $W/3$ away from right edge of groove
 C = Middle central third of groove

After levelling the reference areas of the 3D profile to a best fit plane, the mean 3D profile of the data set was extracted. Using this mean 3D profile, the step height (δ) was then calculated by averaging the z height of the two sections of the reference area (A and B) either side of the groove. The mean z height of the middle central third of the profile of the groove (C) was then calculated and the difference between the two values was quantified as the step height δ as shown in Equation 3 below.

Figure 22 Schematic of the step height measurement technique of the 0.3 μm , 3 μm , 17 μm and 30 μm soft gauges using Mountains® reference software

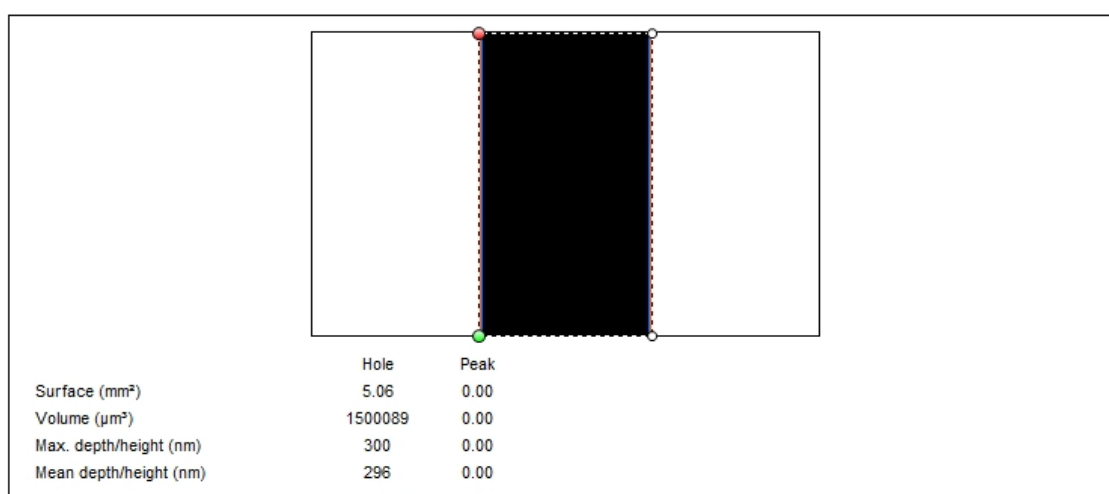


Equation 3 Formula for calculation of step height using Mountains® surface analysis software

$$\delta = ((A+B)/2) - (C)$$

For calculation of the volume of the 0.3 μm common 3D data set using Mountains® reference software, the entire groove was selected using the ‘measure volume of a hole’ function, by placing four markers at the corners of the groove, as shown in Figure 23 below. Finally, in order to ‘normalise’ the volume following previously published protocols (Rodriguez and Bartlett, 2010), the total volume was then divided by the total length in the y axis (3 mm) and the volume was expressed as $\text{M } \mu\text{m}^3/\text{mm}$.

Figure 23 Schematic of the volume measurement technique of the 0.3 μm , 3 μm , 17 μm and 30 μm soft gauges using Mountains® reference software



The test software for step height measurement were BODDIES® (BODDIES® v 2.09, TaiCaan Technologies Ltd., Southampton, UK) and a custom designed step height macro operating under ImageJ (ImageJ v1.42q, Rasband, W. S., U. S. National Institutes of Health, Bethesda, Maryland, USA).

The test software for volume measurement was a custom designed step height macro operating under ImageJ surface analysis software (ImageJ v1.42q, Rasband, W. S., U. S. National Institutes of Health, Bethesda, Maryland, USA).

For step height measurement with BODDIES®, the image analysis work flow was as follows. Images were firstly opened and levelled by removing a best fit plane from the reference (flat) areas of the reference standard. This ensured that the areas either side of the groove were

levelled to a zero plane in the z axis, so that the reference area surrounding the groove became a datum plane with an average z height value of 0. Data from the area of the groove (including the sides and the bottom of the valley) were then isolated by cutting off all data with a z height value ≥ 0 . All remaining data were exported to an Excel spreadsheet (Microsoft® Office Excel® 2007, Microsoft® Corporation, USA), where the mean z height value was calculated for all data points. This value represented the mean 3-dimensional step height of the entire groove in the step height reference standard, in relation to the flat reference area.

For step height and volume measurement with ImageJ macros, custom designed macros were written to automatically read and analyse the 3D data set by first opening the data set and converting it into a 32-bit floating-point greyscale image. The 3D data was thus converted into a 2D image with each pixel representing a data point according to the x/y co-ordinates of each of the 150801 (501 x 301) data points and each pixel allocated a grey scale value corresponding to the z height of the data point. Lighter grey values represented data points with a higher z value, therefore the light grey areas of the image corresponded to the flat peripheral areas and the dark grey areas of the image corresponded to the central groove. The lighter grey data points lying within the reference area were selected as reference points and the darker data points (i.e. those data points with a lower z value) were selected as data points in the area of the groove, which also included the sides and the bottom of the valley. The reference data points were then levelled to a zero plane in the z-axis.

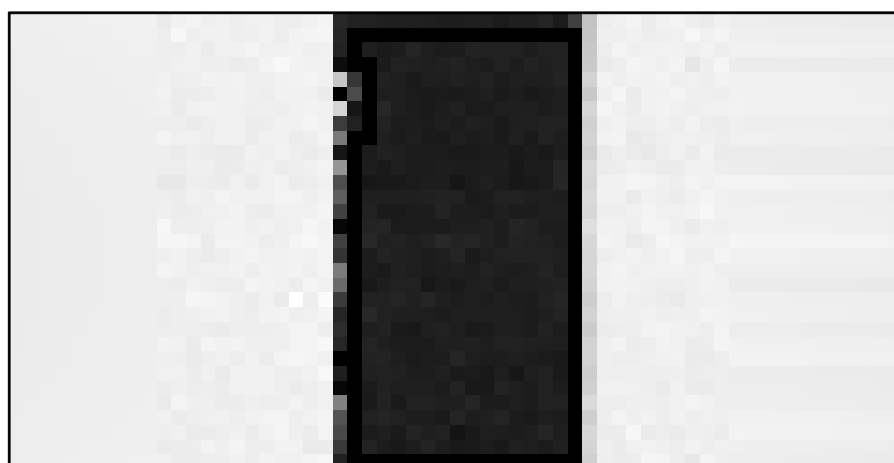
For step height calculation the ImageJ macro was written to calculate the mean z value for all reference points was calculated, which after levelling, should be zero or very close to zero if the identification of reference points and levelling had been carried out successfully. The mean z value of all the non-reference data points (i.e. the sides and wall of the groove) was then calculated and then finally the difference between these two mean z values (μm) was

determined. This z value difference represented the mean step height of the entire groove of the 3D data set, in relation to the flat reference area.

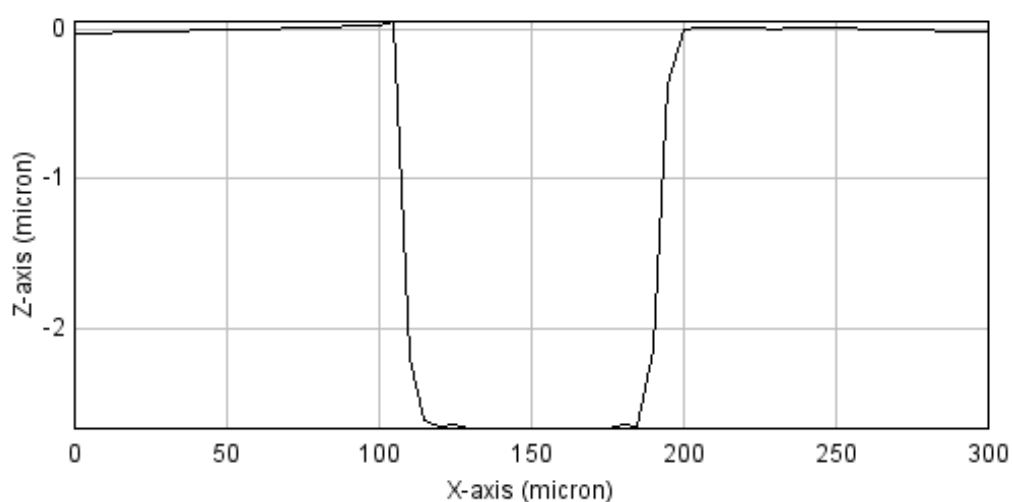
For volume calculation, once the ImageJ macro had carried out grey scale conversion, reference/non-reference identification and levelling as above the macro was written to isolate each one of the 301 y axis line profiles, which as seen in Figure 24 below, thus showed the cross section of the groove and reference plane.

Figure 24 Schematic of the image analysis workflow for calculation of the volume of the 0.3 μm , 3 μm , 17 μm and 30 μm soft gauges using ImageJ volume macro

32-bit greyscale image with reference area levelled and reference/groove areas isolated



Example of extracted profile



The volume macro then calculated the total area (μm^2) of each line profile using the trapezoidal method of integration. In order to derive the total volume of enamel loss (μm^3)

each area was integrated using the 2nd degree Newton–Cotes formulae. In order to ‘normalise’ the volume following previously published protocols (Rodriguez and Bartlett, 2010), the total volume was then divided by the total length in the y axis (3 mm) and the volume was expressed as million (M) $\mu\text{m}^3/\text{mm}$.

Finally, so that the three test software could be validated in comparison to the reference software, the step height and volume outputs from the BODDIES® and ImageJ software were compared with the step height and volume outputs from the Mountains® and ImageJ software.

2.1.2.6 Combine the Standard Uncertainties

Once the individual errors from the flatness deviations, noise, enamel and dentine shrinkage, non-linearity’s and software errors had been investigated and quantified, the Standard Combined Uncertainty of the white light confocal profilometer was then calculated, following a Type B uncertainty evaluation, as outlined in Part 3 of the British Standards Institute Published Document 6461 “*Guide to the Expression of Uncertainty in Measurement*” (GUM) (British Standard Institution, 1995).

As described in Clause 5 of the GUM (pp. 19 -20), the Type B uncertainty evaluation involves the creation of an ‘uncertainty budget’ which states the corresponding variance of the quantity value from each potential source of error. This value is expressed as the Standard Uncertainty. All Standard Uncertainty contributions were then combined and the resulting combined dispersion of values was described as the Standard Combined Uncertainty and in order to make the result understandable, universal and transferable, the Standard Combined Uncertainty was then expressed as a percentage related of the depth/volume of wear being measured.

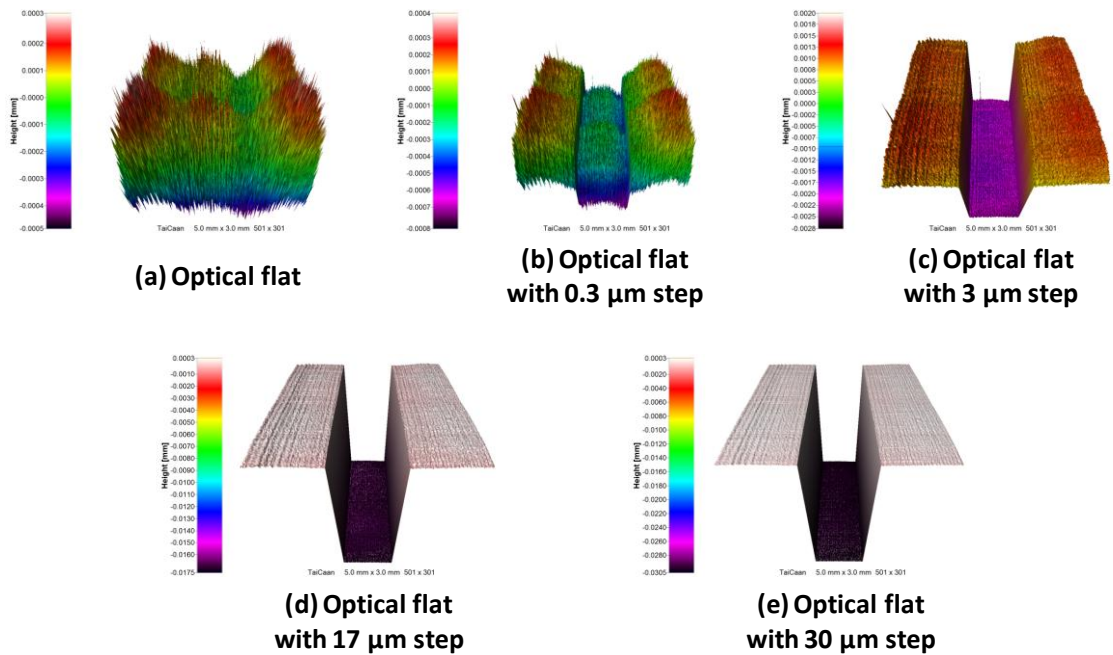
2.1.2.7 Determine the Overall Combined Uncertainty

The Standard Combined Uncertainty calculated in Section 2.1.2.6 above can be considered as the ‘worst case scenario’, whereby the maximum possible effect of the errors on the

uncertainty of measurement was estimated and expressed in percentage terms, according to the depth/volume of the wear being measured. However, in practice, this Standard Combined Uncertainty probably represents an overestimation of the effect of these errors on the measurement. This is partially due to the software reducing the impact of the Standard Uncertainty errors by averaging the result of each of the 301 individual line profiles contained within the overall 5 x 3 mm measurement area. Moreover, the software is designed to further reduce the measurement uncertainty by averaging the step height measurement technique (as shown in Figure 21 above) and normalising the volume measurement technique (as described in Section 2.1.2.5 above).

Therefore, a more realistic effect of the overall effect of all possible errors on the uncertainty associated with step height and volume measurements under the experimental conditions can be assessed by calculating the Overall Combined Uncertainty. This was carried out using the 3D data set created by scanning the NPL optical flat to create 'soft gauge reference standards' with nominally known varying dimensions. Figure 25 below shows 3D images of (a) the 3D data set that was created by scanning the optical flat. This 3D data set was then used to create the 0.3 μm , 3 μm , 17 μm and 30 μm soft gauge reference standards as shown in (b-e) in Figure 25 below. These soft gauges were subsequently used to determine the Overall Uncertainty associated with the step height and volume wear measurements using the white light confocal profilometer.

Figure 25 3D images of (a) the 3D data set created by scanning the optical flat and (b-e) the 0.3 μm , 3 μm , 17 μm and 30 μm soft gauge reference standards



These soft gauges were created by first taking the 3D data set shown in (a) of Figure 25 above, which resulted from a 5 mm x 3 mm scan of the optical flat, as described in Section 2.1.2.1 above. This baseline 3D data set contained all flatness, noise and linearity errors on the x, y and z scales that contributed to the Standard Uncertainty. Using this 3D data set, four simulated wear lesions were created using the ASCII file format to create soft gauges of x/y dimensions of 1670 μm x 3000 μm and z dimensions of 0 μm , 0.3 μm , 3 μm , 17 μm and 30 μm , as shown in (b-e) of Figure 25 above. These dimensions were chosen as they represented the range of geometries that were likely to be created by the tooth wear models used in Chapters 3, 4 and 5 of this thesis.

The step height and volume of these simulated wear lesions contained within these soft gauges was then measured using the BODDIES® (step height) software and ImageJ (step height and volume) macros as described in Section 2.1.2.5 above. These values were then compared with the known “true” values according to the specified x, y and z dimensions (width, length and height) of these cuboid simulated wear lesions that were written into the ASCII file data. The difference between the “true” values and the values from the BODDIES® and ImageJ

software was calculated for both step height and volume and the resulting error was entered into the Overall Uncertainty budgets (in the place of the flatness, noise and linearity errors in the Standard Uncertainties), as described in Section 2.1.2.4 above.

The resulting variances of each potential source of error were then combined, and described as the Overall Uncertainty for each potential source of error. Finally, as in Section 2.1.2.6 above, the Overall Combined Uncertainty was then related to the depth and volume of the wear lesion being measured and the result expressed as a percentage.

2.1.3 Results

2.1.3.1 Flatness and noise errors

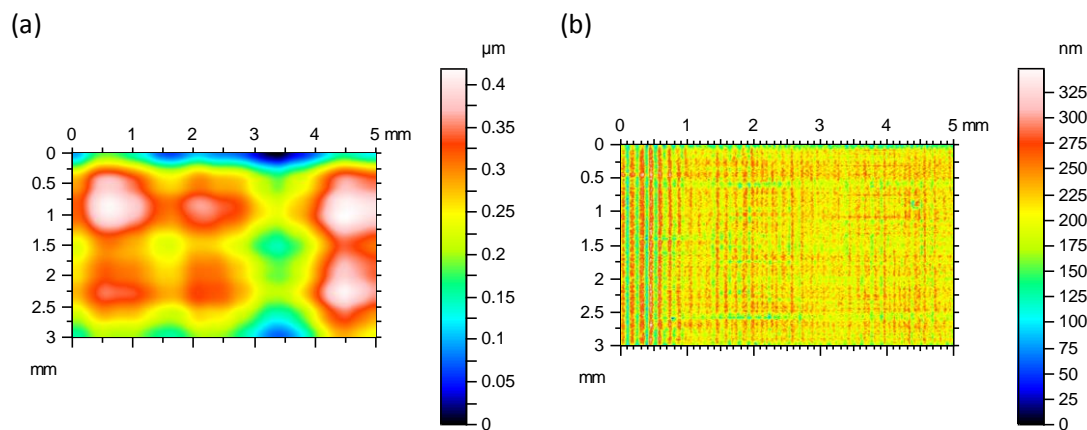
Table 5 below shows the mean (SD) and maximum Sz flatness error (μm) and Sq noise error (μm) of a 5 mm x 3 mm scanned area of the optical flat measured at different locations of the x/y stage. This table shows that the white light confocal profilometer had a mean (SD) 3D flatness error 0.33 (0.09) μm with a maximum flatness error of 0.49 μm over the entire x/y stage. The white light confocal profilometer had a mean (SD) noise error of 0.05 (0.002) μm with a maximum noise error over the entire x/y stage of 0.08 μm .

Table 5 Mean (SD) and maximum Sz flatness error (μm) and Sq noise error (μm) of a 5 mm x 3 mm scanned area of the optical flat measured at different locations of the x/y stage

Measurement position on the x/y stage	Sz flatness error (μm)	Sq noise error (μm)
Bottom left	0.46 (0.03)	0.04 (0.00)
Bottom right	0.24 (0.03)	0.07 (0.00)
Top left	0.26 (0.00)	0.04 (0.00)
Top right	0.33 (0.02)	0.05 (0.00)
Mean (SD)	0.33 (0.09)	0.05 (0.02)
Maximum	0.49	0.08

These flatness and noise errors can be visualised by reference to Figure 26 below which shows representative images of the 3D scans of the optical flat that were analysed with Mountains® surface analysis software in order to assess (a) the flatness errors and (b) the noise errors that contributed to the measurement uncertainty of the white light confocal profilometer.

Figure 26 Representative images of the 3D scans of the optical flat analysed with Mountains® surface analysis software to assess (a) the flatness errors and (b) the noise errors



In Image (a) of Figure 26 above, the flatness deviation from a perfect plane can be seen in the 3D profile of the waviness of the surface. The waviness of this profile shows a deviation from a perfect plane (flatness error) which takes the form of apparently regular 'hills' and 'dales' and has a maximum height of the scale limited surface (S_z) of 0.42 μm. In Image (b) of Figure 26 above, the roughness profile shows a noise error takes the form of an apparently regular criss-crossed pattern which runs parallel to the x and y axis and this has a root mean square height of the scale limited surface (S_q) in the order of 0.04 μm. As discussed in Section 2.1.2.1 above, because a perfectly flat plane cannot exist, even the optical flat has some residual inherent planarity deviations. Therefore, if the white light confocal profilometer had zero flatness errors, the S_z result should be around 0.03 μm and if the white light confocal profilometer had zero noise errors, the S_q result of around 0.003 μm.

2.1.3.2 Enamel and dentine shrinkage errors

Figure 27 below shows the mean percent change (%) of the relative humidity and measured step height of the pre-worn enamel (n =2) and dentine (n =2) samples over time. This shows that over the 360 minute study period, during which three cycles of sample dehydration/rehydration were carried out (with each cycle = 120 minutes) the relative humidity decreased in the immediate environment around the samples over a period of around 30 minutes as the samples initially dehydrated and the immediate environment around the samples. The relative humidity in the immediate environment around the samples increased as the samples were rehydrated. Over the first dehydration cycle, the measured step height of the enamel samples initially increased as the relative humidity decreased/plateaued. The enamel step height subsequently returned to zero change as the enamel samples were rehydrated in deionized water (thus increasing the relative humidity). Subsequent dehydration and rehydration cycles resulted in further step height increases of the enamel sample, which reached a maximum change of 0.03 % over the entire experiment period. In contrast, the measured step height of the dentine samples remained relatively constant over the first dehydration cycle; however as the dentine samples were rehydrated and subsequently dehydrated over time, a decrease in the measured step height was observed, which reached a maximum change of 0.008 % over the entire study period.

Figure 27 Mean percent change (%) of the relative humidity and measured step height of pre-worn enamel (n =2) and dentine (n =2) samples over time

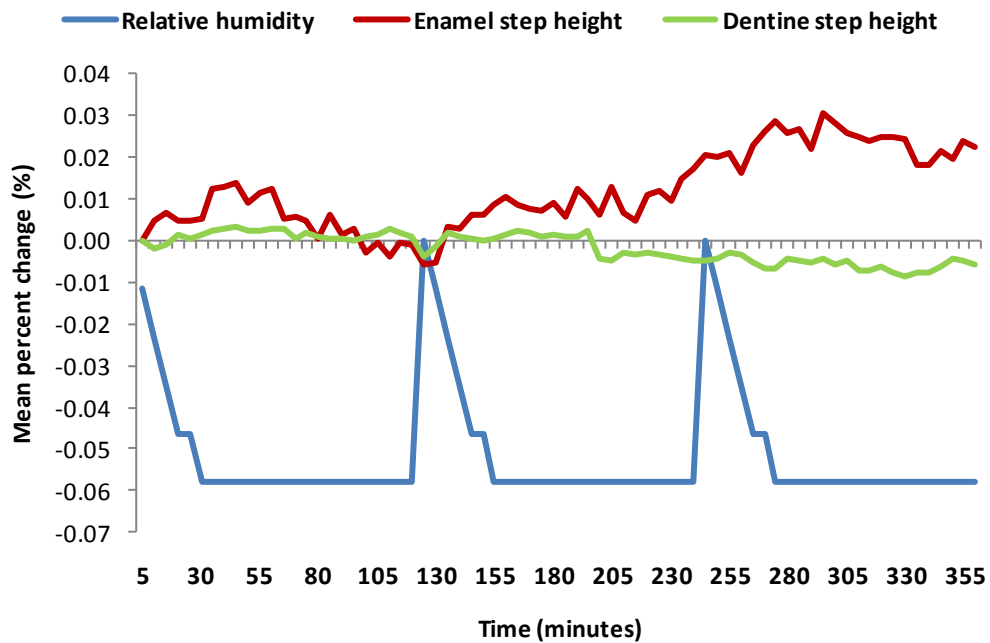
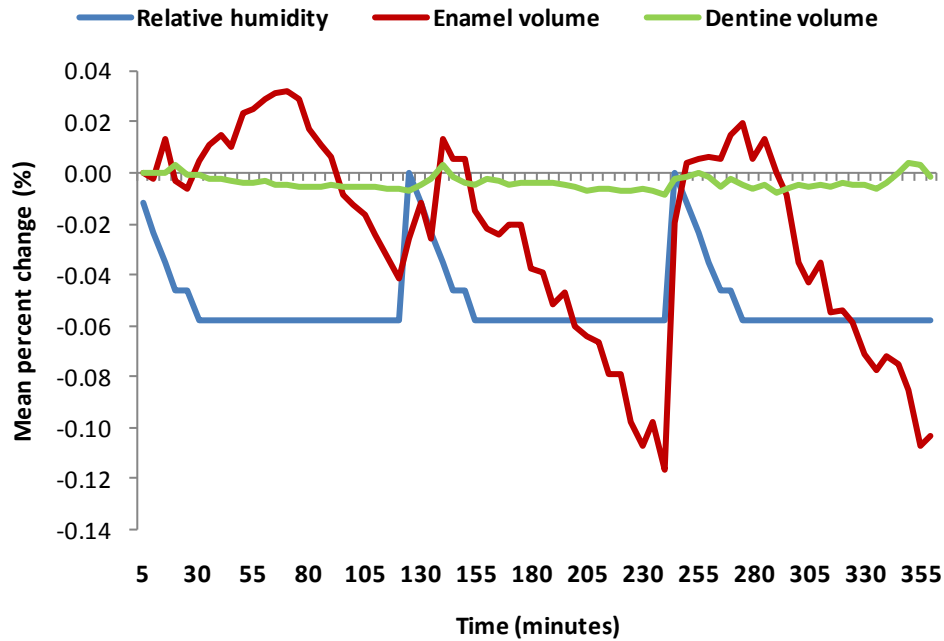


Figure 28 below shows the mean percent change (%) of the relative humidity and measured volume of pre-worn enamel (n =2) and dentine (n =2) samples over time during which three cycles of rehydration and dehydration of the samples was carried out (each cycle = 120 minutes). This figure shows the measured volume of the enamel samples initially increased and then decreased over the first dehydration cycle as the relative humidity decreased and then plateaued. On rehydrating the enamel samples in the deionized water, the measured volume was observed to increase until the relative humidity plateaued once the samples had again dehydrated. The measured volume of the enamel samples subsequently decreased until the samples were rehydrated. Subsequent rehydration and dehydration was observed to cause a similar increase and decrease in the measured volume. Over the entire study period these volume changes reached a maximum change of 0.12 %. Again in contrast to the enamel samples, the measured volume of the dentine samples remained relatively constant over all three dehydration/rehydration cycles, to reach a maximum change of 0.008 % over the entire study period.

Figure 28 Mean percent change (%) of the relative humidity and measured volume of pre-worn enamel (n =2) and dentine (n =2) samples over time



2.1.3.3 Lateral (x,y) scale linearity errors

Figure 29 and Figure 30 below show the mean (SD) linearity error (μm) over 5 mm linear distance in the x and y axis respectively. From these Figures, it can be seen that in both axes, the non-linearity is almost 0 μm at the start and end of the measurement however this non-linearity increased as the central portion of the lateral scale was reached. Thus the non-linearity reached a maximum of 10.22 μm in the x axis and 12.14 μm in the y axis.

Figure 29 Mean (SD) linearity error (μm) on the x axis over 5 mm linear distance

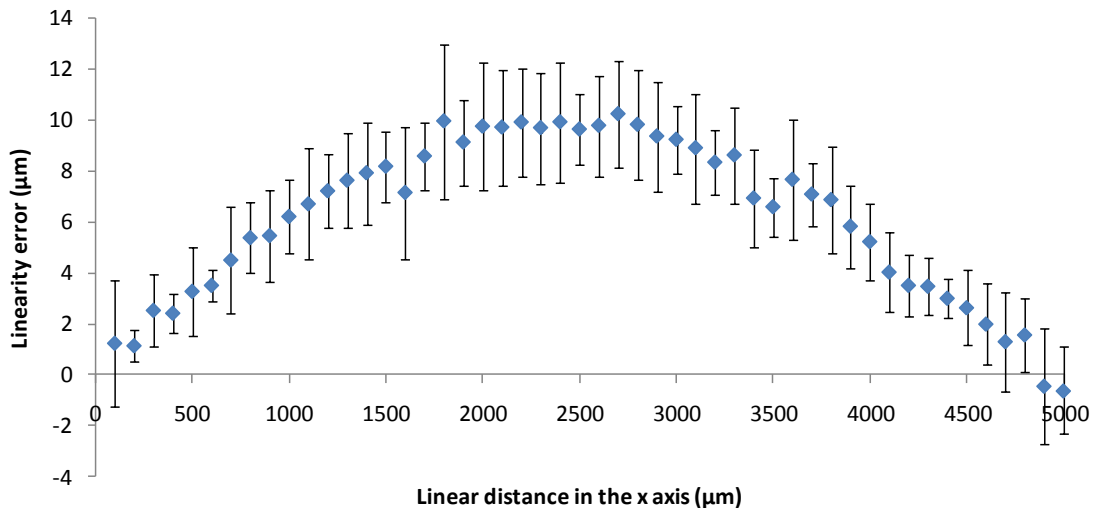
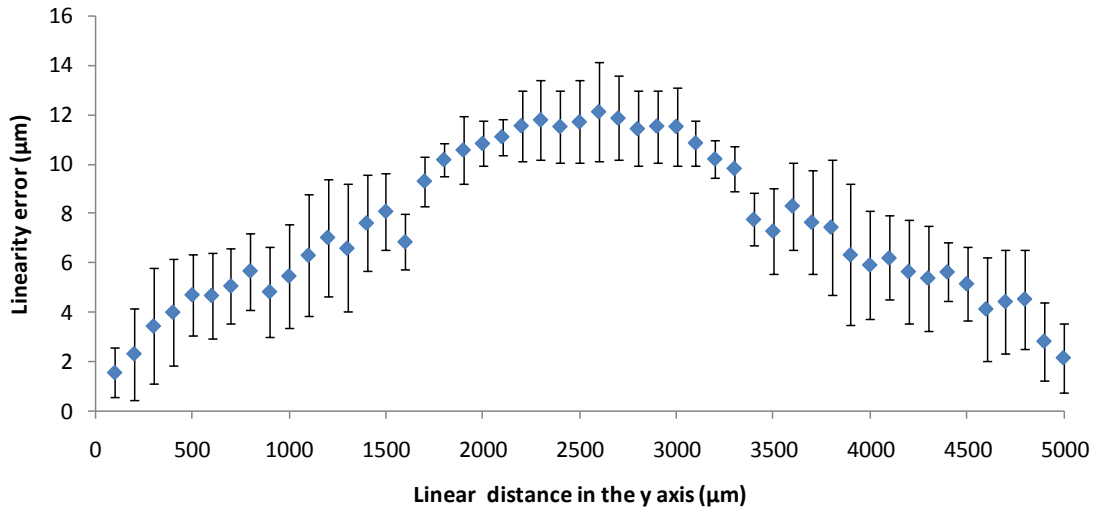


Figure 30 Mean (SD) linearity error (μm) on the y axis over 5 mm linear distance



2.1.3.4 Vertical (z) scale linearity errors

Table 6 below shows the mean (SD) linearity error (μm) on the vertical scale over step heights of 0.3 μm , 2.97 μm , 17 μm and 30 μm . From this Table, it can be seen that the difference between the certified mean step height and the Mountains® step height results varied between 0.01 μm (for the 2.97 μm SH standard) and 0.01 μm (for the 17 μm SH standard). This difference did not vary at any of the ‘low’, ‘medium’ or ‘high’ z axis positions. Converting the overall non-linearity error on the vertical scale into a percentage error revealed that the relative size of this error increased as the total step height being measured decreased. Therefore this measurement error was as high as 10 % during the measurement of the 0.3 μm step height reference standard and this error decreased to 0.007 % during the measurement of the 30 μm step height reference standard.

Table 6 Mean (SD) linearity error (μm) on the vertical scale over step heights of 0.3 μm , 2.97 μm , 17 μm and 30 μm

Certified mean step height (μm)	Mean (SD) Mountains® result (μm)	Non-linearity error on the vertical scale (μm)	Percent error (%)
0.30	0.27 (0.00)	0.03	10.00
2.97	2.96 (0.00)	0.01	0.34

17.03	16.99 (0.00)	0.04	0.23
30.04	30.06 (0.04)	0.02	0.007

2.1.3.5 Software errors

Table 7 below shows the BODDIES® software error (μm) associated with the step height measurement of 0.3 μm , 3 μm , 17 μm and 30 μm soft gauges, in comparison to Mountains® software. This shows that the test and reference software returned results which had perfect agreement and therefore the software error associated with this measurement was 0 μm .

Table 7 BODDIES® software error (μm) associated with the step height measurement of 0.3 μm , 3 μm , 17 μm and 30 μm soft gauges, in comparison to Mountains® software

Step height of soft gauge (μm)	Mountains® result (μm)	Mean (SD) BODDIES® result (μm)	BODDIES® SH error (μm)
0.3	0.30	0.30 (0)	0
3	3.00	3.00 (0)	0
17	17.00	17.00 (0)	0
30	30.00	30.00 (0)	0

Table 8 below shows the ImageJ step height (SH) macro software error (μm) associated with the step height measurement of 0.3 μm , 3 μm , 17 μm and 30 μm soft gauges, in comparison to Mountains®. This shows that the test and reference software returned results which had perfect agreement and therefore the Image J SH macro error associated with this measurement was 0 μm .

Table 8 ImageJ step height (SH) macro software error (μm) associated with the step height measurement of 0.3 μm , 3 μm , 17 μm and 30 μm soft gauges, in comparison to Mountains® software

Step height of soft gauge (μm)	Mountains® result (μm)	Mean (SD) ImageJ SH macro result (μm)	ImageJ SH macro error (μm)
0.3	0.30	0.30 (0)	0
3	3.00	3.00 (0)	0
17	17.00	17.00 (0)	0
30	30.00	30.00 (0)	0

Table 9 below shows the ImageJ volume (Vol) macro software error ($\text{M } \mu\text{m}^3/\text{mm}$) associated with the volume measurement of 0.3 μm , 3 μm , 17 μm and 30 μm soft gauges, in comparison to Mountains® software. This shows that the difference between the test and reference software results varied between 970.36 $\text{M } \mu\text{m}^3/\text{mm}$ and 96998.88 $\text{M } \mu\text{m}^3/\text{mm}$ as the size of the soft gauge increased from 0.3 μm to 30 μm . Converting the ImageJ Vol macro error into a percentage error revealed that the relative size of this error was constant at 0.19 % of the total volume being measured.

Table 9 ImageJ volume (Vol) macro software error ($\text{M } \mu\text{m}^3/\text{mm}$) associated with the volume measurement of 0.3 μm , 3 μm , 17 μm and 30 μm soft gauges, in comparison to Mountains® software

Step height of soft gauge (μm)	Mountains® result ($\text{M } \mu\text{m}^3/\text{mm}$)	Mean (SD) ImageJ Vol macro result ($\text{M } \mu\text{m}^3/\text{mm}$)	ImageJ Vol macro error ($\text{M } \mu\text{m}^3/\text{mm}$)	Percent error (%)
0.3	500030	501000 (0)	970.36	0.19
3	5000333	501000 (0)	9666.71	0.19
17	28335000	28390002 (0)	55001.54	0.19
30	50003000	50099999 (0)	96998.88	0.19

2.1.3.6 Standard Combined Uncertainty

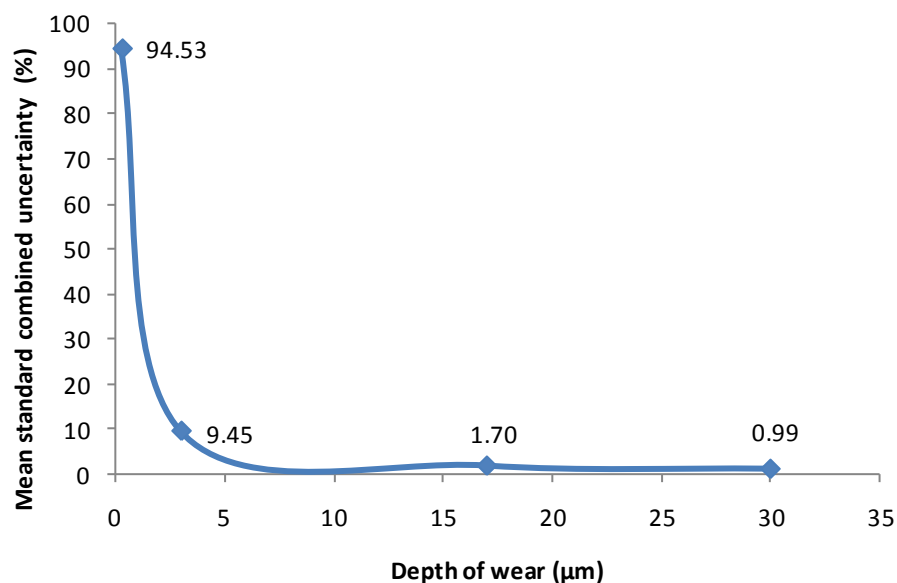
Table 10 below shows the standard combined uncertainties associated with the step height (μm) and volume ($\text{M } \mu\text{m}^3/\text{mm}$) measurements of 0.3 μm , 2.97 μm , 17 μm and 30 μm step height reference standards. This shows that that for step height and volume measurement, the standard uncertainty in μm and $\mu\text{m}^3/\text{mm}$ remained at around the same values, even as the measured z height increased. Therefore, for step height values, this value was 0.28 μm and for volume this value was 850000 to 855000 $\text{M } \mu\text{m}^3/\text{mm}$. Therefore, as the depth of the wear increased, the standard uncertainty of measurement stayed around the same value for both types of measurement.

Table 10 Standard combined uncertainties associated with the step height (μm) and volume ($\text{M } \mu\text{m}^3/\text{mm}$) measurements of 0.3 μm , 2.97 μm , 17 μm and 30 μm step height reference standards

Step height of reference standard (μm)	Standard Combined Uncertainty of step height measurement (μm)	Standard Combined Uncertainty of volume measurement ($\text{M } \mu\text{m}^3/\text{mm}$)
0.3	0.28	850725.29
2.97	0.28	850299.18
17	0.28	851606.83
30	0.28	855394.59

These step height (μm) and volume ($\text{M } \mu\text{m}^3/\text{mm}$) uncertainties were then converted into the mean percent Standard Combined Uncertainty (%) of both step height and volume and plotted by the depth of wear (z axis height) being measured (μm), as seen in Figure 31 below. This figure shows that as the depth and volume of the wear increased, the mean (%) Standard Combined Uncertainty decreased.

Figure 31 Mean Standard Combined Uncertainty (%) of the step height and volume measurement using the white light confocal profilometer by the depth (z axis height) of the wear (μm) being measured



Therefore this evaluation revealed that when the depth and volume of a 0.3 μm deep tooth wear lesion was measured, the uncertainty associated with the measurement would be almost 95 % of the 'true' value. However, there would be less than 1 % uncertainty associated with the depth and volume measurement of a 30 μm wear lesion.

2.1.3.7 Overall Combined Uncertainty

The Standard Combined Uncertainty method for evaluating the uncertainty can be considered as the 'worst case scenario', whereby the maximum possible effect of all errors on the uncertainty of measurement was expressed. However, in practice, the effect of the flatness error on the step height and volume measurements under the experimental conditions can be more realistically assessed though the use of 'soft gauges' with known 'true' dimensions. As shown in Figure 25 above, these soft gauges were created by modifying a 3D image that had been created from the measurement of an optical flat. Therefore this baseline image contained all the flatness and noise errors that were inherent in the system. The subsequently created 0.3 μm , 3 μm , 17 μm and 30 μm simulated wear lesions were then used to determine the Overall Combined Uncertainty associated with the step height and volume measurement.

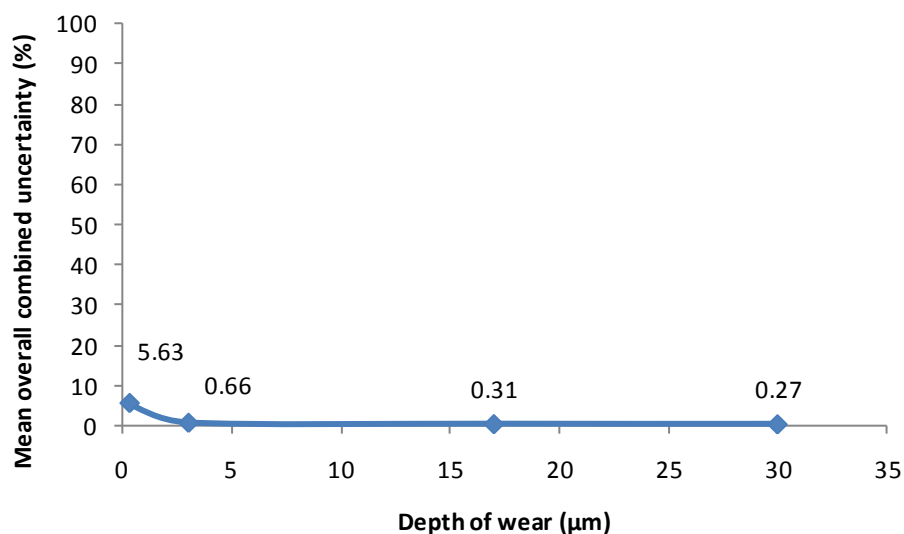
Table 11 below shows the Overall Combined Uncertainty associated with step height (μm) and volume ($\text{M } \mu\text{m}^3/\text{mm}$) measurement of 0.3 μm , 3 μm , 17 μm and 30 μm soft gauge reference standards. Therefore for step height and volume measurement, the standard uncertainty for step height values was 0.02 μm for all z height values and for volume this value ranged from 85000 to 730000 $\text{M } \mu\text{m}^3/\text{mm}$ as the z height values increased.

Table 11 Overall Combined Uncertainty associated with step height (μm) and volume ($\text{M } \mu\text{m}^3/\text{mm}$) measurement of 0.3 μm , 3 μm , 17 μm and 30 μm soft gauge reference standards

Step height (μm)	Step height Overall Combined Uncertainty (μm)	Volume Overall Combined Uncertainty ($\text{M } \mu\text{m}^3/\text{mm}$)
0.3	0.02	84729.41
2.97	0.02	111748.83
17	0.02	421341.71
30	0.02	725280.08

These step height (μm) and volume ($\text{M } \mu\text{m}^3/\text{mm}$) uncertainties were then converted into the mean percent Overall Combined Uncertainty (%) of both step height and volume plotted by the depth of wear (z axis height) being measured (μm). The results of this Overall Combined Uncertainty can be seen in Figure 32 below. This Figure shows that as the depth of the wear increased, the mean Overall Combined Uncertainty decreased, such that the mean Overall Combined Uncertainty was highest (5.63 %) when measuring a simulated depth of wear of 0.3 μm and subsequently decreased sharply as the depth of simulated wear increased.

Figure 32 Mean Overall Combined Uncertainty (%) of the step height and volume measurement using the white light confocal profilometer by the depth (z axis height) of the wear (μm) being measured



2.2 Section 2.2: Validity of microhardness measurement

2.2.1 Introduction

In order to validate the Leitz-Wetzlar Miniload 2 Microhardness Tester (Ernst Leitz GMBH, Wetzlar, Germany) that was to be used to measure Knoop microhardness in this study, the accuracy and precision of the tester was determined.

Accuracy of a measurement system is a quantitative term relating to the ability of a measuring system to provide a quantity value close to the true value of the object being measured (ISO, 2004). Therefore accuracy is greater when the quantity value is closer to the true value and in practice often relates to a comparison between a mean of a set of repeat measurements and the “true” value. Precision is defined as ‘closeness of agreement between measured quantity values obtained by replicate measurements on the same or similar objects under specified conditions’ (ISO 3534-1 1993). Further, the concept of precision encompasses both repeatability and reproducibility, since repeatability is "precision under repeatability conditions (i.e. the same conditions of measurement)," and reproducibility is "precision under reproducibility conditions (i.e. different conditions of measurement)" (BIPM et al., 2008; ISO

3534-1 1993). A comparison of these measurement conditions is shown in Table 12 below and in practice; repeatability and reproducibility may be expressed quantitatively in terms of the dispersion characteristics of the results under the stated conditions of measurement.

Table 12 Varying conditions of measurement used in order to determine the repeatability and reproducibility of a measurement instrument, as described in the International Vocabulary of Metrology (BIPM et al., 2008)

Repeatability conditions	Reproducibility conditions
Same measurement procedure	Different principle or method of measurement
Same observer	Different observer
Same measuring instrument	Different measuring instrument
Same conditions	Different conditions of use
Same location	Different location
Repetition over a short period of time.	Repetition of measurement at a different time

2.2.2 Aim, objectives and null hypothesis

Therefore the aims of Section 2.2 was to:

- Determine the accuracy and precision of the Knoop microhardness tester.

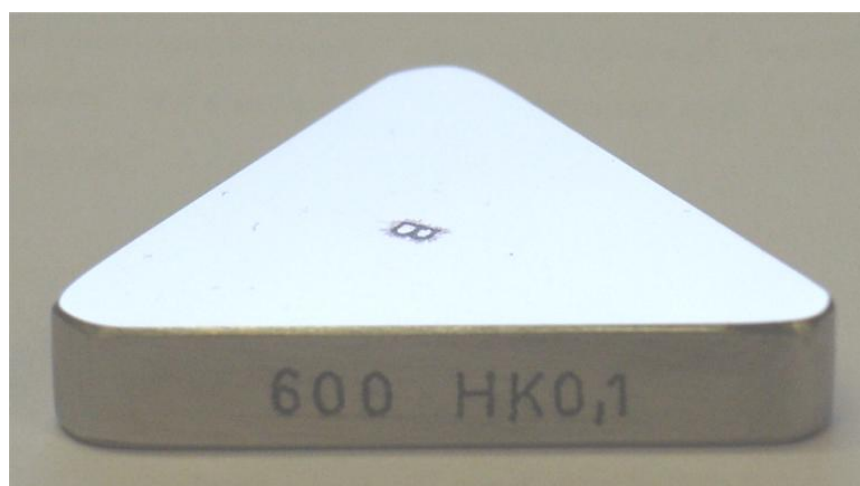
The null hypothesis was that:

- The Knoop hardness tester was neither accurate nor precise.

2.2.3 Materials and methods

In order to assess the accuracy of the Leitz-Wetzlar Miniload 2 Microhardness tester (Ernst Leitz GMBH, Wetzlar, Germany) described in Section 1.3.3 above, a calibrated transfer-standard block was sourced (Staatliches Materialprüfungsamt Nordrhein-Westfalen, Dortmund, Germany). As shown in Figure 33 below, the transfer-standard block was a triangular shaped block of metal with its upper surface mirror-polished flat in order to provide an ideal test surface.

Figure 33 Photograph of the transfer-standard block used to assess the accuracy and precision of the microhardness tester



The transfer-standard block had printed on one side its nominal Knoop hardness number (KHN) which was 600 KHN. The calibration certificate supplied with the transfer-standard described the measurement parameters and values that were used in order to determine the “true” microhardness of the block (DIN 51303, “Haertevergleichsplatten fuer die Pruefung statisher Haertepruefgeraete”, Deutsches Institut fuer Normung e. V., September, 1983). These measurement settings are shown in Table 13 below.

Table 13 Measurement settings used to determine the “true” microhardness of the transfer-standard block as stated in the calibration certificate

Parameter	Value
Application time	10 seconds
Load	100 g (981 mN)
Approximate speed of the indentation body	≤ 0.1 mm/s
Number of indentations	5
Spacing between indentations	100 μ m

Using this information regarding the measurement conditions, the accuracy of the hardness tester was evaluated as follows. The transfer-standard block was placed on the x/y stage of the tester, immediately below an x 100 magnification lens for pre-selection of the indentation site. Once the site was chosen, the Knoop diamond indenter was positioned over the sample and a 100 g (981 mN) tester load was applied. The Knoop indenter was a diamond formed into an

elongated rhombic based pyramid such that an indentation with one diagonal seven times longer than the shorter diagonal was created on the sample surface. Once ready for indentation, the automatic mechanism for slow release of the load was triggered and the indenter was pressed into the surface of the sample for 10 s. After the force had been removed, the x stage micrometer was used to move the sample 100 µm to the left and further four indentations were made. After completion of five indentations, the long diagonals (mm) of the resulting indentations were each measured using an x 500 magnification lens with an integrated micrometer.

On completion of indentation and measurement, the mean Knoop hardness number (KHN) of the five indentations of the test machine was calculated according to the American Society for the Testing of Materials (ASTM) formula for calculation of the Knoop Hardness Number (KHN), as shown in Equation 4 below.

Equation 4 The American Society for the Testing of Materials (ASTM) formula for calculation of the Knoop Hardness Number (KHN)

$$KHN = \frac{F}{C_P L^2}$$

Where F is the load (kg) and L is the length of the long diagonal (mm). C_P is the indenter constant which, as shown in Equation 5 below, is 0.07028 for an indenter with ideal geometry (α angle of 172.5° and β angle of 130° between the opposite edges of the vertex of the diamond).

Equation 5 Indenter constant defined by the angulation of the opposite edges of the vertex of the Knoop diamond indenter

$$C_P = \frac{\tan(\beta/2)}{2\tan(\alpha/2)}$$

The accuracy was then quantified by comparing this mean KHN value of the hardness tester with the “true” mean KHN derived from the calibration certificate, as a percent difference.

In order to assess the repeatability of the hardness tester, the coefficient of variation of these five Knoop hardness values, made as described above under repeatability conditions (i.e. measurements made in the same way over a short time period), was calculated and expressed as a percentage.

In order to assess the reproducibility of the hardness tester, the five Knoop hardness measurements were repeated, as described above, however after a time interval of 24 hours. These measurements were then repeated over the following three days to result in measurements taken at five time intervals under reproducibility conditions (i.e. measurements made in the same way with each group of five measurements made at time intervals of 24 hours). The coefficient of variation of these five mean Knoop hardness values was then calculated and expressed as a percentage.

2.2.4 Statistical analysis

Accuracy was expressed as the percent difference between the mean and standard deviation of the five measurements taken under repeatability conditions and the “true” value provided from the calibration certificate, and a statistical significance between the values was calculated using a two- sample t-test with $p < 0.05$ regarded as statistically significant.

Repeatability and reproducibility were expressed quantitatively by calculating the coefficient of variation of the five measurements made under repeatability conditions and the coefficient of variation of the means of the five groups of five measurements made under reproducibility conditions. Both repeatability and reproducibility results were then expressed as a percentage.

2.2.5 Results

As seen in Table 14 below, the mean (SD) Knoop microhardness values (KHN) of the transfer-standard block using the Leitz-Wetzlar microhardness tester was 560.64 (5.5) and the mean (SD) of the Knoop microhardness values (KHN) from the calibration microhardness tester (as provided in the calibration certificate) 599.97 (5.0). This 6.6 % difference between the two

results was statistically significant ($p = 0.009$) and therefore the accuracy of the Leitz-Wetzlar microhardness tester was 39.33 KHN.

Table 14 Knoop microhardness values (KHN) of the transfer-standard block using the Leitz-Wetzlar microhardness tester and the calibration microhardness tester

Measurement number	Leitz-Wetzlar microhardness values (KHN)	Calibration microhardness values (KHN)
1	562.39	597.49
2	551.37	602.41
3	560.16	595.05
4	564.63	597.49
5	564.63	607.40
Mean (SD)	560.64^a (5.5)	599.97^a (5.0)

Same superscript letters (^{a-a}) between rows = statistically significant difference ($p = 0.009$)

The coefficient of variation of the repeatability results from the Leitz-Wetzlar Microhardness tester under the repeatability conditions was 1.0 % and the coefficient of variation of the reproducibility results from the Leitz-Wetzlar Microhardness tester under the reproducibility conditions was 0.8 %.

2.3 Section 2.3: Validity of remineralisation protocol

2.3.1 Introduction

As discussed in Chapter 1 above, a possible mechanism of action for modification of erosive tooth wear by fluorides is through the promotion of remineralisation and inhibition of demineralisation. The importance of the remineralising potential of saliva should not be underestimated, as saliva not only ensures availability of calcium and phosphate but also promotes calcium binding in the salivary pellicle through proline-rich proteins and statherin in the salivary pellicle (Nekrashevych and Stösser, 2000). These biological factors are important to the potential modification of erosive tooth wear though the action of fluorides (either surface CaF_2 or other fluoride compounds) (Hara et al., 2006b). Therefore, in order to use models simulating erosion, abrasion and attrition *in vitro* to study the effect of fluorides on tooth wear these models must, at the most basic level, be able to simulate the

demineralisation and remineralisation cycles that are thought to occur during erosion and subsequent exposure to saliva *in vivo*.

2.3.2 Aim, objectives and null hypothesis

The aims of Section 2.3 were:

1. To compare the remineralisation potential of an artificial saliva substitute with human saliva.

The hypotheses were that:

1. The remineralising potential of the artificial saliva would be the same as that of previously collected human stimulated parotid saliva, as measured by microhardness recovery.

2.3.3 Materials and methods

2.3.3.1 Study design

The two remineralising solutions under investigation were artificial saliva and human saliva. The remineralising potential of the two solutions was assessed by measuring the surface microhardness recovery over time of eroded enamel samples which had been immersed in one of the two solutions.

2.3.3.2 Sample preparation

Ten enamel samples were prepared as described in Section 2.1.2.2 above. The samples were randomly assigned to the two experimental groups, following a randomization table generated using spreadsheet software (Microsoft® Office Excel® 2007, Microsoft® Corporation, USA).

2.3.3.3 Baseline microhardness measurements

Following sample preparation the baseline Knoop microhardness of all enamel samples was measured, prior to erosion. The surface microhardness was measured by a microhardness

tester (Leitz-Wetzlar Miniload 2, Ernst Leitz GMBH, Wetzlar, Germany) as described in Section 2.2 above.

2.3.3.4 Erosion cycling model

Following sample preparation, all samples were immersed in 50 ml of a citric acid solution for five minutes.

The solution was prepared to a concentration of 0.3 % with the pH adjusted to 3.2 using a sodium hydroxide buffer using a calibrated pH meter and electrode (Oakton pH 510 Benchtop Meter with a WD-35801-00 pH electrode, Eutech Instruments, Nijkerk, Netherlands) (Eisenburger et al., 2001a). The titratable acidity of the solution was measured following previously published protocols (Bartlett and Coward, 2001), using a calibrated pH meter and electrode (Oakton pH 510 Benchtop Meter with a WD-35801-00 pH electrode, Eutech Instruments, Nijkerk, Netherlands). The solution had a titratable acidity of 19.5 ml, measured as the volume of 0.1 M solution of sodium hydroxide required to raise 20 millilitres of the experimental drink to pH 7.0 by adding increasing volumes of sodium hydroxide solution followed by agitation and equilibrium for two minutes until the pH reached 7.0. Each measurement was repeated three times at room temperature ($23\text{ }^{\circ}\text{C} \pm 1\text{ }^{\circ}\text{C}$) and their average calculated.

Following removal from the citric acid solution, the samples were rinsed in deionized water and Knoop microhardness values (KHN) of the eroded enamel were again calculated. Following microhardness measurement, the samples were immersed 40 ml of in the respective remineralising solutions.

2.3.3.5 Artificial saliva

The artificial saliva was prepared according to the protocol used by Eisenburger et al (2001b). The artificial saliva contained the following ingredients in deionized water: $\text{CaCl}_2 \cdot 2\text{H}_2\text{O}$ 0.7 mmol/l; MgCl_2 0.2 mmol/l; KH_2PO_4 4.0 mmol/l; HEPES buffer (acid form) 20.0 mmol/l; KCl 30.0 mmol/l, with the pH being adjusted to 7.0.

2.3.3.6 Human saliva

20 millilitres of stimulated parotid saliva was collected from the author of this thesis, using Lashley cups attached to the oral mucosa surrounding both parotid papillae, whilst a citrus lozenge was allowed to dissolve in the lingual sulcus. The calcium content of the collected parotid saliva was 1.4 mmol/l and therefore a further 20 millilitres of deionised water was added to the saliva in order to equilibrate the calcium concentration of the two solutions to 0.7 mmol/l.

2.3.3.7 Microhardness

As well as the microhardness measurements before erosion and immediately after erosion, the samples were removed from the remineralising solutions for KHN measurement, as described in Section 2.2 above, after 30 minutes, 60 minutes, 2 hours, 6 hours and finally 24 hours. Three indentations per sample were made and following conversion to the KHN using the ASTM formula as described in Section 2.2 above, the mean of the three KHN values was taken as the sample KHN.

Finally, the percent surface microhardness recovery (%SMR) of each enamel sample was then calculated, as shown in Equation 6 below (Gelhard et al., 1979), at each remineralisation time point.

Equation 6 Calculation of percent surface microhardness recovery (%SMR) of eroded enamel samples immersed in either human or artificial saliva over time (Gelhard et al., 1979)

$$\%SMR = 100 * \frac{(KHN \text{ after remin}) - (KHN \text{ after erosion})}{(KHN \text{ at baseline}) - (KHN \text{ after erosion})}$$

2.3.4 Statistical analysis

Data were processed and analysed using Stata 11 software (StataCorp, USA). Frequency distribution assessment showed that for that the step height data in enamel did not conform to a normal distribution at all remineralisation periods and therefore KHN data of the two groups of enamel samples were described using median and inter-quartile range. Data were

assessed for differences between the human and artificial saliva groups at each time point, using the Mann-Whitney-U test. Statistical significance was inferred when $p < 0.05$.

2.3.5 Results

Figure 34 below shows the median (IQR) Knoop microhardness of enamel samples before and after an acid challenge and after immersion in either a diluted solution of stimulated human parotid saliva or an artificial saliva solution over time ($n = 5/\text{gp}$). This figure shows similar median (IQR) baseline KHN values before erosion, following which both groups experienced a similar hardness reduction from five minutes immersion in the 0.3 % citric acid solution. For the human saliva group a 26.2 % reduction in microhardness occurred and for the artificial saliva group a 27.7 % reduction in microhardness occurred. Although the KHN of both enamel groups increased at different rates over time, with the samples immersed in human saliva needing around 2 hours to return to near baseline levels after whereas the samples immersed in artificial saliva required around 24 hours to return to near baseline levels, there were no statistically significant differences in the median (IQR) KHN of both enamel groups at baseline, after erosion and at all subsequent remineralisation time points ($p > 0.05$).

Figure 34 Median (IQR) Knoop microhardness of enamel samples before and after an acid challenge and after immersion in either a diluted solution of stimulated human parotid saliva or an artificial saliva solution over time ($n = 5/\text{gp}$)

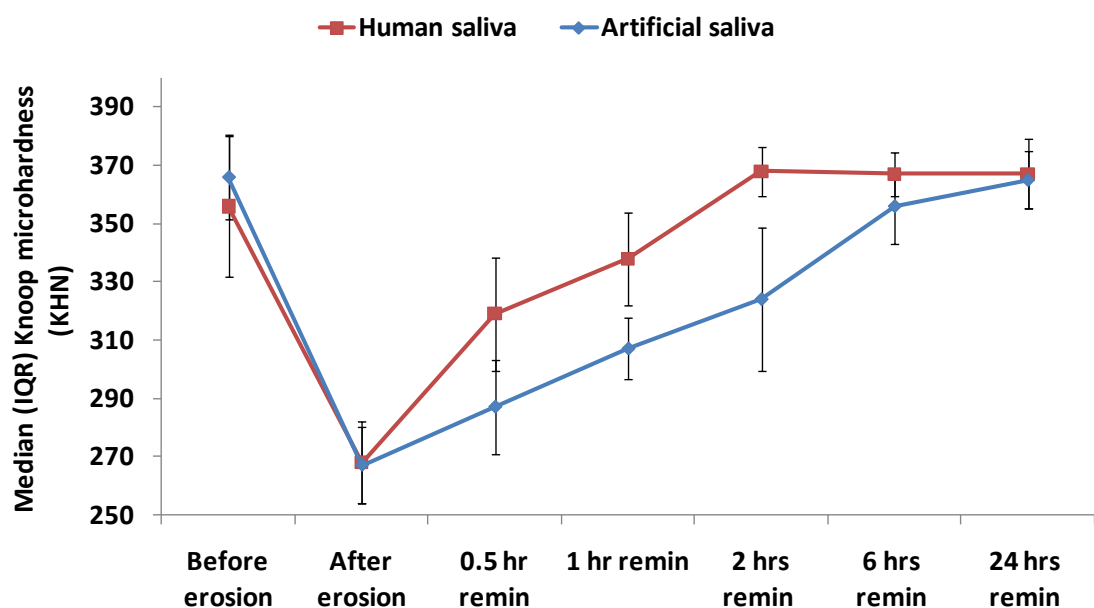
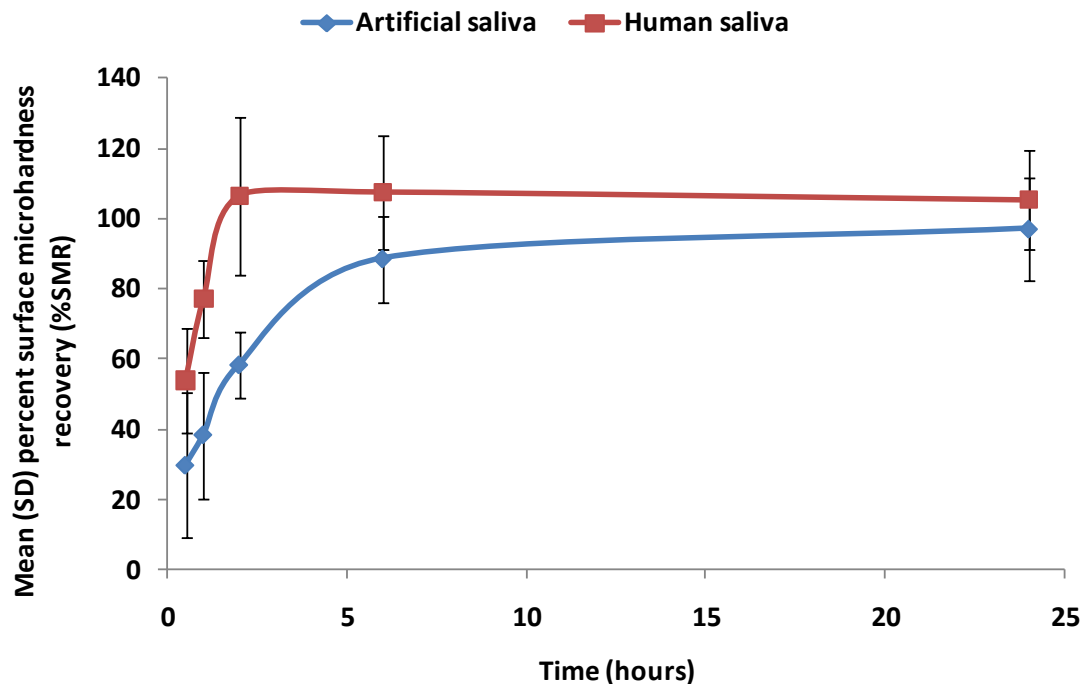


Figure 35 below shows the mean (SD) percent surface microhardness recovery (%SMR) of enamel samples after an acid challenge and after immersion in either a diluted solution of stimulated human parotid saliva or an artificial saliva solution over time (n = 5/gp). This figure shows that following 30 minutes remineralisation, the %SMR of the human saliva group was 54 % and the %SMR of the artificial saliva group was 30 %; following one hour the %SMR was 77 % and 38 % respectively and following two hours 107 % and 58 % respectively. This %SMR trend continued with the samples immersed in human saliva thus requiring two hours to return to baseline hardness values and the samples immersed in the artificial saliva requiring around 24 hours to return to near baseline levels, however there were no statistically significant differences in the median (IQR) KHN of both enamel groups at baseline, after erosion and at all subsequent remineralisation time points (p >0.05).

Figure 35 Mean (SD) percent surface microhardness recovery (%SMR) of enamel samples after an acid challenge and after immersion in either a diluted solution of stimulated human parotid saliva or an artificial saliva solution over time (n = 5/gp)



Discussion

Section 2.1

The concept of measurement uncertainty is based on the fundamental principle that all measurements are subject to some degree of imperfection (ISO, 2004); the extent of which varies according to the specifics of the particular measurement problem being considered. The process of evaluating uncertainty of measurement has been described in detail elsewhere (Bell, 2010; British Standard Institution, 1995), however essentially it requires a systematic assessment of all possible sources of measurement error, which is then expressed as a qualitative value summarising the degree of imperfection of a measurement. In this thesis, the Overall Combined Uncertainty (as opposed to the Standard Combined Uncertainty) was the ultimate outcome used to express the measurement uncertainty of the measurement system that was used to measure enamel and dentine wear in the studies that form Chapters 3, 4 and 5 of this thesis.

Examination of the contribution of each source of error to the uncertainty budgets seen in Table 26 to Table 33 below in Appendix 4 below revealed that the main contributing factor to the Standard Combined Uncertainty was from the flatness, noise and z axis linearity errors. For step height the contribution from the flatness, noise and z axis linearity errors represented 98 – 100 % of the total uncertainty budget and for volume the contribution from the flatness, noise and z axis linearity errors represented 60 - 99 % of the total uncertainty budget. Further consideration of flatness, noise and z axis linearity errors revealed that of these errors, the flatness error was, by far, the greatest contributor. This single contribution to the uncertainty budget therefore represented the single greatest source of error in the entire measurement system.

The cause of this error was as a result of the x/y motion control system being unable to move the stage in a perfectly linear plane during measurement, as seen in panel (a) of Figure 26 above. Further examination of the pattern of the flatness error in Figure 26 above reveals that the flatness error may have been due to the mechanical vibrations or movement of the ball bearing mounted component of the stage. Although the stages are serviced and maintained

yearly, wear of the bearings would contribute to the flatness error. The life span of the ball bearings is recommended by TaiCaan Technologies Ltd. to be around five thousand hours and the current system is reaching that limit. Replacing the ball bearings with new ones or switching to an air bearing mounted x/y stage would both be beneficial options to reduce the flatness and noise contributions to the uncertainty of measurement.

The Standard Combined Uncertainty can be considered to represent the 'worst-case scenario', whereby all sources of error combined to result in the maximum possible measurement uncertainty. Using this Standard Combined Uncertainty, the 10 % tolerance level that was stated as the maximum permissible level of uncertainty in the hypothesis for this Section (on on page 84 above) was exceeded for any measurement of wear less than 3 μm , and reached almost 100 % uncertainty for the measurement of 0.3 μm of wear (Figure 31 above). If this were truly the case, this would render the surface topography measurement system not 'fit for purpose' for use in this thesis and furthermore would negate the ability of other researchers to replicate and interpret any findings from the studies forming Chapters 3, 4 and 5 of this thesis.

However, further examination of the relationship between the main contributory error (i.e. the flatness error) to the Standard Combined Uncertainty and the measurement techniques described in Section 2.1.2.7 above, resulted in the conclusion that the Standard Combined Uncertainty did not represent a realistic estimation of the practical effects of the measurement errors on the tooth wear measurement under the experimental conditions of this thesis. Therefore, the Overall Combined Uncertainty was evaluated, through the use of 'soft gauges', which contained all the flatness, noise and z axis linearity errors as stated above. This evaluation showed that the 10 % tolerance was not exceeded even when the measurement of a 0.3 μm soft gauge was carried out (Figure 32 above) and therefore the Overall Combined Uncertainty was well within the specified 10 % tolerance, which was stated in the hypothesis as being the maximum permissible uncertainty. Therefore, the white light

confocal profilometer and specified software can be considered 'fit for purpose' for use in this thesis.

If this maximal permissible tolerance was exceeded overall, there would have been two main possibilities to further reduce the contribution of the flatness error in the measurement system. The first would have been to move from a ball bearing mounted x/y stage to an air bearing mounted x/y stage, the physical principles of which result in far less potential for a planarity deviation (i.e. flatness error). The second option would have been to evaluate whether the flatness error was a systematic or random type of error. If it were systematic and therefore repeatable, then this could be minimised by scanning an optical flat in the exact same position as the sample was to be measured in. Following the sample measurement, optical flat image could be subtracted from the sample image, which would effectively eliminate the planarity deviation from the scanned sample surface and thus reduce the uncertainty of measurement.

Other research groups using profilometry to measure erosive wear have advocated special precautions, in order to reduce measurement error from shrinkage of enamel and dentine during dehydration. It has been speculated that any potentially significant differences between the amount of wear may be hidden by enamel or dentine "wear", that is actually a result of shrinkage (Ganss et al., 2004b; Ganss et al., 2005; Ganss et al., 2009). In the present study, the step height and volume change during the de/rehydration affected the enamel samples more than the dentine samples. This may be due to the greater thickness of the enamel samples (which also contained subsurface dentine) than the dentine samples. As described in Section 2.1.2.2 above, the enamel and dentine samples were formed from 5mm x 3mm x 2mm sections from the mid-coronal portion of the buccal and lingual surfaces of the teeth and subsequently an outer layer of 400 µm of enamel or approximately 1 mm of enamel and dentine was removed. This meant that the enamel samples had an end thickness of approximately 1.6 mm and the dentine samples approximately 1 mm. This study also found

that the volume measurement changed more than the step height measurement, which perhaps indicates that the volume measurement is a more sensitive outcome measure than the step height measurement. Overall however, the maximum shrinkage errors were relatively low at 0.12 %. Accordingly, the contribution of this error to the uncertainty budget of both the Standard Combined Uncertainty and the Overall Combined Uncertainty was small, totalling less than 5 % of the budget at its maximal percentage contribution (Table 41 below). Therefore enamel and dentine shrinkage was not a major measurement problem in this study.

These findings differ from other similar studies into the impact of storage conditions on profilometry of eroded dental hard tissue (Attin et al., 2009; Ganss et al., 2007b). However, these studies used a stylus profilometer and the comparison of results from optical and stylus profilometry is complicated by the differing fundamental physical principles by which the systems operate (Leach, 2010a). For example, a contacting stylus will cause indentations into the soft collagen structures of demineralised dentine whilst not fully contacting the intact mineralised dentine underlying this layer and it is not possible to use an optical profilometer to measure dentine immersed in water, due to the differing refractive indices of water and air. The previous studies used ceramic discs as reference areas, unlike taped reference areas of the same substrate, as were used in the present study. Moreover, in the latter studies only single line profiles were taken whereas 3D step height and volume measurements were calculated in the present study which is more representative of the dimensional change.

The mean normalised volume of enamel loss ($M \mu\text{m}^3/\text{mm}$) was one of the values used to express tooth wear using the ImageJ macro and the white light confocal profilometer. This specially developed software measured normalised volume of enamel loss corresponding to average trench profile area across the entire wear lesion. Therefore it had the advantage over mean 3D step height measurements of being independent of the surface area of the lesion (i.e. erosion/abrasion length and width of the tape placement). In addition, unlike step height measurements of wear, volume loss is not dependent on the contact dimensions of the

antagonist causing the physical challenge to the substrate surface. Due to the force from the loading weight being evenly distributed along the contact area of the antagonist, a larger abrasive head leads to a shallower wear lesion, whereas the volume of wear is linearly dependent upon the pressure exerted on the substrate surface. The results from a recently published study (Rodriguez and Bartlett, 2010) where 2D and 3D measurements of enamel wear were compared, showed that normalised 3D measurements gave more accurate assessment of *in vitro* tooth wear. By normalising the volume change the amount of wear can be standardised by unit area or length, which compensates for the possible methodological sources of error described above. Vieira et al (2007) have also reported tooth wear both as normalised volume loss ($\mu\text{m}^3/\text{mm}^2$), average wear depth (μm) (volume loss /surface area of wear), max wear depth (μm) and % area of varnish removal, in order to compensate for the irregular surface area of exposed enamel after loss of varnish due to abrasion. Therefore, the choice of outcome measure is an important consideration when using optical profilometry to measure wear, which depends on methodological considerations including the type of antagonist and substrate, order of magnitude of the outcome and sample preparation technique.

Whichever outcome parameter is chosen for erosive wear measured by profilometry, an expression of the quality of the measurement system (i.e. is the measurement technique 'fit for purpose'?) is obligatory so that those who use it can assess the reliability of the measurement system and can readily understand and properly interpret the results of a research study. The validation process described in this section required a comprehensive quantitative expression of the effect of the likely degree of error introduced by the measurement procedures and systems. Even if a comprehensive uncertainty evaluation is not carried out, at the most basic level an assessment of the accuracy and precision of the measurement system under the specified measurement conditions is advised. Without such an indication, measurement results cannot be compared, either among themselves or with reference values given in a specification or standard. The concept of uncertainty as a

quantifiable attribute is relatively new in the history of measurement, although error and error analysis have long been a part of the practice of measurement science (metrology) however there are examples in the tooth wear literature of statistically significant differences being found at a level which is less than the resolution of the measurement system being used. This is an example of using a measurement system which is not 'fit for purpose', such that the poor quality of measurement is likely to result in outcomes which are not able to be replicated or are of reduced clinical significance. In today's global research community, it is imperative that the method for evaluating and expressing uncertainty be uniform throughout the world so that measurements performed in different countries can be easily compared.

This section of the thesis has therefore argued that a thorough understanding of the limitations of the surface topography measurement system is crucial, not only to evaluate and minimise possible sources of error but also to account for the clinical significance of the results of tooth wear studies. The concept of measurement uncertainty has not been widely adopted by many research groups. Most researchers using profilometry fail to report basic contributions to the measurement uncertainty such as the accuracy and repeatability of the measurement system being used and how the system was validated for use in the study. An understanding of the limitations of the measurement tools used and an evaluation of how 'fit for purpose' the system is, remains an important and under investigated area of tooth wear research, which requires further research.

Section 2.2

A full uncertainty analysis was not carried out for the microhardness measurement system. This was partially because this would have required knowledge of the uncertainty associated with the geometry of the diamond indenter, which requires the United Kingdom Accreditation Service (UKAS) to calibrate the Knoop diamond indenter, as well as the uncertainty with all the moving parts of the indentation system, which was not possible. Moreover, the use of microhardness is a mature technology and no new software was developed for use in this

thesis. Therefore, an assessment of accuracy and precision was felt to be sufficient for the validation of the hardness measurement in this thesis. In the UK, the UKAS is the national body responsible for implementing the written standards defining hardness measurements by assessing and accrediting national transfer-standard block machines, in order for these to be used for comparisons between individual machines and fully calibrated national standard machines. The use of a national standard machine and a transfer-standard block are the minimum requirements for the validation of hardness tester. A transfer standard is required because strict repetition of a hardness observation is not possible because a new indentation cannot be made in exactly the same place of the last indentation. Therefore in this thesis, a transfer standard of consistent known 'true' hardness was used. Knoop hardness of a substance is determined by a conventional measurement process that involves a dimensional measurement of an indentation made in a block of the material of interest. The measurement is made according to a written standard which includes a description of the indenter, the construction of the machine by which the indenter is applied and the way in which the machine is to be operated.

Although the accuracy of the hardness tester used in this thesis had a seven percent difference in comparison to the national standard machine, the precision of the system can be considered more important because the relative hardness change (before wear – after wear) was the method by which hardness was measured. Therefore, the good repeatability and reproducibility of the system confirmed that the microhardness tester was 'fit for purpose' for use in this thesis.

Section 2.3

This section demonstrated that the remineralising potential of the artificial saliva was less than that of a human parotid salivary solution of an equivalent calcium concentration solution. However, these differences were not significantly different at any stage of the remineralisation over time ($p > 0.05$).

Artificial saliva is commonly used instead of human saliva due to issues surrounding collection, storage and degradation of human saliva (Hara et al., 2008). In order to ensure that the artificial saliva is similar to the clinical situation it is important to quantify its remineralisation potential and to compare this to human saliva (Levine, 1993). The artificial saliva was formulated as described by Eisenburger et al (2001a). In previous experiments, the saliva was found to optimally remineralise erosive lesions within a six hour period (Eisenburger et al., 2001a; Eisenburger et al., 2001b). However, to date, this artificial saliva had not been compared with human saliva or quantified by microhardness measurements. The results of Section 2.3 of this Chapter seem to agree with Eisenburger et al; however a longer time period was required in the present study to return the enamel samples immersed in the artificial saliva to their baseline hardness values. This perhaps indicates that the artificial saliva solution remineralises eroded enamel at a slower rate than the human saliva. Nevertheless, no statistically significant differences in the KHN or %MHR values were found at any time points ($p > 0.05$).

Following this investigation, a remineralisation time of 60 minutes was chosen for the cyclic tooth wear models that form Chapters 3, 4 and 5 of this thesis. This remineralisation time period resulted in a 40 % surface microhardness recovery of the enamel samples and therefore the models could be considered to be more biased towards demineralisation rather than remineralisation. This remineralisation time was chosen as optimal as a balance between allowing time for a degree of remineralisation to occur, whilst also not prohibiting the use of multiple cycles of tooth wear to be modelled in one day. The specifics of the tooth wear models used will be discussed in more detail below, however, in order to simulate erosive challenges with relevance to the clinical situation, three to five cycles of demineralisation and remineralisation were thought to be desirable. Therefore the 60 minute remineralisation time was ideal to allow maximal number of cycles to be completed during one eight hour day.

Chapter 3 The effect of increasing sodium fluoride concentrations on erosion and attrition of enamel and dentine *in vitro*.

Introduction

The ability of high-concentration fluoride delivery systems to influence erosion and abrasion of enamel and dentine *in vitro* and *in situ* has been well documented (Ganss et al., 2001; Ganss et al., 2004a; Lagerweij et al., 2006; Magalhaes et al., 2009; Wiegand and Attin, 2003), however fewer studies have investigated the effect of fluorides on erosion and attrition. Eisenburger and Addy (2002a; b) investigated the interaction effects of erosion and attrition *in vitro*, using a previously developed enamel-to-enamel attrition machine (Harrison and Lewis, 1975), which simulated concurrent erosion and attrition. This model examined variations in pH, time of erosion (using a 0.3 % citric acid solution at pH 3.2, 5.5 or 7.0 for 10 - 30 minute periods) and variations in load and time of attrition (using loads of 200 g – 600 g for 10 - 30 minute periods). Perhaps somewhat unexpectedly, this study found that additional wear in neutral conditions was significantly greater than attritional wear in acidic conditions ($p < 0.05$); an result which the authors attributed to acid dissolution of the abrasive slurry of enamel and dentine particles which under neutral conditions would have promoted a 3-body wear process. Increasing load and time of attrition was found to significantly increase wear in both acid and neutral conditions, albeit in a non-linear fashion. These interaction effects of erosion and attrition were supported by Kaidonis et al (1998), in a study of the effects of simultaneous erosion and enamel-to-enamel attrition on the rate of enamel wear *in vitro*. This model examined variations in pH, acid (acetic acid solution at pH 3 and a hydrochloric acid solution at pH 1.2), remineralisation (deionized water and human saliva) and in load (loads of 1.7 kg - 16.2 kg). They observed that at pH 1.2, the wear rate was greater than at pH 3.2 and pH 7, for all experimental loads. When the enamel samples were immersed in whole mouth human saliva, at lower loads (9.95 kg) the rate of wear was relatively slow in comparison to deionized water,

however at greater loads (14.2 kg and above), more rapid wear occurred in human saliva than in deionized water.

More recently, *in vitro* research on erosion and attrition has focused on studies of cyclic tooth wear involving periods of demineralisation, mechanical challenges and periods of remineralisation, which may or may not be enhanced by the action of fluoride. Vieira et al (2006b) examined the effect of subjecting bovine enamel to erosion (using a citric acid solution at pH 3.0) prior to attrition (using loads of 600 g) and observed that pre-eroded enamel samples showed significantly greater attritional wear than non-eroded enamel.

This provides some limited evidence supporting the role of combined erosion and attrition as major contributing factors in tooth wear. However, there is a relative paucity of research into the interaction of dental attrition with erosion (Addy and Shellis, 2006) and even fewer studies have investigated the potentially protective effect of fluorides in erosive and attritional conditions. The sole study to date by Li et al (2007), investigated the effect of 24 hours pre-treatment of human dentine by a 22600 ppm sodium fluoride varnish (Duraphat® varnish, Colgate-Palmolive, Piscataway, NJ, USA) and its ability to modify attritional tooth wear *in vitro*. This study found that the fluoride treated groups lost 1.4 µm more dentine than the control groups, a finding that was attributed to the low pH of the fluoride varnish. However this is the sole study in this area and therefore there remains the need for more controlled *in vitro* studies of enamel and dentine attrition.

3.1 Aim, objectives and null hypotheses

The aim of this study was to determine the effect of repeated applications of a sodium fluoride solution of varying concentrations, on *in vitro* attrition and erosion-attrition of enamel and dentine.

The objectives were to:

1. Simulate attrition and erosion-attrition in the laboratory using a cyclic tooth wear model consisting of citric acid erosion, salivary remineralisation and enamel-to-enamel and enamel-to-dentine attrition.
2. Quantify the effect of a sodium fluoride solution of varying concentrations on the mean step height loss of enamel and dentine after five, ten and 15 cycles of simulated attrition and erosion-attrition.

The null hypothesis was that:

1. The amount and rate of wear of enamel and dentine from attrition or erosion-attrition would not be affected by repeated application of an aqueous sodium fluoride solution of varying concentration, in comparison to a deionized water negative control.

3.2 Materials and methods

3.2.1 Study design

The study was a factorial 5 x 2 x 3 x 2 design, according to the split-plot design (Hara et al., 2009). Thus the factors under investigation were:

- a. Aqueous sodium fluoride solution at five levels:
 - i. Deionized water (deionized water)
 - ii. 225 ppm NaF
 - iii. 1450 ppm NaF
 - iv. 5000 ppm NaF
 - v. 19000 ppm NaF
- b. Wear at two levels:
 - i. Attrition
 - ii. Erosion-attrition
- c. Number of wear cycles at three levels:
 - i. Five cycles
 - ii. Ten cycles
 - iii. 15 cycles

- d. Substrate at two levels:
 - i. Enamel
 - ii. Dentine

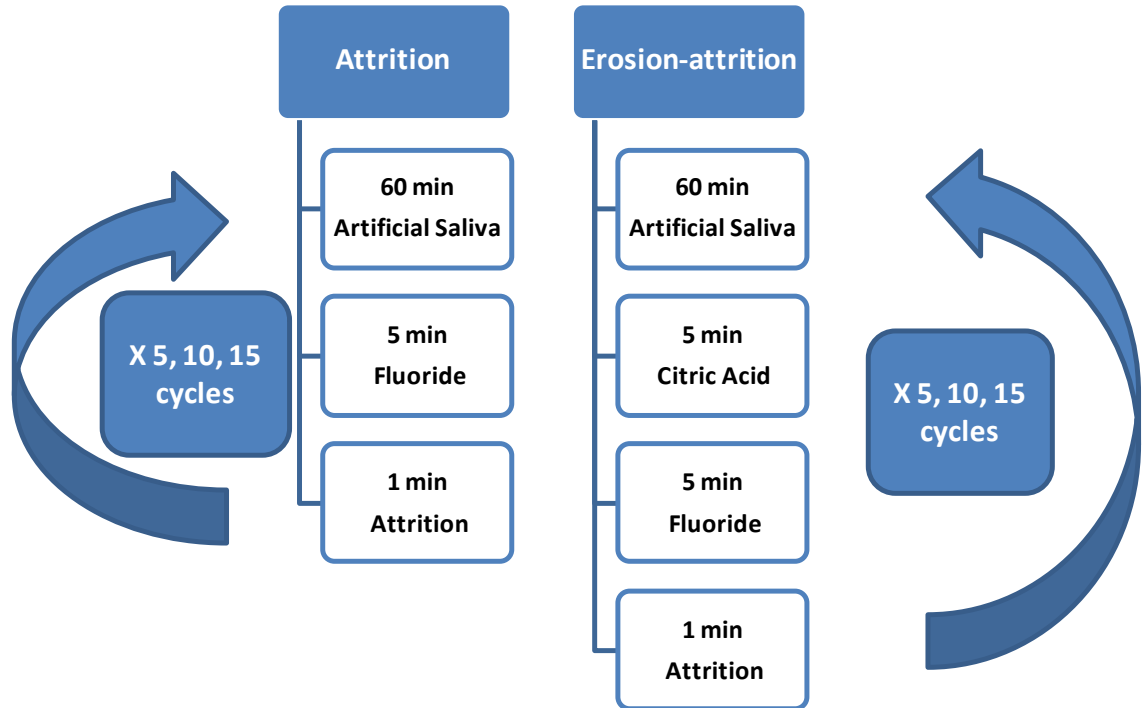
3.2.2 Sample preparation

Enamel and dentine samples (n = 200) were prepared as described in Section 2.1.2.2 above and were randomised using a table of randomly generated numbers obtained from spreadsheet software (Microsoft® Office Excel® 2007, Microsoft® Corporation, USA). Enamel and dentine samples were each allocated to one of ten groups (n =10 per group), according to the five solutions and two wear protocols.

3.2.3 Cyclic tooth wear model

Each group was subjected to a total of 15 attrition or erosion-attrition wear cycles over three days with each day consisting of five cycles of the allocated wear protocol. As shown in Figure 36 below, for the enamel and dentine groups allocated to the attrition wear protocol, one cycle consisted of sixty minutes immersion in artificial saliva, followed by five minutes immersion in sodium fluoride/control solution, followed by one minute of attrition. For the enamel and dentine groups allocated to the attrition and erosion wear protocol, one cycle consisted of sixty minutes immersion in artificial saliva, followed by five minutes demineralisation in citric acid, followed by five minutes immersion in sodium fluoride/control solution and then one minute of attrition.

Figure 36 Flowchart of protocols for the attrition and erosion-attrition



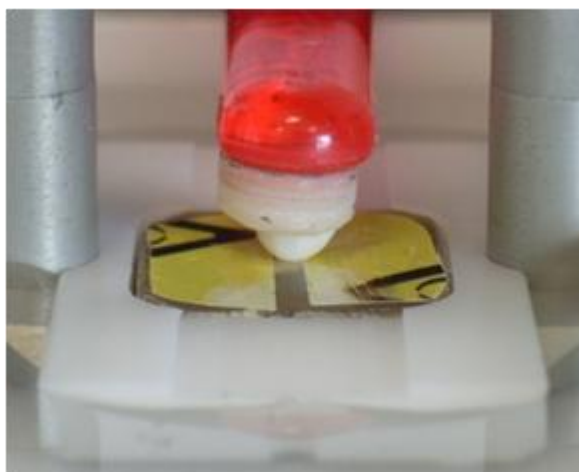
Following sample preparation, all samples were immersed in artificial saliva for sixty minutes. The artificial saliva was formulated as described in Section 2.3.3.5 above. Fresh batches of artificial saliva were mixed daily.

Following removal from the artificial saliva and careful rinsing and blot drying, the samples which were allocated to the erosion-attrition wear protocol were immersed in 50 ml of the citric acid solution static at room temperature ($23\text{ }^{\circ}\text{C} \pm 1\text{ }^{\circ}\text{C}$) for five minutes. The citric acid solution was prepared to a concentration of 0.3 % with the pH adjusted to 3.2 using sodium hydroxide buffer following previously published protocols (Eisenburger et al., 2001a). The solution had a titratable acidity of 19.5 ml, measured as the volume of 0.1 M solution of sodium hydroxide required to raise 20 millilitres of the experimental drink to pH 7.0 by adding increasing volumes of sodium hydroxide solution followed by agitation and equilibrium for two minutes until the pH reached 7.0. Each measurement was repeated three times at room temperature ($23\text{ }^{\circ}\text{C} \pm 1\text{ }^{\circ}\text{C}$) and their average calculated.

Following removal from the citric acid solution (or the artificial saliva for the samples allocated to the attrition wear protocol) and careful rinsing and blot drying, the samples were immersed in 50 ml of the appropriate fluoride solution/control static at room temperature ($23\text{ }^{\circ}\text{C} \pm 1\text{ }^{\circ}\text{C}$) for five minutes. The sodium fluoride solution was made using deionized water (pH 6.8) and 99 % pure sodium fluoride (Sigma-Aldrich Company Ltd., Gillingham, UK). An ionic calibration probe was used to measure the fluoride concentrations of the solutions (Oaklon Ion 510 Series) to ensure consistencies across the solutions. Four solutions were mixed: 225 ppm (0.248 g NaF / 500 g deionized water), 1450 ppm (1.602 g NaF / 500 g deionized water), 5000 ppm (5.255 g NaF / 500 g deionized water) and 19000 ppm (21 g NaF / 500 g deionized water). Deionized water (pH 7.0; 0 ppm F) was used as a negative control.

Following removal from the fluoride/control solution and careful rinsing and blot drying, all samples were immersed in 50 ml of the artificial saliva whilst being subjected to 60 strokes of attrition at room temperature ($23\text{ }^{\circ}\text{C} \pm 1\text{ }^{\circ}\text{C}$). Six enamel antagonists were prepared from previously donated human premolar teeth. The premolar crowns were hemisected and embedded into a disc of bis-acryl composite (Protemp 3, 3M ESPE) before being cemented onto the back of the handle of a tooth brush (Oral B plus size 40, Oral B, UK). The antagonist was mounted in a linear tooth brush testing machine (Syndicad Ingenieurburo, Munich, Germany) with the cusp tip positioned at 90° to the sample surface with a loading weight of 300 g, as shown in Figure 37 below.

Figure 37 Photograph of the set up of the attrition wear machine with taped sample immersed in artificial saliva.



This provided linear attritional strokes across the experimental wear surface. During the attrition, the samples were immersed in artificial saliva as described by Eisenburger (2001b), with fresh batches of artificial saliva mixed daily.

3.2.4 Profilometry

At the end of each round of five, ten and 15 cycles of erosion-attrition, the tape was removed for profilometry using the white light confocal profilometer as described in Section 2.1.2 above. Following profilometry, step height change (μm) was calculated using BODDIES® software as described in Section 2.1.2.5 above. Following measurement, the tape was repositioned using scalpel marks that had been placed at the time of initial tape placement, in order that the next round of attrition or erosion-attrition could be carried out.

3.3 Statistical analysis

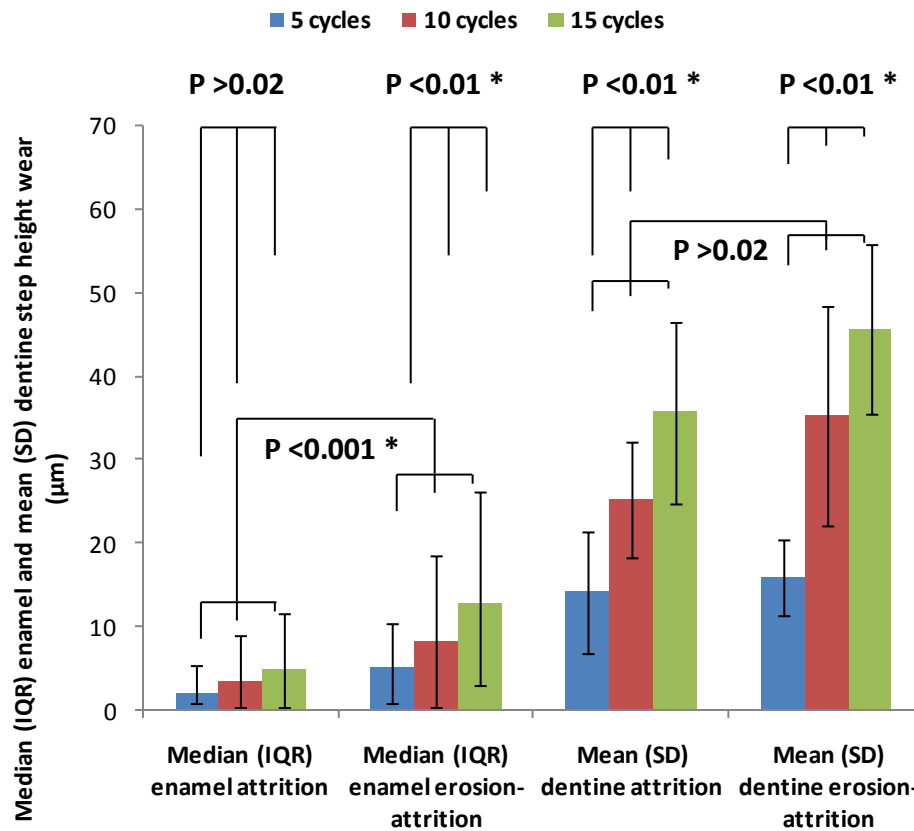
Data were processed and analysed using Stata 11 software (StataCorp, USA). Frequency distribution assessment showed that for that the step height data in enamel did not conform to a normal distribution in all three cycling periods. Enamel data were therefore described using median and inter-quartile range. Analysis was performed after logarithmic transformation to a normal distribution. In contrast, the step height data in dentine did conform to a normal distribution and were described using mean and standard deviation. Both

sets of data were assessed for differences between fluoride concentration, type of wear, number of cycles and substrate using two-way analysis of variance (ANOVA). Post-ANOVA contrasts were performed using a Bonferroni correction for multiple comparisons using a Scheffe comparison. Statistical significance was inferred when $p < 0.02$.

3.4 Results

Figure 38 below shows the median (IQR) enamel step height wear (μm) and mean (SD) dentine step height wear (μm) after five, ten and 15 cycles of attrition and erosion-attrition of the enamel samples allocated to the control group ($n = 10/\text{gp}$). Analysis of these control group results showed that as the number of cycles increased the amount of enamel and dentine wear increased. This increase in wear by group of cycles for the groups treated with deionized water was statistically significant for both dentine attrition and erosion-attrition ($p < 0.01$) and for enamel erosion-attrition ($p < 0.01$), however for enamel attrition the amount of wear did not significantly increase as the number of cycles increased. The enamel attrition group was also observed to experience the least amount of overall wear at all stages of the experiment, when compared to the other wear protocols and substrates. When the amount of wear after 15 cycles of erosion-attrition was compared with that after 15 cycles of attrition, the amount of enamel wear was significantly greater after 15 cycles of erosion-attrition (Table 16) than 15 cycles of attrition alone (Table 15) ($p < 0.001$). However, there were no significant differences between the amount of dentine wear after erosion-attrition, when compared to attrition alone, both at five, ten and 15 cycles.

Figure 38 Median (IQR) enamel step height wear (μm) and mean (SD) dentine step height wear (μm) after five, ten and 15 cycles of attrition and erosion-attrition of the enamel samples allocated to the control group ($n=10/\text{gp}$)



* = statistically significant difference ($p > 0.02$)

Table 15 and Table 16 show the median (IQR) step height (μm) enamel wear after five, ten and 15 cycles of attrition and erosion-attrition, by control and test fluoride solutions ($n=10/\text{gp}$). From these tables showing the results from all fluoride/control groups, it can be seen that the amount of enamel wear generated in the control group was greater than that generated in the fluoride groups for all concentrations at all numbers of cycles. The interaction between experimental fluoride solutions was found to be significantly different for enamel erosion-attrition ($p < 0.02$) (Table 16), with no significant differences between the experimental fluoride solutions found for attrition in enamel (Table 15).

When the effect of the individual fluoride concentrations on all wear protocols and substrates were analysed; only erosion-attrition of enamel showed statistically significant differences, as

seen in Table 16 below. After five cycles of attrition and erosion, the 19000 ppm NaF group showed significantly less wear than both the control group and the 225 ppm NaF group ($p < 0.02$). After ten cycles the 1900 ppm NaF group showed significantly less wear than the control group ($p < 0.02$) and significantly less wear than the 225 ppm NaF ($p = 0.000$), 1450 ppm NaF ($p = 0.001$) and 5000 ppm NaF groups ($p = 0.01$). After 15 cycles, the 1900 ppm NaF and the 5000 ppm NaF groups showed significantly less wear than the control group ($p < 0.02$) and all other experimental fluoride groups showed significantly less wear than the 225 ppm fluoride group ($p < 0.02$).

Table 15 Median (IQR) step height (μm) enamel wear after five, ten and 15 cycles of attrition, by control and test fluoride solutions ($n = 10/\text{gp}$)

	Control	225 ppm	1450 ppm	5000 ppm	19000 ppm
5 cycles	2.05 (3.34-1.2)	0.92 (1.54-0.58)	1.36 (2.11-0.7)	1.16 (3.05-0.14)	0.66 (1.83-0.45)
10 cycles	3.5 (5.44-3.08)	2.07 (2.58-1.54)	2.54 (3.9-2)	2.1 (5.02-1.57)	1.43 (2.6-0.92)
15 cycles	5.04 (6.66-4.53)	2.745 (3.02-2.42)	3.685 (5.99-2.34)	3.58 (6.53-2.56)	2.45 (3.71-1.83)

No statistically significant differences found between fluoride solutions and control ($p > 0.02$) or between fluoride solutions ($p > 0.02$)

Table 16 Median (IQR) step height (μm) enamel wear after five, ten and 15 cycles of erosion-attrition, by control and test fluoride solutions (μm) ($n = 10/\text{gp}$)

	Control	225 ppm	1450 ppm	5000 ppm	19000 ppm
5 cycles	5.11 a (5.31-4.21)	4.73b (9.39-3.36)	2.81 (5.25-1.19)	2.1 (2.81-2.09)	1.67ab (1.89-0.71)
10 cycles	8.265c (10.4-7.98)	8.265d (10.91-6.2)	5.36e (6.9-3.84)	4.04f (5.33-3.61)	2.45cdef (2.94-2.27)
15 cycles	12.86gh (13.24-9.79)	11.57ijk (15.28-10.57)	7.53il (8.93-5.02)	6.25hj (7.33-5.29)	3.456gkl (4.11-3.17)

* indicates statistically significant differences between fluoride solutions and control ($p < 0.02$)
Same superscript letters ^{a-a} by column indicate statistically significant differences between fluoride solutions ($p < 0.02$)

Table 17 and Table 18 show the mean (SD) step height (μm) dentine wear after five, ten and 15 cycles of attrition and erosion-attrition, by control and test fluoride solutions ($n = 10/\text{gp}$). From these tables, the amount of dentine wear generated in the control group was greater than that generated in the fluoride groups for all concentrations at all numbers of cycles, when compared to all experimental fluoride groups, except for the 225 ppm NaF group after five

cycles. Statistical analysis for the dentine results showed no statistically significant differences between experimental fluoride solutions at any levels ($p > 0.02$).

Table 17 Mean (SD) step height (μm) dentine wear after five, ten and 15 cycles of attrition, by control and test fluoride solutions (μm) ($n = 10/\text{gp}$)

	Control	225 ppm	1450 ppm	5000 ppm	19000 ppm
5 cycles	14.16 (7.36)	8.39 (1.8)	10.89 (3.54)	11.88 (4.9)	11.42 (5.11)
10 cycles	25.22 (6.91)	25.17 (7.19)	24.65 (6.87)	25.07 (9.87)	21.91 (6.04)
15 cycles	35.65 (10.97)	32.6 (7.51)	31.38 (6.06)	31.88 (9.28)	27.55 (7.42)

No statistically significant differences found between fluoride solutions and control ($p > 0.02$) or between fluoride solutions ($p > 0.02$)

Table 18 Mean (SD) step height (μm) dentine wear after five, ten and 15 cycles of erosion-attrition, by control and test fluoride solutions ($n = 10/\text{gp}$)

	Control	225 ppm	1450 ppm	5000 ppm	19000 ppm
5 cycles	15.85 (4.55)	16.28 (3.39)	15.6 (5.56)	15.37 (2.95)	14.56 (4.42)
10 cycles	35.31 (13.07)	30.36 (4.31)	29.01 (6.34)	30.18 (6.07)	31.37 (7.84)
15 cycles	45.58 (10.14)	37.96 (5.04)	35.81 (7.78)	37.91 (5.43)	39.54 (8.24)

No statistically significant differences found between fluoride solutions and control ($p > 0.02$) or between fluoride solutions ($p > 0.02$)

Based on the assumption that the baseline step height value of the enamel and dentine samples was zero, Figure 39 to Figure 42 below show the effect of increasing the concentration of the sodium fluoride solution on the mean step height (μm) of enamel and dentine loss by the number of cycles of attrition and erosion-attrition ($n = 10/\text{gp}$), plotted as continuous data. Overall, the gradient of the line graphs can be seen to be reasonably constant which therefore suggests that the rate of wear generated by the experimental attrition and erosion-attrition occurred at a relatively constant rate. A possible exception may be the rate of dentine wear from erosion-attrition, as all groups which showed a decreased rate of wear during the final five cycles of experimental wear; however this effect seems to be independent of fluoride concentration (Figure 42).

Figure 39 Effect of increasing the concentration of the sodium fluoride solution on the mean step height (μm) of enamel loss by the number of cycles of attrition (n =10/gp)

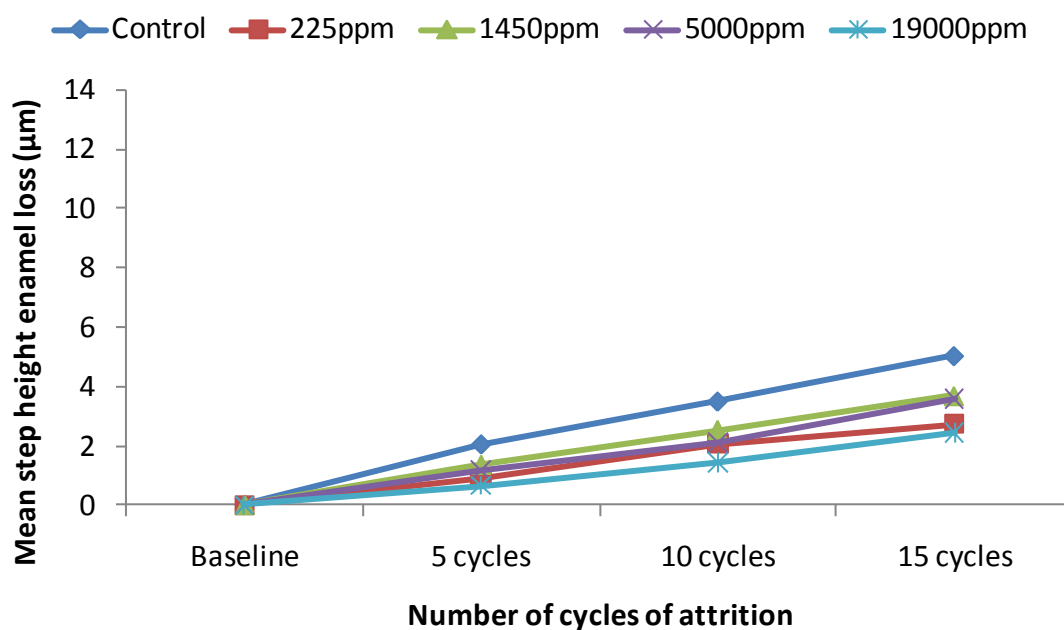


Figure 40 Effect of increasing the concentration of the sodium fluoride solution on the mean step height (μm) of enamel loss by the number of cycles of erosion-attrition (n =10/gp)

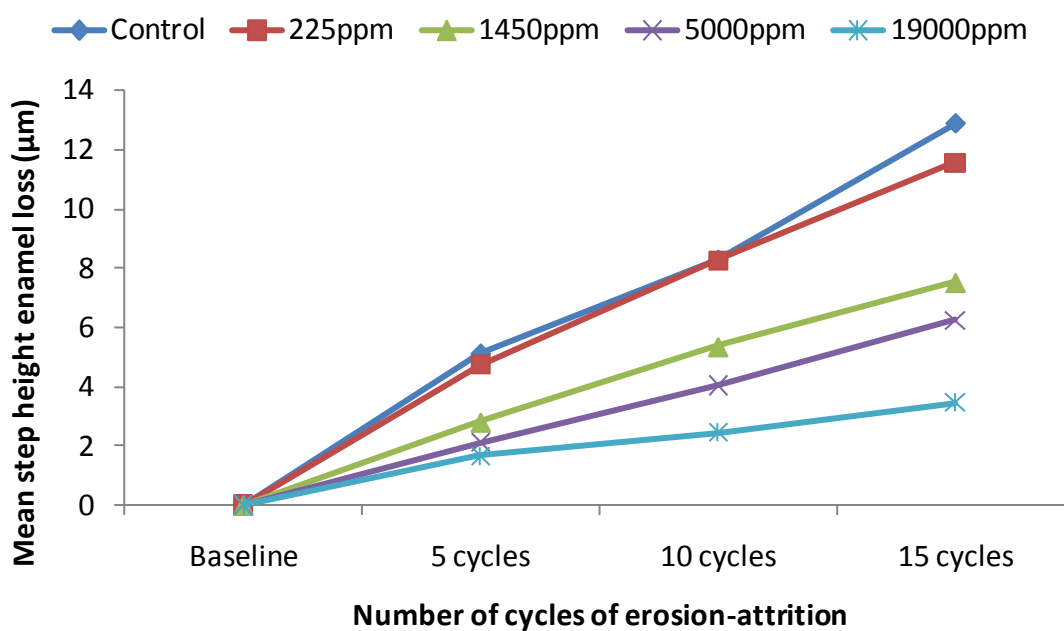


Figure 41 Effect of increasing the concentration of the sodium fluoride solution on the mean step height (μm) of dentine loss by the number of cycles of attrition (n =10/gp)

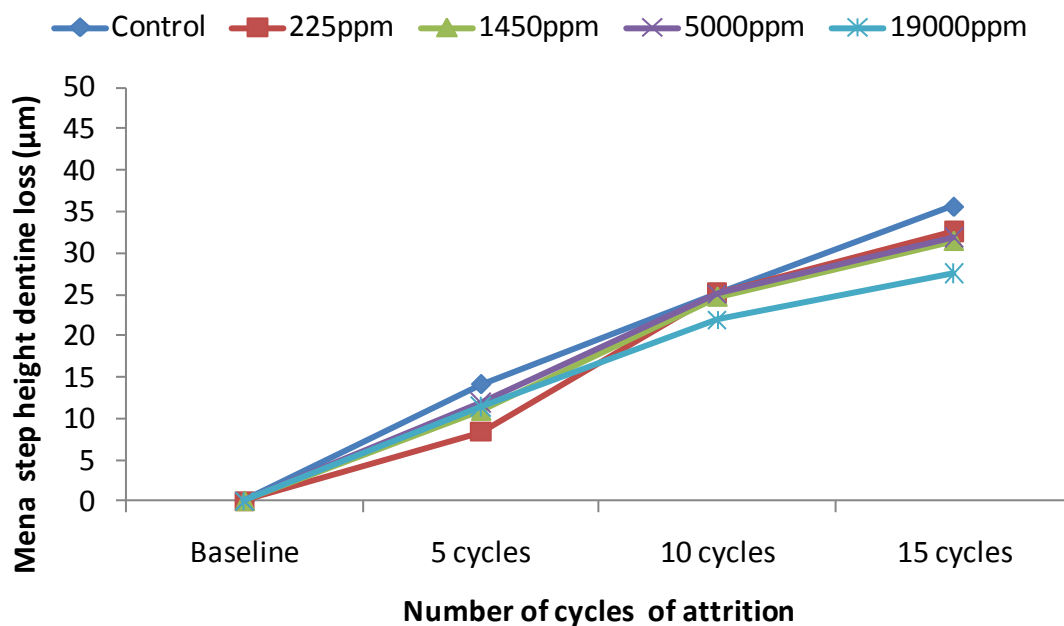
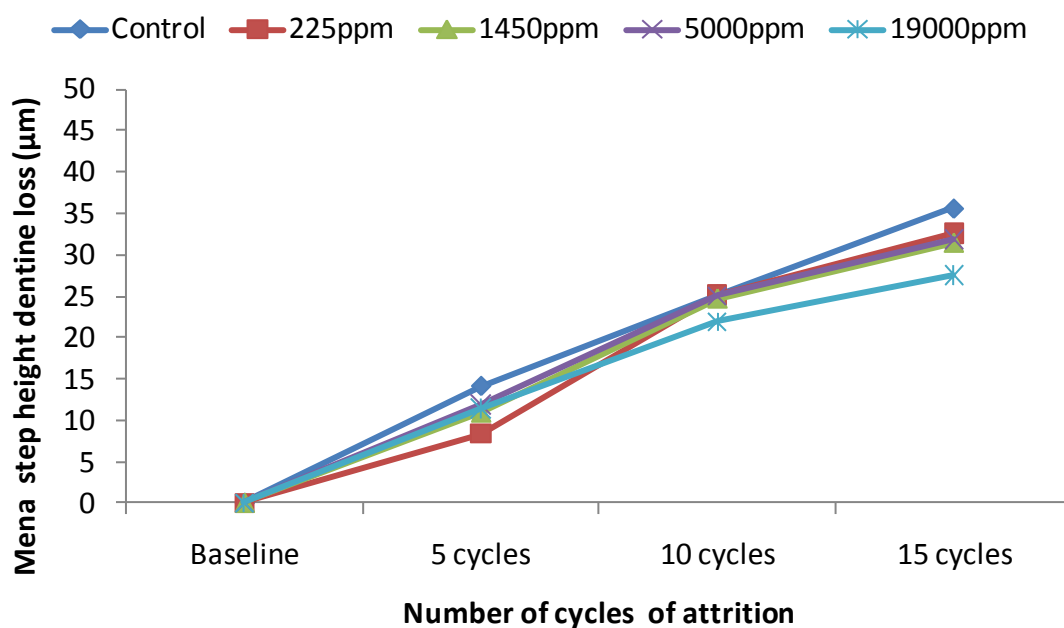


Figure 42 Effect of increasing the concentration of the sodium fluoride solution on the mean step height (μm) of dentine loss by the number of cycles of erosion-attrition (n =10/gp)



Assuming that the rate of wear was constant, the effect of varying the sodium fluoride solutions on the rate of wear (μm enamel or dentine loss per wear cycle) due to attrition and erosion-attrition throughout the entire study can be quantified by calculating the median (IQR)

wear rate of enamel and the mean (SD) wear rate of dentine, the result of which is shown in Figure 43 and Figure 44 below. These figures show that only the 5000 ppm and the 19000 ppm solutions resulted in a statistically significant reduction in the rate of enamel wear and that no such significant differences were shown for dentine wear.

Figure 43 Effect of varying concentration of a sodium fluoride solution on the median (IQR) rate ($\mu\text{m}/\text{cycle}$) of enamel wear by experimental wear method (n=10/gp)

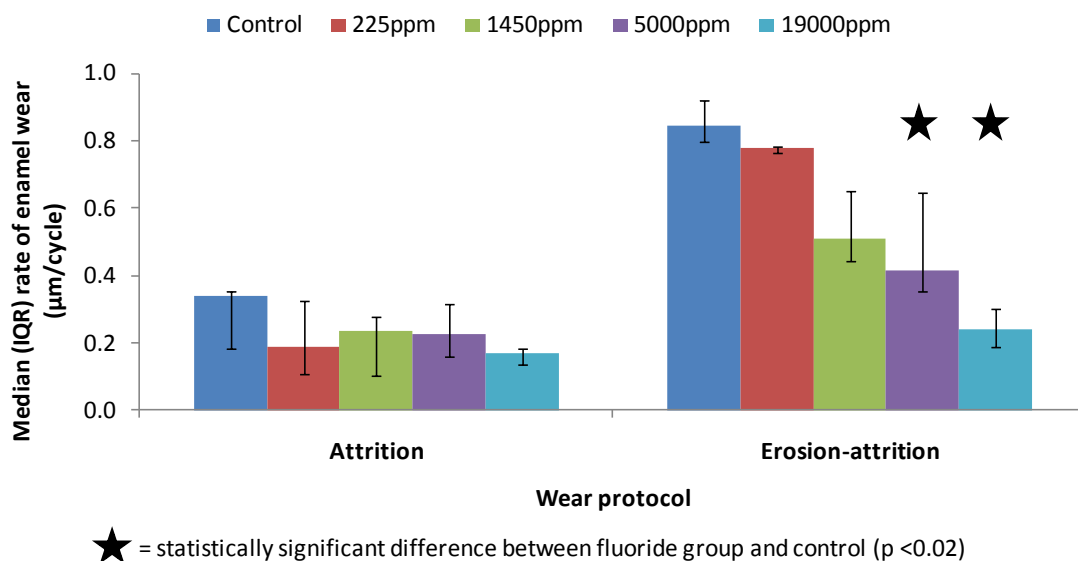
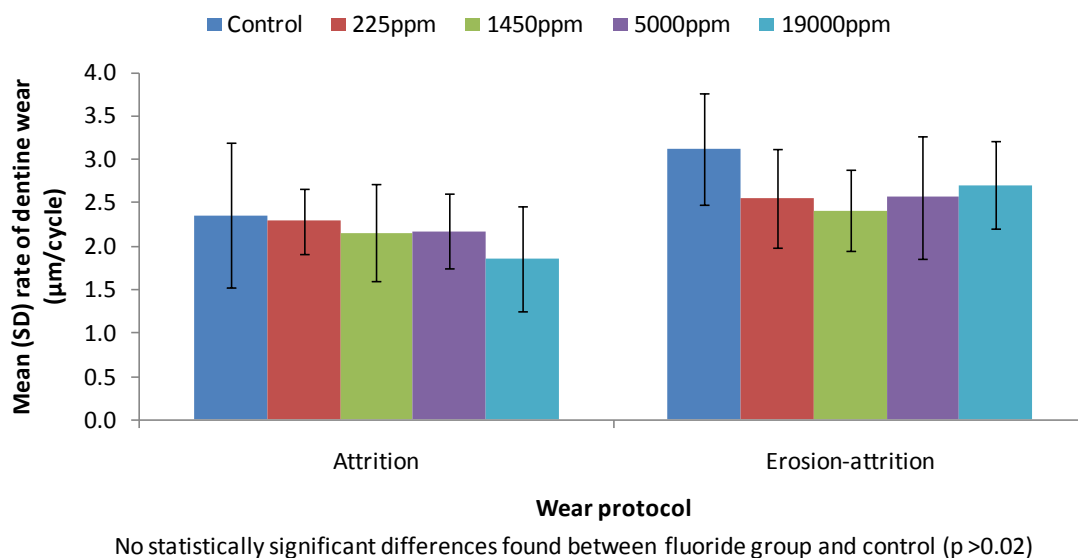


Figure 44 Effect of varying concentration of a sodium fluoride solution on the mean (SD) rate ($\mu\text{m}/\text{cycle}$) of dentine wear by experimental wear method (n=10/gp)



Discussion

These results show that an aqueous sodium fluoride solution formulated at concentrations of 5000 ppm and 1900 ppm resulted in statistically significant reduced enamel wear from erosion-attrition in a laboratory model. Developing and following a standardised sample preparation protocol was important in order to prepare samples with uniform surface characteristics and thus be able to demonstrate the results shown by Figure 43 and Figure 44 above. The grinding-polishing protocol resulted in consistent removal of 400 µm of outer enamel thus ensuring there was no possibility of variation due to the surface layer of fluoride rich enamel. In enamel, the fluoride concentration is greatest in the outer 100 µm of enamel of teeth without fluorosis (Ellwood et al., 2008) and can penetrate up to at least 300 µm in teeth with the most severe forms of fluorosis (Richards et al., 1989), whereas for dentine the 200 – 300 µm from the dentine-pulp interface has the greatest fluoride concentration (Ellwood et al., 2008). Creation of a homogenous area of exposed enamel or dentine with minimum dimensions of 5mm x 3mm required careful quality control of the sample preparation process in order to reject samples which had areas of unwanted exposed enamel or dentine. Perhaps more importantly for the following discussion, the sample preparation protocol was designed to ensure a surface with a flatness profile with a tolerance of ± 0.4 µm and a surface texture with a mean Sa value of 0.11 µm for enamel and 0.14 µm for dentine, as measured by randomly selecting a number of prepared samples for baseline profile and roughness measurement. Uniform surface profile with a flatness tolerance ± 0.4 µm enabled later comparison of step height loss using protected reference areas which were formed from the same substrate as that which was worn away during the simulated tooth wear *in vitro*. These reference areas can therefore be considered to have a baseline step height value of 0. In addition, the enamel and dentine surface was prepared in a plane as parallel as possible to the base of the sample to ensure that the entire surface could be scanned by the profilometer within the 350 µm focal depth of the white light confocal sensor.

Figure 43 and Figure 44 above illustrate the effect of varying the concentration of the sodium fluoride solution on the mean (SD) rate ($\mu\text{m}/\text{cycle}$) of enamel and dentine wear respectively. These figures clearly shows that the rate of wear of dentine was around four times than that of enamel for both types of experimental wear, which is perhaps to be expected considering the use of enamel antagonists against both enamel samples (greater hardness than dentine) and dentine samples (less hardness than enamel). Knoop microhardness testing of all samples at baseline confirmed that the initial mean surface microhardness values (KHN) of the enamel groups were much higher (363.5 ± 20.8) in comparison to the dentine samples (147.6 ± 7.0).

It can be seen from Figure 43 and Figure 44 that although all fluoride groups show a mean rate of enamel and dentine wear less than the control group; the repeated applications of the aqueous fluoride solution only resulted in statistically significant reductions in the rate of wear after repeated application of 5000 ppm ($p = 0.001$) and 19000 ppm ($p < 0.001$) sodium fluoride solutions. Fluoride acts by inhibiting mineral loss from the tooth surface during acid attack through the formation of fluorhydroxyapatite, which is more resistant to subsequent acid attack from caries (ten Cate and Featherstone, 1996), however the role of fluorides against multi-factorial tooth wear is less certain. Several studies have considered the effect of fluoride on cyclic erosion and abrasion (Attin et al., 1998; Attin et al., 1999; Ganss et al., 2007a; Lagerweij et al., 2006; Magalhaes et al., 2007; Ponduri et al., 2005; Vieira et al., 2006a) and most have concluded that fluoride has the potential to protect against tooth wear. This is the first study to demonstrate this protective effect in a cyclic erosion and attrition model. The results of this study concur with previous findings from erosion models that the more intensive the fluoride regime the more protection is afforded to enamel (Wiegand and Attin, 2003).

Prevalence studies of adults diagnosed with tooth wear have shown that the occlusal surfaces of molars and the incisal edges of incisors are the most severely affected surfaces of the dentition (Fares et al., 2009; van't Spijker et al., 2009b). These findings support the contention that attrition is a significant factor in the aetiology of tooth wear (Barbour and Rees, 2006).

However, there are relatively few *in vitro* investigations into the action of attritional tooth wear and therefore the ability of sodium fluoride solutions to protect against simulated erosion/attrition *in vitro* may be under investigated. This may be explained by both difficulties in modelling attrition in a predictive fashion *in vitro* (Lambrechts et al., 2006) and also by difficulties in assessing and quantifying attritive wear (Barbour and Rees, 2006). The development of 3-dimensional surface profilometry techniques and measurement software as described in Section 2.1 above has simplified some of these issues which have previously complicated investigations into multifactorial tooth wear *in vitro*.

The amount of wear generated by this model was significantly greater for enamel erosion-attrition (Table 16) than enamel attrition (Table 15) ($p < 0.001$), however in contrast, the amount of wear for dentine erosion-attrition was not significantly greater than dentine attrition alone ($p > 0.02$). This shows the synergistic impact of erosion in combination with attrition for enamel, however in this model this effect was less pronounced for dentine, possibly due to the 0.3 % citric acid solution not demineralising the dentine to the same extent as the enamel. This may help to explain why the 5000 ppm and 19000 ppm fluoride solutions provided protection to enamel but not to dentine, as the action of fluoride is attributed to inhibiting demineralisation and promoting remineralisation. *In situ*, the rate of fluoride-enhanced remineralisation of dentine has been shown to be slower in comparison to enamel (Fushida and Cury, 1999) and greater concentrations of fluoride are required to inhibit demineralisation of dentine in comparison to enamel (ten Cate and Duijsters, 1983a; b).

In this cyclic erosion and attrition model, artificial saliva was used both for the two hour remineralisation period and to immerse the enamel and dentine samples in during attrition. The model was designed with attrition carried out immediately after erosion in order to be analogous to the clinical situation where an acid challenge may soon be followed by a period of parafunctional activity, which may then be followed by a period of immersion in saliva, thus remineralising any remaining demineralised enamel and/or dentine. The artificial saliva

formulation used in this study was chosen following consideration of previous work (Eisenburger et al., 2001a; 2001b) which modelled similar erosive conditions and following validation experiments as described in Section 2.3 above. Previous work by Kaidonis et al (1998) found that under relatively low loads attritional wear in human saliva progressed less rapidly than attrition in deionized water. This may be have as a result of a lubricating effect of the salivary mucins or due to the promotion of remineralisation of eroded enamel and dentine in the presence of saliva, as measured by an increased surface microhardness recovery. The lack of studies into the role of saliva in erosion-attrition suggests that this area is under investigated in tooth wear research and therefore there may be a need for further studies in this area.

Chapter 4 The effect of a single application of topical fluoride treatments on enamel surfaces subjected to erosion or erosion-abrasion *in vitro*

Introduction

Highly concentrated fluoride solutions and varnishes are believed to promote formation of calcium fluoride (CaF_2) on the enamel surface, which may result in a mineral surface which is less prone to erosive dissolution (Ganss et al., 2001). It has been shown that prolonged (24h) application of a 2.26 % sodium fluoride (NaF) fluoride varnish (Duraphat® Varnish, Colgate-Palmolive, Piscataway, NJ, USA) can inhibit enamel erosion *in vitro* (Sorvari et al., 1994) and that a lower concentration (0.1 % NaF) fluoride varnish (Fluor Protector®, Ivoclar Vivadent, Schaan, Liechtenstein) can reduce erosion and erosion-abrasion *in vitro* (Vieira et al., 2007). These studies support recommendations for using professionally applied fluoride varnishes for prevention of erosion *in vivo* (Imfeld, 1996), in order to take advantage of the potential for gradual release of fluoride over a long period of time (Wiegand and Attin, 2003).

Together with different formulations and concentrations of sodium fluoride, different fluoride species may have varying abilities to influence the progression of enamel erosion (Magalhaes et al., 2008) and in dentine (Wiegand et al., 2008). Both titanium tetrafluoride (TiF_4) solutions and stannous fluoride (SnF_2) solutions can form a surface glaze or coating when applied to enamel, which has resulted in reduced enamel loss in various erosion models (Buyukyilmaz et al., 1997b; Ellingsen, 1986; Ganss et al., 2001; Ganss et al., 2004; Hove et al., 2006; Hove et al., 2007a; Hove et al., 2007b; van Rijkom et al., 2003; Vieira et al., 2005; Wei et al., 1976). The presence of this coating may contribute to the increased ability of TiF_4 and SnF_2 solutions to inhibit simulated gastric erosion using hydrochloric acid, when compared to a NaF solution (Hove et al., 2006; Schlueter et al., 2007). However, there are relatively few studies into the ability of aqueous fluoride solutions such as TiF_4 and SnF_2 to withstand a combined erosive-

abrasive challenge with Vieira et al (2006) reporting that TiF_4 was not able to protect against erosion-abrasion *in vitro*. Although energy dispersive x-ray spectroscopy (EDS) has been used to investigate how single application high concentration fluorides may influence chemical and ultra-structural changes that occur in enamel during erosion (Yu et al., 2010), there remains a lack of certainty about the mechanisms by which fluoride varnishes and different fluoride species may influence the surface chemical and physical changes that occur during repeated cycles of enamel erosion and erosion-abrasion.

High-concentration fluoride varnishes are commonly used in caries prevention and treatment and are formulated to adhere to the tooth surfaces over a longer period of time. It has been shown that prolonged (24h) application of a highly concentrated (2.26 % NaF) shellac-based fluoride varnish (Duraphat® Varnish, Colgate-Palmolive, Piscataway, NJ, USA) can inhibit enamel erosion *in vitro* (Sorvari et al., 1994) and that a lower fluoride concentration (0.1 % NaF) polyurethane-based varnish (Fluor Protector®, Ivoclar Vivadent, Schaan, Liechtenstein) can reduce erosion and erosion-abrasion *in vitro* (Vieira et al., 2007). Together with different formulations and concentrations of sodium fluoride, different fluoride compounds may have varying abilities to influence the progression of erosion in enamel (Magalhaes et al., 2008a) and in dentine (Wiegand et al., 2008) therefore the use of TiF_4 varnish may be a possible treatment in order to reduce enamel loss under mildly erosive conditions

4.1 Aim, objectives and null hypotheses

The aim of this study was to investigate the surface effects of highly concentrated fluoride solutions derived from three different fluorides (titanium tetrafluoride, stannous fluoride, sodium fluoride) and a commercially available highly concentrated sodium fluoride and calcium fluoride varnish (Bifluorid10® varnish, Voco GmbH, Cuxhaven, Germany), on *in vitro* erosion and erosion-abrasion.

The objectives were to:

1. Simulate erosion and erosion-abrasion in the laboratory using a cyclic tooth wear model consisting of hydrochloric acid erosion, salivary remineralisation and tooth brush abrasion.
2. Quantify the effects of a single application of highly concentrated solutions of titanium tetrafluoride, stannous fluoride, sodium fluoride and concentrated sodium fluoride varnish on the mean volume surface gain/loss after three, six and nine cycles of simulated erosion and erosion-abrasion, in comparison to a negative control, using a variety of assessments (optical profilometry, scanning electron microscopy (SEM), energy-dispersive X-ray spectroscopy and surface microhardness).

The null hypotheses were that:

1. Topical fluoride, of varying formulae, applied to the surface had no effect on erosion or erosion/abrasion of enamel and dentine *in vitro*.

4.2 Materials and methods

4.2.1 Study design

The study was a factorial 5 x 2 x 3 design, according to the split-plot design (Hara et al., 2009).

Thus the factors under investigation were:

- a. Fluoride treatments at five levels:
 - i. 0 ppm NaF deionized water (deionized water) negative control
 - ii. NaF solution (0.5M pH 8.0)
 - iii. SnF₂ solution (0.5M pH 2.6)
 - iv. TiF₄ solution (0.5M pH 1.2)
 - v. Bifluorid10® varnish (Sodium fluoride 5%, Calcium fluoride 5%, ethyl acetate, cellulose nitrate, isopentyl propionate)
- b. Experimental wear models at two levels:
 - i. erosion
 - ii. erosion-abrasion
- c. Number of wear cycles at three levels:
 - i. Three cycles

- ii. Six cycles
- iii. Nine cycles

4.2.2 Sample preparation

Enamel samples (n =60) were prepared as described in Section 3.2.2 above and randomised using a Table of randomly generated numbers obtained from spreadsheet software (Microsoft® Office Excel® 2007, Microsoft® Corporation, USA). After randomisation, samples were allocated to one of ten groups (n =6 per group), according to the five surface treatments and two experimental wear protocols.

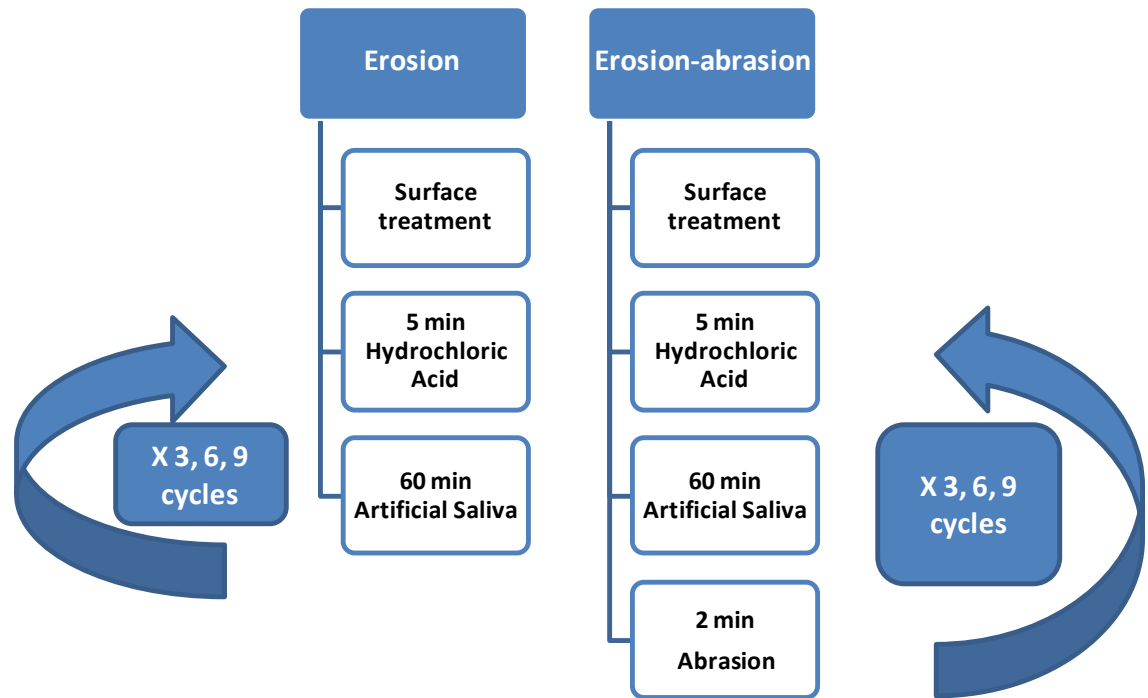
4.2.3 Application of fluoride treatments

Prior to the erosion or erosion-abrasion, each surface treatment was applied to the enamel surface. The NaF, SnF₂ and TiF₄ fluoride solutions were applied by dabbing the enamel surface for two minutes with a cotton pellet saturated in the allocated fluoride solution prior to gentle air drying. The Bifluorid10® varnish was applied according to the manufacturers` instructions for 20 seconds using a micro-brush. Bifluorid10® contains 50 mg NaF (23 mg F) and 50 mg CaF₂ (24 mg F). Deionised water (pH 6.8, 0 ppm F) was then applied to the remaining two enamel groups (controls) using a pipette and allowed to air-dry.

4.2.4 Cyclic tooth wear model

Following application of the surface treatments, each group was subjected to a total of nine cycles of the erosion or erosion-abrasion over three days with each day consisting of three cycles of the allocated protocol, as shown in Figure 45 below.

Figure 45 Flowchart of protocols for the erosion and erosion-abrasion



Following surface treatments, all samples were immersed in 50 ml per sample of freshly prepared hydrochloric acid solution of 0.01 M (pH 2.2) for two minutes at room temperature $21\text{ }^{\circ}\text{C} \pm 1\text{ }^{\circ}\text{C}$ with gentle stirring (Gyrorocker SSL3 at 50 rpm). The hydrochloric acid solution was prepared using 0.833 ml of 37 % HCL, density 1.175-1.188 kg, 12 M, mw 36.46 (Sigma-Aldrich Company Ltd., Dorset, England) with 999.17 ml H_2O following previously published protocols (Hove et al., 2006; Hove et al., 2007a; 2008). The solution had a titratable acidity of 3.46 ml, measured as the volume of 0.1 M solution of sodium hydroxide required to raise 20 ml of the experimental solution to pH 7.0 by adding an increasing volume of sodium hydroxide solution followed by agitation and equilibrium for two minutes until the pH reached 7.0 with each measurement repeated five times at room temperature ($23\text{ }^{\circ}\text{C} \pm 1\text{ }^{\circ}\text{C}$) and an average calculated.

Following removal from the hydrochloric acid solution and careful rinsing and blot drying all samples were immersed for sixty minutes in artificial saliva prepared as previously described in Section 2.3.3.5 above. For the samples allocated to the erosion protocol this completed one cycle of erosion.

For the samples allocated to the erosion-abrasion protocol, following removal from the artificial saliva and careful rinsing and blot drying, were immersed in 50 ml of the artificial saliva whilst being subjected to two minutes of tooth brush abrasion in a standardised tooth brush testing machine (Syndicat Ingenieurbüro, München, Germany) at room temperature ($23^{\circ}\text{C} \pm 1^{\circ}\text{C}$). Each group was brushed with a new TePe medium soft tooth brush (TePe, Preston, UK) loaded to 200 g and subjected to 120 linear reciprocating strokes (one stroke/second) per wear cycle. The samples were immersed in a 1:3 (w/v) slurry of non-fluoridated toothpaste (Kingfisher Natural Toothpaste, Norwich, UK) and artificial saliva during brushing.

4.2.5 Profilometry

At the end three, six and nine cycles of erosion or erosion-attrition, the tape was removed for profilometry using the white light confocal profilometer as described in Section 2.1.2 above. Following profilometry, volume change ($\text{M } \mu\text{m}^3/\text{mm}$) and step height change (μm) were calculated using the ImageJ macros as described in Section 2.1.2.5 above. Following measurement, the tape was repositioned using scalpel marks that had been placed at the time of initial tape placement, in order that the next round of erosion or erosion-abrasion could be carried out.

4.2.6 Scanning electron microscopy (SEM) and energy-dispersive X-ray spectroscopy (EDS)

Two samples per group were randomly chosen for SEM and EDS analysis at three stages of the study; immediately after application of the allocated fluoride treatment, after nine cycles of both erosion and erosion-abrasion. Samples were mounted on an aluminium stub (Agar Scientific, Stansted, UK) with carbon cement (Leit-C Emitech, Ashford, UK), prior to being coated with 50 nm of carbon (K250, Emitech, Ashford, UK). This sample was subsequently examined at x45 magnification in a Hitachi S3500 scanning electron microscope (Hitachi S3500, Hitachi, Wokingham, UK) with an integrated x-ray Spectrometer (Oxford Instruments plc, Tubney Woods, Abingdon, Oxfordshire OX13 5QX). In order to ensure a representative worn

sample surface was imaged , five 150 μm x 150 μm areas of the across the length of the erosion or erosion-abrasion lesion were chosen and these areas were subjected to a 10 KeV x-ray emission for 20 seconds per area, at a working distance of 15 mm. The resulting x-ray spectra of the chosen areas were processed for quantitative analysis by removal of outlying peaks; identification of the elements; removal of the background noise; resolution of the spectral peaks and finally computation of the element concentration as weight percent (wt %). For comparison between samples, at the three stages of the study, the mean (SD) wt % of the five surface areas was calculated pre sample. Because the presence of oxygen and carbon would have mostly represented air within the sample surface and the carbon coating of the samples, the wt % oxygen and carbon were removed from the elemental analysis for between group comparisons. Trace elements (<1 wt %) were also removed as possible contaminants. The remaining element concentrations were expressed as mean weight percent (wt %) of the total elemental composition of the enamel surface at the three stages of the study and between group comparisons carried out.

The remaining enamel sample per fluoride group from at the same three stages of the study described above; was mounted on an aluminium stub (Agar Scientific, Stansted, UK) with carbon cement (Leit-C Emitech, Ashford, UK) prior to being coated with 5 – 7 nm of gold (K250, Emitech, Ashford, UK) for electrical conductivity. A representative central area of the erosion or erosion-abrasion lesion was chosen for imaging at x1500 magnification, maintaining the same orientation, in order to facilitate comparisons between groups at the three stages of the study.

4.2.7 Microhardness

The surface microhardness was measured by the microhardness tester, as described in Section 1.3.3 above. Three indentations were made in the centre of the erosion lesion of all samples at four stages during the study; before application of the allocated fluoride treatment and after the third, sixth and ninth cycle of erosion and a mean Knoop microhardness (KHN) was

calculated per sample and subsequently a mean (SD) KHN was calculated per group (n = 6/gp). The group mean KHN after three, six and nine cycles was then compared to the baseline microhardness and a mean percent Knoop microhardness change (%KHC) was calculated for each fluoride group, in comparison to control. Microhardness was not calculated for the erosion-abrasion groups as this analytical technique is not appropriate for wear studies modelling wear from erosion-abrasion.

4.3 Statistical analysis

From pilot data, it was estimated that in order to have an 80 % chance of detecting a 25 % difference in mean volume change after erosion and after erosion-abrasion between the fluoride groups, at the 5 % level of significance, six samples would be required in each group, assuming that the standard deviation of the volume change in each group was around 2.88 million $\mu\text{m}^3/\text{mm}$.

Data were processed and analysed using Stata 11 software (StataCorp, USA). The profilometry results from the study conformed to a normal distribution and were described using mean and standard deviation. Data were assessed for differences between wear process (erosion/erosion-abrasion) and fluoride group using two-way analysis of variance (ANOVA), and % KHC data were assessed for differences between fluoride groups using two-way analysis of variance (ANOVA). Post-ANOVA Scheffe tests were performed for multiple comparisons. Statistical significance was inferred with $p < 0.05$.

4.4 Results

4.4.1 Profilometry

Table 19 and Table 20 show the mean (SD) volume of surface change ($\text{M } \mu\text{m}^3/\text{mm}$) by fluoride group after three, six and nine cycles of erosion and erosion-abrasion respectively. Statistically significant differences for fluoride groups versus control are annotated using * symbol and

statistically significant differences between groups are annotated using same superscript letters ^{a-a} by column.

Table 19 Mean (SD) volume (M $\mu\text{m}^3/\text{mm}$) surface change by fluoride group after three, six and nine cycles of erosion (n =6/gp)

	3 cycles erosion	6 cycles erosion	9 cycles erosion
Control	-6.32 * (3.58)	-10.52 * (1.70)	-15.20 * (2.08)
NaF	-4.30 ^{ab} (0.72)	-9.90 ^{ef} (1.28)	-14.53 ^{mn} (1.98)
SnF₂	-3.13 ^c (1.39)	-9.27 ^{jk} (1.32)	-15.30 ^{opq} (2.26)
TiF₄	5.05 * ^{acd} (1.35)	2.05 * ^{ejl} (2.26)	-1.38 * ^{mo} (2.25)
Bifluorid10®	1.07 * ^{bd} (2.58)	-4.57 * ^{fkl} (1.32)	-9.42 * ^{npq} (2.01)

* indicates statistically significant differences between treatment and control (p <0.01)
Same superscript letters ^{a-a} by column indicate statistically significant differences between treatments (p <0.01)

Table 20 Mean (SD) volume (M $\mu\text{m}^3/\text{mm}$) of surface change by fluoride group after three, six and nine cycles of erosion-abrasion (n =6/gp)

	3 cycles erosion-abrasion	6 cycles erosion-abrasion	9 cycles erosion-abrasion
Control	-6.57 * (1.09)	-12.47 * (2.33)	-19.08 * (3.77)
NaF	-5.12 ^a (1.47)	-7.45 * ^b (2.30)	-11.88 * (3.67)
SnF₂	-4.05 (1.94)	-7.02 * (1.85)	-12.70 (1.99)
TiF₄	-2.68 * ^a (1.07)	-2.63 * ^b (3.37)	-13.55 (1.48)
Bifluorid10®	-1.98 * (0.88)	-4.48 * (1.28)	-9.53 * (2.93)

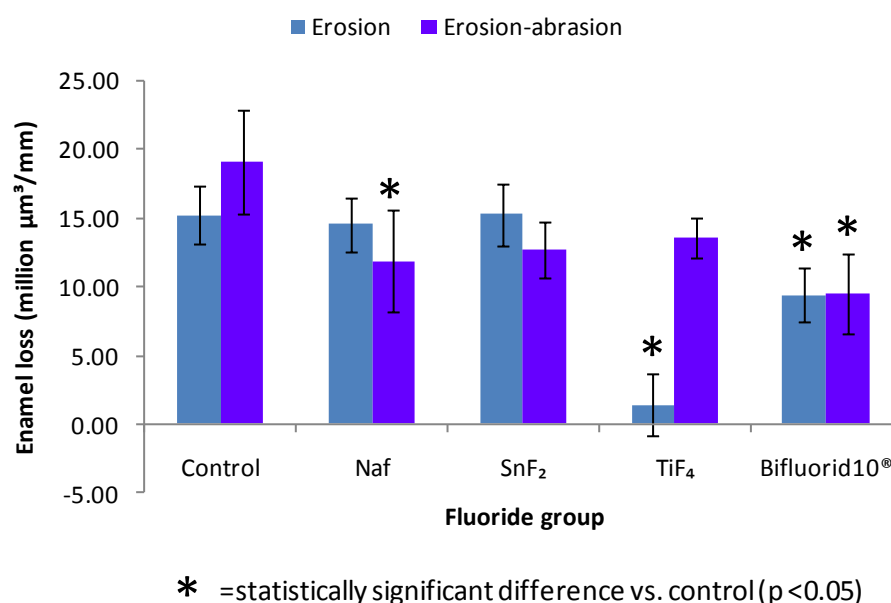
* indicates statistically significant differences between treatment and control (p <0.01)
Same superscript letters ^{a-a} by column indicate statistically significant differences between treatments (p <0.01)

For erosion alone, the NaF, SnF₂ and control groups showed increasing volume loss (negative values) after three, six and nine cycles of erosion (Table 19) but this difference did not reach statistical significance when compared to the controls. The TiF₄ group showed a volume gain after three and six cycles of erosion, but a volume loss after nine cycles of erosion which was statistically significantly less than that of the control, NaF, SnF₂ and Bifluorid10® groups (p <0.001) (Table 19). The Bifluorid10® group showed a volume gain after three cycles of erosion

but volume loss after six and nine cycles of erosion (Table 19) and this difference was statistically significantly less in comparison with the NaF, SnF₂ groups and significantly greater volume loss than TiF₄ after nine cycles of erosion ($p < 0.001$).

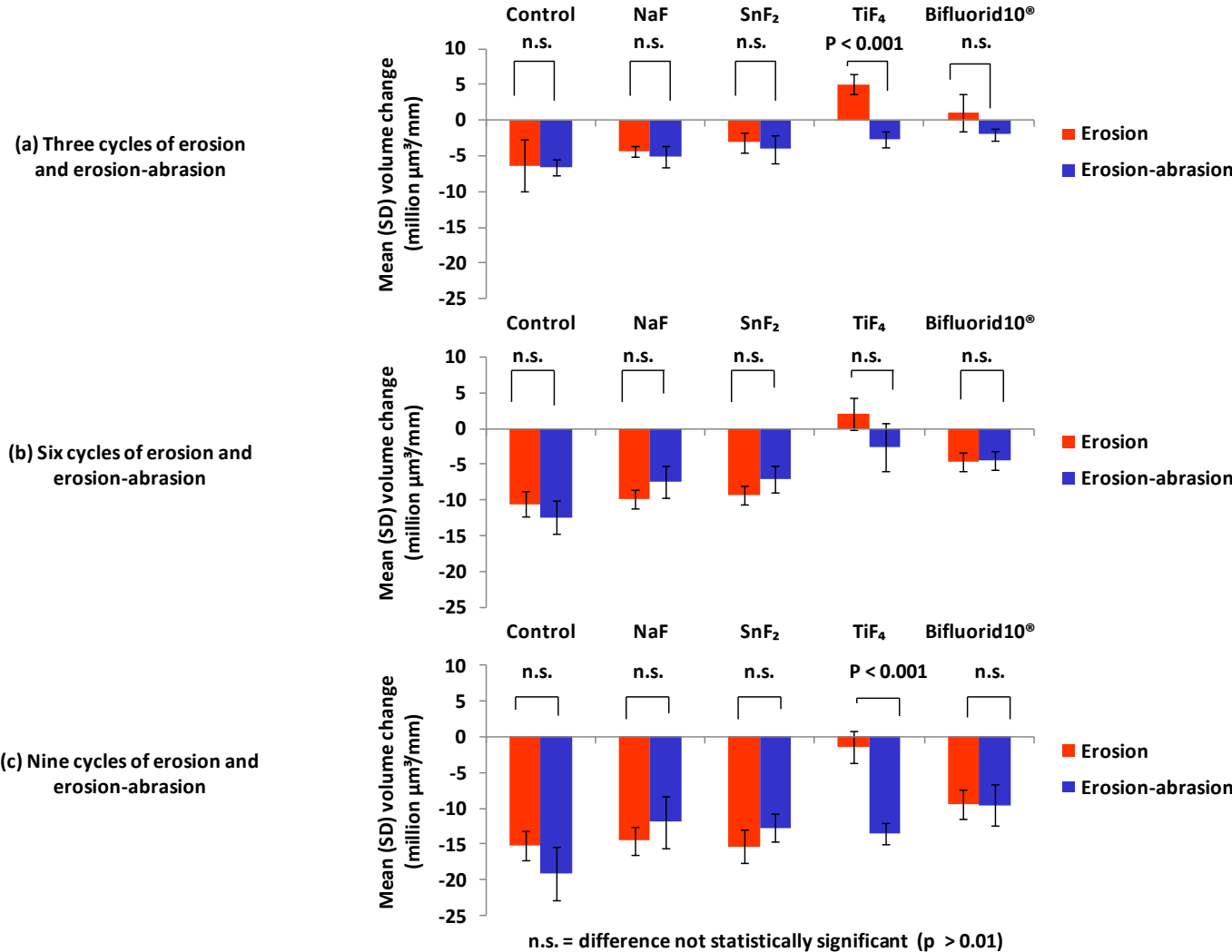
After the third, sixth and ninth cycles of erosion-abrasion all groups showed volume loss (Table 20). There was a statistically significant reduction in volume loss in the groups treated with TiF₄ and Bifluorid10® compared to the controls after three cycles of erosion-abrasion, and for all groups compared to the control after six cycles of erosion-abrasion. Figure 46 below shows the mean (SD) volume of enamel and product loss (M $\mu\text{m}^3/\text{mm}$) after nine cycles of erosion and erosion-abrasion by fluoride/control group ($n = 6/\text{gp}$). This figure shows that at the conclusion of the study, after nine cycles of erosion, the TiF₄ and Bifluorid10® groups were the only groups that showed volume loss significantly less than the control ($p < 0.05$), after nine cycles of erosion-abrasion, the NaF and Bifluorid10® groups were the only groups that showed volume loss significantly less than the control ($p < 0.05$). Between group comparisons revealed no statistically significant comparisons ($p > 0.05$).

Figure 46 Mean (SD) volume of enamel and product loss (M $\mu\text{m}^3/\text{mm}$) after nine cycles of erosion and erosion-abrasion by fluoride/control group ($n = 6/\text{gp}$)



The effect of adding the toothbrush abrasion to the hydrochloric acid erosion can be considered by examining Figure 47 below which shows a comparison of the volume change ($\text{M } \mu\text{m}^3/\text{mm}$) of enamel samples subjected to (a) three cycles (b) six cycles and (c) nine cycles of either erosion or erosion-abrasion by fluoride/control group ($n = 6/\text{gp}$). This Figure shows that only the TiF_4 group had significantly more enamel volume loss after three and nine erosion-abrasion than after the equivalent number of cycles of erosion. No other groups revealed statistically significant differences in the volume of enamel loss after erosion or erosion-abrasion at any stage of the study.

Figure 47 Comparison of volume change (M $\mu\text{m}^3/\text{mm}$) of enamel samples subjected to (a) three cycles (b) six cycles and (c) nine cycles of erosion and erosion-abrasion by fluoride/control group (n = 6/gp)



4.4.2 SEM analysis

Figure 48 below shows representative SEM images from the control treated group, immediately after treatment; after nine cycles of erosion and after nine cycles of erosion-abrasion. These images clearly show an etched enamel prism pattern after nine cycles of erosion, which is characteristic of a Type 1 pattern of etched enamel (Nanci and Ten Cate, 2008) where predominantly the enamel rods are dissolved leaving a demineralised enamel surface, with a delicate inter-prismatic enamel exposed. After nine cycles of erosion-abrasion the etched enamel prisms structure has been removed leaving what appears to be a 'smear layer' with isolated particles of silica-like material, which may be residue from the silica-formulated fluoride free toothpaste used during the abrasion.

Figure 48 Representative SEM images from the control group, immediately after deionized water treatment; after nine cycles of erosion and after nine cycles of erosion-abrasion

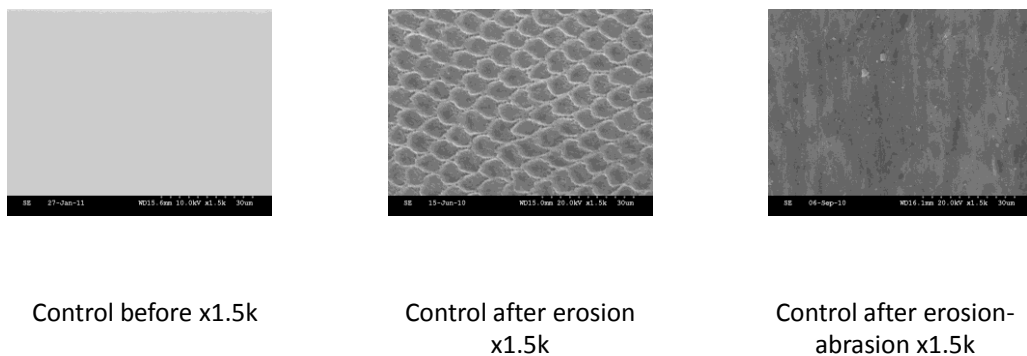
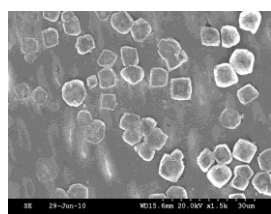
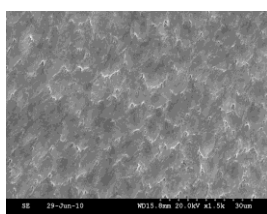


Figure 49 below shows representative SEM images from the NaF treated group, immediately after treatment; after nine cycles of erosion and after nine cycles of erosion-abrasion. These images clearly show the presence of CaF_2 -like globules on the treated surface immediately after treatment, which are approximately three to six μm in diameter. After nine cycles of erosion these CaF_2 -like globules appear to have been completely removed, leaving an etched enamel prism structure, which although clearly etched appears less visibly etched in comparison to the control group sample. After nine cycles of erosion-abrasion again the CaF_2 -like globules are seen to have been completely removed leaving a 'smeared' looking surface with a degree of surface residue present, in a similar fashion to the control group.

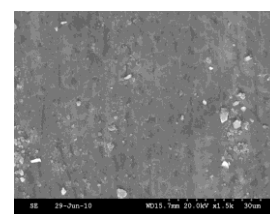
Figure 49 Representative SEM images from the NaF treated group, immediately after treatment; after nine cycles of erosion and after nine cycles of erosion-abrasion



NaF before x1.5k



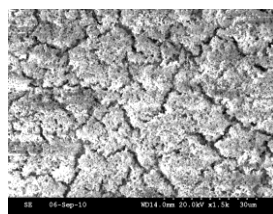
NaF after erosion
x1.5k



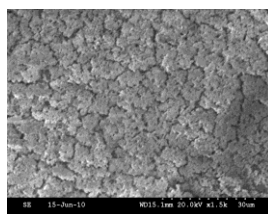
NaF after erosion-
abrasion x1.5k

Figure 50 below shows representative SEM images from the TiF_4 treated group, immediately after treatment; after nine cycles of erosion and after nine cycles of erosion-abrasion. These images clearly show the presence of a complete coating across the entirety of this imaged portion of the treated surface immediately after treatment, which shows a crazed or finely cracked surface. After nine cycles of erosion this coating is clearly seen to remain on the surface in its entirety and does not appear to have been removed resulting in no exposure of enamel. After nine cycles of erosion-abrasion however, the coating is seen to have been almost completely removed leaving an etched enamel prism structure with a degree of surface residue present. This residue is seen to be composed of larger particle size than the control and NaF groups, with particle diameters varying from approximately 3-6 μm , in comparison with particles of less than 3 μm in the control and NaF treated groups.

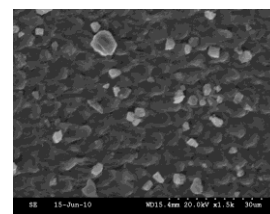
Figure 50 Representative SEM images from the TiF_4 treated group, immediately after treatment; after nine cycles of erosion and after nine cycles of erosion-abrasion



TiF4 before x1.5k



TiF4 after erosion
x1.5k



TiF4 after erosion-
abrasion x1.5k

Figure 51 below shows representative SEM images from the SnF₂ treated group, immediately after treatment; after nine cycles of erosion and after nine cycles of erosion-abrasion. These images show the presence of an incomplete coating across part of this imaged portion of the treated surface immediately after treatment, which shows as patches of coating or residue. After nine cycles of erosion this coating appears to have been removed, resulting in exposure of enamel which shows an etched prism structure. After nine cycles of erosion-abrasion a ‘smeared’ etched enamel prism structure with a degree of surface residue is present, with a particle size and distribution comparable to the control and NaF groups.

Figure 51 Representative SEM images from the SnF₂ treated group, immediately after treatment; after nine cycles of erosion and after nine cycles of erosion-abrasion

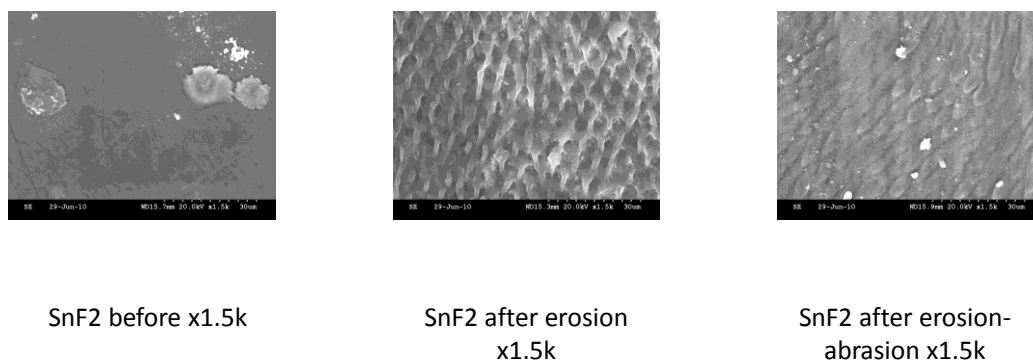
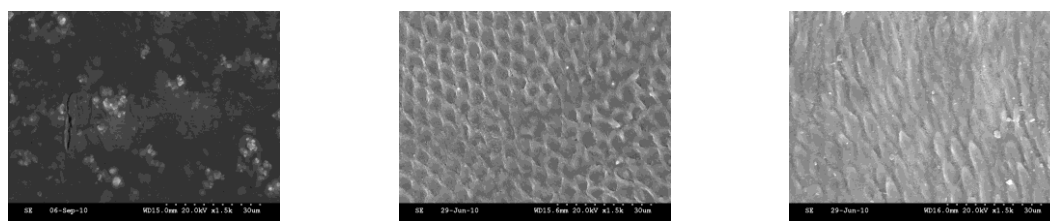


Figure 52 below shows representative SEM images from the Bifluorid10[®] treated group, immediately after treatment; after nine cycles of erosion and after nine cycles of erosion-abrasion. These images clearly show the presence of a complete coating across the entirety of this imaged portion of the treated surface immediately after treatment, which shows a smooth surface with what appears to be embedded CaF₂-like material. After nine cycles of erosion this coating is clearly seen to have been removed from the surface resulting in exposure of enamel which shows an etched prism structure. After nine cycles of erosion-abrasion, the coating is also seen to have been removed leaving an etched enamel prism structure with a degree of surface residue present, with particles of a similar size and distribution to the control and NaF treated groups.

Figure 52 Representative SEM images from the Bifluorid10® treated group, immediately after treatment; after nine cycles of erosion and after nine cycles of erosion-abrasion



Bifluoride before x1.5k

Bifluoride after
erosion x1.5k

Bifluoride after
erosion-abrasion x1.5k

4.4.3 EDS analysis

Figure 53 to Figure 57 below show the elemental surface composition (wt %) of one sample from each group after treatment; after nine cycles of erosion and after nine cycles of erosion-abrasion. Elemental analysis of the TiF_4 treated surface found 3.22 % titanium and 0.26 % fluorine remaining after nine cycles of erosion versus 9.70 % titanium and 8.07 % fluorine immediately after application of the treatment. However all trace of the TiF_4 was removed after erosion-abrasion. For all other fluoride preparations, all elemental traces of the experimental solution were removed after erosion and erosion-abrasion except for 0.16 % fluorine and 0.40 % sodium remaining after erosion-abrasion for the Bifluorid10® varnish treated samples and 0.06 % tin remaining for the SnF_2 treated enamel samples.

Figure 53 Elemental surface composition (wt %) of a sample from the deionized water treated (control) group after application; after nine cycles of erosion and after nine cycles of erosion-abrasion

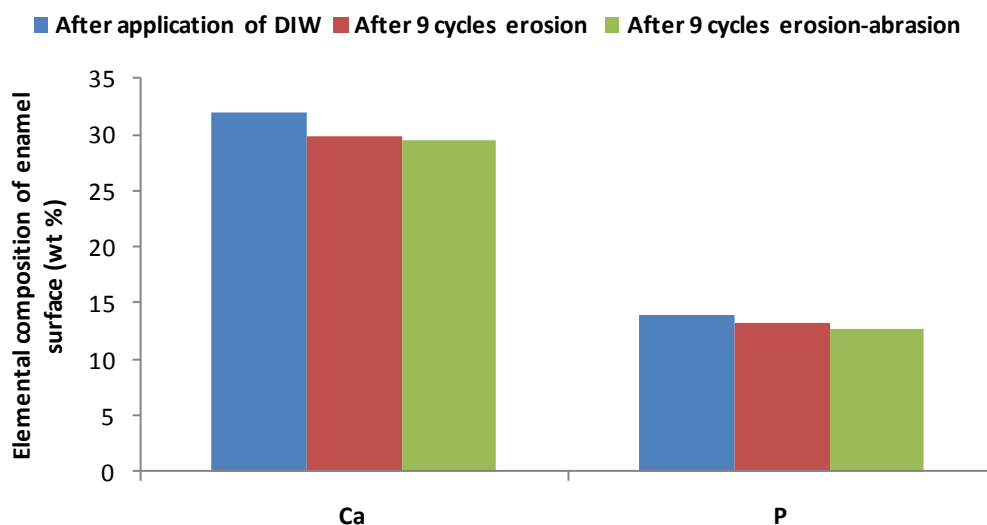


Figure 54 Elemental surface composition (wt %) of a sample from the NaF treated group after treatment; after nine cycles of erosion and after nine cycles of erosion-abrasion

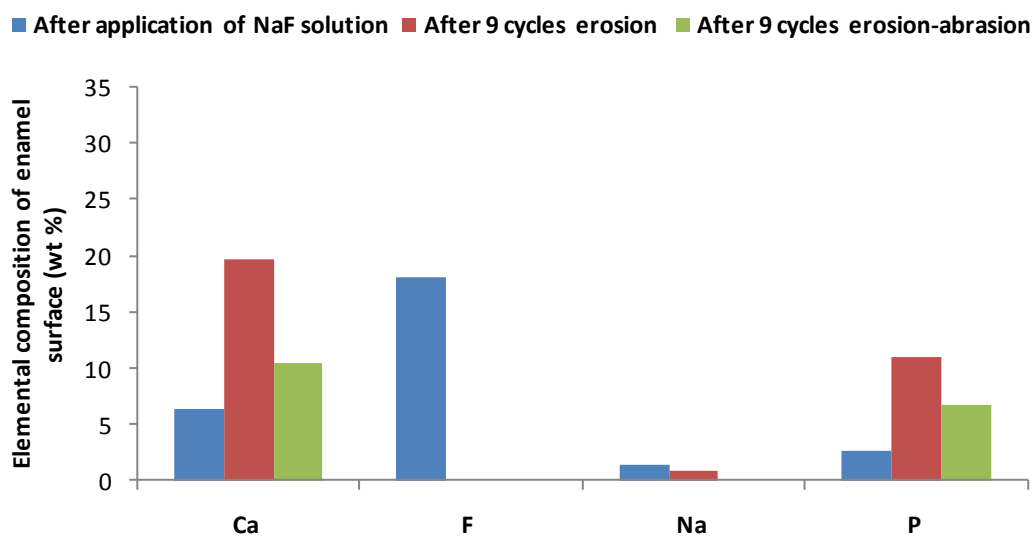


Figure 55 Elemental surface composition (wt %) of a sample from the SnF₂ treated group after treatment; after nine cycles of erosion and after nine cycles of erosion-abrasion

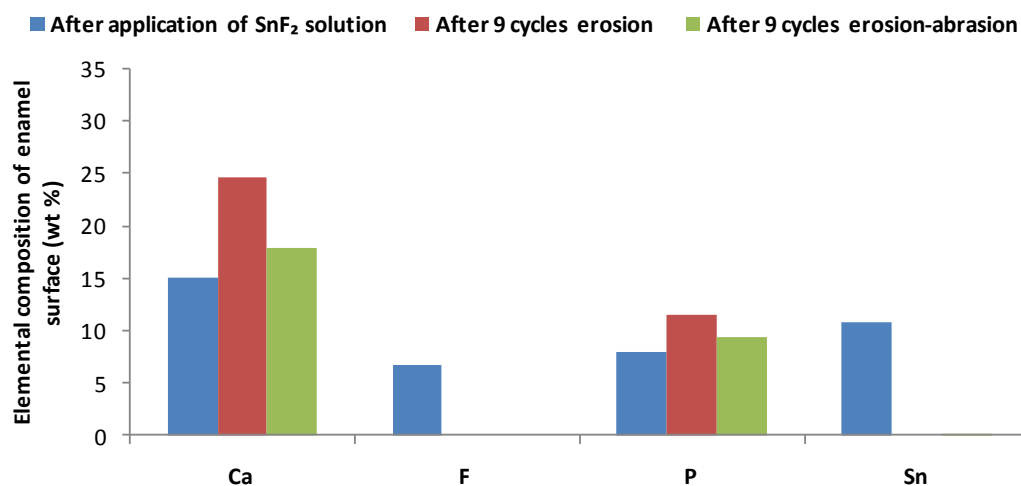


Figure 56 Elemental surface composition (wt %) of a sample from the TiF₄ treated group after treatment; after nine cycles of erosion and after nine cycles of erosion-abrasion

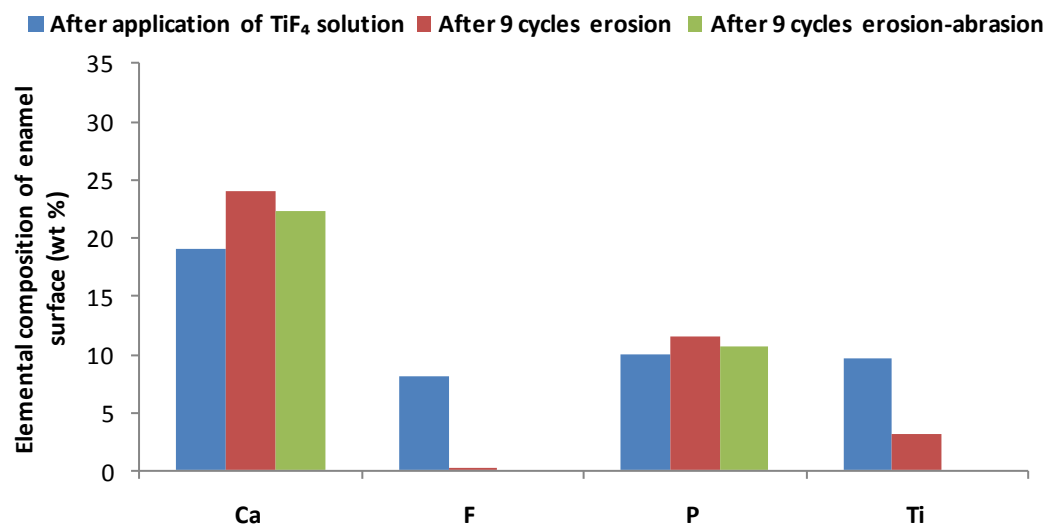
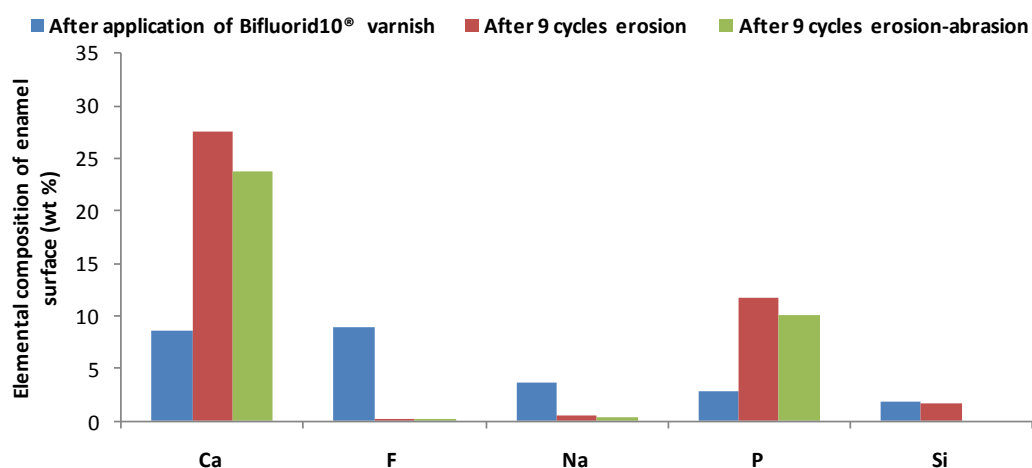


Figure 57 Elemental surface composition (wt %) of a sample from the Bifluorid10® treated group after treatment; after nine cycles of erosion and after nine cycles of erosion-abrasion



4.4.4 Microhardness

It was not possible to measure the Knoop micro-hardness for the TiF_4 group after the experimental procedure due to the nature of the surface coating, which had a mean thickness of 6.25 μm and completely obscured the enamel surface, making it impossible to image the indentations from the diamond indenter.

Figure 58 below shows the mean Knoop microhardness (KHN) of the remaining fluoride groups and control after three, six and nine cycles of erosion. Baseline KHN varied from 358-376 KHN, however no statistically significant differences were noted at baseline among the groups or when individual groups were compared with controls ($P > 0.05$). After three cycles of erosion, a decrease in KHN occurred for all groups, and further smaller reductions in microhardness were noted after six and nine cycles of erosion.

Figure 58 Mean Knoop microhardness (KHN) of fluoride groups and control after 3, 6 and 9 cycles of erosion (n =6/gp)

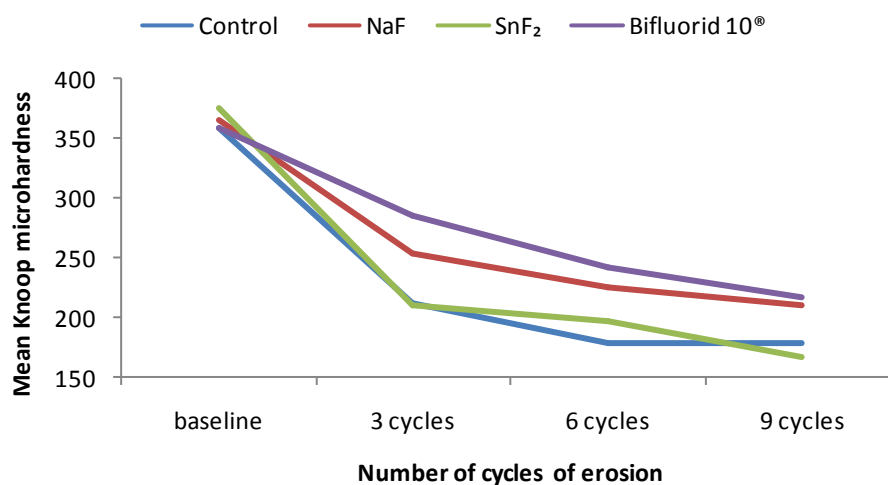
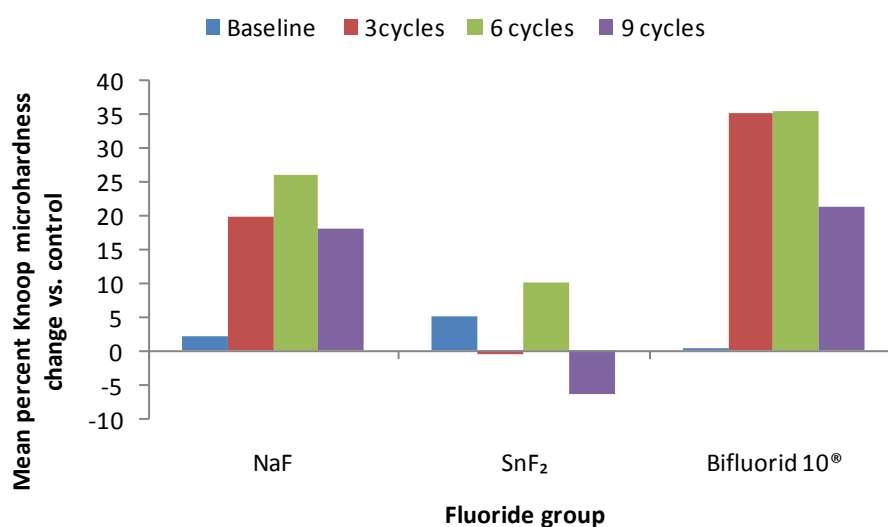


Figure 59 below shows the mean percent Knoop microhardness change (%KHC) of fluoride groups vs. control after three, six and nine cycles of erosion. The %KHC of the Bifluorid10® treated groups decreased significantly less than the control after the third and the sixth cycle ($p < 0.001$) however after nine cycles of erosion, there were no significant differences between the fluoride treated groups and control ($p > 0.05$). Between group comparisons revealed that the Bifluorid10® treated group had statistically significantly less %KHC compared with the SnF₂ treated enamel groups ($p < 0.001$), thus indicating that the enamel hardness reduction of the Bifluorid10® treated groups was significantly less relative to the controls in comparison to enamel hardness reduction of the SnF₂ treated groups relative to the control group.

Figure 59 Mean percent Knoop microhardness change (%KHC) of fluoride groups vs. control after 3, 6 and 9 cycles of erosion (n =6/gp)



Discussion

As with previous studies, application of TiF₄ formed an acid resistant coating on the enamel surface. The coating has been described as a soft but stable structure, hydrophobic and reflecting the spectrum colours (Buyukyilmaz et al., 1997; Hove et al., 2006; Hove et al., 2007b; Hove et al., 2008; Mundorff et al., 1972; Tveit et al., 1983; Tveit et al., 1988; Vieira et al., 2005; Wei et al., 1976). In the present study one single application of 0.5M TiF₄ solution was used in accordance with previous studies (Hove et al., 2008). This coating could be observed visually and was measured using profilometry as positive volume gain after three cycles of erosion. Studies into the ability of TiF₄ to prevent enamel erosion studies report contradictory results, possibly due to differing chemical and physical challenges and different concentrations of TiF₄ solutions used (Magalhaes et al., 2008b).

In the present study, one single application of 0.5M TiF₄ solution reduced enamel loss after three, six and nine cycles of erosion which is in accordance with previous results (Hove et al., 2008). However, although the volume loss in the TiF₄ group was significantly reduced compared with controls after three and six cycles of erosion-abrasion, after nine cycles the volume loss increased by over 40 % in the TiF₄ groups and finally only the NaF and Bifluorid10[®]

showed statistically significant reduction in volume loss after nine cycles of erosion-abrasion compared to the controls. The SEM and EDS results of this *in vitro* study confirmed the profilometry results that following TiF_4 treatment, a surface coating was observed on the enamel samples. This was observed to contain 9.70 % titanium and 8.07 % fluorine using EDS elemental analysis. Following erosion, despite the SEM showing a largely intact surface coating, only 3.22 % titanium and 0.26 % fluorine remained. After nine cycles of erosion-abrasion, no elemental trace of the TiF_4 remained with the coating observed to be almost completely removed using SEM imaging. TiF_4 formed an acid resistant surface coating on the enamel surface after application and in this way acted different from the other fluoride solutions in this study as the NaF and SnF_2 treated groups showed no elemental presence of the fluoride treatment after both nine cycles of erosion and nine cycles of erosion-abrasion.

TiF_4 solutions may reduce enamel mineral loss after acid erosion due to the formation of TiO_2 by complex binding to phosphate bound oxygen in the outer enamel layer and that HF (hydrofluoric acid) formed in the acidic TiF_4 solution may promote a deeper penetration of the F^- and enhance the formation of CaF_2 on the surface (Wiegand et al., 2009). However, studies into the ability of TiF_4 to prevent enamel erosion *in situ* have contradictory findings which may be due to different protocols and different concentrations of TiF_4 solutions used (Hove et al., 2008; Magalhaes et al., 2008b). Overall, the results of this present study suggest that the TiF_4 coating was too fragile to withstand the tooth brushing during the erosion-abrasion, especially after repeated cycles of tooth brushing and HCL acid erosion and this may have ramifications for the ability of a TiF_4 -containing product to provide long term protection against multifactorial tooth wear *in vivo*.

After the cyclic erosion-abrasion protocol the NaF solution and Bifluorid10® varnish showed statistically significant reduction in volume loss after nine cycles of erosion-abrasion compared to the control group; however TiF_4 and SnF_2 showed no statistically significant reduction in volume loss compared to the control group. There are several possible explanations for the

greater protective effect of NaF and Bifluorid10® against the erosion-abrasion protocol compared to TiF_4 seen in this study. Firstly, the low pH of the TiF_4 solution may have demineralised the enamel under the coating thus reducing its resistance to tooth brush abrasion (Skartveit et al., 1989). Secondly, the formulation of the fluoride varnish may have resulted in a surface coating which provided mechanical resistance to abrasion by providing a more stable surface coating which inhibited enamel volume loss even after multiple cycles of erosion-abrasion. Finally, the NaF in both the NaF group and the Bifluoride 10® group, in combination with the fluoride-free toothpaste may have resulted in greater enamel protection from erosion-abrasion via greater chemical interaction with the enamel, as described by previous studies comparing NaF and SnF_2 fluoride toothpastes (Bartlett et al., 1994; Fowler et al., 2009).

Bifluorid10® is a commercial varnish which consists of fluoride both in the form of sodium fluoride 5 % and calcium fluoride 5 % which is the equivalent to 45200 ppm available fluoride (Product information sheet for Bifluorid10 varnish). In the present study, this was the only fluoride treatment that resulted in statistically significant improvements in microhardness reduction compared to control after three and three cycles of erosion-only, however this beneficial effect did not persist after nine cycles of erosion. The EDS analyses also showed that the enamel samples treated with the Bifluorid10® had surface effects which could be detected after nine cycles of erosion abrasion, which although present at trace levels (0.16 % fluorine and 0.4 % sodium) these elements were not present in greater abundance after erosion only (0.09 % fluoride and 0.47 % sodium). The varnish was observed using SEM after application to the enamel as an almost complete layer on top of the surface with embedded CaF_2 -like globules present in the coating. After erosion, this was seen to be partially detached and after nine cycles of erosion-abrasion almost no trace of the varnish remained. Few studies have been performed where the protective effect of sodium fluoride varnishes against erosion-abrasion have been investigated. Vieira et al (2007) documented a gradual detachment of a 0.1

% NaF varnish, which resulted in a similar reduction to cumulative normalized volume loss from dietary erosion-abrasion, as the Bifluorid10® varnish in the present study.

Application of highly concentrated NaF solution at low pH has been shown to reduce enamel erosion (Schlueter et al., 2007) and likewise after intensive fluoridation with NaF in combination with SnF₂ (Ganss et al., 2001). However, unlike this study this required repeated applications of the fluoride to the surface of the substrate being subjected to erosion. The NaF treated group showed the presence of CaF₂-like globules after treatments which were completely removed after nine cycles of erosion and erosion-abrasion. This may be explained by the pH 8 NaF solution causing relatively minor CaF₂ formation in relation to acidulated fluorides (Wiegand and Attin, 2003). However, Yu et al (2010) found that lowering the pH of the NaF solution did not significantly reduce mineral loss when compared with the native NaF solution despite the greater formation of CaF₂-like precipitates on the surface as seen with SEM imaging. Clinically it may be that repeated applications could prolong the protective effect of a fluoride varnish albeit that this topical application with high fluoride concentration has to be performed by dental professionals, which therefore raises cost and time issues. It would therefore be of interest to investigate if lower concentrations of the actual topical agents in the form of a mouth rinse, gel or tooth paste for self-administration could offer a similar protective effect. From the patients point of view this could offer a more biocompatible and practical preventive approach.

Previous studies have shown a protective effect against erosive wear by application of highly concentrated SnF₂ solutions at native pH (Ganss et al., 2001; Ganss et al., 2004a; Ganss et al., 2008; Schlueter et al., 2009; Willumsen et al., 2004; Yu et al., 2010). Although the suggested mode of action is via a formation of CaF₂ as described above, strikingly different results have been reported *in situ* when compared with *in vitro*. Ganss et al (Ganss et al., 2004b) found that *in situ*, intensive SnF₂ fluoridation led to 90 % reduction in enamel loss compared with 20 % reduction *in vitro* (Ganss et al., 2001). A mineral deposit was observed *in situ* consisting of a

stabilised CaF_2 like material possibly due to absorption of HPO_4^{2-} from saliva. The lack of preventive effect against erosion in the SnF_2 fluoridation groups in the present study can be explained by rapid dissolution of the CaF_2 layer from the high titratable acidity/low pH of the HCL acidic challenge simulating vomiting/reflux episodes. The importance of the tin ion has also been investigated and it was speculated that the efficacy of tin-containing fluoride solutions against acids does not stem from precipitates but rather incorporation of tin (saturation principle) and fluoride into dental hard tissue (Schlueter et al., 2009). However, this study has shown that after nine cycles of HCL erosion no elemental presence of the tin remained on the surface despite a 10.85 wt % being present after SnF_2 application. Although 0.06 % tin was detected on the surface after nine cycles of erosion-abrasion the ability of this trace amount of tin to provide protection against erosion-abrasion is uncertain

HCL was chosen as the erosive agent in this study, which is in line with previous studies modelling intrinsic sources of erosion such as gastro-oesophageal reflux disease (GORD) (Hove et al., 2006; Hove et al., 2007a; 2008). GORD is diagnosed by the length of time that pH is below 4 in a given 24h period. Pure gastric acid has a mean pH of 0.9 - 1.5 with gastric acid samples ranging in pH from 1.2 – 6.78 with a mean titratable acidity of 0.68 ml (Bartlett and Coward, 2001) however the pH in the oral cavity is seldom lower than 1.5 due to buffering/dilution effects. Milosevic et al (1997a) measured pH of vomit at 2.9 - 5.0 in bulimia patients. Therefore it was felt that the choice of 0.01 M HCL, pH 2.2 HCL with a titratable acidity of 1.73 ml was relevant to the clinical situation.

In order to simulate multi-factorial tooth wear, tooth brush abrasion was included with the HCL erosion. The observation that the TiF_4 , NaF and SnF_2 surface effects were removed after nine cycles of erosion-abrasion indicates that a coating formed from precipitates of an aqueous fluoride solution are not able to withstand erosion-abrasion *in vitro*. The TiF_4 coating is clearly chemically acid resistant, but it seems to be detached during tooth brushing possibly due to its softness. The Knoop indentations were difficult to read for the TiF_4 treated groups,

which led to the assumption that the surface coating formed by TiF_4 was soft, which is in accordance with the observations presented by Büyükyılmaz et al (1997). In addition a soft (demineralised) zone beneath the coating could have been present as has been demonstrated in previous studies (Skartveit et al., 1989). Wiegand et al (2010) found greater protective effect in a recent *in situ* study which included both erosion and erosion-abrasion in a three day protocol, where a single application of 0.05M TiF_4 solution reduced erosion-abrasion compared with controls. In the latter study a soft drink was used in order to mimic an extrinsic erosive challenge whereas in the present study a 0.01M (pH 2.2) The HCL solution was used, in order to simulate gastric erosion. Furthermore, this study used artificial saliva, which did not contain mucin or salivary proteins which could have acted as a permeable membrane or diffusion barrier in a similar way as a pellicle. However, Hove et al (2008) *in situ* erosion-only study using the same erosive challenge and TiF_4 concentration failed to find any significant differences for TiF_4 versus control.

Energy Dispersive X-Ray Spectroscopy (EDS) provides information about the elemental composition of the surface of the sample being investigated (Woldseth, 1973). The advantage of EDS for dental erosion assessment is that it can reliably detect ion concentrations with a concentration of as little as 1 wt % within a highly mineralised tissue such as enamel. This ability to detect minor ion concentrations has led the technique to be used such as for detection of CaF_2 (Harding et al., 1994) and in studies investigating the effects of amine fluoride on eroded enamel (Rosin-Grget et al., 2000) as well as investigating the remineralising potential of fluoride toothpastes on enamel erosion (Arnold et al., 2006; Arnold et al., 2007). More recently the technique has been compared with profilometry for investigation of TiF_4 , AmF_3 , and SnF_2 *in vitro* (Yu et al., 2010). However this is the first study which has used EDS to assess the ability of a single application of surface fluoride treatments to be able to create surface effects which are able to withstand a physical as well as a chemical challenge. Future uses of the technique could include more frequent elemental assessment of the enamel

surface during the erosive-abrasive cycle to elucidate in more detail at what stage the surface effects of a fluoride treatment are lost.

Chapter 5 The effect of sodium fluoride varnishes and a resin-based adhesive on enamel erosion-attrition *in vitro*

Introduction

Previous research has shown that *in vivo* a single application of a resin-based adhesive system to the palatal surfaces of worn and eroded anterior teeth reduced erosive wear for up to three months (Sundaram et al., 2007a) and that resin-based adhesives protect dentine from erosion-abrasion *in situ* (Azzopardi et al., 2004). Further *in vitro* studies compared the ability of resin based adhesive systems to reduce erosion-abrasion of dentine (in comparison with a fluoride mouthwash) and concluded that the adhesive conferred greater protection to the dentine than the fluoride mouthwash (Sundaram et al., 2007b). However the interpretation of these findings is limited by the lack of knowledge as to whether the protection was purely due to the physical presence of the coating mechanically reducing erosion-abrasion or whether the presence of fluoride in a coating was chemically reducing the erosion. Therefore the potential for oral care products (such as topical fluoride varnishes and resin-based adhesives) to protect enamel against simulated erosion and attrition *in vitro* is an important clinical question which requires further investigation.

5.1 Aim, objectives and null hypothesis

The aim of this study was to investigate the surface effects of a single application of two highly concentrated sodium fluoride varnishes (Bifluorid10® varnish and Duraphat® varnish) and a resin-based adhesive (Adper™ Prompt™ Self-Etch Adhesive) on *in vitro* erosion-abrasion.

The objectives were to:

1. Simulate erosion-attrition in the laboratory using a cyclic tooth wear model consisting of citric acid erosion, salivary remineralisation and enamel-to-enamel attrition.
2. Quantify the effects of a single application of two highly concentrated sodium fluoride varnishes (Bifluorid10® varnish and Duraphat® varnish) and a resin-based adhesive (Adper™ Prompt™ self-etch adhesive) after five, ten and 15 cycles of simulated erosion-attrition, in comparison to a negative control, using optical profilometry, scanning electron microscopy (SEM) and energy-dispersive X-ray spectroscopy (EDS).

The null hypotheses were that

1. A single application of a fluoride varnish or a resin-based adhesive would not influence enamel erosion-attrition *in vitro*.

5.2 Materials and methods

5.2.1 Study design

The study was a factorial 4 x 3, according to the split-plot design. Thus the factors under investigation were:

1. Surface treatment at 4 levels:
 - i. Deionized water (deionized water)
 - ii. Adper™ Prompt™ self-etch adhesive
 - iii. Bifluorid10® varnish
 - iv. Duraphat® varnish
2. Number of wear cycles at three levels:
 - i. Five cycles
 - ii. Ten cycles
 - iii. 15 cycles

5.2.2 Sample preparation

Enamel samples (n = 72) were prepared as described in Section 3.2.2 above, before being randomised using a Table of randomly generated numbers obtained from spreadsheet

software (Microsoft® Office Excel® 2007, Microsoft® Corporation, USA). Samples were allocated to one of four groups (n =18/gp) according to the four surface treatments.

5.2.3 Application of surface treatments

Deionised water was applied using a pipette to the enamel surface and allowed to air dry. The fluoride concentrations, pH and composition of the self-etch adhesive and the fluoride varnishes are shown in Table 21 below. All products were applied following the manufacturer's instructions. Adper™ Prompt™ self-etch adhesive was applied for 15 seconds using a rubbing motion, followed by air drying, followed by a second layer (no rubbing or waiting time), followed by air drying. The second layer was light activated for ten seconds using a curing light. Light activation was performed using a halogen light-curing unit (XL-2500, 3M ESPE, St. Paul, MN, USA) with an output power intensity of 600 mW / cm², at a standardized distance of 5 mm from the enamel surface. The Bifluorid10® varnish was applied for 20 seconds using a micro-brush. The Duraphat® varnish was applied according as a thin layer to the enamel surface using a micro-brush and a drop of deionized water applied to the surface of the varnish, following which the varnish was allowed to set.

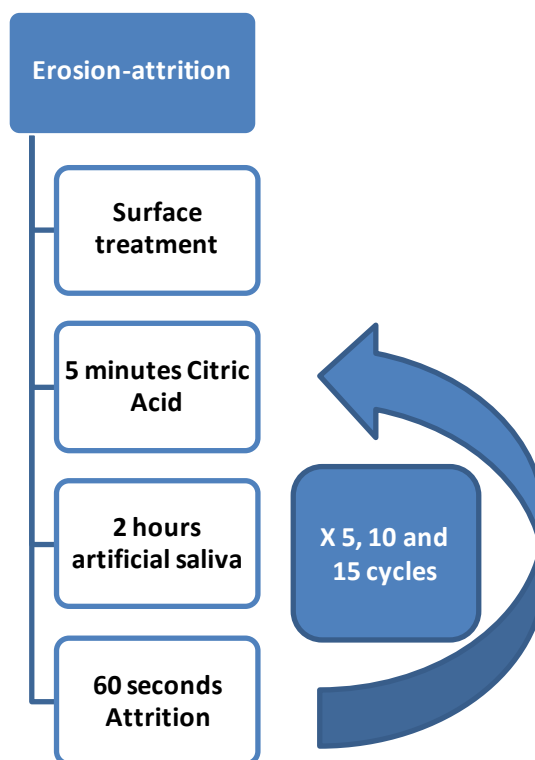
Table 21 Fluoride concentration (ppm), starting pH and composition of the self-etch adhesive and the two fluoride varnishes applied to the enamel samples prior to erosion-attrition

Product name	Fluoride concentration (ppm)	Starting pH	Composition
Deionized water	0	6.8	Water
Adper™ Prompt™ self-etch adhesive	0	0.88	Phosphate methacrylates, water, ethanol, silanated colloidal silica, photoinitiator.
Bifluorid10® varnish	45200	5.5	Ethyl acetate, cellulose nitrate, isopentyl propionate, sodium fluoride 5%, calcium fluoride 5%.
Duraphat® varnish	22600	4.5	Ethanol, colophonium, copal, flavouring, white wax (E901) shellac (E904), sodium fluoride 2.26 %

5.2.4 Cyclic tooth wear model

Following application of the surface treatments, the first ten samples of each group were subjected to a total of 15 wear cycles over five days with each day consisting of five cycles of erosion-attrition. As shown in Figure 60 below, one cycle of erosion-attrition consisted of five minutes immersion in citric acid, followed by 60 minutes immersion in artificial saliva, followed by sixty seconds of attrition.

Figure 60 Flowchart of the protocols for the erosion-attrition



Following surface treatment, the samples were immersed in 50 ml of the citric acid solution static at room temperature ($23\text{ }^{\circ}\text{C} \pm 1\text{ }^{\circ}\text{C}$) for five minutes. The citric acid solution was prepared as described in Section 2.3.3.4 above. Following sample preparation, all samples were immersed in artificial saliva for sixty minutes. The artificial saliva was formulated as described in Section 2.3.3.5 above. Fresh batches of artificial saliva were mixed daily. Following removal from the fluoride/control solution and careful rinsing and blot drying, all samples were immersed in 50 ml of the artificial saliva whilst being subjected to 60 strokes of attrition at room temperature ($23\text{ }^{\circ}\text{C} \pm 1\text{ }^{\circ}\text{C}$), as described in Section 3.2.3 above.

Following profilometry, the tape was repositioned according to scalpel marks that had been placed in the acrylic at the time of initial tape placement, demarcating the borderline between the worn and unworn (reference) areas.

5.2.5 Profilometry

At the end of each round of five, ten and 15 cycles of erosion-attrition, the tape was removed for profilometry using the white light confocal profilometer as described in Section 2.1.2

above. Following profilometry, volume change ($M \mu\text{m}^3/\text{mm}$) and step height change (μm) were calculated using the ImageJ macros as described in Section 2.1.2.5 above. Following measurement, the tape was repositioned using scalpel marks that had been placed at the time of initial tape placement, in order that the next round of erosion-attrition could be carried out.

5.2.6 Scanning electron microscopy (SEM) and energy-dispersive X-ray spectroscopy (EDS)

Two samples per group were randomly chosen for SEM and EDS analysis (as described in Section 4.2.6 above), at four stages of the study; after application of the surface treatment; after five cycles of erosion-attrition, after ten cycles of erosion-attrition and after 15 cycles of erosion-attrition.

5.3 Statistical analysis

The primary outcome was change in volume ($M \mu\text{m}^3/\text{mm}$) and step height (μm) after five, 10 and 15 cycles of experimental wear. Data were processed and analysed using Stata 11 software (StataCorp, USA). Both 'step height' and 'volume' exhibited frequency distributions deviated from a Normal distribution so data were described using a median and inter-quartile range. The data were not amenable to transformation to a Normal distribution and the difference between baseline and subsequent measures was initially chosen for initial analysis. Two-way Analysis of Variance (ANOVA) indicated that there was considerable interaction between treatment group and the stages of erosion/attrition. Subsequently, Kruskal-Wallis ANOVA was chosen to analyse the differences between treatments at each stage and the differences between each stage within treatments. Post-ANOVA contrasts were performed using a Wilcoxon matched-pairs, signed-ranks test within treatments and a Mann-Whitney-U test between treatments. A p value less than 0.01 was regarded as indicating statistical significance.

5.4 Results

5.4.1 Profilometry

After application of the surface treatments to the enamel surfaces, the step height and volume change was quantified using ImageJ SH and vol macros. Table 22 and Table 23 show the median (IQR) step height (μm) and volume ($\text{M } \mu\text{m}^3/\text{mm}$) surface change of the treated enamel surfaces after application of product/ deionized water (deionized water) and after five, 10 and 15 cycles of erosion-attrition, ($n = 10/\text{gp}$). For the control group, application of the deionized water resulted in a median step height and volume surface change of $0.0 \mu\text{m}$ and $0.7 \text{ M } \mu\text{m}^3/\text{mm}$ respectively. The Duraphat® varnish treated samples showed the greatest median step height ($56.9 \mu\text{m}$) and volume ($227.4 \text{ M } \mu\text{m}^3/\text{mm}$) surface change after application; followed by the Bifluorid10® varnish treated samples which had a step height and volume surface change of $32.3 \mu\text{m}$ and $72.5 \text{ M } \mu\text{m}^3/\text{mm}$ respectively; followed by the Adper™ Prompt™ self-etch adhesive treated samples, which had a median step height of $21.3 \mu\text{m}$ and volume surface change of $20.2 \text{ M } \mu\text{m}^3/\text{mm}$ after product application.

Table 22 Median (IQR) step height (μm) surface change of treated enamel surface after application of product/deionized water (deionized water) and after five, ten and 15 cycles of erosion-attrition, by product group ($n = 10/\text{gp}$)

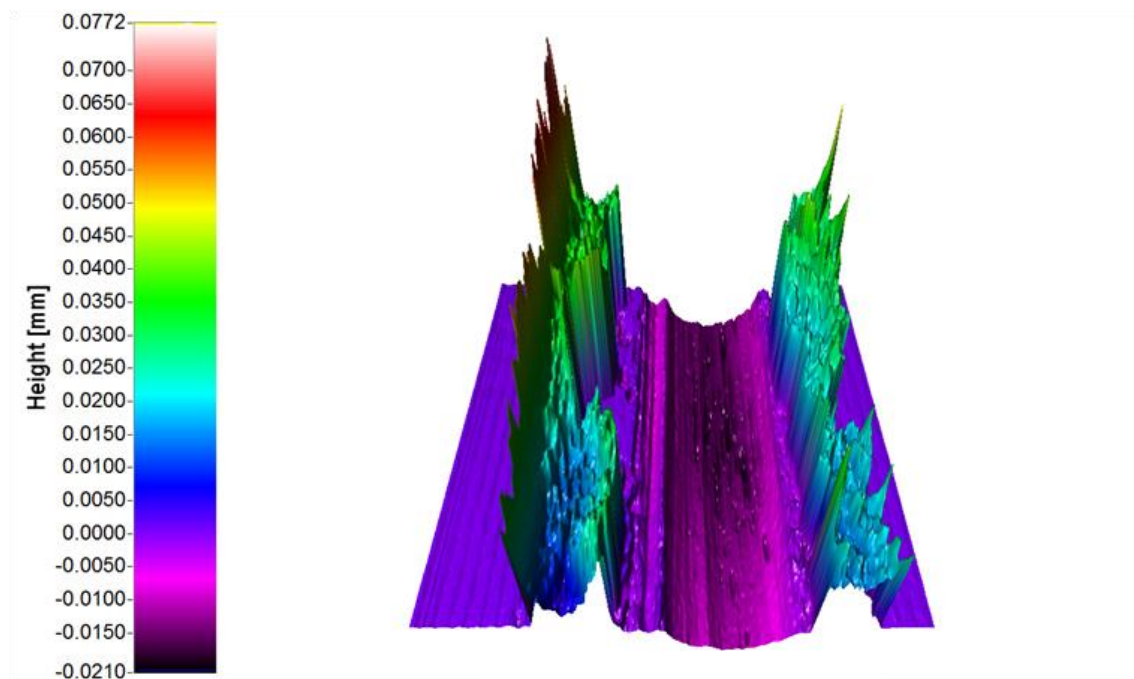
	After application ($\text{M } \mu\text{m}^3/\text{mm}$)	Five cycles ($\text{M } \mu\text{m}^3/\text{mm}$)	Ten cycles ($\text{M } \mu\text{m}^3/\text{mm}$)	15 cycles ($\text{M } \mu\text{m}^3/\text{mm}$)
deionized water Control	0.0 (0.00)	-3.0 (1.46)	-4.1 (2.34)	-4.9 (2.54)
Bifluorid10® varnish	32.3 (10.39)	27.3 (9.55)	25.5 (22.38)	16.4 (17.20)
Adper™ Prompt™ self-etch adhesive	21.3 (5.48)	14.7 (4.83)	9.6 (14.64)	8.7 (5.05)
Duraphat® varnish	56.9 (14.27)	46.8 (43.86)	28.0 (46.03)	23.7 (59.23)

Table 23 Median (IQR) volume (M $\mu\text{m}^3/\text{mm}$) surface change after application of product/deionized water and after five, ten and 15 cycles of erosion-attrition, by product group (n = 10/gp)

	After application (M $\mu\text{m}^3/\text{mm}$)	Five cycles (M $\mu\text{m}^3/\text{mm}$)	Ten cycles (M $\mu\text{m}^3/\text{mm}$)	15 cycles (M $\mu\text{m}^3/\text{mm}$)
Deionized water	0.7 (0.50)	-4.5 (2.97)	-15.4 (4.67)	-21.6 (8.22)
Bifluorid10® varnish	72.5 (11.36)	23.2 (23.00)	5.0 (22.05)	0.1 (22.61)
Adper™ Prompt™ self-etch adhesive	20.2 (24.95)	0.6 (10.18)	-2.5 (0.55)	-11.7 (27.38)
Duraphat® varnish	227.4 (110.18)	40.3 (83.47)	37.0 (69.05)	33.7 (69.84)

All treatment groups showed significant higher volumes compared to the controls after application ($p > 0.05$). All groups showed a subsequent reduction in median step height and volume surface change after five, ten and 15 cycles of erosion-attrition, these significant differences were maintained throughout the study and therefore the initial step height and volume surface changes that were seen after application of the products/deionized water were carried over across all subsequent measurements. The same between group differences that were observed immediately after surface treatment were noted after 15 cycles of erosion attrition, the reason for this can be explained with reference to Figure 61 below. This Figure shows a representative image of Bifluorid10® treated enamel sample after ten cycles of erosion attrition. From this image it can be seen that central area of enamel loss is bordered on both sides by an area of retained surface coating, the presence of which skewed the step height and volume measurements and therefore masked the true extent of enamel loss.

Figure 61 Representative image of Bifluorid10® treated enamel sample after ten cycles of erosion attrition



The retention of the coating was caused by the exact repositioning of the attrition antagonist in the same location which therefore caused a central attrition-erosion lesion of enamel loss, whereas the varnish on the periphery of the exposed enamel area was able to resist dissolution by the action of the citric acid alone. Therefore, as can be seen in Table 22 and Table 23 above, the enamel samples treated with the varnishes and the resin-based adhesive had large variances which prevented between group comparisons revealing any statistically significant differences and therefore these measurements cannot be used to determine the relative protective effects of the fluoride varnishes and self-etch adhesive used in this study.

Therefore, in order to just measure the loss of enamel (as opposed to the loss of coating and the loss of enamel), BODDIES® software was used to virtually remove the coating, as shown in Figure 62 below.

Figure 62 Images from a representative enamel sample (a) after application of Duraphat® varnish (b) after ten cycles of erosion-attribution and (c) after virtual removal of the coating using BODDIES® software

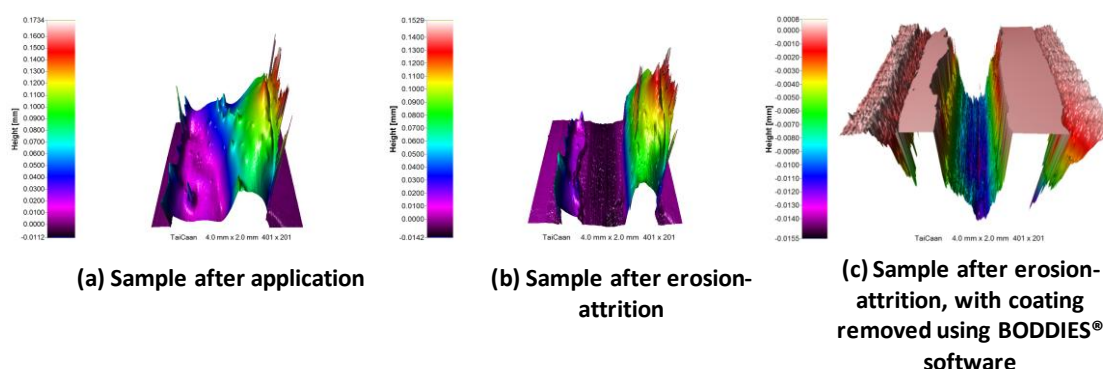


Image (b) and image (c) from this Figure were from the same 3D data set, however in image (c) BODDIES® software had been used to remove the remaining Duraphat® by cutting off all 3D data with a z value greater than 0. This can be justified by the standardised polishing procedure (described in Section 2.1.2.2 above) which provided a flat enamel surface. Thus the virtual removal of these data points would only preferentially remove the coating produced by the products whilst preserving all 3D data regarding the loss of enamel. Finally the cut off data points were filled using a first order polynomial which thus allocated all these data points a z height value of 0 (i.e. approximating the situation if there had not been any enamel wear). The subsequent ImageJ macro step height and volume measurement therefore treated these data points as neither enamel loss nor gain, a desired outcome based upon the likelihood that the enamel had not been damaged by the application of the coating and moreover, that the product had protected the covered enamel from any wear. Thus this virtual removal of the coating preserved all the information needed to determine the outcome of the study, which was whether the single application of the fluoride varnishes or the resin-based adhesive would influence enamel erosion-attribution *in vitro*.

The median (IQR) step height (μm) and volume ($\text{M } \mu\text{m}^3/\text{mm}$) enamel loss after application of product/deionized water and after five, ten and 15 cycles of erosion-attribution can be seen in Table 24 and Table 25 below. These tables show that after application of product / deionized water (deionized water) there were no statistically significant differences in median step

height (μm) and volume ($\text{M } \mu\text{m}^3/\text{mm}$) enamel loss of the treated enamel surface, either between the product groups themselves ($p > 0.01$) or between the product groups and the control group, which therefore suggested that the virtual removal of the enamel coating using the software was carried out successfully. After five cycles of erosion attrition, the Adper™ Prompt™ self-etch adhesive treated samples, showed significantly greater median step height ($3.50 \mu\text{m}$) and volume ($9.80 \text{ M } \mu\text{m}^3/\text{mm}$) enamel loss than the Duraphat® varnish treated samples ($p < 0.01$) which had $1.94 \mu\text{m}$ median step height and $1.60 \text{ M } \mu\text{m}^3/\text{mm}$ median volume enamel loss and the Bifluorid10® varnish treated samples ($p < 0.01$) which had $2.17 \mu\text{m}$ median step height and $1.79 \text{ M } \mu\text{m}^3/\text{mm}$ median volume enamel loss. After five cycles of erosion-attrition, when the Adper™ Prompt™ self-etch adhesive treated group was compared with the control group, the median step height and volume of enamel loss was greater in the treatment group than the control group, however this difference was only significantly different for the volume of enamel loss ($p < 0.01$), not for the step height difference ($p > 0.01$). Moreover, after ten and 15 cycles of erosion-attrition the enamel loss of the Adper™ Prompt™ self-etch adhesive treated group returned to a lower step height and volume value than the control group.

Table 24 Median (IQR) step height (μm) enamel loss after application of product/deionized water and after five, ten and 15 cycles of erosion-attrition, by product group (n = 10/gp)

	After application	Five cycles	Ten cycles	15 cycles
Control	0.21 (0.18-0.23)	3.19 (2.2-3.53)	4.48 (3.85-5.91)	6.38 (4.75-8.06)
Adper™ Prompt™ self-etch adhesive	0.26 (0.17-0.28)	3.50 ^{ab} (3.04-5.14)	5.31 (4.03-6.66)	6.81 (5.16-7.80)
Bifluorid10® varnish	0.25 (0.18-0.35)	2.17 ^a (1.65-2.90)	5.07 (4.41-6.09)	7.37 (6.79-9.39)
Duraphat® varnish	0.27 (0.24-0.32)	1.94 ^b (1.40-2.39)	3.44 (3.07-3.75)	5.98 (5.26-7.10)

* indicates statistically significant differences between treatment and control ($p < 0.01$)
 Same superscript letters ^{a-b} by column indicate statistically significant differences between treatments ($p < 0.01$)

Table 25 Median (IQR) volume (M $\mu\text{m}^3/\text{mm}$) enamel loss after application of product/deionized water and after five, ten and 15 cycles of erosion-attrition, by product group (n = 10/gp)

	After application	Five cycles	Ten cycles	15 cycles
Control	0.18 (0.08-0.21)	5.66 (4.65-7.75)	19.57 (16.88-20.60)	27.83 (20.53-43.39)
Adper™ Prompt™ self- etch adhesive	0.03 (0.02-0.03)	9.80 * ^{ab} (7.39-12.85)	13.12 ^{bc} (9.93-22.45)	16.33 (10.30-29.50)
Bifluorid10® varnish	0.03 (0.02-0.06)	1.79 * ^a (1.09-3.23)	5.59 * ^b (4.87-8.88)	12.64 * (8.26-16.36)
Duraphat® varnish	0.04 (0.03-0.04)	1.60 * ^b (0.26-2.46)	4.17 * ^c (3.38-5.93)	10.02 * (6.77-12.90)

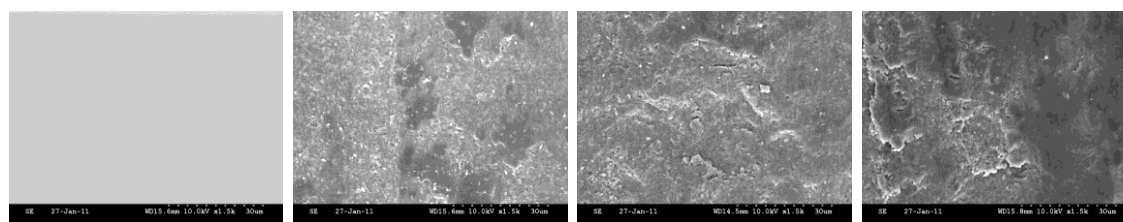
* indicates statistically significant differences between treatment and control (p < 0.01)

Same superscript letters ^{a-b} by column indicate statistically significant differences between treatments (p < 0.01)

5.4.2 SEM analysis

Figure 63 below shows the SEM images from a sample from the control group: after application of de-ionized water (deionized water); after five, ten and 15 cycles of erosion-attrition (x 1.5 k magnification). After application of deionized water, no trace of eroded enamel prisms can be seen and the enamel surface appears intact. After five cycles of erosion-attrition, these images clearly show a damaged looking enamel surface which, in comparison to the previous image appears to have had sections of enamel gouged from its surface. There is not a clear etch pattern surface, with no evidence of remaining delicate inter-prismatic material. After ten and 15 cycles of erosion-attrition the enamel surface has been further damaged with apparent removal of further material. Isolated residue-like particles of material are scattered across the enamel surface, however there is not extensive 'slurry' like coating or smear layer material present.

Figure 63 SEM images from a sample from the control group: after application of de-ionized water (deionized water); after five, ten and 15 cycles of erosion-attribution (x 1.5 k magnification)



After application of DIW

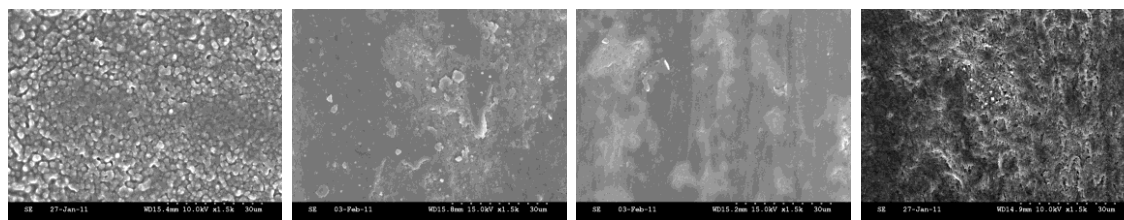
After five cycles of erosion-attribution

After ten cycles of erosion-attribution

After fifteen cycles of erosion-attribution

Figure 64 below shows the SEM images from a sample from the Adper™ Prompt™ self-etch adhesive group: after application of Adper™ Prompt™ self-etch adhesive; after five, ten and 15 cycles of erosion-attribution (x 1.5 k magnification). These images clearly show the presence of a complete coating across the entirety of this imaged portion of the treated surface immediately after application of the Adper™ Prompt™ self-etch adhesive, which shows a finely globular or beaded surface. After five cycles of erosion-attribution this coating appears to not be present resulting in exposure of the enamel surface which is seen to be damaged in a similar fashion to that of the equivalent control group image above. After ten cycles of erosion-attribution however, a more ‘smeared’ looked enamel surface is seen. After 15 cycles of erosion-attribution, a particularly damaged looking surface is apparent with no ‘smear layer’ or coating/residue visible.

Figure 64 SEM images from a sample from the Adper™ Prompt™ self-etch adhesive group: after application of Adper™ Prompt™ self-etch adhesive; after five, ten and 15 cycles of erosion-attrition (x 1.5 k magnification)



**After application of
Adper™ Prompt™ self
etch adhesive**

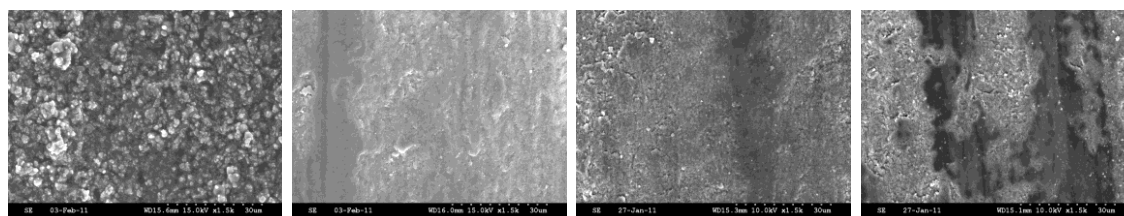
**After five cycles of
erosion-attrition**

**After ten cycles of
erosion-attrition**

**After fifteen cycles of
erosion-attrition**

Figure 65 below shows the SEM images from a sample from the Bifluorid10® varnish group: after application of Bifluorid10® varnish; after five, ten and 15 cycles of erosion-attrition (x 1.5 k magnification). These images clearly show the presence of CaF_2 -like globules on the treated surface immediately after treatment, which are similar to the appearance of the Bifluorid10® coating seen in Figure 52 above. After five cycles of erosion-attrition these CaF_2 -like globules appear to have been completely removed, leaving a 'gouged' or scratched looking enamel surface. After ten and 15 cycles of erosion-attrition again the CaF_2 -like globules are seen to have been completely removed leaving a 'smeared' and 'gouged' looking surface with a degree of surface residue present, in a similar fashion to the control and Adper™ Prompt™ treated groups.

Figure 65 SEM images from a sample from the Bifluorid10® varnish group: after application of Bifluorid10® varnish; after five, ten and 15 cycles of erosion-attrition (x 1.5 k magnification)



**After application of
Bifluorid10® varnish**

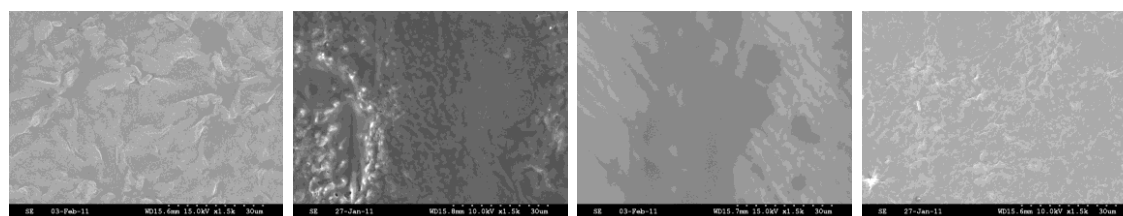
**After five cycles of
erosion-attrition**

**After ten cycles of
erosion-attrition**

**After fifteen cycles of
erosion-attrition**

Figure 66 below shows SEM images from a sample from the Duraphat® varnish group: after application of Duraphat® varnish; after five cycles of erosion-attrition, after ten cycles of erosion-attrition and after 15 cycles of erosion-attrition (x 1.5 k magnification). These images clearly show the presence of a complete coating across the entirety of this imaged portion of the Duraphat® treated surface immediately after treatment, which shows an irregular surface, however no embedded CaF_2 -like material is visible. After five cycles of erosion-attrition this coating is seen to have been partially removed from the surface resulting in exposure of enamel from around two-thirds of the image. The exposed enamel shows a degree of damage to the surface. After ten cycles of erosion-attrition, a degree of surface residue is present, with a 'smeared' or perhaps finely scratched surface visible. Finally, after 15 cycles of erosion-attrition a 'gouged' enamel surface can be seen, however this surface appears to not be as damaged looking as the other group images at the comparable stage of erosion-attrition.

Figure 66 SEM images from a sample from the Duraphat® varnish group: after application of Duraphat® varnish; after five cycles of erosion-attrition, after ten cycles of erosion-attrition and after 15 cycles of erosion-attrition (x 1.5 k magnification)



After application of
Duraphat® varnish

After five cycles of
erosion-attrition

After ten cycles of
erosion-attrition

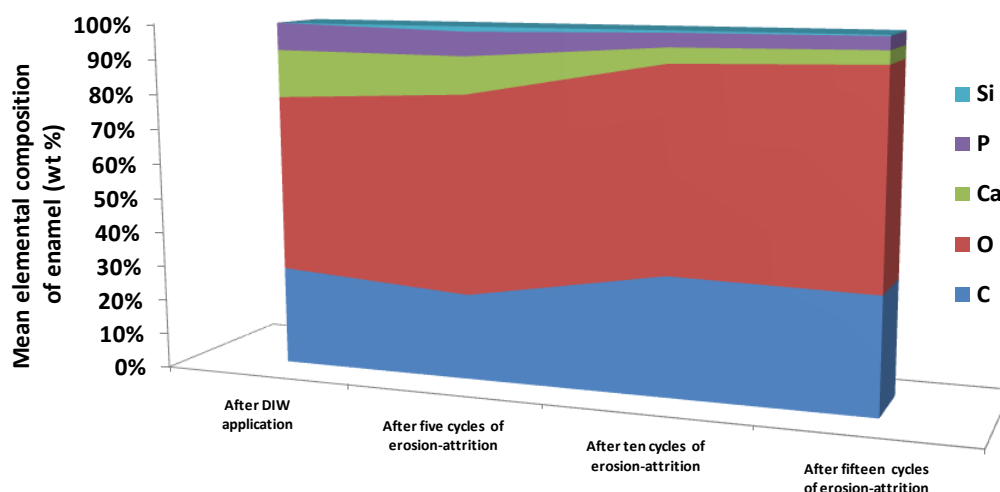
After fifteen cycles of
erosion-attrition

5.4.3 EDS analysis

Figure 67 to Figure 70 below shows the mean elemental composition (wt %) of the enamel surface after application of deionized water (deionized water) and after five, ten and 15 cycles of erosion-attrition for each treatment/control. Elemental analysis of the deionized water treated surface (Figure 67 below) showed that as the number of cycles of erosion-attrition increased, the calcium and phosphate mean wt % of the enamel surface increased. In terms of

the presence of elements other than calcium, phosphorus, oxygen and carbon, the presence of 1 wt % silica was detected in the enamel surface after five and ten cycles of erosion-attrition.

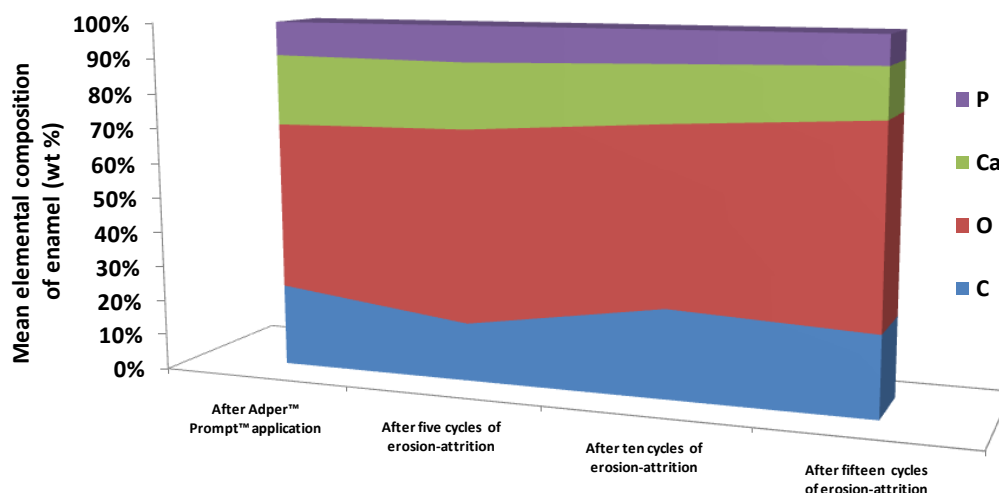
Figure 67 Mean elemental surface composition (wt %) of the enamel surface of a sample from the control group after application of deionized water (deionized water) and after five, ten and 15 cycles of erosion-attrition



	After DIW application	After five cycles of erosion-attrition	After ten cycles of erosion-attrition	After fifteen cycles of erosion-attrition
Si	0	1	1	0
P	8	7	4	4
Ca	14	11	4	4
O	50	57	57	60
C	28	24	34	33

Figure 68 below shows that after application of Adper™ Prompt™ self-etch adhesive the calcium and phosphorus mean elemental composition (wt %) of the enamel was 20 % and 9 % respectively. As the number of cycles increased the proportion of calcium and phosphorus in the overall mean elemental composition (wt %) declined gradually, to end after 15 cycles of erosion-attrition at 14 % and 8 % respectively. In terms of the presence of elements other than calcium, phosphorus, oxygen and carbon, no other element was identified in the enamel surface at all stages of the experiment.

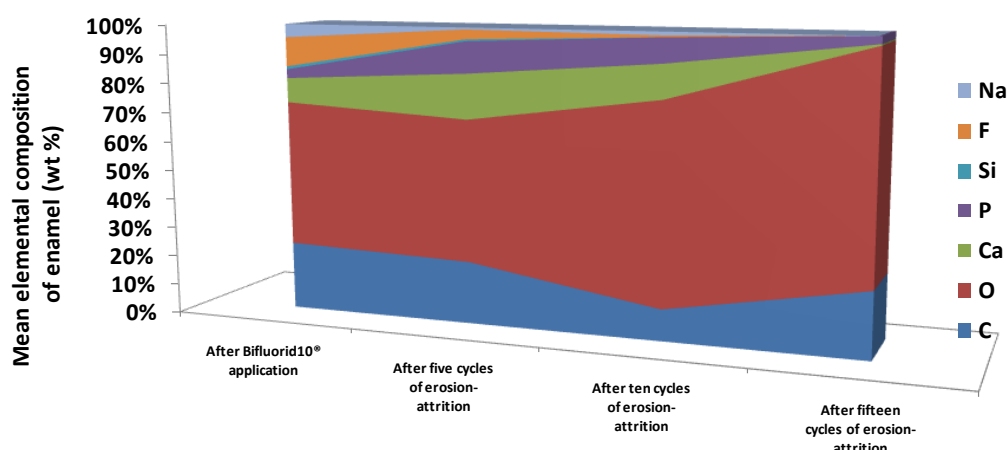
Figure 68 Mean elemental surface composition (wt %) of the enamel surface of a sample from the Adper™ Prompt™ treated group after application of Adper™ Prompt™ self-etch adhesive and after five, ten and 15 cycles of erosion-attribution



	After Adper™ Prompt™ application	After five cycles of erosion-attribution	After ten cycles of erosion-attribution	After fifteen cycles of erosion-attribution
P	9	10	9	8
Ca	20	19	16	14
O	47	55	50	56
C	23	17	25	23

Figure 69 below shows that after application of Bifluorid10® varnish the calcium and phosphorus mean elemental composition (wt %) of the enamel was 8 % and 3 % respectively. As the number of cycles increased the proportion of calcium and phosphorus in the overall mean elemental composition (wt %) increased up to 15 % calcium and 8 % phosphorus after five cycles of erosion-attribution; however the mean elemental composition of these elements subsequently declined to result in 0 % and 2 % respectively, after 15 cycles of erosion-attribution at the completion of the study. In terms of the presence of elements other than calcium, phosphorus, oxygen and carbon, after application of the Bifluorid10® varnish the presence of 1 % silica, 10 % fluorine and 5 % sodium was detected. These values of silica, fluorine and sodium subsequently declined, such that after 15 cycles of erosion-attribution, no presence of these elements was detected.

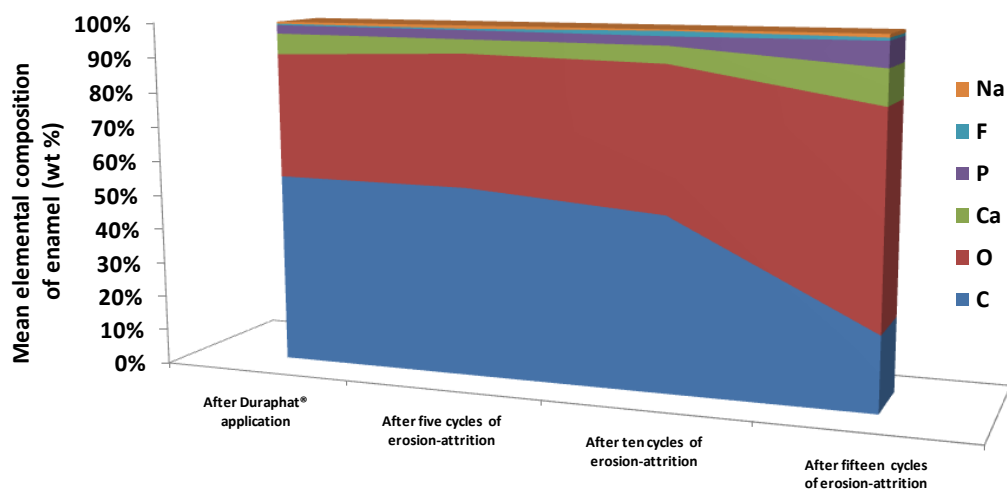
Figure 69 Mean elemental surface composition (wt %) of the enamel surface of a sample from the Bifluorid10® varnish treated group after application of Bifluorid10® varnish and after five, ten and 15 cycles of erosion-attribution



	After Bifluorid10® application	After five cycles of erosion-attribution	After ten cycles of erosion-attribution	After fifteen cycles of erosion-attribution
Na	5	1	1	0
F	10	3	1	0
Si	1	1	0	0
P	3	11	8	2
Ca	8	15	11	0
O	50	48	68	75
C	23	21	11	22

Figure 70 below shows that after application of Duraphat® varnish the calcium and phosphorus mean elemental composition (wt %) of the enamel was 6 % and 2 % respectively. As the number of cycles of erosion-attribution increased the proportion of calcium and phosphorus in the overall mean elemental composition (wt %) decreased down to 5 % calcium and 2 % phosphorus after ten cycles of erosion-attribution; however the mean elemental composition of these elements subsequently increased to result in 10 % and 7 % respectively, after 15 cycles of erosion-attribution at the end of the study. In terms of the presence of elements other than calcium, phosphorus, oxygen and carbon, after application of the Duraphat® varnish the presence of 1 % sodium was detected and subsequently after 15 cycles of erosion-attribution, 1 % of sodium and 1 % of fluorine was detected on the enamel surface at the completion of the study.

Figure 70 Mean elemental surface composition (wt %) of the enamel surface of a sample from the Duraphat® treated group after application of Duraphat® varnish and after five, ten and 15 cycles of erosion-attribution



	After Duraphat® application	After five cycles of erosion-attribution	After ten cycles of erosion-attribution	After fifteen cycles of erosion-attribution
Na	1	1	0	1
F	0	0	1	1
P	2	3	2	7
Ca	6	4	5	10
O	36	38	41	60
C	55	54	50	21

Discussion

This study modelled enamel loss from dietary erosion and attrition. This type of tooth wear has been successfully modelled and measured previously in Chapter 3 of this thesis and by Vieira et al (Vieira et al., 2006b). In comparison to these studies however, the present study examined the effect of treatments that have previously been shown to form a surface coating. As previously discussed in Chapter 4 above; the coatings formed by these products complicates the measurement of enamel and dentine loss from simulated multifactorial tooth wear *in vitro*. Conventional surface topography measurement techniques are not able to distinguish between loss of the surface coating and the loss of enamel/dentine during tooth wear. Consequently, many research groups currently investigating the effect of such products on enamel and dentine erosive wear are required to physically remove the coating from the enamel/dentine surface (Magalhaes et al., 2008a). The surface is then investigated

microscopically to ensure complete removal prior to profilometry. This has obvious disadvantages in terms of potential for iatrogenic damage to delicate eroded enamel and dentine structures. Furthermore as this removal is irreversible, the removal of the coating prevents the samples being used for any further tooth wear modelling. However, physical removal is essential for stylus profilometry of enamel/dentine wear as the presence of a coating would create errors. Therefore a major advantage of optical profilometry, in combination with software that allows for virtual removal of the surface coating, is the non-destructive nature which allows simulation of further tooth wear and subsequent re-measurement. Moreover, as tooth wear simulated *in vitro* attempts to mimic the clinical situation, where the coating may prove to resist abrasive or attrition forces, premature removal of the coating may result in loss of information regarding its durability.

The Adper™ Prompt™ self-etch adhesive used in this study was chosen as a fluoride free 'positive control', in comparison to the fluoride varnishes. This was required to determine if any protective effect from the varnishes was due to the formation of a coating or due to the fluoride content of the varnish. The Adper™ Prompt™ self-etch adhesive treated samples showed greater step height and volume enamel loss after five cycles of erosion-attrition in comparison to the controls ($p < 0.01$). This may be explained by the low starting pH of the self-etch adhesive. This was pH 0.88, in comparison with pH 5.5 for the Bifluorid10® varnish and pH 4.5 for the Duraphat® varnish. Therefore, the initial low pH may have produced wear however after ten and 15 cycles this effect would have dissipated.

Previous studies have investigated the role of self-etch adhesives in erosion-abrasion (Azzopardi et al., 2000a; 2004; Sundaram et al., 2007a; Sundaram et al., 2007b) however this is the first such study to have investigated the effect of a self-etch adhesive on erosion-attrition. The measurement techniques demonstrated in the present study lend themselves well to the measurement of enamel and dentine loss, even with the retention, or partial retention of a surface treatment that forms a coating. The results from this study did not conclusively show

that the self-etch adhesive was able to protect the enamel against erosion-attrition; however the limitations of translating the results of this *in vitro* methodology to the clinical situation must be borne in mind.

Bifluorid10® varnish was shown in Chapter 4 to significantly reduce enamel loss compared with the control, NaF and SnF₂ solutions after nine cycles of erosion-abrasion. However, in this present study, although the Bifluorid10® varnish significantly reduced enamel loss after five, ten and 15 cycles this difference was only statistically significant for the volume and not for the step height ($p > 0.01$). A similar pattern of significant reductions vs. control for volume loss only was also seen for the Duraphat® varnish treated samples. The reasons for and significance of the differing patterns of results for step height and volume enamel loss will be discussed further in Chapter 6 below. Therefore, despite the physical and chemical loss of the varnish, the profilometry suggested that the fluoride varnish was able to protect the enamel from erosion-attrition.

Although the chemical analysis revealed the presence of 10 % fluorine and 5 % sodium after application of the Bifluorid10® varnish, these values were reduced to 0 % after ten cycles. The chemical analysis showed Ca and P were lost from the controls which is what would have been expected under the experimental conditions. The other groups also lost the same ions apart from Duraphat which gained Ca and P as the number of cycles increased, possibly because some form of protective effect from the varnish.

Duraphat® varnish (2.26 % NaF) has been shown to inhibit enamel erosion (Sorvari et al., 1994), whilst both Duraphat® and Duofluorid® varnish (2.71 % NaF/2.92 % CaF₂) reduced enamel loss significantly after several acid attacks in an erosion-remineralisation protocol *in vitro* (Magalhaes et al., 2008a). Vieira et al (2007) showed that an experimental fluoride varnish of lower concentrations (0.1 % NaF) reduced enamel wear after erosion and erosion-abrasion *in situ*. Therefore the present study is the first to have investigated the effect of a varnish on enamel after erosion-attrition. In the only similar study of its kind, Li et al (2007)

investigated the effect of Duraphat® varnish on dentine attrition and reported that the varnish resulted in greater dentine wear than the negative control (water). In comparison however, the present study investigated the effect of erosion-attrition and used a different method to simulate attrition. It is possible that the higher loading of the antagonist during the previous study overcame any protective effect from the fluoride varnish (Li et al., 2007).

There is currently little consensus on what could be considered clinically relevant parameters for the modelling of erosion-attrition *in vitro*. The methodological parameters chosen for this study were considered to be as close as possible to a valid erosion-attrition model, whilst ensuring that the conditions were not overly aggressive. In the clinical situation, maximal bite forces of 911 N in the molar region and 569 N in the incisal region have been reported (Bates et al., 1975), whereas in this model 300 g of loading was chosen. This is towards the lower end of forces generated during the physiological masticatory cycle (Waltimo et al., 1994). The synergistic role of erosion and attrition in tooth wear is thought to be due to acids creating surface/subsurface softening of tooth tissue which is then mechanically removed by the attritional or abrasive elements (Barbour and Rees, 2006). This hypothesis is supported by findings from Vieira et al (2006b) using a similar cyclic erosion-attrition model and by Shabanian and Richards (2002) who found that enamel attritional wear was much greater at pH 1.2 and pH 3.3 compared with wear at pH 7.0. The cyclic design and relatively low load of the erosion-attrition models used in this thesis were chosen to minimise the complex tribochemical interactions at the enamel-to-enamel and enamel-to-dentine interface that previous *in vitro* studies have found increased the rate of wear under neutral conditions (Eisenburger and Addy, 2002a; b; Kaidonis et al., 1998; Mair, 2000).

The formulation of a fluoride delivery product will affect the amount and thickness of the fluoride-rich surface coating which may in turn affect the ability of the product to allow for gradual release of available fluoride ion, from the CaF₂ globules contained within the varnish. Whereas Bifluorid10® varnish is based on ethyl acetate (Safety Data Sheet for Bifluorid10,

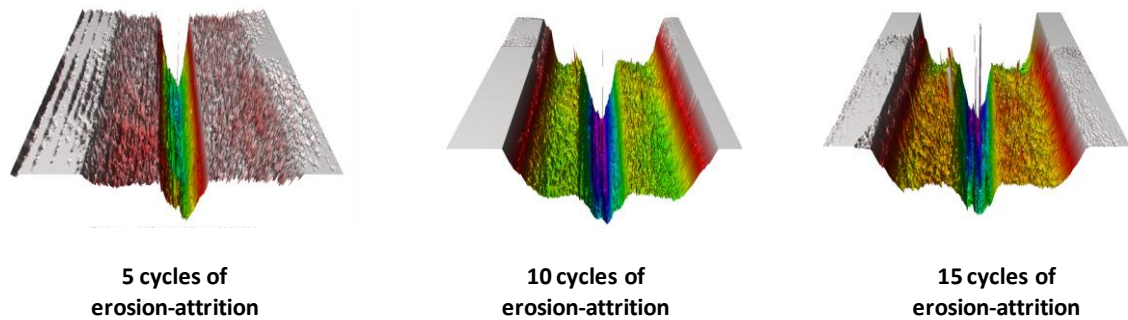
2008), Duraphat® varnish is formulated on a base of white wax (E901) and shellac (E904) (Colgate-Palmolive, 2010) in order to provide adhesion to enamel and dentine. The CaF_2 globules act as a fluoride reservoir and leads to formation of fluorhydroxyapatite and the thickness of the CaF_2 layer may delay the enamel dissolution rate (Ganss et al., 2001). Although chemical traces of the varnishes were observed to be eliminated during the erosion-attrition and the removal of the varnish was also seen in the SEM images; there was still remnants of the varnishes remaining on the enamel surface, either side of the wear scar. It could be argued that this would approximate the clinical situation, whereby varnish would be removed relatively rapidly from the smooth surfaces and wear facets, however would remain protected in the interproximal areas, embrasures and in pits and fissures. Therefore, based on the profilometry results which found that the varnishes did protect the enamel whereas the self-etch adhesive did not suggests that the fluoride may have had a role to play in protecting the enamel from erosion-attrition in this present study.

Chapter 6 General discussion and conclusions; clinical implications and suggestions for future work

General discussion

The aim of Chapter 2 was to validate the techniques used to measure tooth wear modelled *in vitro*; in particular the use of white light confocal profilometry in combination with a range of generic and bespoke software for volume and step height measurement of enamel and dentine wear. The results of the uncertainty evaluation showed that the Overall Combined Uncertainty was less than 5 % for almost all subsequent tooth wear measurements carried out in the subsequent studies of the thesis. The finding in prevalence studies that the occlusal surfaces of molars and the incisal edges of incisors are the surfaces of the dentition most severely affected by tooth wear (Fares et al., 2009; van't Spijker et al., 2009) supports the suspected multifactorial nature of tooth wear which contends that attrition is a significant factor in the aetiology of tooth wear (Addy and Shellis, 2006). Although investigations modelling erosion and attrition have increased understanding of the complex tribochemical tooth wear processes at the enamel-to-enamel and enamel-to-dentine interfaces (Eisenburger and Addy, 2002a; Eisenburger and Addy, 2002b; Kaidonis et al., 1998; Ranjitkar et al., 2008) this thesis has been the first to develop and validate a technique for measuring the effect of surface treatments that form a coating on multi-factorial (erosion-abrasion and erosion-attrition) tooth wear *in vitro*. These techniques resulted in both a step height and volume outcomes to express the loss of enamel or dentine. The advantages and disadvantages of these outcomes measures can be considered in relation to the differing geometry of the erosion-abrasion and erosion-attrition lesions seen in the *in vitro* tooth wear models in this thesis. Whereas an erosion-abrasion lesion is a steep-sided groove with a flat bottom and therefore as the lesion develops the step height measurement should proportionally represent the increase in wear. However, in comparison, an erosion-attrition lesion develops as shown in Figure 71 below.

Figure 71 Geometry of a developing erosion-attrition lesion *in vitro*



Thus the geometry of the lesion begins with a central narrow steep-sided groove with a concave bottom, bordered by a shallower area of erosion. As the lesion develops and the antagonist creates more attrition, the central groove deepens and widens and the erosion results in a flat sided area either side of the attrition. Therefore, a step height measurement may not be the most representative method for describing the enamel or dentine loss caused by erosion-attrition, and the normalised volume loss may be more representative.

2D and 3D measurements of enamel wear have been compared (Rodriguez and Bartlett, 2010) and this study concluded that normalised 3D measurements gave more accurate assessment of *in vitro* tooth wear. By normalising the volume change the amount of wear can be standardised by unit area or length, which compensates for the possible sources of error as described above. Vieira et al (2007) have also reported tooth wear both as normalised volume loss ($\mu\text{m}^3/\text{mm}^2$), average wear depth (μm) (volume loss /surface area of wear), max wear depth (μm) and % area of varnish removal, in order to compensate for the irregular surface area of exposed enamel after loss of varnish due to abrasion.

The rationale for use of normalised volume measurements can be further explored by examining the scatter plots shown in Figure 72 to Figure 74 below. These Figures explore the the relationship between step height (μm) and volume ($\text{M } \mu\text{m}^3/\text{mm}$) of enamel loss after multiple cycles of erosion; erosion-abrasion and erosion-attrition *in vitro*. Using a Pearson's or Spearman Rank correlation coefficient (according to a normal and non normal distribution respectively) to assess whether and how strongly the two outcome measures are related,

these Figures show that step height and volume data are most strongly related for the measurement of erosion ($R = 0.93$), followed by erosion-abrasion ($R = 0.90$) followed by erosion-attrition ($R = 0.86$).

Figure 72 Scatter plot showing the relationship between step height enamel loss and volume enamel loss ($M \mu m^3/mm$) after multiple cycles of erosion ($n = 55$)

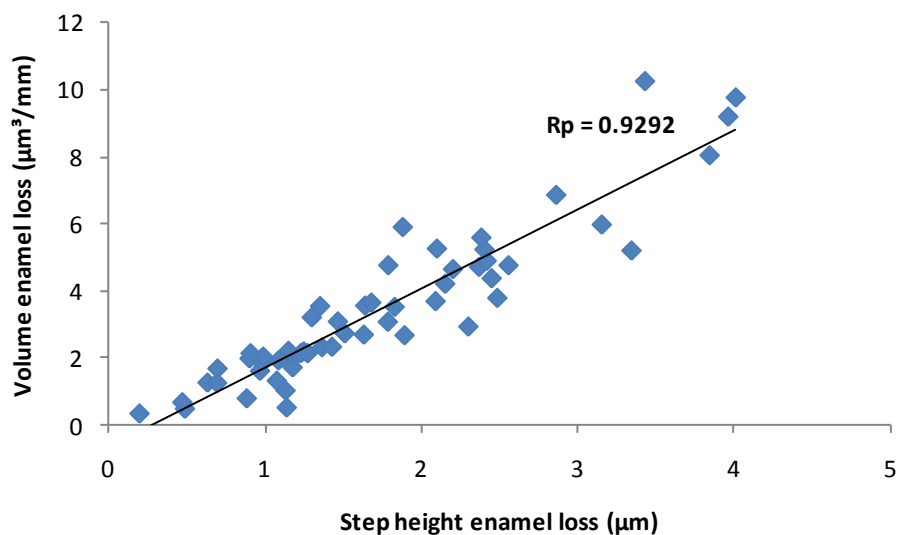


Figure 73 Scatter plot showing the relationship between step height enamel loss and volume enamel loss ($M \mu m^3/mm$) after multiple cycles of erosion-abrasion ($n = 36$)

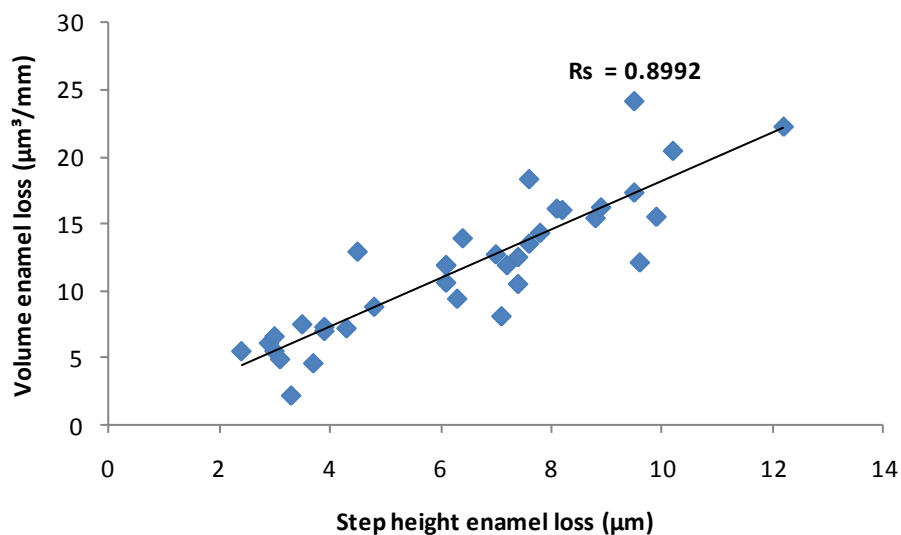
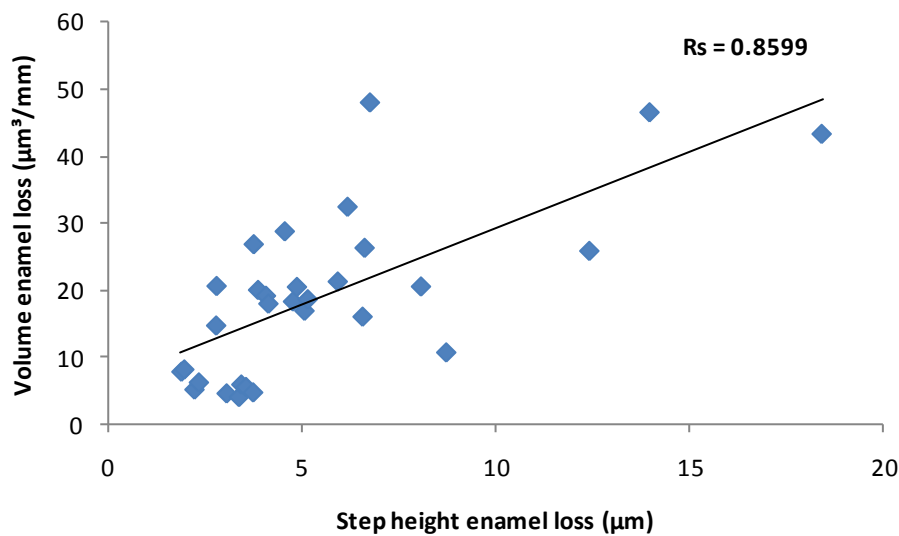


Figure 74 Scatter plot showing the relationship between step height enamel loss and volume enamel loss ($M \mu\text{m}^3/\text{mm}$) after multiple cycles of erosion-abrasion ($n = 30$)



These results supports the argument that as the geometry of the lesion becomes more complex, a simple step height measurement may not be the most appropriate outcome to report. Therefore it can be concluded that step height of wear is the most appropriate measurement outcome for *in vitro* erosion and volume (ideally normalised volume) of wear is the most appropriate measurement outcome for *in vitro* erosion-attrition. When reporting *in vitro* erosion-abrasion, either measurement outcome may be suitable according to the specifics of the tooth wear model used and the measurement technique employed.

Conclusions

Referring back to the aims of Chapters 3, 4 and 5, it can be concluded that:

1. The amount and rate of wear of enamel from 15 cycles of erosion-attrition *in vitro* was significantly reduced by the repeated application of an aqueous sodium fluoride solution of 5000 ppm and 19000 ppm concentrations, in comparison to a deionized water negative control.
2. The volume surface change of enamel samples from nine cycles of erosion *in vitro* was significantly reduced after a single application of highly concentrated titanium

tetrafluoride solution and a highly concentrated sodium fluoride varnish, in comparison to a deionized water negative control.

3. The volume surface change of enamel samples from nine cycles of erosion-abrasion *in vitro* was significantly reduced after a single application of highly concentrated sodium fluoride solution and a highly concentrated sodium fluoride varnish, in comparison to a deionized water negative control.
4. The volume enamel loss of enamel samples from 15 cycles of erosion-attrition *in vitro* was significantly reduced after a single application of highly concentrated sodium fluoride varnishes, in comparison to a deionized water negative control and a self-etch adhesive.
5. In conclusion, the overall null hypothesis of this thesis is not supported and these studies therefore demonstrate that varying fluoride concentrations compounds and formulae can reduce multi-factorial wear in laboratory studies.

Clinical implications

Oral health has been defined as ‘...the state of the mouth and associated structures where no disease exists, future disease is inhibited’ whereby ‘the occlusion is sufficient to masticate food and the (appearance of the) teeth are of a socially acceptable standard’ (Yewe-Dyer, 1993). Tooth wear leading to impairments such as tooth loss may result in social disabilities with speaking and chewing and in psychological disabilities with health perceptions such as appearance (Elias and Sheiham, 1998). Studies investigating how aging and tooth loss affect oral health related quality of life have concluded that tooth loss is associated with more negative impacts than increasing age *per se*. Therefore, those older people with a complete or almost complete natural dentition are likely to have the best oral health-related quality of life (Steele et al., 2004).

In the UK, the median age of the population will rise from the current median age of 39.3 years to 42.2 years by 2033 (Statistical Bulletin: 2008-based National population projections, 21 October 2009). As the population ages, the numbers of ‘older people’ (classified as those over 65 years of age) will increase the fastest and for this section of the population it is estimated that by 2028 total tooth loss will be eliminated in those aged under 65 years and significantly reduced in the population under the age of 75 years (Kelly et al., 1998). As the projected age structure of populations change, so do oral health trends. Older people of today have higher expectations of oral health (Walls and Steele, 2001) and recent systematic reviews have shown that the prevalence of erosive wear amongst children and adults increases with age (Kreulen et al., 2010; Van't Spijker et al., 2009a).

These data reinforce the need to develop effective preventative strategies for dental erosion, such as through the effective use of fluoride products. The erosion inhibiting effects of different fluorides have been investigated in many *in vitro* studies. Patients with dental erosion are exposed to regular acid impacts, which can result in tooth wear. Therapeutic measures of dental erosions aim to reduce mineral loss, which can be achieved, for example, by the

frequent application of fluorides with a low concentration. High-concentrated sodium fluoride applications have been shown to improve the abrasion resistance of eroded enamel and dentine *in vitro* and *in situ*. The results of this thesis suggest that an aqueous solution of high concentration sodium fluoride (5000 ppm and 19000 ppm) provided benefit to enamel in an erosive and attritional *in vitro* tooth wear model which simulated dietary erosion and light attritional forces.

The application of a varnish or a highly concentrated solution may be suitable for therapy of dental erosions; however these preparations have to be applied in the dental practice and cannot be applied by the patients themselves. This thesis has shown that a highly concentrated fluoride varnish provided protection to enamel from both simulated gastric erosion-tooth brush abrasion and from simulated dietary erosion-enamel attrition. The main disadvantage of these professionally applied products in comparison to self-applied fluoride products are that the patients are required to visit the dental practice frequently, in order to re-apply these products and are therefore, reliant to their dentists. Therefore, if these products are to be recommended for use in dental erosion, they need to be proven to be able to protect enamel against erosion for a long period of time, an effect that should be independent of the mechanical protection provided by surface protection agents such as resin-based adhesives. As the skill mix of the dental team evolves and widens, there is great potential for increased delegation and use of dental care professionals (DCPs) to deliver preventative treatments for the elderly (Gallagher et al., 2010). This implementation of simple preventative care by DCPs will complement and prolong the long-term success of holistic restorative dentistry, whilst at the same time ensuring that GDPs are able to optimize the use of their chair-side time, by managing more complex restorative dental treatments.

However, to date the only *in vivo* study into the long term effects of fluoride products on tooth wear has been a retrospective cohort study by Pieterse et al (2006) into the oral health status a group of school children who used a fluoride rinse in comparison with a control group that

did not use a fluoride mouthrinse. This study, nevertheless, found that group that did not use a fluoride rinse had higher levels of dental erosion than those that did. This interesting finding is limited by the inherent weaknesses of the retrospective study design and prospective controlled clinical studies into the role of fluorides in tooth wear remain keenly awaited.

This thesis has therefore argued that topical fluorides in varying concentrations, compounds and formulae have a role to play in the prevention and management of erosive tooth wear. Bearing in mind the limitations of the research techniques employed herein, this thesis has successfully demonstrated that highly concentrated fluoride delivery systems can protect enamel from multifactorial tooth wear, above and beyond any mechanical protection afforded by resin-based adhesive systems. Therefore, further work is justified to assess the clinical effectiveness of such products in managing erosive tooth wear.

Future developments

- 1 Translate the high quality *in vitro* tooth wear measurement techniques for use in further *in vitro* and clinical (*in situ* and *in vivo*) studies, such as investigations into the clinical effectiveness of pharmaceutical and health care products such as toothpastes, gels, mouthrinses and varnishes.
- 2 Further develop and utilise a broad range of expertise in optical techniques for tooth wear measurement.
- 3 Further develop and utilise a broad range of expertise in 3D image analysis for tooth wear measurement, include surface texture and morphology analysis using ISO defined 3D surface parameters for classifying tooth wear.
- 4 Utilise these non-destructive measurement techniques to further investigate the biological factors that influence and modify the tooth wear process such as interactions between the salivary pellicle, fluoride compounds and erosive wear of enamel and dentine.

Appendices

Appendix 1 Effect of varying measurement control settings on the time and accuracy of *in vitro* tooth wear measurement using the white light confocal profilometer

Figure 75 Time taken (minutes) for the white light confocal profilometer to scan a 15 mm² measurement area at 5 x 5 μm , 10 x 10 μm and 15 x 15 μm x/y measurement spacing and at 'fast', 'medium' and 'slow' measurement speeds

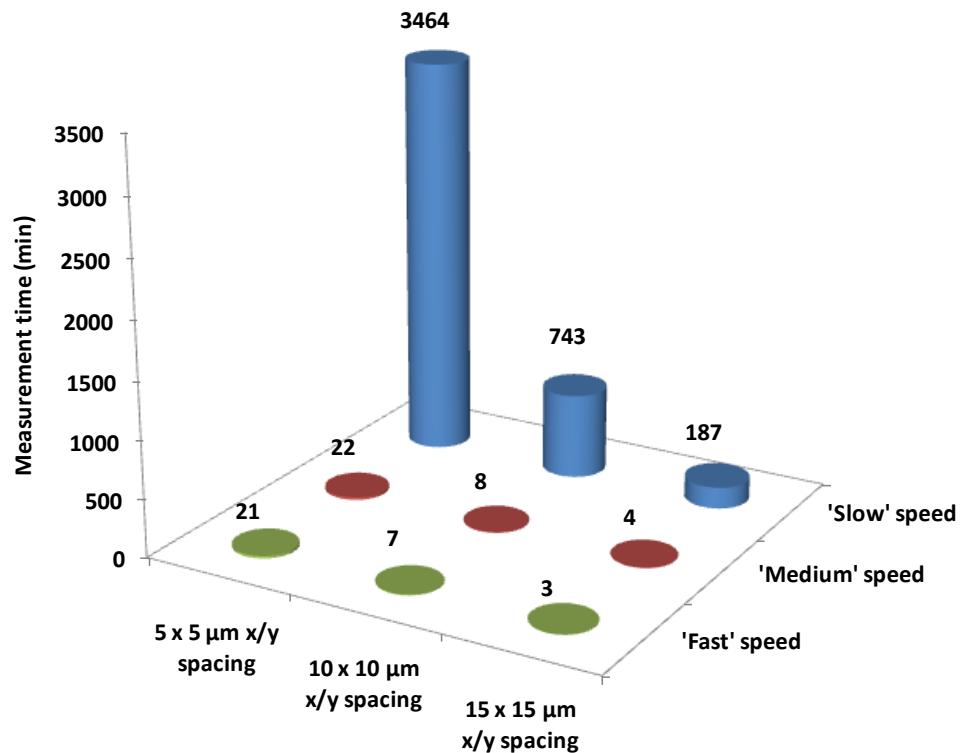
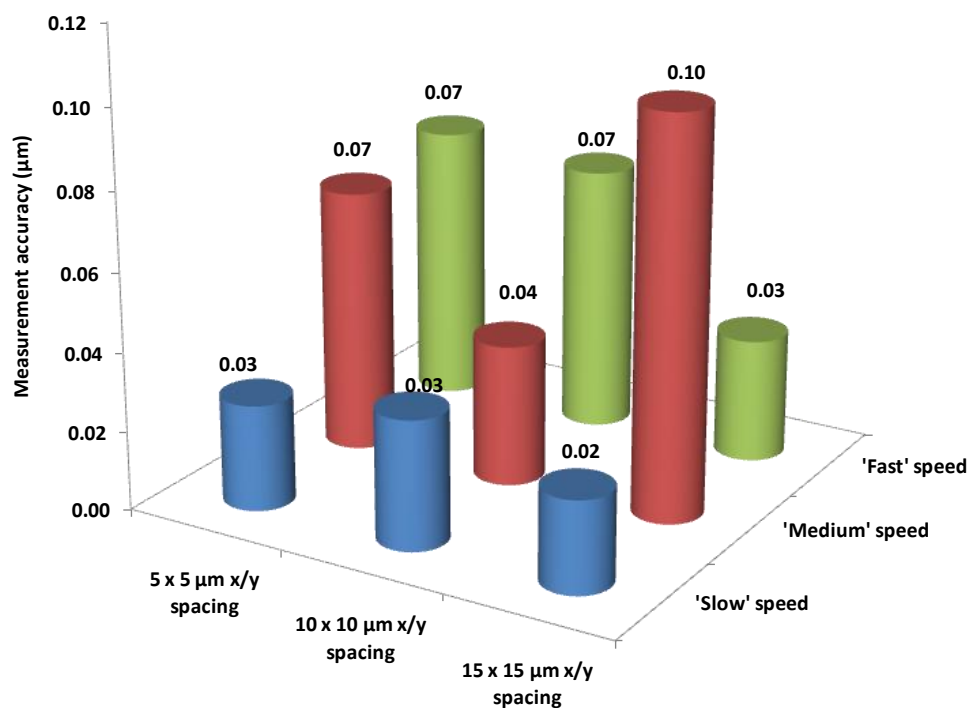


Figure 76 Mean accuracy (μm) of the white light confocal profilometer at measuring a Taylor-Hobson $0.39\ \mu\text{m}$ and a $2.64\ \mu\text{m}$ step height reference standard measured at $5 \times 5\ \mu\text{m}$, $10 \times 10\ \mu\text{m}$ and $15 \times 15\ \mu\text{m}$ x/y measurement spacing and at 'fast', 'medium' and 'slow' measurement speeds



Appendix 2 Patient Information Sheet (PIS) for donation of extracted teeth

Guy's, King's and St Thomas' Dental Institute Department of Fixed and Removable Prosthodontics	29 th Floor, Guy's Tower Guy's Hospital London Bridge London SE1 9RT Tel 0207 188 5390 Fax 0207 188 7486	KING'S College LONDON	King's College Hospital NHS Foundation Trust Guy's and St Thomas' NHS Foundation Trust
--	---	------------------------------	--

Volunteer information sheet (Version 2 Dated December 1st, 2009)
Title of project: Protection of erosive tooth wear (donation of extracted tooth)
REC ref: 09/H0808/109
Investigator: Professor David Bartlett

You will be given a copy of the information sheet and a signed consent form to keep.

Part 1 **Invitation paragraph**

You are being invited to donate your tooth for a research study. Before you decide it is important for you to understand why the research is being done and what it will involve:

Part 1 tells you the purpose of the study and what will happen if you decide to participate.
Part 2 gives you more detailed information about the conduct of the study.

Please take time to read the following information carefully. Ask us if there is anything that is not clear. Talk to others about the research if you wish and the following organization could give you independent advice:

King's College Hospital NHS Foundation Trust Patient Advice and Liaison Service
Telephone 0203 299 3625 or 0203 299 3601 email: pals@kch.nhs.uk
Post: Volunteer Advice and Liaison Service King's College Hospital London SE5 9RS

What is the purpose of the study?

Tooth wear is a condition where the teeth wear away faster than normal and is caused by acid erosion (from acidic foods and drinks and stomach acid), tooth grinding and over brushing. Tooth wear is a common condition that can affect anyone and it appears to be happening more and more nowadays. Severe tooth wear can cause teeth to become very sensitive, as well as causing cosmetic and chewing problems due to shortened teeth and even in severe cases can cause tooth loss. Certain toothpastes and mouth rinses have the potential to prevent and treat tooth wear. However the scientific evidence for this is lacking. This study will us help to identify products that can be beneficial in preventing and treating tooth wear and improve the advice that we can give Volunteers on preventing tooth wear.

Why have I been chosen?

You are suitable for this study because you are a healthy individual who needs a wisdom tooth (third molar) removed.

Do I have to take part?

It is up to you to decide whether or not to take part. If you do, you will be given this information sheet to keep and be asked to sign a consent form. You are still free to withdraw at any time and without giving a reason. A decision to withdraw at any time, or a decision not to take part, will not affect the standard of care you receive.

What will happen to me if I decide to take part?

At your first visit, when you are consulted about the tooth extraction, you will be invited to join the study by a clinician. At your second visit we will confirm that you still want to donate your tooth and then you will have your tooth removed in the normal way. After your tooth is extracted it will be transferred to the Biomaterials laboratory at King's College Hospital Dental Institute (Department of Biomaterials, 17th Floor, Guy's Tower, Guy's Hospital, London Bridge SE1 9RT). Once the tooth is extracted your participation in the study is over.

What do I have to do?

You will just have to attend your set appointments as normal.

What is the drug, device or procedure being tested?

Fluoride toothpaste and fluoride mouth rinse are being tested in this study on the extracted tooth.

What are the alternatives for diagnosis or treatment?

The research does not involve any Volunteer treatment and you will receive your routine standard treatment as usual.

What are the side effects of any treatment received when taking part?

There are no risks associated with this study, other than the usual risks of a tooth extraction which will be explained to you by the clinical team who are carrying out the treatment.

What are the other possible disadvantages or risks of taking part?

There are no risks associated with this study, other than the usual risks of a tooth extraction which will be explained to you by the clinical team who are carrying out the treatment.

What are the possible benefits of taking part?

We do not expect that you will receive any benefit from taking part in this study.

What happens when the research study stops?

We aim to publish the results in medical journals.

What if there is a problem? And contact details:

No problems can be foreseen however the contact number for complaints or concerns is for: Professor David Bartlett 0207 188 5390 or email david.bartlett@kcl.ac.uk

Will my taking part in the study be kept confidential?

We will not be collecting any information about you and your confidentiality is safeguarded during and after the study. Our procedures for handling, processing, storage and destruction of your data are compliant with the Data Protection Act 1998.

Guy's, King's and St
Thomas' Dental Institute
Department of Fixed and
Removable
Prosthodontics

25th Floor, Guy's Tower
Guy's Hospital
London Bridge
London
SE1 9RT
Tel 0207 188 5390
Fax 0207 188 7486



Contact for further information:

Professor David Bartlett 0207 188 5390 or email david.bartlett@kcl.ac.uk

This completes Part 1 of the Information Sheet. If the information sheet in Part 1 has interested you and you are considering participation, please continue to read the additional information in Part 2 before making any decision.

Part 2

What if relevant new information becomes available?

We are a leading establishment in this area of research and if any new information relevant to this study becomes available the researchers will discuss this with you. You are free to withdraw from the study at any time.

What will happen if I don't want to carry on with the study?

You can withdraw from treatment at any time. Just advise the clinician treating you that you do not want to donate your tooth and your tooth will be disposed of once extracted, or you can keep it to take home. Information collected may still be used.

What if there is a problem?

If you have any concern about any aspect of this study, you should ask to speak with the researchers who will do their best to answer their questions.

Professor David Bartlett 0207 188 5390 or email david.bartlett@kcl.ac.uk

If you remain unhappy and wish to complain formally, you can do this through the NHS complaints procedure. If you are harmed by taking part in this research project there are no special compensation arrangements. If you are harmed due to someone's negligence, then you may have grounds for a legal action but you may have to pay privately for it. Regardless of this, if you wish to complain, or have any concerns about any aspect of the way that you have been approached or treated during the course of this study, the normal NHS complaints mechanisms should be available to you.

Details of how to complain can be obtained from the Volunteer Advice and Liaison Service (PALS)

King's College Hospital NHS Foundation Trust Patient Advice and Liaison Service

Telephone 0203 299 3625 or 0203 299 3601 email: pals@kch.nhs.uk

Post: Volunteer Advice and Liaison Service King's College Hospital London SE5 9RS

Will my taking part in this study be kept confidential?

We will not be collecting any information about you and your confidentiality is safeguarded during and after the study. Our procedures for handling, processing, storage and destruction of your data are compliant with the Data Protection Act 1998.

What will happen to any samples that I give?

After your tooth has been removed, it will be anonymised (i.e. there will be no way of linking the tooth to your personal data or medical records) and then transported to the Biomaterials laboratory at King's College Hospital Dental Institute (Department of Biomaterials, 17th Floor, Guy's Tower, Guy's Hospital, London Bridge SE1 9RT). The tooth will be used for one of two studies, both of which are investigating the ability of fluoride toothpastes and mouth rinses in preventing and treating tooth wear. The first study is a laboratory experiment which involves simulating tooth brushing and acid erosion on the tooth in the laboratory, as well as exposure to protective fluoride toothpastes and mouth rinses. Following this, measurements of the amount of wear on the tooth surface are taken. The second study is called an in situ study (see below for definition). This involves sterilizing the tooth and placing it into a mouth guard for use in a study where the mouth guard will be worn in someone else's mouth for ten days. The tooth sample will be subjected to simulated tooth brushing and acid erosion as well as exposure to protective fluoride toothpastes and mouth rinses. Following this, measurements of the amount of wear on the tooth surface are taken.

Once the study is completed the tooth samples will be carefully disposed of in accordance with local and national guidelines.

Definitions:

In situ study:

An in situ study involves testing experimental tooth wear on small sections of tooth which are worn in a human subject's mouth. This has an advantage over the laboratory study because it takes into account biological factors such as saliva and pellicle formation and the movement of the tongue and cheeks.

What will happen to the results of the research study?

The results of the study will be published in medical journals. Participants will not be identified in any report or publication.

Who has reviewed the study?

This study was given a favourable ethical opinion for conduct in the NHS by King's College Hospital Research Ethics Committee.

Will any genetic tests be done?

No.

Thank you for considering taking part and for taking time to read this sheet – please ask any questions if you need to.

Appendix 3 Informed Consent Form (ICF) for donation of extracted tooth



Consent Form (Version 1 Dated Tuesday, October 20, 2009)
Title of project: Protection of erosive tooth wear (donation of extracted tooth)
REC ref: 09/H0808/109
Investigator: Professor David Bartlett

Please complete this form after you have read the Information Sheet and/or listened to an explanation about the research

Patient Identification:

Date

Thank you for considering taking part in this research. The person organising the research and/or a member of the clinical team who is trained for this purpose must explain the project before you agree to take part.

If you have any questions arising from the Information Sheet or explanation given to you, please ask the researcher before you decide whether or not to join in. You will be given a copy of this Consent Form to keep and refer to at any time.

I confirm that I have read and understand the information sheet dated 1st December 2009 (version 2) for the above study.

I have had the opportunity to consider the information, ask questions and have had these answered satisfactorily.

I understand that my participation is voluntary and that I am free to withdraw at any time without giving any reason, without my medical care or legal rights being affected.

I agree to take part in the above study.

Name of Patient.....
Signature.....Date.....

Name of Person taking consent.....
Signature.....Date.....

1 for patient, 1 for researcher site file, 1 (original) to be kept in medical notes, 1 to be kept with donated tooth

Page 1 of 1

Appendix 4 Uncertainty budget used to evaluate the Standard Combined Uncertainty of the step height and volume measurement with the white light confocal profilometer

Table 26 Individual uncertainty budget contributions from each source of error to the Standard Combined Uncertainty (μm and %) of the step height measurement of a $0.3 \mu\text{m}$ step height reference standard

Contribution	Standard Uncertainty (μm)	Percent contribution to the Standard Combined Uncertainty (%)
Flatness, noise and z axis linearity errors	0.28	99.98
Step height software error	0.00	0.00
Enamel/dentine shrinkage error	0.00	0.02
Standard Combined Uncertainty	0.28	100

Table 27 Individual uncertainty budget contributions from each source of error to the Standard Combined Uncertainty (μm and %) of the step height measurement of a $2.97 \mu\text{m}$ step height reference standard

Contribution	Standard Uncertainty (μm)	Percent contribution to the Standard Combined Uncertainty (%)
Flatness, noise and z axis linearity errors	0.28	99.80
Step height software error	0.00	0.00
Enamel/dentine shrinkage error	0.00	0.20
Standard Combined Uncertainty	0.28	100

Table 28 Individual uncertainty budget contributions from each source of error to the Standard Combined Uncertainty (μm and %) of the step height measurement of a $17 \mu\text{m}$ step height reference standard

Contribution	Standard Uncertainty (μm)	Percent contribution to the Standard Combined Uncertainty (%)
Flatness, noise and z axis linearity errors	0.28	98.90
Step height software error	0.00	0.00
Enamel/dentine shrinkage error	0.00	1.10
Standard Combined Uncertainty	0.28	100

Table 29 Individual uncertainty budget contributions from each source of error to the Standard Combined Uncertainty (μm and %) of the step height measurement of a 30 μm step height reference standard

Contribution	Standard Uncertainty (μm)	Percent contribution to the Standard Combined Uncertainty (%)
Flatness, noise and z axis linearity errors	0.28	98.08
Step height software error	0.00	0.00
Enamel/dentine shrinkage error	0.01	1.92
Standard Combined Uncertainty	0.28	100

Table 30 Individual uncertainty budget contributions from each source of error to the Standard Combined Uncertainty ($\text{M } \mu\text{m}^3/\text{mm}$ and %) of the volume measurement of a 0.3 μm step height reference standard

Contribution	Standard Uncertainty ($\text{M } \mu\text{m}^3/\text{mm}$)	Percent contribution to the Standard Combined Uncertainty (%)
Flatness, noise and z axis linearity errors	850725.29	99.35
x axis linearity error	3495.81	0.41
y axis linearity error	1335.09	0.16
Enamel/dentine shrinkage error	166.53	0.02
Volume software error	560.24	0.07
Standard Combined Uncertainty	850733.73	100

Table 31 Individual uncertainty budget contributions from each source of error to the Standard Combined Uncertainty ($\text{M } \mu\text{m}^3/\text{mm}$ and %) of the volume measurement of a 2.97 μm step height reference standard

Contribution	Standard Uncertainty ($\text{M } \mu\text{m}^3/\text{mm}$)	Percent contribution to the Standard Combined Uncertainty (%)
Flatness, noise and z axis linearity errors	850299.18	93.87
x axis linearity error	34958.06	3.86
y axis linearity error	13350.93	1.47
Enamel/dentine shrinkage error	1665.35	0.18
Volume software error	5581.08	0.62
Standard Combined Uncertainty	851142.14	100

Table 32 Individual uncertainty budget contributions from each source of error to the Standard Combined Uncertainty (M $\mu\text{m}^3/\text{mm}$ and %) of the volume measurement of a 17 μm step height reference standard

Contribution	Standard Uncertainty (M $\mu\text{m}^3/\text{mm}$)	Percent contribution to the Standard Combined Uncertainty (%)
Flatness, noise and z axis linearity errors	851606.83	73.00
x axis linearity error	198095.67	16.98
y axis linearity error	75655.25	6.49
Enamel/dentine shrinkage error	9436.98	0.81
Volume software error	31755.15	2.72
Standard Combined Uncertainty	878235.31	100

Table 33 Individual uncertainty budget contributions from each source of error to the Standard Combined Uncertainty (M $\mu\text{m}^3/\text{mm}$ and %) of the volume measurement of a 30 μm step height reference standard

Contribution	Standard Uncertainty (M $\mu\text{m}^3/\text{mm}$)	Percent contribution to the Standard Combined Uncertainty (%)
Flatness, noise and z axis linearity errors	855394.59	60.62
x axis linearity error	349580.59	24.77
y axis linearity error	133509.27	9.46
Enamel/dentine shrinkage error	16653.50	1.18
Volume software error	56002.33	3.97
Standard Combined Uncertainty	935491.75	100

Appendix 5 Uncertainty budget used to evaluate the Overall Combined Uncertainty of the step height and volume measurement with the white light confocal profilometer

Table 34 Individual uncertainty budget contributions from each source of error to the Overall Combined Uncertainty (μm and %) of the step height measurement of a 0.3 μm soft gauge reference standard

Contribution	Combined Uncertainty (μm)	Percent contribution to the Overall Combined Uncertainty (%)
Flatness, noise and z axis linearity errors	0.02	99.67
Enamel/dentine shrinkage error	0.00	0.00
Step height software error	0.00	0.33
Overall Combined Uncertainty	0.02	100

Table 35 Individual uncertainty budget contributions from each source of error to the Overall Combined Uncertainty (μm and %) of the step height measurement of a 3 μm soft gauge reference standard

Contribution	Combined Uncertainty (μm)	Percent contribution to the Overall Combined Uncertainty (%)
Flatness, noise and z axis linearity errors	0.02	96.85
Enamel/dentine shrinkage error	0.00	0.00
Step height software error	0.00	3.15
Overall Combined Uncertainty	0.02	100

Table 36 Individual uncertainty budget contributions from each source of error to the Overall Combined Uncertainty (μm and %) of the step height measurement of a 17 μm soft gauge reference standard

Contribution	Combined Uncertainty (μm)	Percent contribution to the Overall Combined Uncertainty (%)
Flatness, noise and z axis linearity errors	0.02	86.76
Enamel/dentine shrinkage error	0.00	0.00
Step height software error	0.00	13.24
Overall Combined Uncertainty	0.02	100

Table 37 Individual uncertainty budget contributions from each source of error to the Overall Combined Uncertainty (μm and %) of the step height measurement of a 30 μm soft gauge reference standard

Contribution	Combined Uncertainty (μm)	Percent contribution to the Overall Combined Uncertainty (%)
Flatness, noise and z axis linearity errors	0.02	74.16
Enamel/dentine shrinkage error	0.01	0.00
Step height software error	0.00	25.84
Overall Combined Uncertainty	0.02	100

Table 38 Individual uncertainty budget contributions from each source of error to the Overall Combined Uncertainty ($\text{M } \mu\text{m}^3/\text{mm}$ and %) of the volume measurement of a 0.3 μm soft gauge reference standard

Contribution	Combined Uncertainty ($\text{M } \mu\text{m}^3/\text{mm}$)	Percent contribution to the Overall Combined Uncertainty (%)
Flatness, noise and z axis linearity errors	84422.19	88.70
x axis linearity error	6054.91	6.36
y axis linearity error	3861.79	4.06
Enamel/dentine shrinkage error	278.11	0.29
Volume software error	560.24	0.59
Overall Combined Uncertainty	84729.41	100

Table 39 Individual uncertainty budget contributions from each source of error to the Overall Combined Uncertainty ($\text{M } \mu\text{m}^3/\text{mm}$ and %) of the volume measurement of a 3 μm soft gauge reference standard

Contribution	Combined Uncertainty ($\text{M } \mu\text{m}^3/\text{mm}$)	Percent contribution to the Overall Combined Uncertainty (%)
Flatness, noise and z axis linearity errors	85389.58	44.26
x axis linearity error	60549.13	31.39
y axis linearity error	38617.89	20.02
Enamel/dentine shrinkage error	2781.13	1.44
Volume software error	5581.08	2.89
Overall Combined Uncertainty	111748.83	100

Table 40 Individual uncertainty budget contributions from each source of error to the Overall Combined Uncertainty (M $\mu\text{m}^3/\text{mm}$ and %) of the volume measurement of a 17 μm soft gauge reference standard

Contribution	Combined Uncertainty (M $\mu\text{m}^3/\text{mm}$)	Percent contribution to the Overall Combined Uncertainty (%)
Flatness, noise and z axis linearity errors	103236.47	14.49
x axis linearity error	343111.76	48.14
y axis linearity error	218834.70	30.71
Enamel/dentine shrinkage error	15759.76	2.21
Volume software error	31755.15	4.46
Overall Combined Uncertainty	421341.71	100

Table 41 Individual uncertainty budget contributions from each source of error to the Overall Combined Uncertainty (M $\mu\text{m}^3/\text{mm}$ and %) of the volume measurement of a 30 μm soft gauge reference standard

Contribution	Combined Uncertainty (M $\mu\text{m}^3/\text{mm}$)	Percent contribution to the Overall Combined Uncertainty (%)
Flatness, noise and z axis linearity errors	79797.07	6.91
x axis linearity error	605491.34	52.41
y axis linearity error	386178.88	33.43
Enamel/dentine shrinkage error	27811.34	4.85
Volume software error	56002.33	2.41
Overall Combined Uncertainty	725280.08	100

Bibliography

Ablal M, Kaur J, Cooper L, Jarad F, Milosevic A, Higham S *et al.* (2009). The erosive potential of some alcopops using bovine enamel: an in vitro study. *Journal of Dentistry* 37(11):835-839.

Addy M, Hunter ML (2003). Can tooth brushing damage your health? Effects on oral and dental tissues. *International dental Journal* 53(Suppl-86).

Addy M, Shellis RP (2006). Interaction between attrition, abrasion and erosion in tooth wear. In: Dental Erosion from Diagnosis to Therapy. A Lussi editor. Basel: Karger.

Albrecht M, Takats R, Fosse G, Sapi Z, Banoczy J (1991). [Dental enamel hardness tests in diabetics]. *Fogorv Sz* 84(12):363-366.

Amaechi B, Higham S, Edgar W, Milosevic A (1999). Thickness of acquired salivary pellicle as a determinant of the sites of dental erosion. *Journal of Dental Research* 78(12):1821-1825.

Amaechi B, Higham S, Podoleanu A, Rogers J, Jackson D (2001). Use of optical coherence tomography for assessment of dental caries: quantitative procedure. *Journal of Oral Rehabilitation* 28(12):1092-1093.

Anderson P, Elliott J (2000). Rates of mineral loss in human enamel during in vitro demineralization perpendicular and parallel to the natural surface. *Caries Research* 34(1):33-40.

Angmar-Mansson B, Ten Bosch J (2001). Quantitative light-induced fluorescence (QLF): a method for assessment of incipient caries lesions. *Dentomaxillofacial Radiology* 30(6):298-232.

Aoba T, Fejerskov O (2002). Dental fluorosis: chemistry and biology. *Critical Reviews in Oral Biology & Medicine* 13(2):155-159.

Arnold WH, Dorow A, Langenhorst S, Gintner Z, Banoczy J, Gaengler P (2006). Effect of fluoride toothpastes on enamel demineralization. *BMC Oral Health* 6(8).

Arnold WH, Haase A, Hacklaender J, Gintner Z, Banoczy J, Gaengler P (2007). Effect of pH of amine fluoride containing toothpastes on enamel remineralization in vitro. *BMC Oral Health* 7(14).

Attin T, Koidl U, Buchalla W, Schaller HG, Kielbassa AM, Hellwig E (1997). Correlation of microhardness and wear in differently eroded bovine dental enamel. *Archives of Oral Biology* 42(3):243-250.

Attin T, Zirkel C, Hellwig E (1998). Brushing abrasion of eroded dentin after application of sodium fluoride solutions. *Caries Research* 32(5):344-350.

Attin T, Deifuss H, Hellwig E (1999). Influence of acidified fluoride gel on abrasion resistance of eroded enamel. *Caries Research* 33(2):135-139.

Attin T, Meyer K, Hellwig E, Buchalla W, Lennon A (2003). Effect of mineral supplements to citric acid on enamel erosion. *Archives of Oral Biology* 48(11):753-759.

Attin T, Siegel S, Buchalla W, Lennon AM, Hannig C, Becker K (2004). Brushing abrasion of softened and remineralised dentin: an in situ study. *Caries Research* 38(1):62-66.

Attin T (2006). Methods for assessment of dental erosion. *Monographs in Oral Science* 20:152-172.

Attin T, Becker K, Roos M, Attin R, Paque F (2009). Impact of storage conditions on profilometry of eroded dental hard tissue. *Clinical Oral Investigations* 13(4):473-478.

Attramadal A, Svaton B (1980). Uptake and retention of tin by *S. mutans*. *Acta Odontologica* 38(6):349-354.

Azzopardi A, Bartlett DW, Watson TF, Sherriff M (2000a). The protection given by dentine-bonding agents to prevent erosion - an in-vitro study. *Caries Research* 34(5).

Azzopardi A, Bartlett DW, Watson TF, Smith BGN (2000b). A literature review of the techniques to measure tooth wear and erosion. *European Journal of Prosthodontics and Restorative Dentistry* 8:93-97.

Azzopardi A, Bartlett DW, Watson TF, Sherriff M (2004). The surface effects of erosion and abrasion on dentine with and without a protective layer. *British Dental Journal* 196(6):351-354.

Bakhos Y, Brudevold F, Aasenden R (1977). In-vivo estimation of the permeability of surface human enamel. *Arch Oral Biol* 22(10-11):599-603.

Bakhos Y, Brudevold F (1982). Effect of initial demineralisation on the permeability of human enamel to iodide. *Archives of Oral Biology* 27:193-196.

Barbour ME, Parker DM, Allen GC, Jandt KD (2003a). Human enamel dissolution in citric acid as a function of pH in the range 2.30 < or = pH < or = 6.30--a nanoindentation study. *Eur J Oral Sci* 111(3):258-262.

Barbour ME, Parker DM, Allen GC, Jandt KD (2003b). Enamel dissolution in citric acid as a function of calcium and phosphate concentrations and degree of saturation with respect to hydroxyapatite. *Eur J Oral Sci* 111(5):428-433.

Barbour ME, Parker DM, Jandt KD (2003c). Enamel dissolution as a function of solution degree of saturation with respect to hydroxyapatite: a nanoindentation study. *J Colloid Interface Sci* 265(1):9-14.

Barbour ME, Rees JS (2004). The laboratory assessment of enamel erosion: a review. *Journal of Dentistry* 32(8):591-602.

Barbour ME, Rees GD (2006). The role of erosion, abrasion and attrition in tooth wear. *Journal of Clinical Dentistry* 17(4):88-93.

Barbour ME, Shellis RP (2007). An investigation using atomic force microscopy nanoindentation of dental enamel demineralization as a function of undissociated acid concentration and differential buffer capacity. *Phys Med Biol* 52(4):899-910.

Bardsley PF (2008). The evolution of tooth wear indices. *Clinical Oral Investigations* 12(Suppl-9).

Bartlett DW, Smith BGN, Wilson RF (1994). Comparison of the effect of fluoride and non-fluoride toothpaste on tooth wear in vitro and the influence of enamel fluoride concentration and hardness of enamel. *British Dental Journal* 176:346-348.

Bartlett DW (1995). The relationship between gastro-oesophageal reflux and palatal dental erosion, University of London.

Bartlett DW (1997). The causes of dental erosion. *Oral Diseases* 3:209-211.

Bartlett DW, Blunt L, Smith BGN (1997a). Measurement of tooth wear in patients with palatal erosion. *British Dental Journal* 182:179-184.

Bartlett DW, Evans DF, Smith BGN (1997b). Oral regurgitation after reflux provoking meals: a possible cause of dental erosion? *Journal of Oral Rehabilitation* 24:102-108.

Bartlett DW, Smith BGN (2000). Definition, classification and clinical assessment of attrition, erosion and abrasion of enamel and dentine. In: Tooth wear and sensitivity - clinical advances in restorative dentistry. M Addy, G Embery, WM Edgar and R Orchardson editors. London: Martin Dunitz.

Bartlett DW, Coward PY (2001). Comparison of erosive potential of gastric juice and a carbonated drink in vitro. *J Oral Rehabil* 28:1045-1047.

Bartlett DW (2005). The implication of laboratory research on tooth wear and erosion. *Oral Diseases* 11(1):3-6.

Bartlett DW, Shah P (2006). A critical review of non-carious cervical (wear) lesions and the role of abfraction, erosion, and abrasion. *JDent Res* 85(4):306-312.

Bates JF, Stafford GD, Harrison A (1975). Masticatory function: A review of the literature II Speed of movement of the mandible, rate of chewing and forces developed in chewing. *Journal of Oral Rehabilitation* 2:349-361.

Bell S (2010). A beginner's guide to Uncertainty of Measurement NPL Good Practice Guide No 11: National Physical Laboratory.

Berg-Beckhoff G, Kutschmann M, Bardehle D (2008). Methodological considerations concerning the development of oral dental erosion indexes: literature survey, validity and reliability. *Clinical Oral Investigations* 12(Suppl-8).

Berry DC, Poole DFG (1974). Masticatory function and oral rehabilitation. *Journal of Oral Rehabilitation* 1:191-205.

Bhushan B, Williams VS, Shack RV (1988). In-Situ Nanoindentation Hardness Apparatus for Mechanical Characterization of Extremely Thin Films. *Journal of Tribology* 110(3):563-571.

BIPM, IEC, IFCC, ILAC, ISO, IUPAC *et al.* (2008). International vocabulary of metrology — Basic and general concepts and associated terms (VIM). 3rd ed.: JCGM 200: 2008.

Blunt L (2008). Instrumentation for Surface Texture Analysis. Measurement and Characterisation of Surface Topography. National Physical Laboratory, Teddington, UK.

Blunt L, Jiang X, Leach R, Harris P, Scott P (2008). The development of user-friendly software measurement standards for surface topography software assessment. *Wear* 264(5-6):389-393.

Boltryk PJ, Hill M, McBride JW, Nascè A (2008). A comparison of precision optical displacement sensors for the 3D measurement of complex surface profiles. *Sensors and Actuators A: Physical* 142(1):2-11.

Boltryk PJ, Hill M, McBride JW (2009). Comparing laser and polychromatic confocal optical displacement sensors for the 3D measurement of cylindrical artefacts containing microscopic grooved structures. *Wear* 266(5-6):498-501.

Bowen W (1995). The role of fluoride toothpastes in the prevention of dental caries. *Journal of the Royal Society of Medicine* 88(9):505-509.

Boyde A, Lester KS (1967). Electron microscopy of resorbing surfaces of dental hard tissues. *Z Zellforsch Mikrosk Anat* 83(4):538-548.

British Standard Institution (1995). Part 3: Guide to the Expression of Uncertainty in Measurement. PD 6461. London: BSI.

Brudevold F, Tehrani A, Cruz R (1982). The relationship among the permeability to iodide, pore volume, and intraoral mineralization of abraded enamel. *Journal of Dental Research* 61(5):645-649.

Buyukyilmaz T, Ogaard B, Rolla G (1997). The resistance of titanium tetrafluoride-treated human enamel to strong hydrochloric acid. *European Journal of Oral Sciences* 105(5):473-477.

Caldwell RC, Muntz ML, Gilmore RW, Pigman W (1957). Microhardness Studies of Intact Surface Enamel. *Journal of Dental Research* 36(5):732-738.

Camosci D, Tinanoff N (1984). Anti-bacterial determinants of stannous fluoride. *Journal of Dental Research* 63(9):1121-1126.

Castillo J, Milgrom P, Kharasch E, Izutsu K, Fey M (2001). Evaluation of fluoride release from commercially available fluoride varnishes. *The Journal of the American Dental Association* 132(10):1389-1394.

Centerwall BS, Armstrong CW, Funkhouser LS, Elzay RP (1986). Erosion of dental enamel among competitive swimmers at a gas-chlorinated swimming pool. *Am J Epidemiol* 123(4):641-647.

Chadwick RG, Mitchell HL, Cameron I, Hunter B, Tulley M (1997). Development of a novel system for assessing tooth and restoration wear. *Journal of Dentistry* 25(1):41-47.

Chadwick RG, Mitchell HL, Manton SL, Ward S, Ogston S, Brown R (2005). Maxillary incisor palatal erosion: no correlation with dietary variables? *J Clin Pediatr Dent* 29(2):157-163.

Chana H, Kelleher M, Briggs P, Hooper R (2000). Clinical evaluation of resin-bonded gold alloy veneers. *The Journal of Prosthetic Dentistry* 83(3):294-300.

Cheng ZJ, Wang XM, Cui FZ, Ge J, Yan JX (2009). The enamel softening and loss during early erosion studied by AFM, SEM and nanoindentation. *Biomedical Materials* 4(1):1502-1506.

Clarkson J, Ellwood R, Chandler R (1993). A comprehensive summary of fluoride dentifrice caries clinical trials. *American Journal of Dentistry* 6(S59).

Colgate-Palmolive (2010). Product information: Colgate Duraphat Varnish 50mg/ml Dental Suspension.

Craig RG, Peyton FA (1958). The micro-hardness of enamel and dentin. *Journal of Dental Research* 37(4):661-668.

Cuenat A (2010). Scanning probe and particle beam microscopy In: Fundamental Principles of Engineering Nanometrology. RK Leach editor. Oxford: Elsevier.

Curzon MEJ, Cutress TW (1983). Trace elements and dental disease Boston: John Wright.

de Josselin de Jong E, van der Linden A, Ten Bosch J (1987). Longitudinal microradiography: a non-destructive automated quantitative method to follow mineral changes in mineralised tissue slices. *Physics in Medicine and Biology* 32(10):1209.

De Josselin de Jong E, Van Der Linden A, Borsboom P, Ten Bosch J (1988). Determination of mineral changes in human dental enamel by longitudinal microradiography and scanning optical monitoring and their correlation with chemical analysis. *Caries Research* 22(3):153-159.

Dean HT, Arnold Jr FA, Jay P, Knutson JW (1950). Studies on mass control of dental caries through fluoridation of the public water supply. *Public Health Reports* 65(43):1403-1408.

DeVries W, Li C (1985). Algorithm to deconvolve stylus geometry from surface profile measurements. *J ENG IND* 107(2):167-174.

Dodds MW, Gragg PP, Rodriguez D (1997). The effect of some Mexican citric acid snacks on in vitro tooth enamel erosion. *PediatrDent* 19(5):339-340.

DoH/BASCD (2009). Delivering better oral health: An evidence-based toolkit for prevention: Department of Health.

Duschner H, Gotz H, Walker H, Lussi A (2000). Structural changes of acid etched enamel examined under confocal laser scanning microscope. In: Tooth wear and sensitivity. M Addy, G Embery and R Orchardson editors. London: Martin Dunitz.

Eccles JD (1979). Dental erosion of nonindustrial origin. A clinical survey and classification. *Journal of Prosthetic Dentistry* 42:649-653.

Egerton RF (2008). Physical principles of electron microscopy: an introduction to TEM, SEM and AEM. 2 ed.: Springer.

Eisenburger M, Addy M, Hughes JA, Shellis RP (2001a). Effect of time on the remineralisation of enamel by synthetic saliva after citric acid erosion. *Caries Research* 35(3):211-215.

Eisenburger M, Hughes JA, West NX, Shellis RP, Addy M (2001b). The use of ultrasonication to study the remineralisation of eroded enamel. *Caries Research* 35:61-66.

Eisenburger M, Addy M (2002a). Erosion and attrition of human enamel in vitro part I: interaction effects. *Journal of Dentistry* 30(7-8):341-347.

Eisenburger M, Addy M (2002b). Erosion and attrition of human enamel in vitro part II: influence of time and loading. *Journal of Dentistry* 30(7-8):349-352.

Eisenburger M, Addy M (2003). Influence of liquid temperature and flow rate on enamel erosion and surface softening. *Journal of Oral Rehabilitation* 30(11):1076-1080.

Ekstrand J (1996). Fluoride Metabolism. In: Fluoride in dentistry. O Fejerskov, J Ekstrand and BA Burt editors. Copenhagen: Munksgaard.

Elias A, Sheiham A (1998). The relationship between satisfaction with mouth and number and position of teeth. *Journal of Oral Rehabilitation* 25(9):649-661.

Ellwood R, Fejerskov O, Cury JA, Clarkson BH (2008). Fluorides in caries control. In: Dental caries : the disease and its clinical management. O Fejerskov and EAM Kidd editors. Oxford; Ames, Iowa: Blackwell Munksgaard, pp. 287-327.

Elton V, Cooper L, Higham S, Pender N (2009). Validation of enamel erosion in vitro. *Journal of Dentistry* 37(5):336-341.

Evans RW, Stamm JW (1991). An epidemiologic estimate of the critical period during which human maxillary central incisors are most susceptible to fluorosis. *Journal of Public Health Dentistry* 51(4):251-259.

Fares J, Shirodaria S, Chiu K, Ahmad N, Sherriff M, Bartlett DW (2009). A new index of tooth wear. Reproducibility and application to a sample of 18- to 30-year-old university students. *Caries Research* 43(2):119-125.

Faria Ac Fau - Rodrigues RCS, Rodrigues Rc Fau - Macedo AP, Macedo Ap Fau - Mattos MdGCd, Mattos Mda G Fau - Ribeiro RF, Ribeiro RF Accuracy of stone casts obtained by different impression materials. 1807-3107 (Electronic)).

Featherstone JD, Lussi A (2006). Understanding the chemistry of dental erosion. *Monographs in Oral Science* 20:66-76.

Fejerskov O, Clarkson BH (1996). Dynamics of caries lesion formation. In: Fluoride in Dentistry. O Fejerskov, J Ekstrand and BA Burt editors. Copenhagen: Munksgaard.

Fejerskov O, Richards A, DenBesten L (2009). The effect of fluoride on tooth mineralization. In: Fluoride in dentistry. O Fejerskov, J Ekstrand and BA Burt editors. Copenhagen: Munksgaard.

Field J, Waterhouse P, German M (2010). Quantifying and qualifying surface changes on dental hard tissues in vitro. *Journal of Dentistry* 38(3):182-190.

Finke M, Jandt K, Parker D (2000). The early stages of native enamel dissolution studied with atomic force microscopy. *Journal of colloid and interface science* 232(1):156-164.

Flack DR, Hannaford J (2005). Fundamental good practice in dimensional metrology *NPL Good practice guide No. 80* Teddington: National Physical Laboratory.

Fomon SJ, Ekstrand J (1996). Fluoride intake. In: Fluoride in dentistry. O Fejerskov, J Ekstrand and BA Burt editors. Copenhagen: Munksgaard, pp. 40-49.

Fosse G, Rosengren B, Skaale S, Leknes K, Wulff L (1986). An in vivo method for microhardness measurements on human teeth. *ScandJ Dent Res* 94(1):27-37.

Fowler C, Gracia L, Edwards M, Brown A, Rees G (2009). Fluoride penetration from toothpastes into incipient enamel erosive lesions investigated using dynamic secondary ion mass spectrometry. *The Journal of clinical dentistry* 20(6):186.

Frant MS, Ross JW (1966). Electrode for sensing fluoride ion activity in solution. *Science* 154(1553-1555).

Fushida C, Cury J (1999). Evaluation of enamel-dentine erosion by beverage and recovery by saliva and fluoride. *J Dent Res* 78:410.

Gallagher J, Kleinman E, Harper P (2010). Modelling workforce skill-mix: how can dental professionals meet the needs and demands of older people in England? *British dental journal* 208(3):E6-E6.

Ganss C, Klimek J, Schaffer U, Spall T (2001). Effectiveness of two fluoridation measures on erosion progression in human enamel and dentine in vitro. *Caries Research* 35(5):325-330.

Ganss C, Klimek J, Brune V, Schurmann A (2004a). Effects of two fluoridation measures on erosion progression in human enamel and dentine in situ. *Caries Research* 38(6):561-566.

Ganss C, Klimek J, Starck C (2004b). Quantitative analysis of the impact of the organic matrix on the fluoride effect on erosion progression in human dentine using longitudinal microradiography. *Archives of Oral Biology* 49(11):931-935.

Ganss C, Lussi A, Klimek J (2005). Comparison of calcium/phosphorus analysis, longitudinal microradiography and profilometry for the quantitative assessment of erosive demineralisation. *Caries Research* 39(3):178-184.

Ganss C (2006). Definition of erosion and links to tooth wear. In: Dental Erosion from Diagnosis to Therapy. A Lussi editor. Basel: Karger.

Ganss C, Schlueter N, Friedrich D, Klimek J (2007a). Efficacy of waiting periods and topical fluoride treatment on toothbrush abrasion of eroded enamel in situ. *Caries Research* 41(2):146-151.

Ganss C, Schlueter N, Hardt M, von HJ, Klimek J (2007b). Effects of toothbrushing on eroded dentine. *European Journal of Oral Sciences* 115(5):390-396.

Ganss C (2008). How valid are current diagnostic criteria for dental erosion?. [Review] [52 refs]. *Clinical Oral Investigations* 12(Suppl-9).

Ganss C, Schlueter N, Hardt M, Schattenberg P, Klimek J (2008). Effect of fluoride compounds on enamel erosion in vitro: a comparison of amine, sodium and stannous fluoride. *Caries Research* 42(1):2-7.

Ganss C, Lussi A, Scharmann I, Weigelt T, Hardt M, Klimek J *et al.* (2009). Comparison of Calcium Analysis, Longitudinal Microradiography and Profilometry for the Quantitative Assessment of Erosion in Dentine. *Caries Research* 43(6):422-429.

Gelhard T, Ten Cate J, Arends J (1979). Rehardening of Artificial Enamel Lesions *in vivo*. *Caries Research* 13(2):80-83.

Gilmour AG, Beckett HA (1993). The voluntary reflux phenomenon. *British Dental Journal* 175(10):368-372.

Giunta JL (1983). Dental erosion resulting from chewable vitamin C tablets. *Journal of American Dental Association* 107:253-256.

Good Clinical Practice and Current Regulations (2010). London: The Institute of Clinical Research.

Good practice in research and consent to research (2010). General Medical Council.

Goodhew PJ, Humpheys FJ, Beanland R (2000). Electron microscopy and analysis: Taylor and Francis.

Grenby TH, Phillips A, Desai T, Mistry M (1989). Laboratory studies of dental properties of soft drinks. *British Journal of Nutrition* 62:451-464.

Grenby TH (1996). Methods of assessing erosion and erosive potential. *European Journal of Oral Sciences* 104(2):207-214.

Grenness MJ, Tyas MJ, Osborn JE (2009). Mapping a non-carious cervical lesion using stereoimagery and dental casts incorporating optical texture. *Journal of Dentistry* 37(3):191-197.

Habelitz S, Marshall GW, Jr., Balooch M, Marshall SJ (2002). Nanoindentation and storage of teeth. *J Biomech* 35(7):995-998.

Hall AF, Sadler JP, Strang R, Josselin de Jong ED, Foye RH, Creanor SL (1997). Application of transverse microradiography for measurement of mineral loss by acid erosion. *Advances in Dental Research* 11(4):420-425.

Hannig C, Hamkens A, Becker K, Attin R, Attin T (2005). Erosive effects of different acids on bovine enamel: release of calcium and phosphate in vitro. *Arch Oral Biol* 50(6):541-552.

Hannig M, Hess N, Hoth-Hannig W, De Vrese M (2003). Influence of salivary pellicle formation time on enamel demineralization—an in situ pilot study. *Clinical Oral Investigations* 7(3):158-161.

Hannig M, Joiner A (2006). The structure, function and properties of the acquired pellicle. *Monographs in Oral Science* 19:29.

Hara AT, Ando M, Gonzalez-Cabezas C, Cury JA, Serra MC, Zero DT (2006a). Protective effect of the dental pellicle against erosive challenges in situ. *Journal of Dental Research* 85(7):612-616.

Hara AT, Lussi A, Zero DT (2006b). Biological factors. In: Dental Erosion from Diagnosis to Therapy. A Lussi editor. Basel: Karger.

Hara AT, Gonzalez-Cabezas C, Creeth J, Zero DT (2008). The effect of human saliva substitutes in an erosion-abrasion cycling model. *European Journal of Oral Sciences* 116(6):552-556.

Hara AT, Kelly SA, Gonzalez-Cabezas C, Eckert GJ, Barlow AP, Mason SC *et al.* (2009). Influence of fluoride availability of dentifrices on eroded enamel remineralization in situ. *Caries Res* 43(1):57-63.

Harding AM, Zero DT, Featherstone JD, McCormack SM, Shields CP, Proskin HM (1994). Calcium fluoride formation on sound enamel using fluoride solutions with and without lactate. *Caries Research* 28(1):1-8.

Harrison A, Lewis TT (1975). The development of an abrasion testing machine for dental materials. *Journal of Biomedical Materials Research* 9(3):341-353.

Helfenstein U, Steiner M (1994). Fluoride varnishes (Duraphat): A meta analysis. *Community Dentistry and Oral Epidemiology* 22(1):1-5.

Hemingway C, Shellis R, Parker D, Addy M, Barbour M (2008). Inhibition of Hydroxyapatite Dissolution by Ovalbumin as a Function of pH, Calcium Concentration, Protein Concentration and Acid Type. *Caries Research* 42(5):348-353.

Holbrook WP, Ganss C (2008). Is diagnosing exposed dentine a suitable tool for grading erosive loss? *Clinical Oral Investigations* 12(Suppl-9).

Holme B, Hove LH, Tveit AB (2005). Using white light interferometry to measure etching of dental enamel. *Measurement* 38(2):137-147.

Horowitz HS, Ismail AI (1996). Topical fluorides in caries prevention. In: Fluoride in Dentistry. O Fejerskov, J Ekstrand and BA Burt editors. Copenhagen: Munksgaard.

Hove L, Holme B, Ogaard B, Willumsen T, Tveit AB (2006). The protective effect of TiF₄, SnF₂ and NaF on erosion of enamel by hydrochloric acid in vitro measured by white light interferometry. *Caries Research* 40(5):440-443.

Hove LH, Holme B, Young A, Tveit AB (2007a). The erosion-inhibiting effect of TiF₄, SnF₂, and NaF solutions on pellicle-covered enamel in vitro. *Acta Odontologica Scandinavica* 65(5):259-264.

Hove LH, Young A, Tveit AB (2007b). An in vitro study on the effect of TiF₄ treatment against erosion by hydrochloric acid on pellicle-covered enamel. *Caries Research* 41(1):80-84.

Hove LH, Holme B, Young A, Tveit AB (2008). The protective effect of TiF₄, SnF₂ and NaF against erosion-like lesions in situ. *Caries Research* 42(1):68-72.

HTA Codes of Practice (2009). Human Tissue Authority. <http://www.hta.gov.uk/> (accessed 30 Sept 2008)

Human Tissue Act (2004). www.legislation.hmso.gov.uk/acts/acts2004/20040030.htm (accessed 30 Sept 2008).

ISO 3274 (1996). Geometrical product specifications (GPS) – Surface texture: Profile method – Nominal characteristics of contact (stylus) instruments: International Organisation of Standardization.

ISO 3534-1 (1993). Statistics - Vocabulary and symbols - Part 1: Probability and general statistical terms International Organisation of Standardization.

ISO 4287 (1997). Geometrical product specifications (GPS) – Surface texture: Profile method – Terms, definitions and surface texture parameters International Organisation of Standardization.

ISO 25178-2 (2010). Geometrical product specifications (GPS) -- Surface texture: Areal -- Part 2: Terms, definitions and surface texture parameters.

ISO 25178-602 (2010). Geometrical product specifications (GPS) -- Surface texture: Areal -- Part 602: Nominal characteristics of non-contact (confocal chromatic probe) instruments International Organisation of Standardization.

ISO (1996). Surface texture: Profile method—Nominal characteristics of contact (stylus) instruments. Geometrical product specifications. Geneva.

ISO (2004). International vocabulary of basic and general terms in metrology (VIM). *International Organization For Standardization*.

Ivoclar-Vivadent (2010). Fluor Protector Gel Scientific Documentation. Schaan, Liechtenstein.

Jaeggi T, Lussi A (1999). Toothbrush abrasion of erosively altered enamel after intraoral exposure to saliva: an in situ study. *Caries Research* 33(6):455-461.

Jensdottir T, Nauntofte B, Buchwald C, Bardow A (2005). Effects of sucking acidic candy on whole-mouth saliva composition. *Caries Research* 39(6):468-474.

Jensdottir T, Nauntofte B, Buchwald C, Bardow A (2007). Effects of calcium on the erosive potential of acidic candies in saliva. *Caries Research* 41(1):68-73.

Joiner A, Pickles MJ, Tanner C, Weader E, Doyle P (2004a). An in situ model to study the toothpaste abrasion of enamel. *Journal of Clinical Periodontology* 31(6):434-438.

Joiner A, Weader E, Cox TF (2004b). The measurement of enamel wear of two toothpastes. *Oral Health PrevDent* 2(4):383-388.

Jones R, Lydeard S (1989). Prevalence of symptoms of dyspepsia in the community. *British Medical Journal* 298:30-32.

Jones R, Darling C, Featherstone J, Fried D (2006). Imaging artificial caries on the occlusal surfaces with polarization-sensitive optical coherence tomography. *Caries Research* 40(2):81.

Joziak MT, Morgan AM, Prencipe M (2011). Resistance to Acid Exposure from 5000 ppm Fluoride Dentifrices. IADR/AADR/CADR 89th General Session and Exhibition. San Diego, California, USA.

Kaidonis JA, Richards LC, Townsend GC, Tansley GD (1998). Wear of human enamel: a quantitative in vitro assessment. *Journal of Dental Research* 77(12):1983-1990.

Karlsson L (2010). Caries detection methods based on changes in optical properties between healthy and carious tissue. *International Journal of Dentistry* 2010:1-9.

Kelly M, Steele J, Nuttall N, Bradnock G, Morris J, Nunn J *et al.* (1998). Adult dental health survey. *Oral health in the United Kingdom*:257–288.

Kreulen C, Van't Spijker A, Rodriguez J, Bronkhorst E, Creugers N, Bartlett D (2010). Systematic Review of the Prevalence of Tooth Wear in Children and Adolescents. *Caries Research* 44(2):151-159.

Lagerweij MD, Buchalla W, Kohnke S, Becker K, Lennon AM, Attin T (2006). Prevention of erosion and abrasion by a high fluoride concentration gel applied at high frequencies. *Caries Research* 40(2):148-153.

Lambrechts P, Debels E, Van LK, Peumans M, Van MB (2006). How to simulate wear? Overview of existing methods. *DentMater* 22(8):693-701.

Larsen MJ (2001). Prevention by means of fluoride of enamel erosion as caused by soft drinks and orange juice. *Caries Research* 35(3):229-234.

Larsen MJ, Richards A (2002). Fluoride is unable to reduce dental erosion from soft drinks. *Caries Research* 36(1):75-80.

Larsen MJ (2008). Erosion of the teeth. In: Dental caries : the disease and its clinical management. O Fejerskov and EAM Kidd editors. Oxford; Ames, Iowa: Blackwell Munksgaard.

Last JM (2000). A dictionary of epidemiology. New York: Oxford University Press.

Layer T (2009). Formulation considerations for developing toothpastes suitable for those at risk from erosive tooth wear. *The Journal of clinical dentistry* 20(6):199.

Leach RK (13th August 2008). Introduction and profile characterisation. Measurement and Characterisation of Surface Topography. National Physical Laboratory, Teddington, UK.

Leach RK Limitations of stylus instruments. Measurement and characterisation of surface topography 2008, National Physical Laboratory, Teddington, UK.

Leach RK, Brown L, Jaing X, Blunt R, Conroy M, Mauger D (2008). Guide to the measurement of Smooth Surface Topography using Coherence Scanning Interferometry: Measurement Good Practice Guide No. 108: National Physical Laboratory.

Leach RK (2010a). Surface topography measurement instrumentation. In: Fundamental principles of engineering nanometrology. Oxford; Amsterdam: William Andrew ; Elsevier Science.

Leach RK (2010b). Surface topography characterisation. In: Fundamental principles of engineering nanometrology. Oxford; Amsterdam: William Andrew ; Elsevier Science.

Leach RK (2010c). Fundamental principles of engineering nanometrology. Oxford; Amsterdam: William Andrew ; Elsevier Science.

Leach RK (2010d). Some basics of measurement. In: Fundamental principles of engineering nanometrology. Oxford; Amsterdam: William Andrew ; Elsevier Science.

Lee WC, Eakle WS (1984). Possible role of tensile stress in the aetiology of cervical erosive lesions of teeth. *Journal of Prosthetic Dentistry* 52:374-379.

Levine MJ (1993). Development of Artificial Salivas. *Critical Reviews in Oral Biology & Medicine* 4(3):279-286.

Li H, Watson TF, Sherriff M, Curtis R, Bartlett DW (2007). The influence of fluoride varnish on the attrition of dentine. *Caries Research* 41(3):219-222.

Lissera RG, Luna Maldonado ER, Battellino LJ (1998). In vitro erosive capacity of some fruit juices and soft or low alcoholic strength beverages on human teeth. *Acta Odontol Latinoam* 11(1):55-71.

Litonjua LA, Andreana S, Bush PJ, Tobias TS, Cohen RE (2003). Noncarious cervical lesions and abfractions: a re-evaluation. *Journal of American Dental Association* 134(7):845-850.

Lussi A, Jaggi T, Scharer S (1993). The influence of different factors on in vitro enamel erosion. *Caries Research* 27(5):387-393.

Lussi A, Jaeggi T, Jaeggi-Scharer S (1995). Prediction of the erosive potential of some beverages. *Caries Research* 29(5):349-354.

Lussi A, Portmann P, Burhop B (1997). Erosion on abraded dental hard tissues by acid lozenges: an in situ study. *Clin Oral Investig* 1(4):191-194.

Lussi A, Kohler N, Zero DT, Schaffner M, Megert B (2000). A comparison of the erosive potential of different beverages in primary and permanent teeth using an in vitro model. *EurJ Oral Sci* 108(2):110-114.

Lussi A, Hellwig E (2001). Erosive potential of oral care products. *Caries Research* 35(Suppl-6).

Lussi A (2002). Dental erosion; clinical diagnosis and case history taking. *EurJ Oral Sci* 104:191-198.

Lussi A, Jaeggi T, Gerber C, Megert B (2004). Effect of amine/sodium fluoride rinsing on toothbrush abrasion of softened enamel in situ. *Caries Research* 38(6):567-571.

Lussi A, Jaeggi T (2006). Chemical factors. In: Dental Erosion from Diagnosis to Therapy. A Lussi editor. Basel: Karger.

Magalhaes AC, Rios D, Delbem AC, Buzalaf MA, Machado MA (2007). Influence of fluoride dentifrice on brushing abrasion of eroded human enamel: an in situ/ex vivo study. *Caries Research* 41(1):77-79.

Magalhaes AC, Kato MT, Rios D, Wiegand A, Attin T, Buzalaf MA (2008a). The effect of an experimental 4% Tif4 varnish compared to NaF varnishes and 4% TiF4 solution on dental erosion in vitro. *Caries Research* 42(4):269-274.

Magalhaes AC, Rios D, Honorio HM, Jorge AM, Jr., Delbem AC, Buzalaf MA (2008b). Effect of 4% titanium tetrafluoride solution on dental erosion by a soft drink: an in situ/ex vivo study. *Archives of Oral Biology* 53(5):399-404.

Magalhaes AC, Wiegand A, Rios D, Honorio HM, Buzalaf MA (2009). Insights into preventive measures for dental erosion. *Journal of Applied Oral Science* 17(2):75-86.

Maggio B, Mason S, Zero DT, Kelly S, Guibert GB, Karwal R (2010). Evaluation of Dentifrice/Mouthrinse Regimens in an In Situ Erosion Model. 88th General Session and Exhibition of the International Association for Dental Research

Mair LH (2000). Wear in the mouth: the tribological dimension. In: Tooth wear and sensitivity: Clinical advances in Restorative Dentistry. M Addy, G Embery, WM Edgar and R Orchardson editors. London: Martin Dunitz.

Marshall G, Chang Y, Gansky S, Marshall S (2001). Demineralization of caries-affected transparent dentin by citric acid: an atomic force microscopy study. *Dental materials: official publication of the Academy of Dental Materials* 17(1):45.

Mason SC (2009). New in vitro and in situ evidence for a toothpaste formulated for those at risk from erosive tooth wear. *J Clin Dent* 20(6):175-177.

McCool J (1984). Assessing the effect of stylus tip radius and flight on surface topography measurements. *Journal of Tribology* 106:202.

McNally LM, Barbour ME, O'Sullivan DJ, Jagger DC (2006). An in vitro investigation of the effect of some analgesics on human enamel. *JOral Rehabil* 33(7):529-532.

Meredith N, Sherrieff M, Setchell DJ, Swanson SA (1996). Measurement of the microhardness and Young's modulus of human enamel and dentine using an indentation technique. *Archives of Oral Biology* 41(6):539-545.

Meurman JH, Frank RM (1991). Progression and surface ultrastructure of in vitro caused erosive lesions in human and bovine enamel. *Caries Research* 25:81-87.

Millward A, Shaw L, Smith AJ, Rippin JW, Harrington E (1994). The distribution and severity of tooth wear and the relationship between erosion and dietary constituents in a group of children. *International Journal of Paediatric Dentistry* 4:151-157.

Millward A, Shaw L, Harrington E, Smith AJ (1997). Continuous monitoring of salivary flow rate and pH at the surface of the dentition following consumption of acidic beverages. *Caries Research* 31:44-49.

Milosevic A, Slade PD (1989). The orodental status of anorexics and bulimics. *British Dental Journal* 167:66-70.

Milosevic A, Brodie DA, Slade PD (1997a). Dental erosion, oral hygiene, and nutrition in eating disorders. *International Journal of Eating Disorders* 21(2):195-199.

Milosevic A, Kelly MJ, McLean AN (1997b). Sports supplement drinks and dental health of competitive swimmers and cyclists. *British Dental Journal* 182(303-308).

Milosevic A, Agrawal N, Redfearn P, Mair L (1999). The occurrence of toothwear in users of Ecstasy (3,4-methylenedioxymethamphetamine). *Community Dentistry & Oral Epidemiology* 27(4):283-287.

Milosevic A, Bardsley PF, Taylor S (2004). Epidemiological studies of tooth wear and dental erosion in 14-year old children in North West England. Part 2: The association of diet and habits. *BrDent J* 197(8):479-483.

Mitchell HL, Chadwick RG (1998). Mathematical shape matching as a tool in tooth wear assessment - development and conduct. *Journal of Oral Rehabilitation* 25:921-928.

Mühlemann H, Schmid H, König K (1957). Enamel solubility reduction studies with inorganic and organic fluorides. *Helv Odont Acta* 1:23-33.

Mundorff SA, Little MF, Bibby BG (1972). Enamel dissolution. II. Action of titanium tetrafluoride. *Journal of Dental Research* 51(6):1567-1571.

Murray JJ, Rugg-Gunn AJ, Jenkins GN (1991). Fluorides in caries prevention Oxford: Wright/Butterworth-Heinemann.

Nakagaki H, Koyama Y, Sakakibara Y, Weatherell JA, Robinson C (1987). Distribution of fluoride across human dental enamel, dentine and cementum. *Archives of Oral Biology* 32(9):651-654.

Nanci A, Ten Cate AR (2008). Ten Cate's oral histology : development, structure, and function St. Louis, Mo.: Mosby Elsevier.

Nekrashevych Y, Stösser L (2000). Protective influence of experimentally formed salivary pellicle on enamel erosion. *Caries Research* 37(3):225-231.

NPL Optical Dimensional Standard For Vision Machines & Microscopy Range 1 µm - 60 mm. http://www.npl.co.uk/upload/pdf/ods_photomask.pdf. In: National Physical Laboratory editor.

Nunn JH (2000). Prevalance and distribution of tooth wear. In: Tooth wear and sensitivity - clinical advances in restorative dentistry. M Addy, G Embery, WM Edgar and R Orchardson editors. London: Martin Dunitz.

Nyvad B, Machiulskiene V, Baelum V (2003). Construct and predictive validity of clinical caries diagnostic criteria assessing lesion activity. *Journal of Dental Research* 82(2):117.

Nyvad B (2008). Role of oral hygiene. In: Dental caries : the disease and its clinical management. O Fejerskov and EAM Kidd editors. Oxford; Ames, Iowa: Blackwell Munksgaard.

O'Sullivan EA, Milosevic A (2007). Diagnosis, prevention and management of dental erosion: Faculty of Dental Surgery of the Royal College of Surgeons of England.

O'Donnell K (1993). Effects of finite stylus width in surface contact profilometry. *Applied Optics* 32(25):4922-4928.

Øgaard B, Seppä L, Rolla G (1994). Professional topical fluoride applications—clinical efficacy and mechanism of action. *Advances in Dental Research* 8(2):190-194.

Oxford English Dictionary "model, n. and adj.": OED Online: Oxford University Press. <http://www.oed.com/> (accessed 21 January 2011)

Oxford English Dictionary (November 2010). "surface, n.". OED Online: Oxford University Press. <http://www.oed.com/> (accessed 20 February 2011)

Peck SL (2004). Simulation as experiment: a philosophical reassessment for biological modeling. *Trends in Ecology & Evolution* 19(10):530-534.

Petersen PE, Gormsen C (1991). Oral conditions among german battery factory workers. *Community Dental Oral Epidemiology* 19:104-106.

Petzold M (2000). The Influence of Different Fluoride Compounds and Treatment Conditions on Dental Enamel: A Descriptive in vitro Study of the CaF₂ Precipitation and Microstructure. *Caries Research* 35(1):45-51.

Pieterse S, de JN, de VN (2006). Does fluoride rinsing have an effect on teeth status? Evaluation of preventive dental health activities for the youth of Woudenberg, The Netherlands. *International Journal of Dental Hygiene* 4(3):133-139.

Pintado MR, Anderson GC, DeLong R, Douglas WH (1997). Variation in tooth wear in young adults over a two-year period. *Journal of Prosthetic Dentistry* 77:313-320.

Ponduri S, MacDonald E, Addy M (2005). A study in vitro of the combined effects of soft drinks and tooth brushing with fluoride toothpaste on the wear of dentine. *International Journal of Dental Hygiene* 3(1):7-12.

Poulsen S, Larsen M (1975). Dental caries in relation to fluoride content of enamel in the primary dentition. *Caries Research* 9(1):59-65.

Pretty I, Edgar W, Higham S (2004). The validation of quantitative light-induced fluorescence to quantify acid erosion of human enamel. *Archives of Oral Biology* 49(4):285-294.

Pretty IA, Edgar WM, Higham SM (2003). The erosive potential of commercially available mouthrinses on enamel as measured by Quantitative Light-induced Fluorescence (QLF). *Journal of Dentistry* 31(5):313-319.

Product information sheet for Bifluorid10 varnish: VOCO GmbH.

Richards A, Kragstrup J, Josephsen K, Fejerskov O (1986). Dental fluorosis developed in post-secretory enamel. *Journal of Dental Research* 65(12):1406-1409.

Richards A, Fejerskov O, Baelum V (1989). Enamel fluoride in relation to severity of human dental fluorosis. *Advances in Dental Research* 3(2):147-152.

Rios D, Honorio HM, Magalhaes AC, Buzalaf MA, Palma-Dibb RG, Machado MA *et al.* (2006). Influence of toothbrushing on enamel softening and abrasive wear of eroded bovine enamel: an in situ study. *BrazOral Res* 20(2):148-154.

Rios D, Honorio HM, Magalhaes AC, Silva SM, Delbem AC, Machado MA *et al.* (2008). Scanning electron microscopic study of the in situ effect of salivary stimulation on erosion and abrasion in human and bovine enamel. *BrazOral Res* 22(2):132-138.

Ripa L (1991). A Critique of Topical Fluoride Methods (Dentifrices, Mouthrinses, Operator , and Self applied Gels) in an Era of Decreased Caries and Increased Fluorosis Prevalence. *Journal of Public Health Dentistry* 51(1):23-41.

Robb ND, Smith BGN (1990). Prevalence of pathological tooth wear in patients with chronic alcoholism. *British Dental Journal* 169:367-369.

Robinson C, Kirkham J, Weatherell JA (1996). Fluoride in teeth and bone. In: Fluoride in dentistry. O Fejerskov, J Ekstrand and BA Burt editors. Copenhagen: Munksgaard.

Rodriguez J, Bartlett D (2010). A comparison of two-dimensional and three-dimensional measurements of wear in a laboratory investigation. *Dental Materials* 26(10):221-225.

Rodriguez JM, Curtis RV, Bartlett DW (2009). Surface roughness of impression materials and dental stones scanned by non-contacting laser profilometry. *Dental Materials* 25(4):500-505.

Rodriguez JM, Austin RS, Bartlett DW (2011). The measurement of tooth wear in vivo of 63 patients over 24 months. *Caries Research (in press)*

Rodriguez JM, Austin RS, Bartlett DW (2011). A method to evaluate profilometric tooth wear measurements. *Journal of Dental Research (in press)*.

Rosin-Grget K, Lincir I, Tudja M (2000). Effect of amine fluoride on enamel surface morphology. *Coll Antropol* 24(2):501-508.

Safety Data Sheet for Bifluorid10 (2008). VOCO GmbH.

Sales-Peres SH, Pessan JP, Buzalaf MA (2007). Effect of an iron mouthrinse on enamel and dentine erosion subjected or not to abrasion: an in situ/ex vivo study. *ArchOral Biol* 52(2):128-132.

Scheie AA, Peterson FC (2008). Antimicrobials in caries control. In: Dental caries : the disease and its clinical management. O Fejerskov and EAM Kidd editors. Oxford; Ames, Iowa: Blackwell Munksgaard.

Schlueter N, Ganss C, De SS, Klimek J (2005). Evaluation of a profilometrical method for monitoring erosive tooth wear. *EurJ Oral Sci* 113(6):505-511.

Schlueter N, Ganss C, Mueller U, Klimek J (2007). Effect of titanium tetrafluoride and sodium fluoride on erosion progression in enamel and dentine in vitro. *Caries Research* 41(2):141-145.

Schlueter N, Hardt M, Lussi A, Engelmann F, Klimek J, Ganss C (2009). Tin containing fluoride solutions as anti erosive agents in enamel: an in vitro tin uptake, tissue loss, and scanning electron micrograph study. *European Journal of Oral Sciences* 117(4):427-434.

Schmidlin PR, Gohring TN, Schug J, Lutz F (2003). Histological, morphological, profilometric and optical changes of human tooth enamel after microabrasion. *Am J Dent* 16 Spec No(4A-8A).

Sciences et Techniques Industrielles de la Lumière (STIL) (2007). Optical Principles Confocal Chromatic Sensor. 595, rue Pierre Berthier – Domaine St Hilaire – 13855 Aix en Provence Cedex 3 - France.

Shabanian M, Richards LC (2002). In vitro wear rates of materials under different loads and varying pH. *Journal of Prosthetic Dentistry* 87(6):650-656.

Shaffner TJ, Van Veld RD (1971). 'Charging' effects in the scanning electron microscope. *Journal of Physics E: Scientific Instruments* 4(9).

Shellis RP, Finke M, Eisenburger M, Parker DM, Addy M (2005). Relationship between enamel erosion and liquid flow rate. *European Journal of Oral Sciences* 113(3):232-238.

Shrestha BM (1983). Titanium. In: Trace elements and dental disease. MEJ Curzon and TW Cutress editors. Boston: John Wright.

Siddall G, Willey P (1970). Flat-surface wringing and contact error variability. *Journal of Physics D: Applied Physics* 3(8).

Sirdeshmukh L, Sirdeshmukh BD, Subhadra KG (2006). Hardness. In: Micro- and Macro-Properties of Solids: Thermal, Mechanical and Dielectric Properties. Berlin: Springer Berlin Heidelberg.

Skartveit L, Tveit A, Klinge B, Tørtedal B, Selvig K (1989). In vivo uptake and retention of fluoride after a brief application of TiF₄ to dentin. *Acta Odontologica* 42(2):65-68.

Smith BGN, Knight JK (1984a). An index for measuring the wear of teeth. *British Dental Journal* 156:435-438.

Smith BGN, Knight JK (1984b). A comparison of patterns of tooth wear with aetiological factors. *British Dental Journal* 157:16-19.

Smith BGN (1991). Some facets of tooth wear. *Annals of Royal College of Dental Surgery* 11:37-51.

Sorvari R, Meurman JH, Alaluusua S, Frank MR (1994). Effect of fluoride varnish on enamel in vitro. *Caries Research* 28:227-232.

Sorvari R, Pelttari A, Meurman JH (1996). Surface ultrastructure of rat molar teeth after experimentally induced erosion and attrition. *Caries Research* 30:163-168.

Stachowiak GW, Batchelor AW, Stachowiak GB (2004). Experimental methods in tribology Amsterdam: Elsevier.

Statistical Bulletin: 2008-based National population projections (21 October 2009). Office for National Statistics.

Steele JG, Sanders AE, Slade GD, Allen PF, Lahti S, Nuttall N *et al.* (2004). How do age and tooth loss affect oral health impacts and quality of life? A study comparing two national samples. *Community Dentistry and Oral Epidemiology* 32(2):107-114.

Stout KJ, Blunt L (1995). Application of 3-D topography to bio-engineering. *International Journal of Tools and Manufacturing* 35(2):219-229.

Suga N (2007). Metrology Handbook: The Science of Measurement. Andover: Mitutoyo (UK) Ltd.

Sundaram G, Bartlett DW, Watson T (2004). Bonding to and protecting worn palatal surfaces of teeth with dentine bonding agents. *J Oral Rehabil* 31(5):505-509.

Sundaram G, Bartlett DW, Watson TF, Wilson R (2007a). Clinical measurement of palatal tooth wear following coating by a resin sealing system. *Operative Dentistry* 32(6):539-543.

Sundaram G, Wilson R, Watson TF, Bartlett DW (2007b). Effect of resin coating on dentine compared to repeated topical applications of fluoride mouthwash after an abrasion and erosion wear regime. *Journal of Dentistry* 35(10):814-818.

Takats R, Albrecht M, Fosse G, Sapi Z, Banoczy J (1991). [Testing of dental enamel hardness by an in vivo method]. *Fogorv Sz* 84(5):145-148.

ten Cate J, Duijsters P (1983a). Influence of fluoride in solution on tooth demineralization. I. Chemical data. *Caries Research* 17(3):193-195.

ten Cate J, Duijsters P (1983b). Influence of fluoride in solution on tooth demineralization. II. Microradiographic data. *Caries Research* 17(6):513-515.

ten Cate J (1997). Review on fluoride, with special emphasis on calcium fluoride mechanisms in caries prevention. *European Journal of Oral Sciences* 105(5 Pt 2):461-466.

ten Cate JM, Featherstone JD (1996). Physicochemical aspects of fluoride-enamel interactions. In: Fluoride in dentistry. O Fejerskov, J Ekstrand and BA Burt editors. Copenhagen: Munksgaard.

ten Cate JM, Larsen MJ, Pearce E, Fejerskov O (2008). Chemical interactions between the tooth and oral fluids. In: Dental caries : the disease and its clinical management. O Fejerskov and EAM Kidd editors. Oxford; Ames, Iowa: Blackwell Munksgaard.

Tranæus S, Al-Khateeb S, Björkman S, Twetman S, Angmar-Månsson B (2001). Application of quantitative light-induced fluorescence to monitor incipient lesions in caries-active children. A comparative study of remineralisation by fluoride varnish and professional cleaning. *European Journal of Oral Sciences* 109(2):71-75.

Tveit A, Hals E, Isrenn R, Tødtal B (1983). Highly acid SnF₂ and TiF₄ solutions. Effect on and chemical reaction with root dentin in vitro. *Caries Research* 17(5):412-418.

Tveit A, Klinge B, TÖTDAL B, Selvig K (1988). Long-term retention of TiF₄ and SnF₂ after topical application to dentin in dogs. *European Journal of Oral Sciences* 96(6):536-540.

Van't Spijker A, Kreulen CM, Creugers NHJ (2007). Attrition, occlusion,(dys) function, and intervention: a systematic review. *Clinical oral implants research* 18:117-126.

Van't Spijker A, Rodriguez J, Kreulen C, Bronkhorst E, Bartlett D, Creugers N (2009a). Prevalence of tooth wear in adults. *The International journal of prosthodontics* 22(1):35-42.

van't Spijker A, Rodriguez JM, Kreulen CM, Bartlett DW, Creugers NH (2009b). Prevalence of Tooth Wear in Adults. *International Journal of Prosthodontics* 22(1):35-42.

van der Veen MH, de Josselin de Jong E (2000). Application of quantitative light-induced fluorescence for assessing early caries lesions. *Monogr Oral Sci* 17:144-162.

Van Meerbeek B, Willems G, Celis JP, Roos JR, Braem M, Lambrechts P *et al.* (1993). Assessment by nano-indentation of the hardness and elasticity of the resin-dentin bonding area. *Journal of Dental Research* 72(10):1434-1442.

van Rijkom H, Ruben J, Vieira A, Huysmans MC, Truin GJ, Mulder J (2003). Erosion-inhibiting effect of sodium fluoride and titanium tetrafluoride treatment in vitro. *European Journal of Oral Sciences* 111(3):253-257.

Venasakulchai A, Williams NA, Gracia L, Rees GD (2009). Erosion Protection by Mouthrinses in a 5-Day Cycling Model 88th General Session and Exhibition of the International Association for Dental Research Barcelona, Spain.

Venkateswarlu P, Vogel GL (1996). Fluoride analytical methods. In: Fluoride in Dentistry. O Fejerskov, J Ekstrand and BA Burt editors. Copenhagen: Munksgaard.

Vieira A, Ruben JL, Huysmans MC (2005). Effect of titanium tetrafluoride, amine fluoride and fluoride varnish on enamel erosion in vitro. *Caries Research* 39(5):371-379.

Vieira A, Lugtenborg M, Ruben JL, Huysmans MC (2006a). Brushing abrasion of eroded bovine enamel pretreated with topical fluorides. *Caries Research* 40(3):224-230.

Vieira A, Overweg E, Ruben JL, Huysmans MC (2006b). Toothbrush abrasion, simulated tongue friction and attrition of eroded bovine enamel in vitro. *Journal of Dentistry* 34(5):336-342.

Vieira A, Jager DH, Ruben JL, Huysmans MC (2007). Inhibition of erosive wear by fluoride varnish. *Caries Research* 41(1):61-67.

Walls A, Steele J (2001). Geriatric oral health issues in the United Kingdom. *International dental Journal* 51(3 Suppl):183-186.

Waltimo A, Nystrom M, Kononen M (1994). Bite force and dentofacial morphology in men with severe dental attrition. *Scandinavian Journal of Dental Research* 102(2):92-96.

Waters NE (1980). Some mechanical and physical properties of teeth. In: The mechanical properties of biological materials. JFV Vincent and JD Currey editors. Cambridge: Cambridge University Press.

Wei SH, Soboroff DM, Wefel JS (1976). Effects of titanium tetrafluoride on human enamel. *Journal of Dental Research* 55(3):426-431.

Wei SHY, Forbes WC (1974). Electron microprobe investigations of stannous fluoride reactions with enamel surfaces. *Journal of Dental Research* 53(1):51-55.

West N, Hughes J, Addy M (2001). The effect of pH on the erosion of dentine and enamel by dietary acids in vitro. *Journal of Oral Rehabilitation* 28(9):860-864.

West NX, Maxwell A, Hughes JA, Parker DM, Newcombe RG, Addy M (1998). A method to measure clinical erosion: the effect of orange juice consumption on erosion of enamel. *Journal of Dentistry* 26(4):329-335.

West NX, Jandt KD (2000). Methodologies and instrumentation to measure tooth wear: future perspectives. In: Tooth wear and sensitivity - clinical advances in restorative dentistry. M Addy, G Embery, WM Edgar and R Orchardson editors. London: Martin Dunitz.

West NX, Hooper S, MacDonald E, Barker ML, He T (2011). In-situ Erosion Study of a Stannous Containing Sodium Fluoride Dentifrice. IADR/AADR/CADR 89th General Session and Exhibition. San Diego, California, USA.

Whitford GM (1996). Fluoride toxicology and health effects. In: Fluoride in dentistry. O Fejerskov, J Ekstrand and BA Burt editors. Copenhagen: Munksgaard.

Whittaker DK (2000). Historical and forensic aspects of tooth wear. In: Tooth wear and Sensitivity - clinical advances in restorative dentistry. M Addy, G Embery, WM Edgar and R Orchardson editors. London: Martin Dunitz.

Wiegand A, Attin T (2003). Influence of fluoride on the prevention of erosive lesions--a review. *Oral Health PrevDent* 1(4):245-253.

Wiegand A, Meier W, Sutter E, Magalhaes AC, Becker K, Roos M *et al.* (2008). Protective effect of different tetrafluorides on erosion of pellicle-free and pellicle-covered enamel and dentine. *Caries Research* 42(4):247-254.

Wiegand A, Magalhaes A, Attin T (2009). Is titanium tetrafluoride (TiF 4) effective to prevent carious and erosive lesions? A review of the literature. *Oral Health and Preventive Dentistry* 8(2):159-64.

Wiegand A, Hiestand B, Sener B, Magalhães A, Roos M, Attin T (2010). Effect of TiF (4), ZrF (4), HfF (4) and AmF on erosion and erosion/abrasion of enamel and dentin in situ. *Archives of Oral Biology* 55(3):223-8.

Wilder-Smith C, Wilder-Smith P, Kawakami-Wong H, Voronets J, Osann K, Lussi A (2009). Quantification of Dental Erosions in Patients With GERD Using Optical Coherence Tomography Before and After Double-Blind, Randomized Treatment With Esomeprazole or Placebo. *The American Journal of Gastroenterology* 104(11):2788-95.

Willershausen B, Callaway A, Azrak B, Kloss C, Schulz-Dobrick B (2009). Prolonged in vitro exposure to white wines enhances the erosive damage on human permanent teeth compared with red wines. *Nutrition Research* 29(8):558-567.

Willumsen T, Ogaard B, Hansen BF, Rolla G (2004). Effects from pretreatment of stannous fluoride versus sodium fluoride on enamel exposed to 0.1 M or 0.01 M hydrochloric acid. *Acta Odontologica Scandinavica* 62(5):278-281.

Winsberg E (2001). Simulations, models, and theories: Complex physical systems and their representations. *Philosophy of Science* 68(3):442-454.

Woldseth R (1973). All you ever wanted to know about X-ray energy spectrometry: KeVeX Corporation, Burlingame.

World Health Organisation (1992). Application of the international classification of diseases to dentistry and stomatology, ICD-DA Geneva.

Xhonga FA, Sognnaes RA (1973). Dental erosion: progress of erosion measured clinically after various fluoride applications. *Journal of American Dental Association* 87:1223-1228.

Xhonga FA (1977). Bruxism and its effect on the teeth. *Journal of Oral Rehabilitation* 4:65-76.

Xhonga FA, Wolcott RB, Sognnaes RF (1995). Clinical measurements of dental erosion progress. *Journal of American Dental Association* 84:577-582.

XYRIS Series Precision 3D Surface Profilers Brochure (2009). TaiCaan Technologies Ltd <http://www.taicaan.com> 2 Venture Road, Southampton Science Park, Southampton, SO16 7NP, UK.

Yewe-Dyer M (1993). The definition of oral health. *British Dental Journal* 174(7):224-227.

Young A, Thrane PS, Saxegaard E, Jonski G, Rolla G (2006). Effect of stannous fluoride toothpaste on erosion-like lesions: an in vivo study. *Eur J Oral Sci* 114(3):180-183.

Young A, Amaechi BT, Dugmore C, Holbrook WP, Nuutinen P, Nunn JH *et al.* (2008). Current erosion indices--flawed or valid? Summary. *Clinical Oral Investigations* 12(Suppl-63).

Yu H, Attin T, Wiegand A, Buchalla W (2010). Effects of Various Fluoride Solutions on Enamel Erosion in vitro. *Caries Research* 44(4):390-401.

Zero DT, Rahbek I, Fu J, Proskin HM, Featherstone JD (1990). Comparison of the iodide permeability test, the surface microhardness test, and mineral dissolution of bovine enamel following acid challenge. *Caries Research* 24(3):181-188.

Zheng J, Xiao F, Qian LM, Zhou ZR (2009). Erosion behavior of human tooth enamel in citric acid solution. *Tribology International* 42(11-12):1558-1564.